Title
Development and Applications of Well-Defined Antibody and Antibody Fragment Bioconjugates

Author
Netirojjanakul, Chawita

Publication Date
2014

Peer reviewed|Thesis/dissertation

Development and Applications of Well-Defined Antibody and Antibody Fragment Bioconjugates

by

Chawita Netirojjanakul

A dissertation submitted in partial satisfaction of the

requirements for the degree of

Doctor of Philosophy

in

Chemistry

in the

Graduate Division

of the

University of California, Berkeley

Committee in charge:

Professor Matthew B. Francis, Chair
Professor Christopher J. Chang
Professor David V. Schaffer

Spring 2014

Development and Applications of Well-Defined Antibody and Antibody Fragment Bioconjugates

by Chawita Netirojjanakul

Abstract

Development and Applications of Well-Defined Antibody and Antibody Fragment Bioconjugates

by

Chawita Netirojjanakul

Doctor of Philosophy in Chemistry
University of California, Berkeley
Professor Matthew B. Francis, Chair

Antibodies have been widely used in many biological applications, including reseach tools, imaging, and therapeutics, due to their excellent binding specificity and affinity. As therapeutics, the ability to elicit immune effector functions and plasma half-life extension through the function of the constant domain (Fc) render antibodies superior to small molecules in these aspects. This work describes the use of chemical-based bioconjugation techniques to develop novel bioconjugates from antibody fragments and full-sized antibodies for therapeutic and imaging purposes. The complex structures of this class of biomolecules — with the presence of multiple polypeptide chains, extensive disulfide networks, and critically important glycosylation patterns — make it difficult to manipulate these biomolecules in a controlled manner. Thus, protein modification techniques play important roles in enabling the development of these constructs. In this work, we discuss the generation of Fc-synthetic molecule hybrids as antibody mimics, full-sized antibody-synthetic molecule conjugates as bispecific antibodies, and MS2-antibody conjugates as targeted delivery vehicles. The ability to conjugate different moieties into one molecule provides the ability to shuffle and combine synergistic advantages of the component molecules.

To my parents, my finest starting materials,
and everyone in my family,

with all my love and gratitude.

Table of Contents

Preface

Had I not attended the immunology class at UC Berkeley, my PhD dissertation might have been much different from this one. I started my PhD career in the Francis Group conducting research on cell patterning of cardiac myoblasts and on the attachment of aptamer on cells for appplications in homing stem cells to an organ or cytotoxic T cells to target cells, using the technology developed by Dr. Sonny Hsiao. We reached the point where the biological assessment was beyond our capability at the time (though looking back with my current knowledge, it might be possible). Then came along the Fc-synthetic molecule hybrid idea, which was perhaps the very first grand idea of mine that actually developed into a research project. The idea emerged during one of the immunology lectures in the Spring semester of my first year. Why did I take immunology? My curiosity led me, and the more I learned, the more fascinated I have become with the complexity of human body. We were learning the basic pathways of the innate immune system — complement pathways. The main character here was a molecule called the antibody, which I really did not know much about at the time. I remember vividly looking at each component of the pathways and fixating on a part of the antibody called the Fc or crystallizable fragment (often known as the constant domain). The Fc is responsible for recruiting the complement proteins and initiates the cytotoxicity cascade. I asked myself, "what if we can create an antibody mimic by attaching a synthetic targeting group to the N-termini of Fc?" I asked the immunology professor right after class whether this idea could work. He said, "Yes," and everything began shortly after another "yes" from Prof. Matt Francis, my adviser.

For the Ab-DNA project, the idea came from a small project in collaboration with Prof. Garry Nolan at Stanford Medical School. They would like to find alternative approach to generate antibody-DNA conjugates. Since both antibodies and DNA oligonucleotides are relatively large and costly biomolecules, an oxidative coupling reaction with its fast kinetics was a reaction of choice. Growing beyond the initial collaboration, I then had an idea that we can create an Ab-aptamer conjugates to function as bispecific antibodies. The collaboration from this group also expanded to the MS2-antibody project as well when we decided to generate a better mass cytometry (CyTOF) probes using MS2-encapsulated nanoparticles. Despite widespread uses of antibodies as targeting groups, the Francis group has never tried attaching them to MS2. If we can generate MS2-antibody conjugates that still retain the binding specificity and affinity of the antibody, it could be useful for many other applications, including *in vivo* imaging and drug delivery.

Writing about what I have done for the past five years reminds me of the time I applied to PhD program at Berkeley. In my statement of purpose, I asked a question, "Will my small step make a giant leap for mankind?" and my answer was "For me, just a tiny possibility to influence many lives other than my own makes it worth an attempt. Then, my journey in science will be more than mere satisfaction of my own…Just as a trickle of light from a jellyfish can be to the benefit of us humans!" During this PhD journey, what I was hoping to do has been, in some way, accomplished. Even though the usefulness of my modified proteins, as of now, is nowhere near that of the fluorescent proteins from jellyfish, I hope that this Jelly has put in her small contribution to the field as originally intended and will continue to do so. Just like the wish I gave myself at the start of my PhD, now it is for the next adventure I am taking...Bon Voyage, Jelly(fish)!

To those who are reading my dissertation, I am very grateful for your attention, and I hope that it will be of some values to you.

Acknowledgements

My journey has been beyond what I had expected both intellectually and spiritually. Not only have I acquired a great deal of knowledge and skills in science, I have learned a great deal more about my very own self. Without the following people, I will not be a person I am today.

I would like to thank my "boss," Prof. Matthew B. Francis for his guidance not only in research but in life! Thank you for giving me space to explore my imagination and being very patient with my stubbornness in proposing and continuing ideas that might not have much to do with the lab expertise. Regardless of the results (mostly failing), his optimitic attitude and unfailing support invaluably kept me going through difficult challenges. I also very much appreciate his advice in career options and his openness to talk to me about anything.

All my previous mentors, Prof. John Essigmann and Dr. Peter Rye at MIT, Prof. Steven Ley and Dr. Alexander Oelke at Cambridge, and Dr. Songpon Deechongkit previously at Chulabhorn Research Institute, have also helped shaping me to be a scientist I am today. I am very much indebted for all their mentorship.

My graduate career would not have been so fulfilling without my awesome labmates! Starting my PhD career in the "sweat shop" (739 Latimer) was, as I shall put, very interesting! This very small room, originally intended to house a maximum of two students, did contain four graduate students, one postdocs, and perhaps four undergrads at one point! However, this seemingly "intimate" space have stimulated and enforced scientific and personal exchanges among the incumbents. Sonny Hsiao was a wonderful mentor for my very first projects, and he was a very accomplished scientist himself. It was a perfect start for me. I am very grateful for all his advice for the projects he mentored and beyond. I continued to ask him questions even after he graduated! Michel Dedeo was kind enough to share this "precious" bench space with me and Dr. Michelle Farkas. He is also a brilliant molecular biology master and "fixing anything" mechanic who I have probably bugged the most with scientific and random questions. Dr. Michelle Farkas, a postdoc who joined the lab at almost the same time as me, has been my "biology" buddy! Since not many other people in the lab have much to do with "biology," Michelle and I often exchanged thoughts and plans for our experiments. She also guided me through many fellowship, conference, and job application processes. If she may allow me, I was almost like her first graduate student! I truly appreciated her mentorship. Kareem El Muslemany, a graduate student who also joined the lab at the same time as me, has always come up with interesting ideas in science and thoughts about the world. Despite the lack of space, I have enjoyed very much being in this room!

After three years or so, I have "graduated" from a "legendary" desk space in the sweat shop to a new, shiny, spacious desk and bench space in 733 Latimer, soon after Zac Carrico left the lab to start his postdoc. Despite being rather quiet, Zac has been very helpful in answering any molecular biology or MS2 questions! Gary Tong and Chris Behrens were funny and witty. In addition to their scientific contribution to my PhD career, they have been very good friends to hang out with outside of the lab even after they graduated. Gary and I can always share personal stories (aka dramas!). Abby Knight is definitely one of the most cheerful people in the lab! I have enjoyed her company both in the lab and outside. She has been a very good friend of mine, and I really appreciate all her good intention for the Francis Group. The end of "fraternity" and the rise of "sorority" era in the 733 happened when Chris and Gary left the group. Kanwal and Ioana were our fantastic new additions. I have worked with them on the Rapoport's salt and the antibody-MS2 projects, respectively. They are bright and hard-working. The successor of my desk was Joel Finbloom. I have not

interacted wtih him much, but I have only heard good things about him. I am really quite certain that all these younger generations will do very well here. If the sweat shop was a happy beginning, 733 was a very happy ending. I will definitely miss the 733 crew!

The Francis Group do not just have two roomful of brilliant students, but so many others have made this group "the place to be!" Nich Stephanopoulos not only struck me as a very smart and well-rounded scientist, but also often entertained me with this question, "are you ready for this, Jelly?" Leah Witus was probably the happiest person in the world and definitely the Francis Group's mama! She was also my absolutely helpful and optimistic mentor and collaborator. We collaborated on both PLP and Rapoport's salt projects, and it was my true pleasure to work with her. Kristen Seim has become the CAN master. Her bench was always filled with buffers and colorful dyes! Despite such a young age for her class, Allie Obermeyer has defeinitely impressed me with all her knowledge in science. She seems to know everything! I always go to her for many of my random questions, especially about MS2 and HPLC! I also would like to thank Wesley Wu and Kanna Palaniappan for answering my random questions. Kanna, by this point, probably knows more about Thailand and Southeast Asia than I do! Mike Coyle has been a good resource for anything DNA-related. He also helped me start many of my projects with his knowledge in biology. I also would like to thank Amy Twite, Troy Moore, and Dan Finley for all their help. Amy knows so much about biology; it was interesting to talk about Asian culture with Troy, the master in this subject; and Dan helped me with anything computer-related! Also without them, the parties in the Francis Group would have been much less entertaining. My classmates in the Francis Group, Jeff Glasgow, Stacy Capehart, Katherine Mackenzie, and Kareem El Muslemany, have made this group even more interesting intellectually and personally. Not only have we pursued such diverse research interests, but we also each have very distinct characters. I have been unsuccessfully requesting to see a shaved look of Jeff Glasgow. Stacy always have the cutest animal pictures and videos. Katherine often baked the most delicious goodies! Moreover, she built a bar in 733! Besides those I already mentioned, the other younger classes, Jess Lee, Jenna Bernard, Jim MacDonald, Richard Kwant, Jake Jaffe, Matt Smith, Matt White, and Am (Rapeepat Sangsuwan), are all brilliant. I am very happy to get to know Am, to help her throughout her transition to the U.S. and to learn that she decided to join the Francis Group. I am sure she will do very well here.

Besides Dr. Michelle Farkas, our postdocs, Dr. Adel Elsohly, Dr. Meera Rao, Dr. Henrik Munch, and Dr. Praveena Garimella, have brought much expertise, especially in organic synthesis, to the lab. It was definitely my honor and pleasure to collaborate with Adel on the MS2-antibody project. We have gone through many phases of success and failure and also through many trips to Stanford. His complementary thinking process has made our collaboration a truly stimutaing and enjoyable one. He knows so much about literally so many branches of maths and sciences, with all his undergraduate and master degress as a confirmation. He possesses a rare breadth of knowledge.

The last lot I need to acknowledge in the Francis Group is our undergrads! The group has been very successful in attracting the best and brightest undergraduate students: Nielson Weng, Forrest Jones, Effie Zhou, Betty Shum, Peter Palmere, Josh Zweig, Jacqueline Cox, James Brady, and Hyun Shin Park. I was very fortunate to mentor Nielson Weng and Forrest Jones, both of whom made it seem very easy to be a mentor! Nielson was definitely more than what I could have asked for in an undergrad. He was genuine, hard-working, smart, and meticulous in everything he does. I often said to him, "If I started my career in academia and he were my first graduate student, I should be all set for the rest of my career." I am also grateful for his company during my late night experiments, and I cherish our friendship. Despite my brief mentorship to Forrest, he was also a

great addition to the team Jelly! He is a very smart and quick learner. I wish them both the best in their future, Nielson as an MD PhD student at Stanford and Forrest as a master student in public health at Yale. I am indeed very proud of them.

Apart from all the support I got from the group, I am indebted for all the help and scientific contribution I obtained from all my collaborators. I would like to thank Prof. Volkmar Heinrich, Chek Ounkomol, and Chengyuk Lee at UC Davis for their help in the neutrophil projects. Funnily, this collaboration just came from a conversation between Chek and me over pizza and wine! I very much enjoyed learning more about immunology through them, not to mention observing the phagocytosis event in real time. It was amazing! I am also very grateful to Prof. Garry Nolan at Stanford for the collaboration in the antibody-DNA and MS2-antibody projects. In particular, I would like to thank Astraea Jager for her patience in assisting us through many of our failing CyTOF experiments and definitely for her expertise in running the instrument. Our experiment finally worked! I would like to thank Sean Bendall for his guidance in designing and running the CyTOF experiments. Besides those two collaborations, I have also consulted with many others on my projects. I would like to thank Jonathan Sockolosky in the Szoka Lab at UCSF for his expertise and advice in FcRn-related experiments. I am also very grateful for the FcR- and FcRn-expressing cells, kind gifts from the Ravetch Lab at Rockefeller Institute and the Roopenian Lab at the Jackson Laboratory, respectively. In particular, I would like to thank Patrick Smith and Dr. Stylianos Bournazos from the Ravetch Lab, and Dr. Greg Christianson and Dr. Victor Sun from the Roopenian Lab for their assistance throughout the material transfer process and their guidance in the cell maintenance. I would also like to thank Prof. Thomas Kodadek, Manuel Tapia, and Prof. D. Gomika Udugamasooriya for our collaboration and their advice on the peptoid screening project, which Ioana will continue. Lastly, I would like to thank Dr. Anthony Iavarone from the mass spectrometry facility, Ann Fischer from the cell facility, and the Bertozzi Group for the use of their instrument.

During my studies at Berkeley, I also enjoyed participating in other activities outside of the lab. I have very much enjoyed attending meeting and conferences where I met such great scientists, in particular Dr. Paul Carter from Genentech, whose work I admire very much, and Prof. Robert Tjian, who started the HHMI International Fellow Scholarship. My internship experience at Eureka Therapeutics has also prepared me well for my future job in industry, thank to great mentoship of Dr. Cheng Liu and Dr. Jingyi Xiang. The Mayfield Fellow Program has been a great experience in entrepreneurship. I am thankful to Prof. Andrew Isaacs and Rajeev Batra for their mentorship and introduction to the entreprenuerial and venture capital world. I have also been fortunate to have met, traveled, and been friends with such a great group of the 2012 Mayfield fellows (Vimal Kini, Carla Vazquez, Tony Le Verger, Raja Muthuraman, Vivien Leong, Luis Navarro, Patrick Wendell, and Alan Yiu) and all the alumni.

My classmates, Pim (Munchuta Dangkulwanich), Maya Sen, and Sam Sternberg, have become very good friends and great people to chat with about science. Sam Sternberg has become an expert for all my "K_d" problems. Maya and her family have been wonderful hosts for some of our gathering. I have known Pim from high school (which is more than 10 years ago!), and I am very happy that we reunite and continue our friendship at UC Berkeley.

It would not have been fair if I do not also thank Geoffrey Supran. I appreciated his existence. I learned a great deal about my life through him.

I am also very thankful for the Thai community at Berkeley and in the Bay Area. It is always very difficult being miles away from home but these people make me feel like here is also

home, my second home! P' Parn (Yada Duangsawai) has become my local big sissy, who has very similar character to me! I adopted N' Kaew (Penporn Koanantakool) as my local younger sissy, who I can share my thoughts and let out my stress after a long day. Oak (Kan Kanjanapas), despite being older in age, has claimed a spot as my local little brother, who is my tennis partner, my life counseler, and perhaps my business partner for our future commedy show. Despite their short presence at Berkeley, I somehow managed to become besties with Nicky (Nuttanuch Arnuntapunpong), who spent a year doing LLM, and Apple (Luksanawan Wannaluk), who was only here for a week for the Global Social Venture Competition at Haas. In the latter case, serendipity has brought us together as I overheard some Thai speaking in the bathroom queue! I am very glad to have shared happy, exciting, stressful, and failing moments with other Thai graduate students, who entered the PhD life at the same or almost the same time as me, Jack (Subprasiri Sirivirivakul), Champ (Chayut Thanapirom), Chao Kusollerschariya, Fook (Poomyos Wimonkittiwat), Pim, Natth, and Oak. I have also become very close to a few of Thammasart exchange students, expecially N' Tae (Thitiwat Kaewwattanaborworn) and N' Firm Thiengtham, who seemed to leave me too soon. Last but not least, I am very fortunate to have met my "dhamma gang," Kruba Bird (Tanachai Limpaitoon), Nattha (Natth Benjaburanin), and Hung' (Summa Sriprachyaanan), who introduced me to inner peace. I am also very grateful for all the dhamma lessons and practice they have shared with me and for the trips to Abhayagiri Buddhist Monastery, where I had a first glimpse of true Buddhism and met great "Ajarns" (i.e., teachers). For those I did not mention the names, I appreciate your presence much the same.

I would like to thank my lovely roommates who make home the best place to come back to everyday: Chip (Nalat Yulong), who has stayed with me the longest and always cook and bake such yummy food; N' Kaew, who has impressed me very much with her kindness and selflessness; P' Van (Sirilata Yotphan) and P' May Srikun, whom I could always chat with about research and exchange some gossips in the department.

Eleven years ago, I began my "random walk" outside of my hometown, starting in the U.S., with a brief visit to the UK. Many of the friendships throughout my journey have been transient, but I am very much indebted to those that last. My beloved roommates from MIT, Patricia Zheng (my peanut butter!) and Sophia Lee (my bean!), have made my stay in the U.S. one of the most memorable. We share everything, and I cannot imagine my life without them. Emily Teller, who worked in the academic office at Middlesex School, has become one of my very first friends in the U.S., and we still cherish our friendship until today. Ping (Sakdapong Chavanaves) was my tennis coach at Cambridge, UK, and I thank him for being by my side when I had nowhere to go. I also enjoy my complaining session about life with Pann (Pakpong Chirarattananon), another friend from Cambridge who was lured to come do PhD in the U.S. He has indeed done very well.

This may seem odd but I would like to thank myself for deciding to come to Berkeley. From the first moment I visited until now, I still enjoyed every moment I have been here. The hippies, the homeless, the creeks, the hills, the sunset over the Golden Gate, the food, the lively music by the Bart station, the rigorous academic settings, the collaborative research environment, the friendship...Shall I just say "the everything"?

I very much appreciate all the financial support I received throughout my education: Scholarship from Institute for the Promotion of Teaching Science and Technology in Thailand for Bachelor, Gates Cambridge Scholarship for Master, and Abramson Graduate Scholarship and Howard Hughes Medical Institute (HHMI) International Student Research Fellowship for PhD. Without these financial supports, I would not have the oppotunities to accomplish any of these degrees in

such world-class academic institutes.

Finally, I would like to thank my family, without whom I am nobody and definitely nowhere. I owed everything I have to them. Thank to my dad, who has always been my cheerleader and my great academic supporter, I had the urge to pursue my PhD studies. Lacking the opportunity to pursue any education beyond primary school themselves, my mom and my dad (Mrs. Walaiporn and Mr. Adul Netirojjanakul) have always encouraged me to reach my full potential in everything I do. I just happened to be quite good at school so here I am, finishing one of the highest degrees one can aim for. I always joke with them, "If I continued studying, I would just become a 'professional student' until I retire!" I still remember vividly, just like it happened yesterday, a pticture of a little primary school girl who went over her book and recited her English vocabulary with her dad, using one of the shoe stalls in his shop as her desk. Sometimes she pretended to fall asleep while her dad patiently read her English conversation from one of those "self-learning English" books. If she fell asleep for too long, she could very well find herself picking up the book from a trash can with tears in her eyes at any point during the studying time with her dad. Coincidentally or not, the cover of that English conversation book features a picture of Margaret Thatcher, the UK's first female priminister. Perhaps, her dad secretly implied something here. That little girl was me 20 years ago. Now everytime I go back to Thailand, my dad still picked up the "Margaret Thacher book," but instead I am reading off those English conversation to him. It just dawned on me where my continuous curiosity and my fondness in learning come from, perhaps along with a "stubborness gene." My mom contributed no less than my dad in my "educational tour" (the word my dad used when he wanted me to study extra time outside of school. Instead of going to the mall, we went on this so called educational tour!). She has gone with me to all these tutoring schools and never ever once complained how late at night or how long she had to wait. Thoughout this educational tour, a picture of a little girl sitting on her mom's lap on a crowded bus getting stuck in a heavy traffic in Bangkok would not have been an exaggeration. With all their supports, my parents gave me the flexibility to explore my path and to choose what I want to study and who I want to become. Among all the steps in my "professional student" career, the decision to pursue a PhD in chemistry was the most difficult one to make, and this five-year journey has also been the most challenging intellectually and mentally. Not knowing how my research will unfold or when it could end, I often found myself exhausted from not knowing the unknowns. However, the value of education and the thirst for knowledge my parents have instilled in me have left me no fear to tackle all these challenges. In fact, I quite enjoyed the process of solving problems and figuring out the unknowns. Their encouragement throughout this "scientific marathon" has also been tremendous. Apart from my parents, my siblings, J' Nok (Sansanee Netirojjanakul), Ken (Wisit Netirojjanakul), and Book (Wasan Wanarungruedee), have been such a great source of joy, encouragement, and advice. When I fall from any challenges in life, they never once failed to give me the invisible hands to pick me back up. Ken also introduced me to Vipassana practice by Ajarn Goenka, which helped me realize that "the happiness is here and now." Without my family, there would not be me today. If it is karma, I must have done something good.

ขอขอบคุณป๊า ม้า เจ๊นก เคน บุ๊ค ที่คอยเป็นกำลังใจให้ตลอดมานะคะ ความสำเร็จที่ลีมีในวันนี้จะเป็นไปไม่ได้เลยหากปราศจากกำลังใจและความรักจากทุกคน รักทุกคนมากเช่นกัน ขอบคุณป๊าม้าที่ดูแลเลี้ยงดูและหล่อหลอมให้ลีเป็นลีทุกวันนี้ คงไม่มีคำขอบคุณใดจะสามารถทดแทนบุญคุณของป๊ากับม้าได้ แต่ลีอยากจะบอกว่าลีรักป๊าม้ามากและอยากทำตัวให้ดีให้ป๊ากับม้าภูมิใจ อยากดูแลป๊ากับม้าตลอดไป

I have been so fortunate about many things in my life, and these five years have also been

yet another highlight. I appreciated all the precious moments, the friendship, the opportunities, and the fun I have had. I really cannot believe it has already been five years! Thank you everyone for all your support! I did it!!!

Chapter 1

Advance in Antibody Engineering and Alternative Antibody Platforms

Abstract

This chapter gives an overview of the recent advancements in antibody engineering with a focus on the cancer therapeutic applications. In the past, antibodies have been widely used as research tools in various applications. It was not until the 1970s when Georges Köhler and César Milstein developed the hybridoma technology for production of monoclonal antibodies (mAbs) that the concept of using antibodies as "magic bullet" therapeutics was realized. Antibody engineering has further improved the properties of mAbs, and at this time, there are more than 20 antibodies already being used in the clinic. Following the success of antibodies, many other platforms, such as antibody fragments, bispecific antibodies, and antibody-drug conjugates, have been investigated as alternatives. Here, we discuss the mechanisms of actions of therapeutic mAbs based on the functions of each antibody fragment, the advancement in antibody engineering, and alternative antibody mimic and antibody-based platforms.

1.1 Significance of Antibodies in Therapeutics

Over a century ago, Paul Ehrlich proposed the "magic bullet" concept for drugs that go straight to their targets [1]. However, it was not until Georges Köhler and César Milstein developed the hybridoma technology for production of monoclonal antibodies (mAbs) in 1975 that the possibility of using mAbs for therapeutics became a viable option [2]. In the past, mAbs originating from mice often had limited clinical applicability due to their immunogenicity and poor ability to induce immune effector responses in humans [3]. The advance in antibody engineering led to the development of mouse/human chimeric antibodies [4], humanized antibodies [5], and fully human monoclonal antibodies [6,7], which satisfactorily addressed many of these problems [3]. This breakthrough has allowed the use of antibodies as therapeutic agents [8]. To date, there are more than 20 mAbs approved as therapeutic agents for a variety of diseases, nine of which are for cancer therapy (Table 1.1) [9]. In this chapter, we focus on these anti-cancer antibody therapeutics and discuss their structures and mechanisms of action, advance in antibody engineering, and lastly alternative antibody-based platforms.

Table 1.1. Approved antibodies for cancer therapy (Table adapted from Ref. [10])

Generic name (trade name)	Target	Antibody Form	Mechanisms of Action	Approved indications
Cetuximab (Erbitux)	EGFR	Chimeric IgG1	Block ligand binding; inhibit receptor dimerization; induction of apoptosis; ADCC; sensitization of cells to chemotherapy and radiotherapy	Metastatic colorectal cancer; head and neck cancer
Panitumumab (Vectibix)	EGFR	Human IgG2	Block ligand binding; inhibit receptor dimerization; induction of apoptosis	Metastatic colorectal carcinoma
Trastuzumab (Herceptin)	HER2	Humanized IgG1	Inhibit receptor dimerization; inhibit HER2 shedding; ADCC; sensitization of cells to chemotherapy	HER2-overexpressing breast cancer
Pertuzumab (Perjeta)	HER2	Humanized IgG1	Inhibit receptor dimerization; ADCC	HER2-positive metastatic breast cancer
Bevacizumab (Avastin)	VEGFA	Humanized IgG1	Neutralization of VEGFA activity	Metastatic colorectal cancer
Ipilimumab (Yervoy)	CTLA4	Human IgG1	Blockade of CTLs inhibitory mechanism	melanoma
Rituximab (Rituxan)	CD20	Chimeric IgG1	Induction of apoptosis, ADCC; CDC; sensitization of cells to chemotherapy	Non-Hodgkin's lymphoma, RA and CLL
Ofatumumab (Arzerra)	CD20	Human IgG1	ADCC; CDC	CLL
Alemtuzumab (Campath)	CD52	Humanized IgG1	ADCC	CLL

ADCC, antibody-dependent cellular cytotoxicity; CD, cluster of differentiation; CDC, complement-dependent cytotoxicity; CLL, chronic lymphocytic leukaemia; CTLs, cytotoxic T lymphocytes; CTLA4, cytotoxic T lymphocyte antigen-4; EGFR, epidermal growth factor receptor, HER2, human epidermal growth factor receptor 2; RA, rheumatoid arthritis; VEGFA, vascular endothelial growth factor A

1.2 Antibody Structures and Mechanisms of Action

1.2.1 Antibody structures

Antibodies are grouped into five classes based on the sequence of their heavy chain constant regions: IgM, IgD, IgG, IgE, and IgA. Of the five classes, IgG, in particular the IgG1 isotype, is the most frequently used for cancer immunotherapy [3,10,12]. Human IgG1 is a heterodimer of ~150 kDa, comprised of heavy and light chains, shown in blue and purple, respectively (Figure 1.1). It can be subdivided into two distinct functional units, the fragment of antigen binding (Fab) and the crystallizable fragment (Fc, also known as constant fragment), connected through a flexible polypeptide called the hinge region (Figure 1.1). In addition, human IgG1 contains two

N-linked oligosaccharides covalently attached at the asparagine 297 (Asn297) in the C_H2 domain (Figure 1.1). These oligosaccharides are composed of a mannosyl-chitobiose core structure in the presence or absence of a fucose, a bisecting *N*-acetylglucosamine (GlcNAc), and terminal galactose and sialic acid, yielding a heterogeneous mixture of 30 or more glycoforms [8,13,14,15].

Antigen binding specificity can be achieved through the Fab fragment, which contains three hypervariable complementarity determining regions (CDRs) that form the antigen binding site of the antibody. Antibodies elicit various immune effector functions via the Fc fragment by initiating complement-dependent cytotoxicity (CDC) and binding to Fc γ-receptors (FcγR) for the antibody-dependent cellular cytotoxicity (ADCC) and antibody-dependent cellular phagocytosis (ADCP) effects [16-20]. The presence of oligosaccharides is also critical for the binding of Fc to FcRs and complement proteins and plays a critical role in inducing effector functions [15,21,22]. Moreover, the Fc can also bind to the neonatal Fc receptor (FcRn), which allows the Ab to be protected from degradation in the endosome and recycled to plasma [23,24]. The Fc-FcRn interaction is thus important for the plasma half-life extension of antibodies.

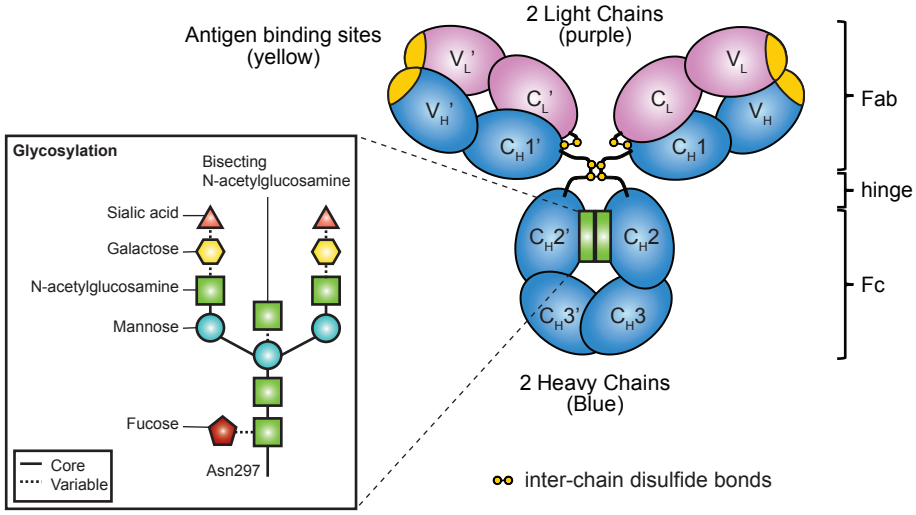

Figure 1.1. Human immunoglobulin G1 (IgG1) structure. Antibodies comprise two heavy and two light chains, shown in blue and purple, respectively. The light chain has two domains: variable (V_L) and constant (C_L). The heavy chain contains four domains, three of which are constant C_H1, C_H2, and C_H3, and the other is variable V_H. The variable and the first constant domain of heavy and light chain form the antigen binding fragment (Fab), where hypervariable loops or complementarity determining regions (CDRs; shown in yellow) form antigen binding sites. The other two constant domains of the heavy chain form the crystallizable fragment, also known as constant fragment (Fc). The flexible linkage between Fab and Fc is called the hinge region. Two dimers of IgG1 are connected through two inter chain disulfide bonds (yellow dots represent Cys residues of inter chain disulfide bonds) in the hinge region. There is also another inter-chain disulfide connecting heavy and light chains, as well as one intra-chain disulfide in each domain. The human IgG1 isotype also contains one glycan linked to each heavy chain at Asn297 (shown in green). The glycan comprises of mannosyl-chitobiose core (connection shown in solid lines) with variable galactose, sialic acid, core fucose, and bisecting GlcNAc residues (connection shown in dotted lines).

1.2.2 Antibody mechanisms of action

In this section, we discuss the mechanisms of action that therapeutic antibodies can use to treat cancer, classified according to two major components of antibodies: the Fab and the Fc fragments. The Fab confers specific binding to any target antigens with high affinity. This domain can thus be designed to perturb growth signaling cascades, induce apoptosis pathways, or inter-

fere with the tumor microenvironment to prevent important nutrients or signaling molecules from supplying tumor cells. The Fc can induce various cytotoxic events through immune effector cells, such as ADCC, CDC, and ADCP (Figure 1.2). Moreover, it has been shown to induce the adaptive immunity through cross-presentation of antigen presenting cells (APCs) to T-cells (Figure 1.2).

1.2.2.1 The use of Fab for specific binding of antigens

Specific binding of Fab can interfere with the growth of cancer cells through several mechanisms, including the blocking of ligand binding, perturbation of signaling pathways, and interference with the tumor microenvironment [3]. Blocking ligand-receptor interactions and perturbing signaling pathways have been the earliest mechanisms for tumor targeted therapeutics. The main targets are members of the epidermal growth factor receptor (EGFR) family, including EGFR (also known as ERBB1), Human epidermal growth factor receptor 2 (HER2, also known as ERBB2), HER3 (also known as ERBB3), and HER4 (also known as ERBB4), which are frequently overexpressed in solid tumors [3]. Many of the antibodies targeting these receptors have already been approved by the FDA and are summarized in Table 1.1. These antibodies function by preventing binding of activating ligand and/or by preventing receptor dimerization, thus blocking downstream growth signaling events. Other mechanisms of action may also include those triggered by interaction of Fc with immunologically relevant proteins and/or receptors. The Fc-induced cytotoxicity will be discussed in the following section.

Cetuximab and penitumumab both target EGFR but at different epitopes. They exhibit similar modes of action, i.e., blocking the binding of EGF and inhibiting receptor dimerization [25-27], except that penitumumab, as an IgG2, does not elicit ADCC responses [27]. Other EGFR-targeting antibodies in clinical trials include nimotuzumab (approved in India and several countries in South America) [28] and necitumumab [29]. In addition to targeting the complete form of EGFR, efforts are underway to target a truncated form of the receptor, EGFRvIII, one of the most common mutations in glioblastomas, occurring in about 50% of cases where the EGFR gene is amplified and also found in head and neck cancer and lung squamous cell carcinoma [30-32]. An in-frame deletion of exons II–IV leads to the elimination of 267 amino acids from the extracellular domain, and the insertion of a novel glycine at the fusion junction, resulting in a mutant EGFR that is unable to bind any known ligand but capable of constitutive signaling .

HER2 has also been a very successful target for antibody therapy. HER2 was found to be overexpressed in many types of cancers: 25-30% of breast, 44% of bladder, 26% of pancreatic, and smaller percentages in ovarian and lung cancers [33,34]. Even though the natural ligand for HER2 has not been discovered, homodimerization and/or heterodimerization with other EGFR family members (EGFR, HER3, and HER4) leads to tyrosine phosphorylation of these receptors and triggers a variety of signaling cascades that play a critical role in tumorigenesis [35]. Thus, the antibodies targeting this receptor have been raised primarily to inhibit receptor homo- and hetero-dimerization and internalization, rather than by blocking ligand-binding [35]. Trastuzumab (Herceptin), a humanized IgG1, was the first anti-HER2 antibody to be approved for invasive breast cancer that exhibits gene amplification and overexpression of HER2. Besides blocking of receptor dimerization, this antibody can activate ADCC [19,37] and inhibit the shedding of the HER2 extracellular domain, which leads to a truncated form (HER2 p95) with potentially enhanced signaling activity [36]. Whether trastuzumab induces HER2 downregulation and subsequent degradation in HER2-overexpressing breast cancer cells is currently subject of discussion [38-40]. Pertuzumab (Perjeta), which binds to different epitope of HER2 extracellular domain, was approved in 2012

for the treatment of HER2-positive metastatic breast cancer. Its mechanism of action is similar to that of trastuzumab, but its ability to block HER2 shedding has not been proven [41]. Given that pertuzumab and trastuzumab target different epitopes on HER2, they can be used together in combination therapy to achieve more comprehensive blockade of HER2 signaling [41-43]. Efforts in targeting HER3 and HER4 are relatively recent and as of now, no antibodies have been approved; however, many promising studies have been reported [44,45].

Another strategy is to target critical events within the tumor microenvironment. Vascular endothelial growth factor (VEGF), which is expressed by many solid tumors to stimulate angiogenesis upon binding to VEGF receptor (VEGFR) on the vascular endothelium, has become one of the main targets. A VEGF-specific humanized monoclonal antibody, such as bevacizumab (Avastin), has been developed and approved for the treatment of breast, colorectal and non-small cell lung cancer in combination with cytotoxic chemotherapy [46]. Other efforts also include developing antibodies against VEGFR [47] and platelet-derived growth factor receptor (PDGFR) [48]. PDGF, another proangiogenic mediator, was found to be upregulated during treatment with bevacizumab, increasing the occurence of bevacizumab-resistant tumors. Thus, the blockade of PDGFR-signaling via a PDGFRβ-specific antibody has been shown to have a synergistic effect with that of VEGF-VEGFR signaling pathway [48,49].

In addition to the angiogenesis pathways, many studies have targeted relevant receptor-ligand interactions of the immune systems in the tumor microenvironment, including transforming growth factor β (TGFβ), an immunosuppressive cytokine that inhibits T cell activation, proliferation, and differentiation, cytotoxic T lymphocyte antigen-4 (CTLA4), a negative regulator of T cell activation, and CD40, a member of the tumor necrosis factor receptor (TNFR) family expressed by APCs [3,50-53]. Both antagonists to TGFβ and CTLA4 and agonists to CD40 have been shown to have anti-tumor activities [50-53].

1.2.2.2 The use of Fc for immune effector functions

1.2.2.2.1 Antibody-dependent cellular cytotoxicity (ADCC) and antibody-dependent cellular phagocytosis (ADCP)

ADCC and ADCP are natural mechanisms designed to remove or destroy pathogens such as viruses or bacteria that could invade the body [54]. These pathogens are first recognized by specific antibodies, followed by recognition and destruction of the antibody-bound particles by FcR-expressing immune effector cells [54]. The FcγRs family, comprised of FcγRI (CD64), FcγRII (CD32), and FcγRIII (CD16) in humans, are expressed on a variety of immune cells, such as natural killer (NK) cells, neutrophils, and macrophages [54]. These receptors are specific to the Fc of IgGs, with the highest affinity to IgG1 and IgG3 [54]. The crosslinking of FcγRs on immune effector cells upon binding to Fc-bound antigens triggers the signaling and subsequent immune responses, such as release of inflammation mediators, B cell activation, endocytosis, phagocytosis, and cytotoxic attack [15,55]. The main players in ADCC are NK cells, which use an analogous mechanism of attack to that of cytotoxic T-cells, involving the release of cytoplasmic granules containing granzyme or perforin to attack target cells (Figure 1.2a). ADCP is an effect of the interaction of Fc with FcγRs on phagocytes, such as neutrophils and macrophages (Figure 1.2b).

The engagement of the Fc fragment of the antibody with Fcγ receptors (FcγRs) has been shown to be important for the anti-tumor effects of several mAbs. An *in vivo* study in FcγR-deficient mice showed reduced anti-tumor activity of trastuzumab and rituximab, as compared to their

effects in wild-type mice [19]. Moreover, the FcγR polymorphisms, which lead to high binding of antibodies to FcγR, are also associated with high response rates to rituximab [56,57], trastuzumab [58], and cetuximab [59], highlighting the importance of ADCC for these therapeutic antibodies. Unlike ADCC, there have been several reports of the ADCP effect *in vitro* [60-62], but few examples are available for studies *in vivo* or in clinical settings [63].

1.2.2.2.2 Complement-dependent cytotoxicity (CDC)

Another strategy that antibodies use to eliminate foreign pathogens is to activate the cascade of complement proteins or the so-called complement-dependent cytotoxicity (CDC) [54]. Complement activation occurs upon binding of C1q to an IgM (existing in pentameric form) or two or more bound IgG molecules. The complement cascade then proceeds via a series of proteolytic cleavage reactions and finally results in the polymerization of C9 molecules into a pore-forming structure called the membrane-attack complex, which destroys the target cells (Figure 1.2c) [54]. For cancer therapeutics, one of the most studied CDC effects is that of anti-CD20 and anti-CD52 antibodies. CDC was shown to be critical to the anti-cancer efficacy of rituximab (Rituxan); anti-tumor protection by rituximab was completely abolished in C1q knockout mice [64]. Depletion of complement by using cobra venom factor (CVF) also reduced therapeutic activity of rituximab in a xenograft model of human B-cell lymphomas [65]. Studies using ofatumumab, another anti-CD20 antibody that binds a different epitope from rituximab, and alemtuzumab (Campath), which recognizes CD52, also reveal the importance of CDC [66,67]. One hypothesis suggests that effectiveness of CDC may depend on the distance between the plasma membrane and the Fc of the bound antibody. Thus, mAbs directed at membrane proximal targets such as CD20 and CD52 lead to more effective CDC than the mAbs that target the receptor epitopes farther away from cell surface [66].

1.2.2.2.3 Induction of T cell immunity through cross-presentation

Early research on the anti-tumor effects of therapeutic antibodies focused on the induction of cytotoxic effects via innate immunity, ADCC and CDC. Not until recently did several studies suggest the role of the adaptive immune system in mediating the long-term benefit or "vaccinal" effect of mAbs [68]. Tumors coated with antibodies were able to enhance cross-presentation by dendritic cells (DCs), which are antigen-presenting cells (APCs), in an FcγR-dependent fashion [68-71]. DCs can also engulf the resultant apoptotic tumor cells from ADCC and subsequently present tumor antigens on MHC class I and II molecules. This dual presentation leads to the generation of $CD8^+$ T cells, causing direct tumor cytotoxicity, and the generation of $CD4^+$ T cells, which can prime B cells for the production of tumor-specific host antibodies (Figure 1.2d). However, DC presentation of engulfed tumor antigens can lead to either adaptive immunity, as mentioned above, or tolerance, which suppresses immune response, based on the tumor microenvironment. Accordingly, adjuvant therapy (GM-CSF, Flt-3 ligand, and IFN-α) promoting the cross-presentation or strategies aimed at blockade of immunosuppressive factors, e.g., TGFβ and CTLA4, and activation of inflammatory pathways, such as via CD40 in the microenvironment, as mentioned in section 1.2.2.1, may have a synergistic effect with tumor-directed antibody therapy by enhancing cross-presentation and breaking local tolerance [50,68].

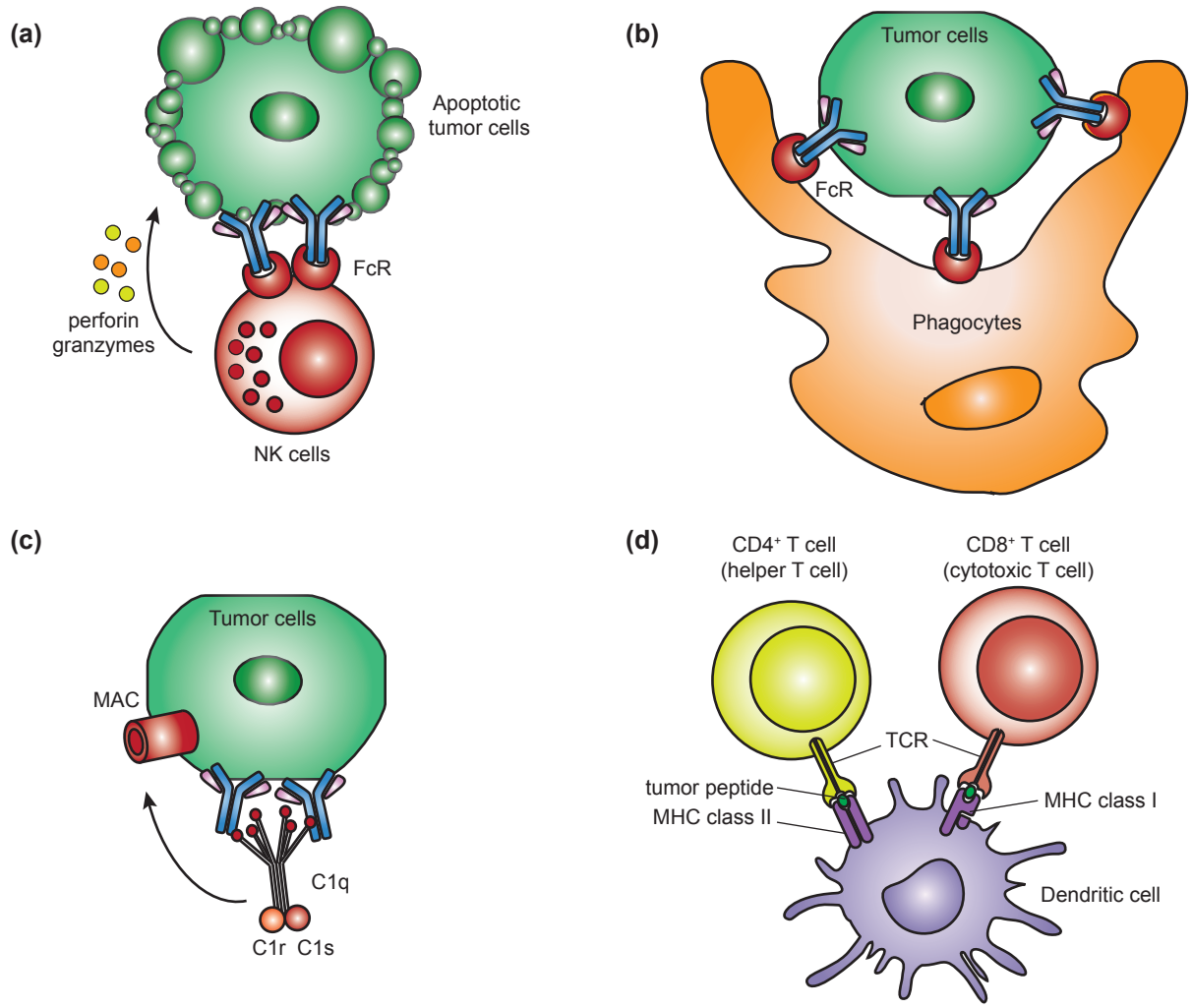

Figure 1.2. Anti-tumor mechanisms induced by interactions between Fc and immunologically relevant proteins. (a) Antibody-dependent cellular cytotoxicity (ADCC). The antibody-bound tumor cell is recognized by FcγRs on immune effector cells such as NK cells. The crosslinking of FcγRs on NK cells triggers the release of cytoplasmic granules containing granzyme or perforin to attack target cells. (b) Antibody-dependent cellular phagocytosis (ADCP). The IgG-coated tumor cells can bind FcγRs on phagocytes and initiate Fc- dependent phagocytosis, leading to the lysosomal degradation of the tumor cells. (c) Complement-dependent cytotoxicity (CDC). Upon binding of antibodies to target tumor cells, the Fc recruits C1q complement protein to initiate the complement cascade, resulting in tumor cell lysis by the membrane attack complex (MAC). (d) Induction of T cell immunity through cross presentation. Antigen presenting cells (APCs) such as dendritic cells (DCs) can engulf IgG-coated apoptotic tumor cells and present these tumor antigens, which are peptides derived from lysosomal degradation of tumor cells, on MHC class I and II molecules, leading to activation of $CD8^+$ cytotoxic T cells and $CD4^+$ helper T cells, respectively. (Figure adapted from Ref. [3])

1.3 Advances in Antibody Engineering

As discussed in the previous section, numerous studies suggest that interactions between the Fc and immunological relevant proteins (FcRs and complements) are critically important for the cytotoxic effect of antibodies in cancer immunotherapy. The Fc-FcRn interaction also prolongs the plasma half-life of antibodies. To enhance the ADCC, CDC, and also increase the half-life, various efforts in engineering Fc for higher affinity to activating FcRs, complements, and FcRn have been conducted [8]. We will focus on the improvement in ADCC, one of the most studied

and a major mechanism of action of cancer therapeutic antibodies, such as cetuximab, rituximab, and trastuzumab. Two main approaches to modify the Fc domain for enhanced ADCC include (1) amino acids alteration of Fc domains and (2) modification of Fc domain oligosaccharides.

1.3.1 Protein engineering

Enhancing ADCC activity by modifying the amino acid sequence of the Fc domain has been extensively studied. Shields *et al*. reported a detailed mutational analysis of IgG1 Fc regions based on the co-crystal structure of IgG and FcγRIIIa [72] and identified up to three key mutations, S298A, E333A, and K334A, which increase the binding of IgG1 to the activating receptor FcγIIIa and reduce the binding to the inhibitory receptor FcγIIb [18]. These mutants were shown to enhance capacity for ADCC in *in vitro* studies. Using a yeast display system, Stavenhagen *et al*. have screened a number of comprehensive Fc mutants. The best variant, containing five mutations (F243L, R292P, Y300L, V305I, and P396L), showed ~10-fold higher binding affinity to FcγRIIIa and ~100-fold improved ADCC activity [73]. Computational design algorithms based on structural information of the Fc/FcγR interface have also been used to design IgG1 Fc variants. Lazar *et al*. computationally designed amino acid modifications of the Fc region that provide more favorable interaction at the Fc/FcγR interface while maintaining the stability and solubility of the IgG [55]. The variant of Fc, containing S239D/A330L/I332E mutations, exhibited a ~100-fold improvement in binding affinity to FcγRIIIa, resulting in remarkably enhanced ADCC activity *in vitro* and in cynomolgus monkeys [55].

1.3.2 Glycoengineering

Another factor that affects the binding of Fc to FcγR is the N-glycosylation at Asn297 in the Fc domain. Antibodies that lack N-glycosylation structures cannot mediate ADCC and CDC as a result of reduced affinity of the Fc domain for the FcγRs and C1q [21,22]. It was hypothesized that the structural change of the Fc domain from "opened" to "closed" conformation upon removal of glycans ablates binding to FcγRs and C1q and abrogates ADCC and CDC [74]. Moreover, the degree of cell-mediated killing is sensitive to the composition of the glycans in the Fc region of the antibody [75].

Many studies have investigated the effect of each sugar component on the glycans. Even though other sugar residues (such as bisection of GlcNAc) may have affected the immune effector functions of the antibody, several studies have revealed that fucose has the most critical role in inhibiting ADCC activity [8]. The absence of fucose from the glycans on the Fc resulted in increased ADCC activity by improving FcγRIIIa binding [76]. Multiple strategies, including cell line engineering and chemical approaches, were taken to produce fucose-deficient glycoforms. In cell line engineering, earlier efforts established the use of Lec13 cells, a variant of Chinese hamster ovary (CHO) cells [77], and rat hybridoma YB2/0 cells [76], which produce low-fucose containing IgG1. Later, knockout CHO cell lines, lacking α-1,6-fucosyltransferase (FUT8), identified to be responsible for the core fucosylation of N-linked oligosaccharide [76], were constructed to produce completely de-fucosylated antibodies with fixed quality and consistently enhanced ADCC activity [78].

Furthermore, other approaches were taken to produce uniform glycoforms of human IgG. Li *et al*. reported novel expression systems using engineered *Pichia pastoris* cell lines, which can perform specific human N-glycosylation reactions with high fidelity [75]. Not only was a library of uniform glycoforms of the anti-CD20 rituximab produced, but these yeast glycoforms, especially

ones lacking fucose, exhibit higher binding affinity to the activating receptor FcγRIIIa, while retaining similar or lower binding affinity to the inhibitory receptor FcγRIIb, as compared to those expressed in mammalian cells [75].

An alternative strategy to produce a uniform glycosylation pattern on antibodies is to chemically modify the glycosylation site. Two interesting approaches have been reported: (1) replacing the Asn297, the natural glycosylation site, with a cysteine residue and then ligating a synthetic oligosaccharide by an asymmetric disulfide conjugation [79]; and (2) performing *in vitro* chemoenzymatic glycosylation based on the transglycosylation activity of endo-β-*N*-acetylglucosaminidases (ENGases) [80]. These two approaches can thus be used to append any glycoform of interest, including ADCC-enhanced ones.

1.4 Alternative Antibody-Based Platforms

The modular nature of immunoglobulins renders the possibility of using each fragment for "customized" therapeutics, with pharmacologic properties optimized for specific applications [81]. Thus, half-life, distribution, valency, affinity, avidity, tissue penetration, and bioactivities could each be controlled by selection of appropriate molecular domains or defined genetic features [81]. Fab can be used on its own, leading to the specific binding properties. Similarly, the Fc may also be fused with other molecules or even used on its own in some applications, such as intravenous immunoglobulin (IVIG) treatment. In this section, we present alternative therapeutic platforms to mAbs, extracting the advantages of each modular domain of an antibody.

1.4.1 Fab, scFv, and nanobodies

Since the specificity of mAbs lies entirely at the CDRs or antigen binding sites in the Fab fragment, the Fc portion may not be necessary in the design of therapeutics that only require the binding event, such as those for ligand sequestration or receptor blockade. The smaller size of fragments may permit cheaper, faster production in microbial systems. However, the lack of Fc and also the smaller size lead to a shorter serum half-life. Even though this property may be useful in other applications, such as imaging, which requires faster clearance of the agents, this section will focus on the use of these fragments as therapeutics. The first Fab therapeutic that received approval was abciximab, an anti-GPIIb/IIIa chimeric Fab [81]. Recently, two more have been approved: ranibizumab (in 2006), an anti-VEGF-A humanized Fab, and certolizumab pegol (in 2008), an anti-TNFα pegylated humanized Fab [81]. For the latter, polyethyleneglycol (PEG) was conjugated to Fab to extend the circulation half-life of the construct.

Other platforms were also developed to shrink the Fab to its core binding modality. The variable regions of light and heavy immunoglobulin chains encoding antigen-binding domains are engineered into a single polypeptide, called single-chain variable fragments (scFvs). Generally, the V_H and V_L sequences are joined by a flexible linker sequence, and a series of variants are generated for optimizing binding affinity and stability [82]. Further attempts to remove domains deemed non-essential for function or to reduce the size of the mAbs resulted in the "nanobodies," which were derived from the antigen-binding variable heavy chain regions (VHHs) of heavy chain antibodies found in camels and llamas [83,84]. These antibodies naturally lack light chains; thus only the CDRs of heavy chains in these species were necessary for the high binding affinity and specificity [83,84].

1.4.2 Fc fusions

Fc fusion proteins are molecules in which the immunoglobulin Fc is fused genetically to a protein of interest, such as an extracellular domain of a receptor, ligand, enzyme, or peptide. The fusion strategy has been invented in order to equip the protein with the favorable attributes of the Fc domains, including the prolongation of serum half-life through FcRn interaction [23], the increase in size limiting renal clearance [85], Fc dependent effector functions [86], and in some cases, improved biophysical properties of its fusion partner [87,88]. Moreover, the Fc may also contribute to several manufacturing advantages, such as high expression, secretion to cell culture medium, and protein A affinity purification of Fc fusion proteins [87]. To date, seven Fc fusion proteins have been approved by the FDA as summarized in Table 1.2. Six of these are receptors fused to Fc, while romiplostim is the only peptide-Fc fusion that has been approved thus far. Most of these Fc-fusions target receptor-ligand interactions, working either as antagonists to block receptor binding (e.g., etanercept, aflibercept, rilonacept, belatacept, abatacept) or as agonists to directly stimulate receptor function to reduce (e.g., alefacept) or increase immune activity (e.g., romiplostim) [89]. Besides therapeutics, Fc-fusion proteins may also be used in other applications, such as vaccines and research tools [89].

Table 1.2. Approved Fc-fusion proteins (Table adapted from Ref. [10],[87])

Generic name (trade name)	Fusion Protein	Target	Mechanisms of Action	Approved indication
Etanercept (Enbrel)	p75 TNFαR	TNF-α	TNF-α inhibitors	RA, JIA, PA, AS, plaque psoriasis
Alefacept (Amevive)	LFA-3	CD2	CD2 antigen inhibitors	Plaque psoriasis
Abatacept (Orencia)	CTLA-4	CD80 and CD86	T cell activation inhibitors	RA and JIA
Romiplostim (Nplate)	Thrombopoietin receptor -binding peptide	Thrombopoietin receptor	Activation of thrombopoietin receptor	Thrombocytopaenia in patients with idiopathic thrombocytopaenic purpura
Rilonacept (Arcalyst)	Binding domains of IL-1R and IL-1RacP	IL-1	IL-1 inhibitors	CAPS
Aflibercept (Eylea)	2nd domain of VEGFR1 and 3rd domain of VFGFR2	VEGF-A and PGF	Angiogenesis inhibitors	Wet macular degeneration
Belatacept (Nulojix)	Mutated CTLA-4	CD80 and CD86	T cell activation inhibitors	Prophylaxis of organ rejection

AS, ankylosing spondylitis; CAPS, cryopyrin-associated periodic syndrome; CD, cluster of differentiation; CTLA4, cytotoxic T lymphocyte antigen-4; IL-1R, Interleukin-1 receptor; IL-1RacP, interleukin-1 receptor accessory protein; JIA, juvenile idiopathic arthritis; LFA-3, lymphocyte function-associated antigen 3; PA, psoriatic arthritis; PGF, placental growth factor; RA, rheumatoid arthritis; TNFαR, tumor necrosis factor α receptor; VEGF-A, vascular endothelial growth factor A

1.4.3 Peptide scaffolds

Over the past few years, a number of alternative scaffolds to antibodies have been designed as new binding proteins [90]. The development of new technologies for selection and evolution from libraries independent of the antibody scaffold has also enabled the finding of these new platforms. Even though high affinity and specificity can be achieved by both antibody and the alternative platforms presented here, other desired properties of engineered affinity proteins make it appealing to discover non-immuglobulin alternatives. Some of the benefits that these molecules may possess include (1) small size, enabling efficient tissue penetration; (2) designed pharmacokinetic properties appropriate for the application (rapid clearance for imaging agents and prolonged half-life for protein drugs); (3) tunable biophysical properties (rapid folding and high chemical, proteolytic and thermal stability); (4) absence of cysteines; (5) cost-efficient production by chemical synthesis or recombinant methods; and (6) flexible engineering for conjugation to other mol-

ecules and generation of bispecific or multispecific constructs [91]. A few of the most important examples are based on either natural protein scaffolds or entirely new designed scaffolds.

Repeat proteins are characterized by small, repeating structural motifs of 20–50 amino acids, important for many protein-protein interactions [90]. In some species, repeat proteins are used in nature instead of antibodies. For example, in jawless vertebrates, the adaptive immune system is based on leucine-rich repeat (LRR) family, instead of the immunoglobulin fold [92]. The major motifs include 2-3 helix repeats, as seen in HEAT (αRep), Armadillo, TPR, and Ankyrin (Table 1.3). Among many scaffolds of repeat proteins, designed ankyrin repeat proteins (DARPins), which has helix-turn-helix-β-hairpin motif, have gained much traction in potential use for therapeutics, such as viral retargeting to tumors and as the targeting moiety for a payload [90]. In order to increase the stability of these repeat proteins, several approaches have been undertaken, including stapled peptides [93-95], D-peptides [96], and α/β peptides [97].

Besides repeat proteins, affibodies, adnectins, anticalins, and knottins form the other subset of non-immunoglobulin alternatives, based-on natural scaffolds (Table 1.3) [91]. These molecules are derived from domain B of staphylococcal protein A, human 10^{th} fibronectin domain, lipocalin, and cysteine knot peptides, respectively [91]. These scaffolds all contain different structural motifs as summarized in Table 1.3. Apart from natural scaffolds, novel designed scaffolds, such as cyclic peptides or bicyclic peptides [98], also offer alternatives for the protein binders. The smaller size and synthetic control of these peptide scaffolds are advantageous.

Table 1.3. Alternative scaffolds to antibodies (Table adapted from Ref. [90],[91])

Protein Scaffold	Origin	Structural Motif	Length (Aa)
Repeat protein scaffold			
HEAT (aRep)	Huntingtin, elongation factor 3 (EF3), subunit A of phosphatase 2A (PP2A), yeast PI3-kinase TOR1	Two α-helices	31
Armadillo (ARM)	Product of the *Drosophila melanogaster* segmentation polarity gene Armadillo	Three α-helices	42
tetratricopeptide (TPR)	Yeast cell division control protein 23 (CDC23)	Helix-turn-helix	34
Ankyrin (DARPin)	Repeated sequence in yeast cell-cycle regulation	Helix-turn-helix-β-hairpin	33
Non-repeat protein scaffold			
Affibody molecules	Protein A domain	Three helical bundle	58
Adnectins/monobodies	^{10}Fn3	β-sandwich structure connected by six loops	94
Anticalins	Lipocalin	β-barrel structure containing four loops	170
Knottins/microproteins	Cysteine knot peptides	Three antiparallel β-strands connected by three disulfide bonds	30

1.4.4 Bispecific antibodies

Bispecific antibodies (bsAb) present another antibody-based platform that combines the benefits of two antibodies into one agent. Complex diseases, such as cancer or inflammatory disorders, can easily develop resistance to a treatment. Due to a redundancy of disease-mediating ligands and receptors, as well as crosstalk between signal cascades, blockade of one signaling pathway may result in upregulation of another with the same action [99]. Blockade of multiple pathways or receptor-ligand interactions simultaneously can be achieved by combination therapy,

which has been shown to help improve the therapeutic efficacy [100]. During the past decade, dual targeting with bispecific antibodies has emerged as an alternative to combination therapy. The concept of dual targeting with bispecific antibodies is based on the targeting of multiple disease-modifying molecules with one drug. From a technological and regulatory perspective, the concept of targeting multiple disease-modifying molecules with one drug makes development and treatment less complex [99]. The manufacturing, preclinical and clinical testing, and treatment regimen are reduced to a single, bispecific molecule.

Dual targeting strategies can be divided into two routes: (1) targeting two receptor-ligand interactions and (2) retargeting effector molecules or effector cells [99,101]. The former may include binding of bsAb to two receptors, one receptor-one ligand, two ligands, or two epitopes on one receptors or ligands simultaneously. In the latter, effort has been put in the retargeting of T cells by binding to CD3, which is part of the T cell receptor complex, or of natural killer (NK) cells by binding to the FcγRIII (CD16) [102-104]. These bispecific, as well as multispecific, antibodies can be produced using various approaches, including assembly of two mAbs, chemical crosslinking, and recombinant fusion of scFvs to each other or to the N- and/or C-terimini of IgG [99,101].

First, the assembly of two mAbs can be achieved via expression in quadromas, i.e., hybrid-hybridromas, or via engineering of the constant regions to promote asymmetric assembly of heavy chains from two different mAbs. Such strategies includes (1) knobs-into-holes, where the contact site between the C_H3 domains are substituted by larger or smaller residues [105,106], (2) charge pair strategy, where charged residues of the C_H3 domain interface were engineered in order to introduce an electrostatic steering effect [107], and (3) strand-exchange engineered domain technology (SEEDbody) with C_H3 sequences composed of alternating segments from human IgA and IgG [108]. Second, the chemical crosslinking approaches have been devised from the use of homo- or hetero-bifunctional coupling reagents or the CovX-Body platform, which comprises a catalytic IgG molecule covalently coupled to a branched peptides targeting two different antigens [109,110]. Third, the scFv-based bispecific platform emerged from the generation of tandem scFVs [111,112] or the fusion of scFv molecules to the N-terminus and the C-terminus of the heavy or light chain of a mAb [113-115]. One of the most successful strategies was the "bispecific T-cell engager" (BiTE) antibodies, which is a combination of anti-CD3 scFV and tumor specific scFv [112].

1.4.5 Antibody-drug conjugates (ADCs)

To improve the cytotoxicity of mAbs, toxins have been conjugated to the mAbs. In this way, mAbs are used to deliver these cytotoxic agents to specific targets. The concept of conjugating an antibody to a cytotoxic agent to produce a synergistic effect has been around for decades, but early products faced technological, targeting, and potency issues that did not allow integrity of the antibody to be maintained [116,117]. The recent approval of brentuximab vedotin [118] and trastuzumab emtansine [119] have ushered in a renaissance in the popularity of ADCs. Many more are in clinical trials and development. To achieve optimal efficacy, each component of ADCs has to contain the following characteristics [9,116,117]:

(1) The target antigen is expressed at high level in the malignant cells as compared to normal cells.

(2) The mAb is internalized following binding and has minimal non-specific binding.

(3) Conjugation sites do not impact stability, binding, internalization, and pharmacokinetics. The heterogeneity of the conjugates is controlled.

(4) The linker is stable in circulation.

(5) The cytotoxic drug is highly potent such that two to four molecules are sufficient, and it is amenable to modification. The drug is stable in circulation and in lysosomes and non-immunogenic.

Here, we will focus on the modification of the mAbs. The most common approach is to modify the lysine or the cysteine (from reduced interchain disulfide bonds) residues, yielding non-site-selective modification. Recently a few studies have shown that sites of conjugation, as well as number of drugs per mAbs, play important roles in efficacy of ADCs [120]. To control the number and site of conjugation, the solvent-accessible cysteines that form the interchain disulfide bonds were replaced with serine, to reduce the eight potential conjugation sites down to 4 or 2 [121]. Various other efforts have also established site-selective modification of mAbs. The thiomabs from Genentech achieve site selectivity by introducing additional Cys residues to the heavy or light chains [122,123]. Upon mild reduction (without reducing endogenous disulfide bonds), two drug molecules per mAbs can be conjugated via maleimide chemistry. Schultz and co-workers introduced the nonnative amino acid *p*-acetylphenylalanine to a specific site for conjugation using oxime formation [124].

1.5 Conclusions

The importance of monoclonal antibodies as therapeutics has been proven over the past several decades. More than 20 antibodies have already been approved for the use in clinical setting, and hundreds more are in clinical trials, making antibodies one of the fastest growing class of biologics. Antibodies possess multiple attractive therapeutic properties, including high specificity and affinity to target ligands or receptors, immune effector functions, and long plasma half-lives. Advances in protein engineering and glycoengineering have reduced immunogenicity, improved binding properties, and enhanced the cytotoxic effects of these molecules. Moreover, antibody fragments, alternative binding scaffolds, and other novel antibody-based platforms, such as bispecific antibodies, ADCs, and Fc fusions, have been developed. In the following chapters, we present our development of Fc-synthetic molecule hybrids and mAb-synthetic molecule hybrids as an alternative antibody-based platform for cancer therapeutic applications. Furthermore, we demonstrate the use of antibodies for the generation of targeted MS2 viral capsids for various applications, including mass cytometry and *in vivo* imaging.

1.6 References

1. Strebhardt, K.; Ullrich, A. *Nat. Rev. Cancer* **2008**, *8*, 473–480.
2. Köhler, G.; Milstein, C. *Nature* **1975**, *256*, 495–497.
3. Weiner, L. M.; Surana, R.; Wang, S. *Nat. Rev. Immunol*. **2010**, *10*, 317–327.
4. Morrison, S. L.; Johnson, M. J.; Herzenberg, L. A.; Oi, V. T. *Proc. Natl. Acad. Sci. U. S. A*. **1984**, *81*, 6851–6855.
5. Jones, P. T.; Dear, P. H.; Foote, J.; Neuberger, M. S.; Winter, G. *Nature* **1986**, *321*, 522–525.
6. Tomizuka, K.; Yoshida, H.; Uejima, H.; Kugoh, H.; Sato, K.; Ohguma, A.; Hayasaka, M.; Hanaoka, K.; Oshimura, M.; Ishida, I. *Nat. Genet*. **1997**, *16*, 133–143.
7. Mendez, M. J.; Green, L. L.; Corvalan, J. R.; Jia, X. C.; Maynard-Currie, C. E.; Yang, X. D.; Gallo, M. L.; Louie, D. M.; Lee, D. V; Erickson, K. L.; Luna, J.; Roy, C. M.; Abderrahim, H.; Kirschenbaum, F.; Noguchi, M.; Smith, D. H.; Fukushima, A.; Hales, J. F.; Klapholz, S.; Finer, M. H.; Davis, C. G.; Zsebo, K. M.; Jakobovits, A. *Nat. Genet*. **1997**, *15*, 146–156.
8. Kubota, T.; Niwa, R.; Satoh, M.; Akinaga, S.; Shitara, K.; Hanai, N. *Cancer Sci*. **2009**, *100*, 1566–1572.
9. Trail, P. *Antibodies* **2013**, *2*, 113–129.
10. Jiang, X.-R.; Song, A.; Bergelson, S.; Arroll, T.; Parekh, B.; May, K.; Chung, S.; Strouse, R.; Mire-Sluis, A.; Schenerman, M. *Nat. Rev. Drug Discov*. **2011**, *10*, 101–111.
11. Carter, P. J. *Nat. Rev. Immunol*. **2006**, *6*, 343–357.
12. Scott, A. M.; Wolchok, J. D.; Old, L. J. *Nat. Rev. Cancer* **2012**, *12*, 278–287.
13. Mizuochi, T.; Taniguchi, T.; Shimizu, A.; Kobata, A. *J. Immunol.* **1982**, *129*, 2016–2020.
14. Harada, H.; Kamei, M.; Tokumoto, Y.; Yui, S.; Koyama, F.; Kochibe, N.; Endo, T.; Kobata, A. *Anal. Biochem*. **1987**, *164*, 374–381.
15. Jefferis, R.; Lund, J. *Immunol. Lett*. **2002**, *82*, 57–65.
16. Iannello, A.; Ahmad, A. *Cancer Metastasis Rev*. **2005**, *24*, 487-499.
17. Gelderman, K. A.; Tomlinson, S.; Ross, G. D.; Gorter, A. *Trends in Immunology* **2004**, *25*, 158–164.
18. Shields, R. L.; Namenuk, A. K.; Hong, K.; Meng, Y. G.; Rae, J.; Briggs, J.; Xie, D.; Lai, J.; Stadlen, A.; Li, B.; Fox, J. A.; Presta, L. G. *J. Biol. Chem*. **2001**, *276*, 6591–6604.
19. Clynes, R. A.; Towers, T. L.; Presta, L. G.; Ravetch, J. V. *Nat. Med*. **2000**, *6*, 443–446.
20. Radaev, S.; Motyka, S.; Fridman, W. H.; Sautes-Fridman, C.; Sun, P. D. *J. Biol. Chem*. **2001**, 276, 16469–16477.
21. Jefferis, R. *Nat. Rev. Drug Discov*. **2009**, *8*, 226–234.
22. Shade, K.-T.; Anthony, R. *Antibodies* **2013**, *2*, 392–414.
23. Roopenian, D. C.; Akilesh, S. *Nat. Rev. Immunol*. **2007**, *7*, 715–725.

24. Ghetie, V.; Ward, E. S. *Ann. Rev. Immunol.* **2000**, *18*, 739–766.

25. Graham, J.; Muhsin, M.; Kirkpatrick, P. *Nat. Rev. Drug Discov*. **2004**, *3*, 549–550.

26. Li, S.; Schmitz, K. R.; Jeffrey, P. D.; Wiltzius, J. J. W.; Kussie, P.; Ferguson, K. M. *Cancer Cell* **2005**, *7*, 301–311.

27. Kim, R. *Lancet Oncol*. **2009**, *10*, 1140–1141.

28. Ramakrishnan, M. S.; Eswaraiah, A.; Crombet, T.; Piedra, P.; Saurez, G.; Iyer, H.; Arvind, A. S. *MAbs* **2009***, 1*, 41–48.

29. Kuenen, B.; Witteveen, P. O.; Ruijter, R.; Giaccone, G.; Dontabhaktuni, A.; Fox, F.; Katz, T.; Youssoufian, H.; Zhu, J.; Rowinsky, E. K.; Voest, E. E. *Clin. Cancer Res*. **2010**, *16*, 1915–1923.

30. Li, D.; Ji, H.; Zaghlul, S.; McNamara, K.; Liang, M.-C.; Shimamura, T.; Kubo, S.; Takahashi, M.; Chirieac, L. R.; Padera, R. F.; Scott, A. M.; Jungbluth, A. A.; Cavenee, W. K.; Old, L. J.; Demetri, G. D.; Wong, K.-K. *J. Clin. Invest*. **2007**, *117*, 346–352.

31. Scott, A. M.; Lee, F.-T.; Tebbutt, N.; Herbertson, R.; Gill, S. S.; Liu, Z.; Skrinos, E.; Murone, C.; Saunder, T. H.; Chappell, B.; Papenfuss, A. T.; Poon, A. M. T.; Hopkins, W.; Smyth, F. E.; MacGregor, D.; Cher, L. M.; Jungbluth, A. A.; Ritter, G.; Brechbiel, M. W.; Murphy, R.; Burgess, A. W.; Hoffman, E. W.; Johns, T. G.; Old, L. J. *Proc. Natl. Acad. Sci. U. S. A*. **2007**, *104*, 4071–4076.

32. Gan, H. K.; Lappas, M.; Cao, D. X.; Cvrljevdic, A.; Scott, A. M.; Johns, T. G. *J. Cell. Mol. Med*. **2009**, *13*, 3993–4001.

33. Slamon, D. J.; Godolphin, W.; Jones, L. a; Holt, J. a; Wong, S. G.; Keith, D. E.; Levin, W. J.; Stuart, S. G.; Udove, J.; Ullrich, A. *Science* **1989**, *244*, 707–712.

34. Ménard, S.; Casalini, P.; Campiglio, M.; Pupa, S.; Agresti, R.; Tagliabue, E. *Ann. Oncol.* **2001**, *12*, S15–S19.

35. Chen, J.-S.; Lan, K.; Hung, M.-C. *Drug Resist. Updat*. **2003**, *6*, 129–136.

36. Molina, M. A.; Codony-Servat, J.; Albanell, J.; Rojo, F.; Arribas, J.; Baselga, J. *Cancer Res*. **2001**, *61*, 4744–4749.

37. Mimura, K.; Kono, K.; Hanawa, M.; Kanzaki, M.; Nakao, A.; Ooi, A.; Fujii, H. *Clin. Cancer Res*. **2005**, *11*, 4898–4904.

38. Valabrega, G.; Montemurro, F.; Aglietta, M. *Ann. Oncol*. **2007**, *18*, 977–984.

39. Austin, C. D.; De Mazière, A. M.; Pisacane, P. I.; van Dijk, S. M.; Eigenbrot, C.; Sliwkowski, M. X.; Klumperman, J.; Scheller, R. H. *Mol. Biol. Cell* **2004**, *15*, 5268–5282.

40. Hudis, C. A. *New Engl. J. Med. Rev*. **2007**, *357*, 39–51.

41. Franklin, M. C.; Carey, K. D.; Vajdos, F. F.; Leahy, D. J.; de Vos, A. M.; Sliwkowski, M. X. *Cancer Cell* **2004**, *5*, 317–328.

42. Scheuer, W.; Friess, T.; Burtscher, H.; Bossenmaier, B.; Endl, J.; Hasmann, M. *Cancer Res*. **2009**, *69*, 9330–9336.

43. Keating, G. M. *Drugs* **2012**, *72*, 353–360.

44. Schoeberl, B.; Pace, E. A.; Fitzgerald, J. B.; Harms, B. D.; Xu, L.; Nie, L.; Linggi, B.; Kalra, A.; Paragas, V.; Bukhalid, R.; Grantcharova, V.; Kohli, N.; West, K. A.; Leszczyniecka, M.; Feldhaus, M. J.; Kudla, A. J.; Nielsen, U. B. *Sci. Signal.* **2009**, *2*, ra31.

45. Hollmén, M.; Määttä, J. A.; Bald, L.; Sliwkowski, M. X.; Elenius, K. *Oncogene* **2009**, *28*, 1309–1319.

46. Ellis, L. M.; Hicklin, D. J. *Nat. Rev. Cancer* **2008**, *8*, 579–591.

47. Wu, Y.; Zhong, Z.; Huber, J.; Bassi, R.; Finnerty, B.; Corcoran, E.; Li, H.; Navarro, E.; Balderes, P.; Jimenez, X.; Koo, H.; Mangalampalli, V. R. M.; Ludwig, D. L.; Tonra, J. R.; Hicklin, D. J. *Clin. Cancer Res*. **2006**, *12*, 6573–6584.

48. Shen, J.; Vil, M. D.; Prewett, M.; Damoci, C.; Zhang, H.; Li, H.; Jimenez, X.; Deevi, D. S.; Iacolina, M.; Kayas, A.; Bassi, R.; Persaud, K.; Rohoza-Asandi, A.; Balderes, P.; Loizos, N.; Ludwig, D. L.; Tonra, J.; Witte, L.; Zhu, Z. *Neoplasia* **2009**, *11*, 594–604.

49. Shen, J.; Vil, M. D.; Zhang, H.; Tonra, J. R.; Rong, L. L.; Damoci, C.; Prewett, M.; Deevi, D. S.; Kearney, J.; Surguladze, D.; Jimenez, X.; Iacolina, M.; Bassi, R.; Zhou, K.; Balderes, P.; Mangalampalli, V. R. M.; Loizos, N.; Ludwig, D. L.; Zhu, Z. *Biochem. Biophys. Res. Commun.* **2007**, *357*, 1142–1147.

50. Rabinovich, G. A.; Gabrilovich, D.; Sotomayor, E. M. *Annu. Rev. Immunol*. **2007**, *25*, 267–296.

51. Arteaga, C. L. *Curr. Opin. Genet. Dev*. **2006**, *16*, 30–37.

52. Leach, D. R.; Krummel, M. F.; Allison, J. P. *Science* **1996**, *271*, 1734–1736.

53. Khalil, M.; Vonderheide, R. H. *Update Cancer Ther*. **2007**, *2*, 61–65.

54. Murphy, K. P.; Travers, P.; Walport, M.; Janeway, C. *Janeway's immunobiology.* **2008**. Garland Science.

55. Lazar, G. A.; Dang, W.; Karki, S.; Vafa, O.; Peng, J. S.; Hyun, L.; Chan, C.; Chung, H. S.; Eivazi, A.; Yoder, S. C.; Vielmetter, J.; Carmichael, D. F.; Hayes, R. J.; Dahiyat, B. I. *Proc. Natl. Acad. Sci. U. S. A*. **2006**, *103*, 4005–4010.

56. Cartron, G. *Blood* **2002**, *99*, 754–758.

57. Weng, W.-K.; Levy, R. *J. Clin. Oncol*. **2003**, *21*, 3940–3947.

58. Musolino, A.; Naldi, N.; Bortesi, B.; Pezzuolo, D.; Capelletti, M.; Missale, G.; Laccabue, D.; Zerbini, A.; Camisa, R.; Bisagni, G.; Neri, T. M.; Ardizzoni, A. *J. Clin. Oncol*. **2008**, *26*, 1789–1796.

59. Bibeau, F.; Lopez-Crapez, E.; Di Fiore, F.; Thezenas, S.; Ychou, M.; Blanchard, F.; Lamy, A.; Penault-Llorca, F.; Frébourg, T.; Michel, P.; Sabourin, J.-C.; Boissière-Michot, F. *J. Clin. Oncol.* **2009**, *27*, 1122–1129.

60. Oflazoglu, E.; Stone, I. J.; Brown, L.; Gordon, K. A.; van Rooijen, N.; Jonas, M.; Law, C.-L.; Grewal, I. S.; Gerber, H.-P. *Br. J. Cancer* **2009**, *100*, 113–117.

61. Petricevic, B.; Laengle, J.; Singer, J.; Sachet, M.; Fazekas, J.; Steger, G.; Bartsch, R.; Jensen-Jarolim, E.; Bergmann, M. *J. Transl. Med*. **2013**, *11*, 307.

62. Richards, J. O.; Karki, S.; Lazar, G. A.; Chen, H.; Dang, W.; Desjarlais, J. R. *Mol. Cancer Ther*. **2008**, *7*, 2517–2527.

63. Tedder, T. F.; Baras, A.; Xiu, Y. *Springer Semin. Immunopathol*. **2006**, *28*, 351–364.

64. Di Gaetano, N.; Cittera, E.; Nota, R.; Vecchi, A.; Grieco, V.; Scanziani, E.; Botto, M.; Introna, M.; Golay, J. *J. Immunol*. **2003**, *171*, 1581–1587.

65. Cragg, M. S.; Glennie, M. J. *Blood* **2004**, *103*, 2738–2743.

66. Coiffier, B.; Lepretre, S.; Pedersen, L. M.; Gadeberg, O.; Fredriksen, H.; van Oers, M. H. J.; Wooldridge, J.; Kloczko, J.; Holowiecki, J.; Hellmann, A.; Walewski, J.; Flensburg, M.; Petersen, J.; Robak, T. *Blood* **2008**, *111*, 1094–1100.

67. Zent, C. S.; Secreto, C. R.; LaPlant, B. R.; Bone, N. D.; Call, T. G.; Shanafelt, T. D.; Jelinek, D. F.; Tschumper, R. C.; Kay, N. E. *Leuk. Res.* **2008**, *32*, 1849–1856.

68. Cartron, G.; Watier, H.; Golay, J.; Solal-Celigny, P. *Blood* **2004**, *104*, 2635–2642.

69. Selenko, N.; Majdic, O.; Jäger, U.; Sillaber, C.; Stöckl, J.; Knapp, W. *J. Clin. Immunol*. **2002**, *22*, 124–130.

70. Rafiq, K.; Bergtold, A.; Clynes, R. *J. Clin. Invest*. **2002**, *110*, 71–79.

71. Dhodapkar, K. M.; Krasovsky, J.; Williamson, B.; Dhodapkar, M. V. *J. Exp. Med*. **2002**, *195*, 125–133.

72. Sondermann, P.; Huber, R.; Oosthuizen, V.; Jacob, U. *Nature* **2000**, *406*, 267–273.

73. Stavenhagen, J. B.; Gorlatov, S.; Tuaillon, N.; Rankin, C. T.; Li, H.; Burke, S.; Huang, L.; Johnson, S.; Koenig, S.; Bonvini, E. *Adv. Enzyme Regul*. **2008**, *48*, 152–164.

74. Feige, M. J.; Nath, S.; Catharino, S. R.; Weinfurtner, D.; Steinbacher, S.; Buchner, J. *J. Mol. Biol*. **2009**, *391*, 599–608.

75. Li, H.; Sethuraman, N.; Stadheim, T. A.; Zha, D.; Prinz, B.; Ballew, N.; Bobrowicz, P.; Choi, B.-K.; Cook, W. J.; Cukan, M.; Houston-Cummings, N. R.; Davidson, R.; Gong, B.; Hamilton, S. R.; Hoopes, J. P.; Jiang, Y.; Kim, N.; Mansfield, R.; Nett, J. H.; Rios, S.; Strawbridge, R.; Wildt, S.; Gerngross, T. U. *Nat. Biotechnol*. **2006**, *24*, 210–215.

76. Shinkawa, T.; Nakamura, K.; Yamane, N.; Shoji-Hosaka, E.; Kanda, Y.; Sakurada, M.; Uchida, K.; Anazawa, H.; Satoh, M.; Yamasaki, M.; Hanai, N.; Shitara, K. *J. Biol. Chem*. **2003**, *278*, 3466–3473.

77. Shields, R. L.; Lai, J.; Keck, R.; O'Connell, L. Y.; Hong, K.; Meng, Y. G.; Weikert, S. H. A.; Presta, L. G. *J. Biol. Chem*. **2002**, *277*, 26733–26740.

78. Yamane-Ohnuki, N.; Kinoshita, S.; Inoue-Urakubo, M.; Kusunoki, M.; Iida, S.; Nakano, R.; Wakitani, M.; Niwa, R.; Sakurada, M.; Uchida, K.; Shitara, K.; Satoh, M. *Biotechnol. Bioeng*. **2004**, *87*, 614–622.

79. Watt, G. M.; Lund, J.; Levens, M.; Kolli, V. S. K.; Jefferis, R.; Boons, G.-J. *Chem. Biol.* **2003**,

10, 807–814.

80. Wei, Y.; Li, C.; Huang, W.; Li, B.; Strome, S.; Wang, L.-X. *Biochemistry* **2008**, *47*, 10294–10304.
81. Nelson, A. L. *MAbs* **2010**, *2*, 77–83.
82. Bird, R. E.; Hardman, K. D.; Jacobson, J. W.; Johnson, S.; Kaufman, B. M.; Lee, S. M.; Lee, T.; Pope, S. H.; Riordan, G. S.; Whitlow, M. *Science* **1988**, *242*, 423–426.
83. Harmsen, M. M.; De Haard, H. J. *Appl. Microbiol. Biotechnol*. **2007**, *77*, 13–22.
84. Muyldermans, S. *Annu. Rev. Biochem.* **2013**, *82*, 775–797.
85. Kontermann, R. E. *Curr. Opin. Biotechnol*. **2011**, *22*, 868–876.
86. Nimmerjahn, F.; Ravetch, J. V. *Methods Mol. Biol*. **2008**, *415*, 151–162.
87. Huang, C. *Curr. Opin. Biotechnol*. **2009**, *20*, 692–699.
88. Carter, P. *J. Exp. Cell Res*. **2011**, *317*, 1261–1269.
89. Czajkowsky, D. M.; Hu, J.; Shao, Z.; Pleass, R. *J. EMBO Mol. Med*. **2012**, *4*, 1015–1028.
90. Boersma, Y. L.; Plückthun, A. *Curr. Opin. Biotechnol.* **2011**, *22*, 849–857.
91. Löfblom, J.; Frejd, F. Y.; Ståhl, S. *Curr. Opin. Biotechnol*. **2011**, *22*, 843–848.
92. Pancer, Z.; Cooper, M. D. *Annu. Rev. Immunol*. **2006**, *24*, 497–518.
93. Schafmeister, C. E.; Po, J.; Verdine, G. L. *J. Am. Chem. Soc.* **2000**, *122*, 5891–5892.
94. Walensky, L. D.; Kung, A. L.; Escher, I.; Malia, T. J.; Barbuto, S.; Wright, R. D.; Wagner, G.; Verdine, G. L.; Korsmeyer, S. J. *Science.* **2004**, *305*, 1466–1470.
95. Verdine, G. L.; Hilinski, G. J. *Meth. Enzymology*. **2012**, *503*, 3–33.
96. Zhao, L.; Lu, W. *Isr. J. Chem*. **2011**, *51*, 868–875.
97. Johnson, L. M.; Gellman, S. H. *Meth. Enzymology*. **2013**, *523*, 407–429.
98. Heinis, C.; Rutherford, T.; Freund, S.; Winter, G. *Nat. Chem. Biol.* **2009**, *5*, 502–507.
99. Kontermann, R. *MAbs* **2012**, *4*, 182–197.
100. Demarest, S. J.; Hariharan, K.; Dong, J. *MAbs* **2011**, *3*, 338–351.
101. Müller, D.; Kontermann, R. E. *BioDrugs* **2010**, *24*, 89–98.
102. Mack, M.; Riethmuller, G.; Kufer, P. *Proc. Natl. Acad. Sci*. **1995**, *92*, 7021–7025.
103. Bargou, R.; Leo, E.; Zugmaier, G.; Klinger, M.; Goebeler, M.; Knop, S.; Noppeney, R.; Viardot, A.; Hess, G.; Schuler, M.; Einsele, H.; Brandl, C.; Wolf, A.; Kirchinger, P.; Klappers, P.; Schmidt, M.; Riethmüller, G.; Reinhardt, C.; Baeuerle, P. A.; Kufer, P. *Science* **2008**, *321*, 974–977.
104. Kügler, M.; Stein, C.; Kellner, C.; Mentz, K.; Saul, D.; Schwenkert, M.; Schubert, I.; Singer, H.; Oduncu, F.; Stockmeyer, B.; Mackensen, A.; Fey, G. H. *Br. J. Haematol*. **2010**, *150*, 574–586.

105. Carter, P. *J. Immunol. Methods* **2001**, *248*, 7–15.

106. Merchant, A. M.; Zhu, Z.; Yuan, J. Q.; Goddard, A.; Adams, C. W.; Presta, L. G.; Carter, P. *Nat. Biotechnol*. **1998**, *16*, 677–681.

107. Gunasekaran, K.; Pentony, M.; Shen, M.; Garrett, L.; Forte, C.; Woodward, A.; Ng, S. Bin; Born, T.; Retter, M.; Manchulenko, K.; Sweet, H.; Foltz, I. N.; Wittekind, M.; Yan, W. *J. Biol. Chem*. **2010**, *285*, 19637–19646.

108. Davis, J. H.; Aperlo, C.; Li, Y.; Kurosawa, E.; Lan, Y.; Lo, K.-M.; Huston, J. S. *Protein Eng. Des. Sel.* **2010**, *23*, 195–202.

109. Graziano, R. F.; Guptill, P. *Methods Mol. Biol*. **2004**, *283*, 71–85.

110. Doppalapudi, V. R.; Huang, J.; Liu, D.; Jin, P.; Liu, B.; Li, L.; Desharnais, J.; Hagen, C.; Levin, N. J.; Shields, M. J.; Parish, M.; Murphy, R. E.; Del Rosario, J.; Oates, B. D.; Lai, J.-Y.; Matin, M. J.; Ainekulu, Z.; Bhat, A.; Bradshaw, C. W.; Woodnutt, G.; Lerner, R. A.; Lappe, R. W. *Proc. Natl. Acad. Sci. U. S. A*. **2010**, *107*, 22611–22616.

111. Holliger, P.; Prospero, T.; Winter, G. *Proc. Natl. Acad. Sci. U. S. A*. **1993**, *90*, 6444–6448.

112. Baeuerle, P. A.; Reinhardt, C. *Cancer Res*. **2009**, *69*, 4941–4944.

113. Dong, J.; Sereno, A.; Snyder, W. B.; Miller, B. R.; Tamraz, S.; Doern, A.; Favis, M.; Wu, X.; Tran, H.; Langley, E.; Joseph, I.; Boccia, A.; Kelly, R.; Wortham, K.; Wang, Q.; Berquist, L.; Huang, F.; Gao, S. X.; Zhang, Y.; Lugovskoy, A.; Martin, S.; Gouvis, H.; Berkowitz, S.; Chiang, G.; Reff, M.; Glaser, S. M.; Hariharan, K.; Demarest, S. J. *J. Biol. Chem*. **2011**, *286*, 4703–4717.

114. Orcutt, K. D.; Ackerman, M. E.; Cieslewicz, M.; Quiroz, E.; Slusarczyk, A. L.; Frangioni, J. V; Wittrup, K. D. *Protein Eng. Des. Sel*. **2010**, *23*, 221–228.

115. Coloma, M. J.; Morrison, S. L. *Nat. Biotechnol*. **1997**, *15*, 159–163.

116. Hughes, B. *Nat. Rev. Drug Discov*. **2010**, *9*, 665–667.

117. Zolot, R. S.; Basu, S.; Million, R. P. *Nat. Rev. Drug Discov*. **2013**, *12*, 259–260.

118. Doronina, S. O.; Toki, B. E.; Torgov, M. Y.; Mendelsohn, B. A.; Cerveny, C. G.; Chace, D. F.; DeBlanc, R. L.; Gearing, R. P.; Bovee, T. D.; Siegall, C. B.; Francisco, J. A.; Wahl, A. F.; Meyer, D. L.; Senter, P. D. *Nat. Biotechnol*. **2003**, *21*, 778–784.

119. Lewis Phillips, G. D.; Li, G.; Dugger, D. L.; Crocker, L. M.; Parsons, K. L.; Mai, E.; Blättler, W. A.; Lambert, J. M.; Chari, R. V. J.; Lutz, R. J.; Wong, W. L. T.; Jacobson, F. S.; Koeppen, H.; Schwall, R. H.; Kenkare-Mitra, S. R.; Spencer, S. D.; Sliwkowski, M. X. *Cancer Res*. **2008**, *68*, 9280–9290.

120. Shen, B.-Q.; Xu, K.; Liu, L.; Raab, H.; Bhakta, S.; Kenrick, M.; Parsons-Reponte, K. L.; Tien, J.; Yu, S.-F.; Mai, E.; Li, D.; Tibbitts, J.; Baudys, J.; Saad, O. M.; Scales, S. J.; McDonald, P. J.; Hass, P. E.; Eigenbrot, C.; Nguyen, T.; Solis, W. A.; Fuji, R. N.; Flagella, K. M.; Patel, D.; Spencer, S. D.; Khawli, L. A.; Ebens, A.; Wong, W. L.; Vandlen, R.; Kaur, S.; Sliwkowski, M. X.; Scheller, R. H.; Polakis, P.; Junutula, J. R. *Nat. Biotechnol*. **2012**, *30*, 184–189.

121. McDonagh, C. F.; Turcott, E.; Westendorf, L.; Webster, J. B.; Alley, S. C.; Kim, K.; Andrey-

ka, J.; Stone, I.; Hamblett, K. J.; Francisco, J. A.; Carter, P. *Protein Eng. Des. Sel.* **2006**, *19*, 299–307.

122. Junutula, J. R.; Raab, H.; Clark, S.; Bhakta, S.; Leipold, D. D.; Weir, S.; Chen, Y.; Simpson, M.; Tsai, S. P.; Dennis, M. S.; Lu, Y.; Meng, Y. G.; Ng, C.; Yang, J.; Lee, C. C.; Duenas, E.; Gorrell, J.; Katta, V.; Kim, A.; McDorman, K.; Flagella, K.; Venook, R.; Ross, S.; Spencer, S. D.; Lee Wong, W.; Lowman, H. B.; Vandlen, R.; Sliwkowski, M. X.; Scheller, R. H.; Polakis, P.; Mallet, W. *Nat. Biotechnol.* **2008**, *26*, 925–932.

123. Junutula, J. R.; Flagella, K. M.; Graham, R. A.; Parsons, K. L.; Ha, E.; Raab, H.; Bhakta, S.; Nguyen, T.; Dugger, D. L.; Li, G.; Mai, E.; Lewis Phillips, G. D.; Hiraragi, H.; Fuji, R. N.; Tibbitts, J.; Vandlen, R.; Spencer, S. D.; Scheller, R. H.; Polakis, P.; Sliwkowski, M. X. *Clin. Cancer Res*. **2010**, *16*, 4769–4778.

124. Tian, F.; Lu, Y.; Manibusan, A.; Sellers, A.; Tran, H.; Sun, Y.; Phuong, T.; Barnett, R.; Hehli, B.; Song, F.; Deguzman, M. J.; Ensari, S.; Pinkstaff, J. K.; Sullivan, L. M.; Biroc, S. L.; Cho, H.; Schultz, P. G.; Dijoseph, J.; Dougher, M.; Ma, D.; Dushin, R.; Leal, M.; Tchistiakova, L.; Feyfant, E.; Gerber, H.-P.; Sapra, P. *Proc. Natl. Acad. Sci. U. S. A*. **2014**, *111*, 1766–1771.

Chapter 2

Site-Selective Modification of Antibody Fc Domains and Its Applications

Abstract

This chapter describes the development of novel antibody mimics by installing synthetic molecules at the N-termini of crystallizable fragment domains (Fc's) via a chemical modification approach. First, a pyridoxal 5′-phosphate (PLP) mediated N-terminal transamination reaction provided a compatible method for site-selectively installing ketones as reactive handles on Fc domains. High levels of conversion were achieved. Two strategies were subsequently used for the ligation of our desired synthetic targeting compounds to the protein: (1) via oxime or hydrazone linkages and (2) via oxidative coupling reaction. In the latter case, we used the ketone as a site to introduce a second reaction handle: an aniline group that can participate in an oxidative coupling reaction. By combining the advantages of synthetic targeting agents (e.g. high stability, low cost, and facile and reproducible production and discovery) with the ability of Fc domains to mediate targeted cell death and extend plasma half-life, these new hybrid agents may possess the best qualities of both. As an initial proof of concept, Fc domains were functionalized with DNA aptamers. The specificity of the aptamers for binding their cellular targets was demonstrated, as was the ability of the modified Fc domains to bind to complement proteins and Fc receptors.

Portions of the work described in this chapter have been reported in a separate publication [1].

2.1 Introduction

Since the early 1980s proteins have emerged as a major new class of pharmaceuticals, with over 200 marketed products currently available for therapeutic, diagnostic, and vaccine use [2-4]. Protein engineering has revolutionized this field by providing tools to customize existing proteins or to create new ones for specific clinical applications. A particularly important advance has been the generation of fusion proteins comprising segments derived from two or more different precursors. This approach allows multiple biological functions, such as binding and therapeutic activity, to be combined in a single entity. Arguably the most clinically and commercially successful fusion protein therapeutics to date contain the crystallizable fragment (Fc) region of immunoglobulins. The Fc fusions can endow attached peptides or proteins with the antibody-like property of long serum half-life (days to weeks) by binding to the neonatal Fc receptor (FcRn) [2-6]. The abilitiy of the Fc to bind to Fc receptors and/or complement proteins can also provide the fusion protein with immunological cytotoxicity functions [2-4,7-10]. Moreover, the smaller size of Fc domains, compared to full-size monoclonal antibodies (mAbs), may also improve tissue penetration [11,12] and allow for alternative routes of administration such as pulmonary delivery [13,14]. They also only require a single gene for expression. However, most approaches involve protein engineering, hence limiting the class of targeting group to peptides or proteins.

In contrast, the chemical protein modification strategy delineated in this chapter combines protein and synthetic targeting groups, which can potentially expand the variety of antibody-like constructs. Barbas and coworkers have previously explored a combination approach by conjugating a targeted small molecule and an RNA aptamer to aldol-catalyzing mAbs [15,16]. The resulting construct exhibited significant increases in the plasma half-lives of the synthetic moieties [15,16]. While these results provide an exciting approach to the creation of antibody fusions using various types of targeting groups, their method required the use of full-size mAbs, with Fab domains that catalyzed the ligation reaction [16]. Thus, the final hybrid products still retain the large size and complexity of full-sized antibodies. Currently, there is no analogous way to conjugate other classes of therapeutics, such as small synthetic molecules, aptamers [17,18], peptoids [19], or chemically-modified peptides [20-26], to only the Fc fragments in order to make Fc-fusions. This is largely due to the complex structure of Fc domains, which contain multiple polypeptide chains, extensive disulfide networks, and essential glycosylation patterns. These components make it very difficult to design chemical approaches that can modify Fc domains site-specifically.

To date the most promising methods for site-selective modification of complex molecules containing disulfide bonds and oligosaccharides have included the double alkylation of cysteines resulting from the reduction of interchain disulfide bonds [20-22], the alkylation of a site-specifically introduced cysteine residue [28], native chemical ligations at the C-termini [29], and the chemical modification of genetically encoded aldehyde tags [30]. The Bertozzi aldehyde tagging method [30] provides a particularly intriguing possibility for subsequent site-selective hydrazone and oxime formation, and could indeed be used as an alternative strategy for the generation of the conjugates described herein. As an additional possibility, artificial amino acids can also be incorporated for the site-selective modification of antibodies. For example, Rader and co-workers have demonstrated the insertion of selenocysteine residue at the C-termini of Fc proteins for an attachment to LLP2A, an α4β1 integrin-binding small molecule [31]. More recently, Schultz and co-workers also showed an incorporation of *p*-acetylphenylalanine to the antigen-binding fragments (Fab) and full-sized antibodies for the attachment of the protein toxin saporin and monomethyl auristatin D (MMAD), respectively [32-34]. The latter method could also potentially

provide the carbonyl groups that are targeted in our strategy.

In this chapter, we present a new method to create antibody mimics by directly conjugating antibody Fc domains to synthetic targeting molecules using chemically-based protein modification methods. This synthesis leads to the production of Fc-synthetic molecule hybrids, where the Fc domains serve as building blocks to improve the pharmacokinetic properties of synthetic agents and potentially endow them with immunological activating properties, such as the ability to induce antibody dependent cell-mediated cytotoxicity (ADCC) and complement dependent cytotoxicity (CDC). These Fc-synthetic molecule hybrids are still much smaller in size compared to mAbs. Moreover, these chemical modification techniques should be extensible for the modification of many other complex biomolecules, including IgG itself, as discussed in chapter 3.

2.2 Design and Strategy

2.2.1 The components

2.2.1.1 Fc protein

In the early stages of this project, I imagined that the described approach could be used to modify any Fc obtained by digesting the IgG1 molecules isolated from a patient's serum. IgG1 is the isotype that is commonly used for therapeutics as it can best induce ADCC and CDC (Table 1). IgG3 is as good as or even slightly better than IgG1 in inducing ADCC and CDC, but has a somewhat shorter half-life, susceptibility of the longer hinge region to proteolysis, and extensive allotypic polymorphism that make it less desirable [35,36].

Table 1. Functions of each immunoglobulin isotype (Table adapted from Ref. [37])

Functional activity	IgM	IgD	IgG1	IgG2	IgG3	IgG4	IgA	IgE
Neutralization	+	-	++	++	++	++	++	-
Opsonization	+	-	+++	*	++	+	+	-
Sensitization for killing by NK cells	-	-	++	-	++	-	-	-
Sensitization of mast cells	-	-	+	-	+	-	-	+++
Activates complement system	+++	-	++	+	+++	-	+	-

+++: major function; ++: lesser function; +: minor function; -: no function
*IgG2 can act as an opsonin in the presence of an Fc receptor of the appropriate allotype, found in about 50% of caucasians.

In practice, IgG1 would be isolated from patients, and Fc would be obtained by digestion at the hinge region. After attaching synthetic molecules to the Fc, the Fc-synthetic conjugates can then be injected back to the same patient for various purposes, e.g., half-life extension of therapeutic drugs for that patient or redirecting the Fc with synthetic targeting groups for immunotherapy. Even though the constant region of most people will be the same or very similar, this method would be applicable to all patients, even those that reject humanized antibodies from other sources.

Within the same species, the Fc regions of the same isotype contain the same primary sequence; therefore, another approach for obtaining Fc is to express the human IgG1 Fc in mammalian cells. The production and purification method of human IgG1 mAbs has been widely studied

as it is the most common isotype for antibody therapeutics.

2.2.1.2 Synthetic groups

Ideally, the synthetic groups could be virtually any molecules you can imagine. In my work, I chose DNA aptamers to start with as the Francis group had prior success using a DNA aptamer as the targeting agent [38].

2.2.2 The methodology

The first protein modification approach I considered was pyridoxal 5'-phosphate (PLP)-mediated N-terminal modification developed in the Francis group [38-45]. However, other N-terminal transamination reactions, including that promoted by Rapoport's salt [46], could also be used. These reactions are advantageous in several ways:

(1) They are site-selective at the N-terminus, which is the preferred modification site for creating antibody mimics. Hence, other residues are not modified;

(2) The reaction conditions are mild and biocompatible (i.e., the protein would not be denatured);

(3) The methodology is applicable to a wide variety of N-terminal amino acids; and

(4) The product of transamination is a glyoxamide (for N-terminal glycine) or pyruvamide derivative (for N-terminal residues other than glycine) that can be subsequently modified by bioorthogonal oxime or hydrazone formation [47-50].

The first strategy is shown as route 1 in Figure 2.1 This strategy, however, is limited as the hydrazone formation between transaminted Fc and hydrazide aptamers requires long reaction times (usually 2 days) and a large excess of oligonucleotides to achieve decent yields. An alternative method using oxidative coupling [51-53] (route 2, Figure 2.1) may prove superior. The oxidative coupling provides a highly efficient ligation strategy requiring very short reaction times

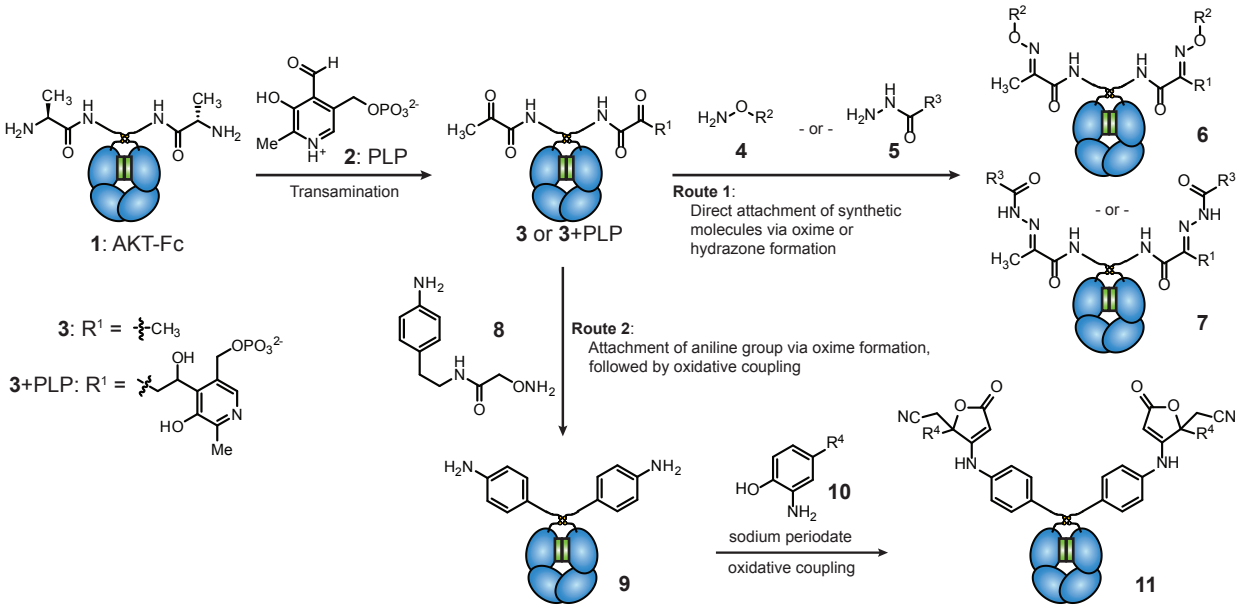

Figure 2.1. Modification of Fc proteins. First, ketone functional groups are installed at the N-termini through PLP-mediated transamination. These groups can then be functionalized using two different approaches. The first involves the direct attachment of molecules of interest via oxime formation (with **4**) or hydrazone formation (with **5**). The second strategy uses a highly efficient oxidative coupling reaction. This approach involves the chemoselective coupling of aniline groups on the Fc proteins (**9**) with aminophenol-containing reagents (**10**). (Figure adapted from Ref. [1]).

(two minutes or less) at room temperature [52]. The enhanced efficiency is a useful feature for the installation of high-value cargo, such as complex drug molecules or the nucleic acid aptamers. Even though the oxime formation between keto-Fc and aniline alkoxylamine is still necessary, aniline alkoxylamine is a much cheaper molecule for the use in excess and also one can imagine producing a large batch of Fc-aniline conjugates that can be stored for subsequent coupling to aminophenol-containing synthetic molecules. Current efforts in N-terminal modification in the Francis group may also be used to bypass the oxime formation step altogether.

2.3 Results and Discussion

2.3.1 Fc production

The Fc domains can be generated via (1) proteolytic digestion of full-sized human IgG1 at the hinge region or (2) expression of human IgG1 Fc protein in mammalian cells.

2.3.1.1 Digestion of human IgG1

I first attempted the digestion of a monoclonal anti-FLAG® antibody produced in mice using papain resins, followed by purification of Fc from Fab using a protein A column that is known to bind only the Fc fragments of antibodies. Papain non-specifically digests antibodies at the hinge region above the disulfide bonds that connect two heavy chains, although predominantly at the C-terminus of His224 residue (in italics) of the human IgG1 heavy chain sequence -Ser-Cys-Asp-Lys-Thr-*His*-Thr-Cys- (See full sequence of the hinge region in Figure 2.12) [54-56]. After a few trials, the digestion and purification to separate Fc from Fab were successfully achieved, as shown by SDS-PAGE (Figure 2.2a) and LCMS analysis of each fraction (data not shown). A similar approach using papain resins, as well as another approach using endoproteinase Lys-C, were explored for digesting human IgG1 mixture isolated from human serum. Limited proteolysis with endoproteinase Lys-C was shown to cleave the antibody in the flexible hinge region between

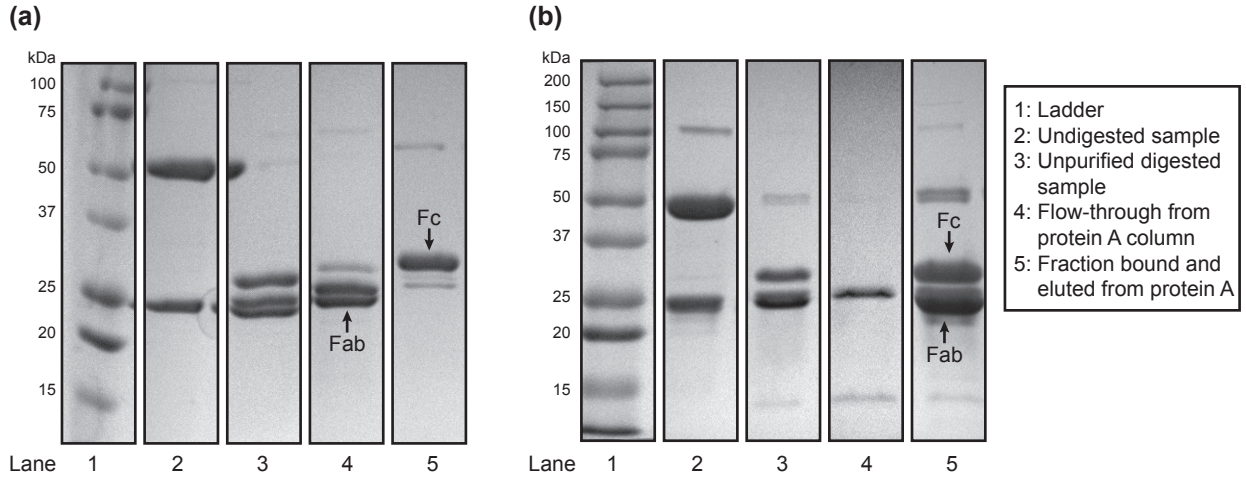

Figure 2.2. SDS-PAGE analysis of digested antibodies. (a) Mouse anti-FLAG® antibodies were digested using papain resins, followed by separation of Fab from Fc fragments using protein A columns. (b) Human IgG1 antibody mixture isolated from human serum was digested using the same strategy as in (a). However, Fab was non-specifically bound to protein A even after elution using high salt (400 mM NaCl) solution. Digestion of human IgG1 antibodies using endoproteinase Lys-C protease also yielded similar results as shown in (b).

Lys222 and Thr223 to produce one Fc and two identical Fab domain fragments, giving a more defined digestion of human IgG1 [56,62]. However, the digested Fab from both strategies seemed to be bound to protein A or protein G column, even after using high salt buffer (400 mM NaCl) to disrupt any non-specific binding of Fab to protein A (Figure 2.2b). LCMS analysis of the protein A bound fraction also confirmed that it contained both Fab and Fc of digested human IgG1 (data not shown).

2.3.1.2 Expression of human IgG1 Fc proteins

An alternative approach to obtaining Fc proteins was to express the protein. However,

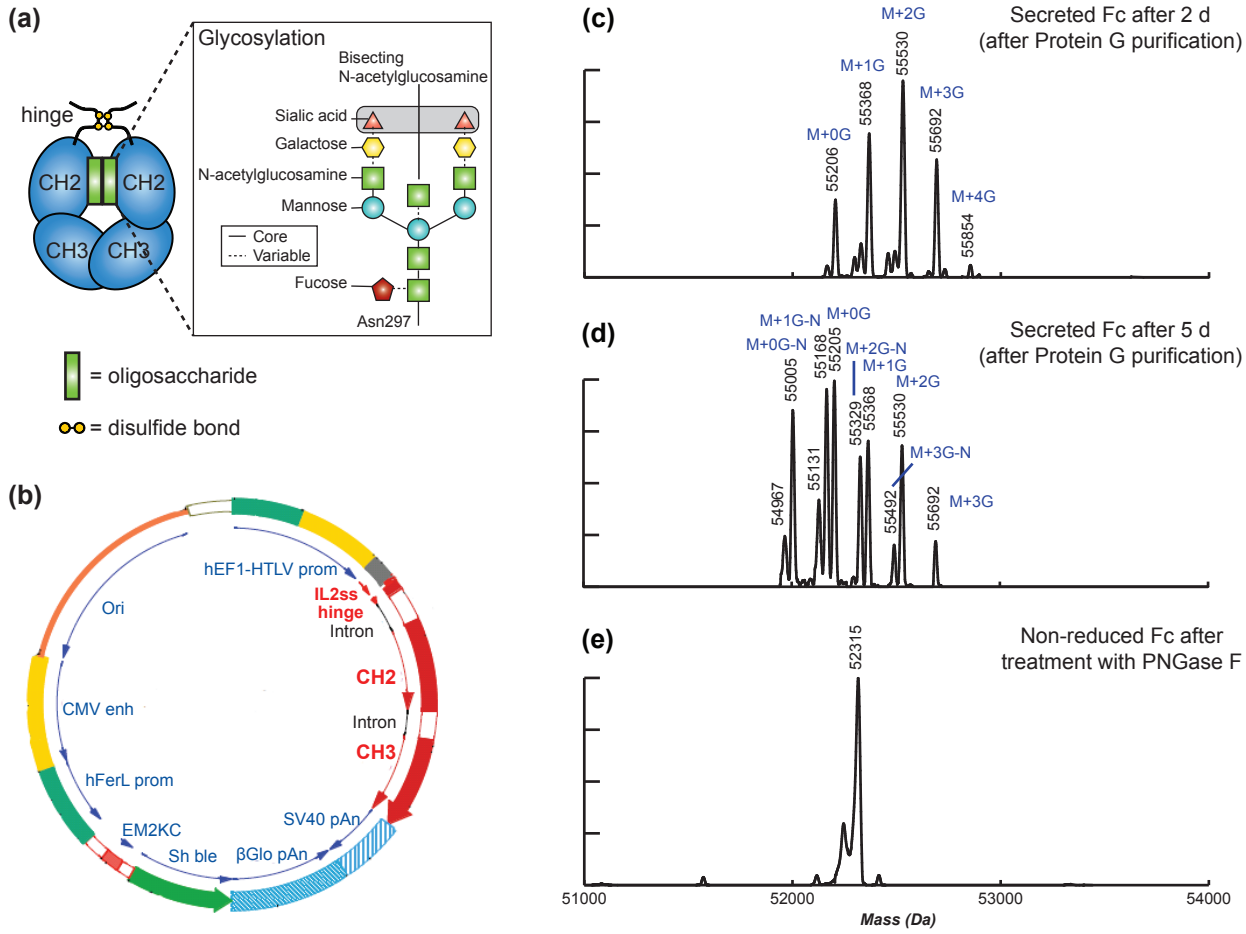

Figure 2.3. Structure, expression vector, and LCMS analysis of human IgG1 Fc. (a) Structure of Fc region of human immunoglobulin G1 (IgG1) is comprised of two monomers, each containing two domains (CH2 and CH3), with glycosylation at Asn297. The hinge region, which contains two disulfide bonds, serves as a flexible spacer between the Fc and the Fab. The sialic acids highlighted in the gray shaded box were not observed using our expression system. (b) A plasmid expressing human IgG1 Fc protein with introns and IL2 signal sequence (IL2ss) was constructed and used for these experiments. The introns helped to increase the expression level of the IgG1 Fc, and IL2ss signaled the secretion of the Fc protein to the extracellular medium. (c-e) LCMS analysis of the Fc protein collected 2 d after transfection, the Fc protein collected 5 d after transfection (fresh Opti-MEM media was replaced after 2 d), and the Fc protein after treatment with PNGase F (both 2 d and 5 d samples were identical). The heterogeneity was a result of differences in the number of galactose (G, 162 Da) and N-acetylglucosamine (N, 203 Da) residues that were incorporated. Because each monomer of the Fc protein could contain up to two galactose residues, there are five possibilities of glycosylation patterns for the Fc dimer, corresponding to a normal distribution of M+0G (55206 Da), M+1G (55368 Da), M+2G (55530 Da), M+3G (55692 Da), and M+4G (55854 Da). Additionally, peaks at 55005, 55166, 55329, and 55492 Da appear to match M+0G-N, M+1G-N, M+2G-N, and M+3G-N, respectively. (Figure adapted from Ref. [1]).

since the oligosaccharide on the Fc domain is important for binding to Fc receptors and complement proteins, the proteins cannot be expressed in *E. coli*. Mammalian and yeast cells can be used instead, with Chinese hamster ovary (CHO) and human embryonic kidney (HEK) cells being the most common as they give the closest glycosylation patterns to those produced in human. Many efforts in glycoengineering have been conducted to improve binding efficiency of Fc to Fc receptor and complement proteins, as reviewed in chapter 1 [57-61].

The plasmid vector for expressing human IgG1 Fc was obtained from InVivogen. Since the efficiency of PLP-mediated transamination depends on the sequence of the N-terminus [41,42], the Fc protein was first mutated to contain a highly reactive alanine-lysine-threonine (AKT) sequence [42] immediately following the IL2 signaling peptide (Figure 2.2; see sequence in materials and methods). This leader peptide was cleaved during the secretion of the AKT-Fc proteins from the host cells. The protein was expressed in glycosylated form in transfected HEK 293T cells (Figure 2.2c-e) and purified using a protein G column.

2.3.2 Fc modification

2.3.2.1 PLP-mediated N-terminal transamination

Reaction conditions for PLP-mediated N-terminal modification were previously optimized [42], and we confirmed that the same conditions were also optimal for modification of Fc proteins (Figure 2.4d). In brief, the AKT-Fc proteins were exposed to a freshly prepared 100 mM solution of PLP in pH 6.5 phosphate buffer at 37 °C for 1 h. Due to the small mass difference (1 Da) corresponding to the transamination of each terminus, the resulting protein was exposed to benzyl hydroxylamine ($BnONH_2$, **4a**) for 2 d at RT before characterization using mass spectrometry. To simplify the analysis, the carbohydrate domain was removed from the samples using PNGase F. As shown for the non-reduced Fc products in Figure 2.4a,b, very high conversion was observed. Two major products were obtained (**6a** and **6a+PLP**), both resulting from the desired oxime formation reaction at the two Fc termini. The higher mass product resulted from an aldol reaction between the aldehyde of PLP and the transaminated terminus during the first reaction step (shown as **3+PLP** in Figure 2.1). The only other product that was evident was a small amount of Fc with a single oxime modification (species **12**). In samples lacking PLP treatment, exposure to $BnONH_2$ led to no observable modification. Oxime formation using AlexaFluor 488 alkoxyamine was also used to detect reaction progress via SDS-PAGE (Figure 2.4e). Fluorescence was detected in the +PLP lanes using both reducing and non-reducing gel loading buffers, suggesting that AKT-Fc underwent transamination by PLP and that the Fc remained in a dimeric state under the reaction conditions. In addition to the expected products, a small amount of residual Fc dimer (~4-7% by densitometry) was observed in the reduced lane. We presume this resulted from an aldol reaction between the two terminal ketones, which are directly adjacent to one another in the dimeric Fc structure. Such a species would still possess a single remaining ketone group, thus allowing its labeling with the dye molecule. The presence of this minor species could also explain species **12** in Figure 2.4b, but the identities of these two byproducts have not been confirmed further due to their very low abundance.

After successful transamination and oxime formation with $BnONH_2$, I then explored the attachment of aniline-ONH_2 (compound **8**), an oxidative coupling partner, to the N-termini of Fc using the transamination/oxime formation procedure described above. Not only did we achieve Fc proteins bearing an aniline group at each of the two termini (species **9**), but much to our surprise,

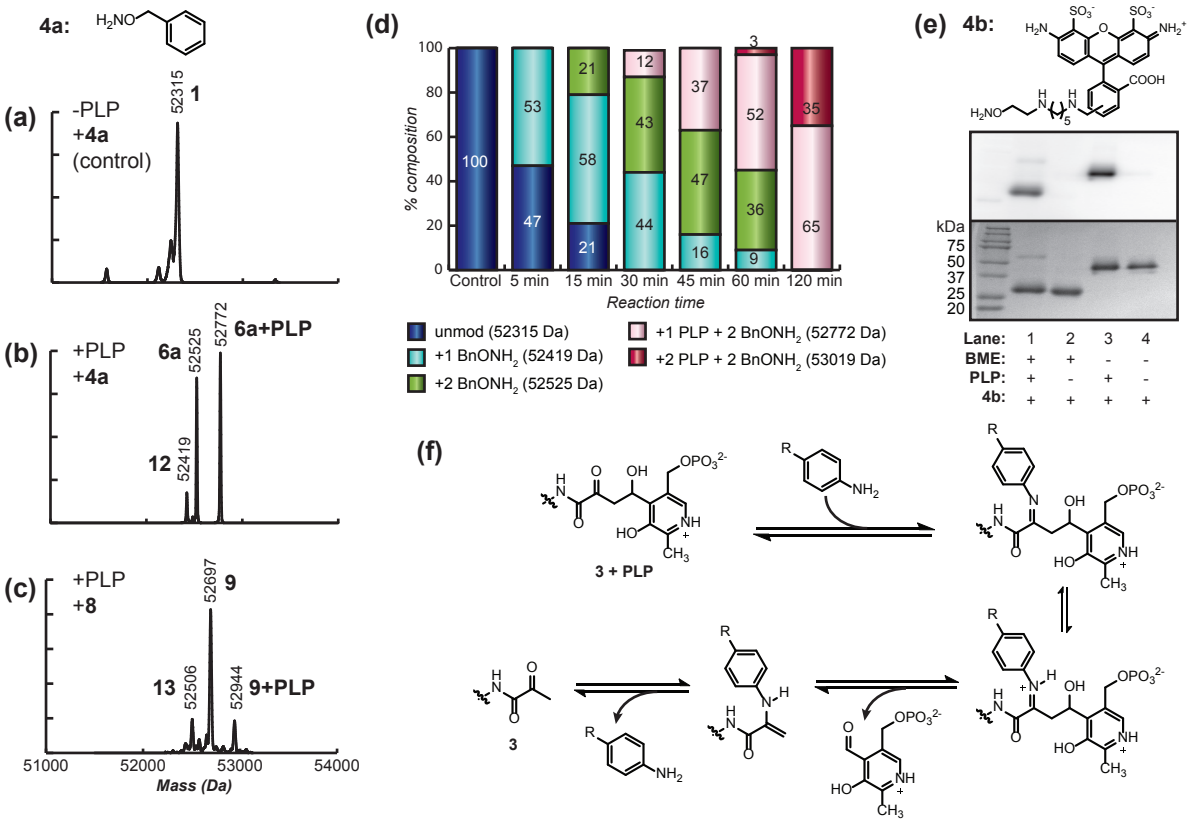

Figure 2.4. Analysis of transamination efficiency for AKT-Fc domains. AKT-Fc (**1**) was exposed to 50 mM **4a** for 40 h at pH 6.5, followed by treatment with PNGase F (a) without prior transamination with PLP (as a negative control), or (b) following transamination with 100 mM PLP at 37 °C for 1 h. The peak at 52315 Da corresponded to unmodified AKT-Fc (expected: 52315 Da). The double-oxime product (**6a**) appeared at 52525 Da (expected: 52523 Da), and the peak at 52772 Da corresponded to product **6a** plus a single PLP addition (expected: 52770 Da). The peak at 52419 Da corresponded to the addition of one molecule of **4a** to the AKT-Fc fragment (**12**, expected: 52419 Da). (c) After transamination using the same condition as in (b), resulting keto-Fc (**3**) was exposed to 25 mM **8** for 40 h at pH 4.5, followed by PNGaseF treatment. The double-oxime product (**9**) appeared at 52697 Da (expected: 52695 Da), and the peak at 52944 Da corresponded to product **9** plus a single PLP addition (expected: 52942 Da). The peak at 52506 Da corresponded to the addition of one molecule of **8** to the AKT-Fc fragment (**13**, expected: 52506 Da). (d) Product distribution of PLP-mediated transamination of the Fc domains at various reaction time, followed by oxime formation with benzyl hydroxylamine (**4a**). Percent yields were calculated by peak area of each product. (e) Samples of AKT-Fc with and without transamination using PLP (100 mM PLP at 37 °C for 1 h) were exposed to 80 μM AlexaFluor 488 alkoxyamine (**4b**) for 43 h in the presence of 100 mM aniline as a catalyst. They were then analyzed by SDS-PAGE under reducing (lanes 1 and 2) or non-reducing conditions (lanes 3 and 4). The fluorescent images of the Fc-AlexaFluor 488 oxime products (top) were taken using a Typhoon imaging system. The bottom gel was stained using Coomassie blue. (f) Proposed mechanism for the decrease of PLP adduct after oxime formation with aniline-ONH_2 (**8**). We hypothesized that aniline can catalyze the reverse aldol reaction releasing PLP from the PLP aldol adduct. (Figure adapted from Ref. [1]).

the amount of PLP adduct (species **9**+PLP) was much reduced when aniline-ONH_2, as compared to other alkoxyamines, was used in the oxime step (Figure 2.4c). We hypothesized that aniline can catalyzed the retro aldol reaction through iminium ion formation (Figure 2.4f). However, simply adding aniline in the oxime formation step of $BnONH_2$ does not achieve the same reduced amount of PLP adduct as using aniline-ONH_2. Further investigation on peptides and proteins is thus necessary to confirm this hypothesis.

2.3.2.2 Oxidative coupling

Following successful installation of aniline groups on the Fc proteins, the oxidative coupling reaction was then investigated using aminophenol containing polyethyleneglycol **10a** (MW

~ 2000 Da) [51-53]. Aniline Fc **9** (10-40 μM) was combined with 100 μM **10a** in pH 6.5 phosphate buffer. A stock solution of sodium periodate was added to a final concentration of 1 mM, and the reaction was incubated for 2 min. The resulting solution was then passed through a NAP-5 gel filtration column to quench and remove the periodate. SDS-PAGE analysis under reducing conditions (and without the use of PNGase F) indicated that 50% of the individual Fc chains were converted to the singly PEGylated product (Figure 2.5a, lane 6), as indicated by optical densitometry. The lower PEGylation yield likely results from the close proximity of the two N-termini in the intact Fc domains, leading to the attachment of only one PEG chain to each protein dimer. Nonetheless, a high degree of modification was observed using very short coupling times.

As one potential concern with this strategy, immunoglobulin proteins contain oligosaccharides that could be cleaved to form aldehydes in the presence of sodium periodate. To determine to what degree the glycan oxidation occurs, unmodified Fc domains were exposed to $NaIO_4$ under the oxidative coupling conditions for 2 min and 1 h. The resulting aldehyde groups were then visualized by subsequent reaction with AlexaFluor 488 alkoxyamine (**4b**). As seen in Figure 2.5c, the oligosaccharides on the Fc protein were only minimally oxidized by $NaIO_4$ at the 2 min time point (compare lanes 2 and 5 to the background labeling for unmodified Fc in lane 1). Furthermore, we found that the addition of 10 mM to 100 mM mannose could suppress this oxidation of the carbohydrate groups completely (Figure 2.5c). Interestingly, the oxidative coupling reaction still proceeded with similar conversion in the presence of 10 mM mannose (Figure 2.5a, lane 7) although a somewhat reduced conversion in the presence of 100 mM mannose (lane 8) was observed. Thus,

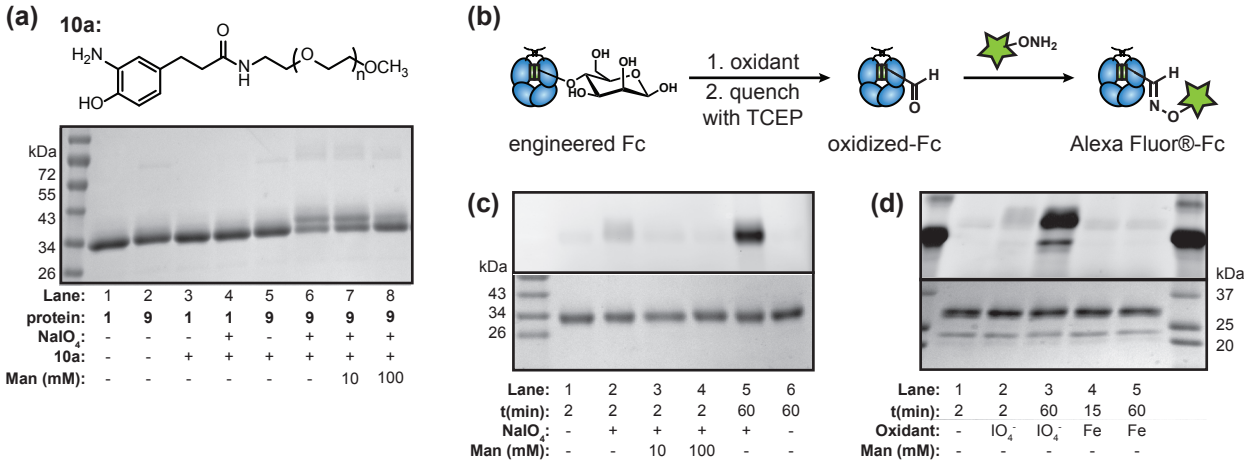

Figure 2.5. Modification of Fc domains via oxidative coupling (O.C.). (a) Samples of unmodified Fc (**1**) and Fc-aniline (**9**) were exposed to 100 μM 2k PEG-aminophenol (**10a**) and 1 mM $NaIO_4$ for 2 min at RT. Lanes 1-5 display negative controls. Only in the presence of both aniline on the Fc and $NaIO_4$ did the attachment of 2k-PEG-aminophenol occur (lane 6). In the presence of 10 mM mannose (lane 7), the O.C. still proceeded; however, the yield suffered when the mannose concentration was increased to 100 mM (lane 8). (b) The reaction scheme for analyzing the extent of oxidation of the oligosaccharides on the Fc protein. The Fc proteins were first exposed to oxidant, followed by addition of TCEP to stop the oxidation. Aldehydes from oxidized saccharides were then detected by oxime formation with AlexaFluor 488-ONH_2. (c) The Fc proteins were exposed to 1 mM $NaIO_4$ for 2 min (the O.C. reaction time) with and without addition of mannose. The fluorescent images of Fc-AlexaFluor 488 oxime products (top) were taken using a Typhoon imaging system. The oligosaccharides on the Fc were minimally oxidized under the O.C. reaction time of 2 min (lane 2) and this oxidation was lowered to background level upon addition of 10 mM mannose or higher concentration (lanes 3 and 4). The oxidation of oligosaccharides on Fc with $NaIO_4$ for 1 h was shown as a positive control (lane 5). Lane 1 and 6 display the background level of oxidized sugar in the absence of $NaIO_4$. (d) The Fc was exposed to either $NaIO_4$ or $K_3Fe(CN)_6$ (abbreviated Fe in the figure) for 2 (lane 2) and 15 min (lane 4), respectively, the reaction time required for completion of the O.C. Exposure to ferricyanide does not result in any detectable oxidation of the glycoprotein even after 1 h (lane 5). (Figure adapted from Ref. [1] and [53]).

this strategy provides a method to protect glycoproteins from undesired oxidation with this procedure. Even though it should be noted that the Fc protein examined here does not contain sialic acids, which are the most susceptible to oxidation, we anticipate that oxidative coupling will still occur in a much shorter timescale in comparison to oxidation of oligosaccharides.

Recently, a new oxidant for the oxidative coupling reaction was reported by Obermeyer *et al*. [53]. Potassium ferricyanide ($K_3Fe(CN)_6$) can be used to achieve similar yield to $NaIO_4$ but did not oxidize the glycans due to both a lower oxidation potential as well as a distinct mechanism of oxidation. Figure 2.5d shows no detectable amount of glycan oxidation even after 1 h incubation with 1 mM $K_3Fe(CN)_6$. This new approach will be useful for reaction on complex molecules with post-translational glycosylation, including the Fc proteins and antibodies.

2.3.3 Attachment of synthetic targeting groups

Since the 1990s, small RNA and DNA aptamers have emerged as a new class of molecules for therapeutic and diagnostic purposes, owing to the successful development of the systematic evolution of ligands by an exponential enrichment process, known as SELEX [17,18,67-71]. Using SELEX, new aptamers can be evolved to bind to cells with high specificity and affinity, often without prior knowledge of the specific molecular targets. These readily evolved binding groups could endow Fc domains with specific cell binding abilities, and, conversely, the Fc domains could improve the *in vivo* circulation times of the oligonucleotides, as shown by Barbas *et al*. [15]. Two aptamers were selected for attachment to the Fc proteins as a proof of principle for the production of Fc-synthetic molecule hybrids: (1) sgc8c, which targets protein tyrosine kinase 7 (PTK7) [67-69] and (2) TD05.1, which targets membrane-bound IgM (mIgM, also known as the B-cell receptor) [70,71]. The sgc8c aptamer has been used in many applications [38,72-75] and shown high specificity to its target. The use of TD05.1 could be advantageous because there is currently no antibody that is specific to mIgM without also binding to circulating IgM in the blood [71]. For use as a negative control in cell binding experiments, a non-specific 41-nucleotide DNA sequence (M2M2) was also attached to Fc.

Using the hydrazone formation strategy with 100 μM hydrazide-oligonucleotides (**5**) and 100 mM aniline as a coupling catalyst [76,77] over a 48 h period, the Fc-aptamer conjugates could be obtained as identified by SDS-PAGE analysis (Figure 2.6b). Due to the high negative charge of the DNA portion, the Fc conjugates could also be separated using anion exchange chromatography (Figure 2.6c,d), allowing more accurate determination of the product ratios. The major product (64%) possessed a single attachment of the oligonucleotide to one of the Fc N-termini, likely due to steric hindrance and electronic repulsion between two DNA molecules. The doubly modified product corresponded to 20% yield, with only 16% of unconjugated Fc protein remaining. The alternative method, the attachment of aminophenol-DNA oligonucleotides (**10b**, 100 μM) to Fc-aniline (**9**) via oxidative coupling reaction, was achieved at RT in 2 min. In this case, 58% of the protein product corresponded to the single aptamer conjugate and 39% corresponded to the double aptamer conjugate, representing a total of >95% of the protein species. The overall yields were therefore slightly higher than those achieved by direct hydrazone formation (Figure 2.6a, lane 4-6), but they were obtained with drastically reduced coupling times. Anion exchange chromatography was again used to obtain pure conjugates for use in subsequent binding studies, Figure 2.6e.

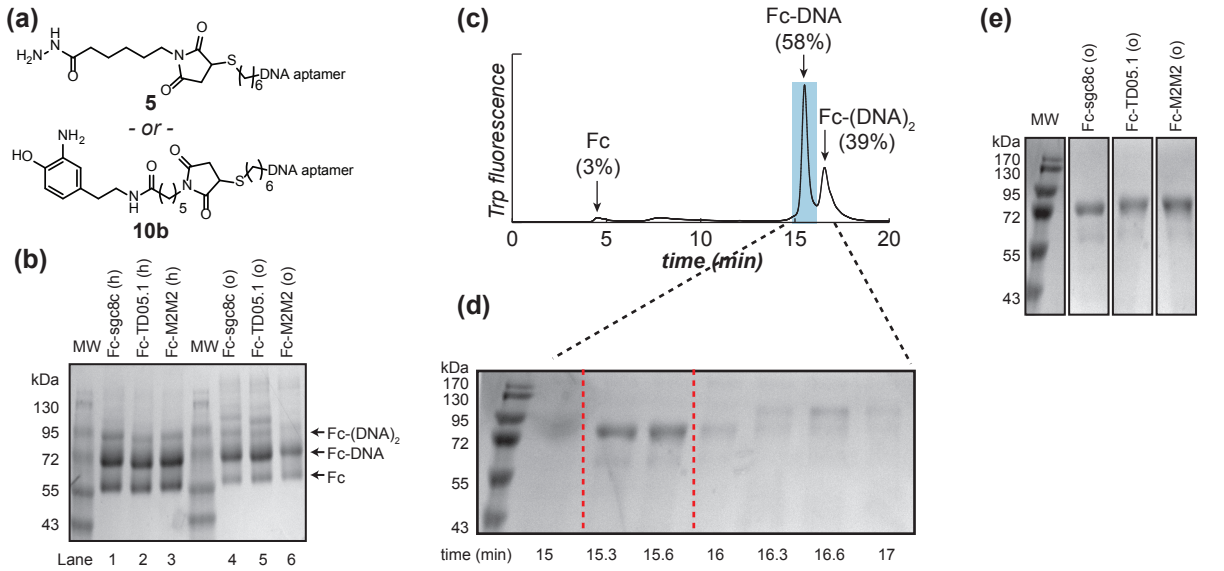

Figure 2.6. Construction of Fc-aptamer conjugates. Two different aptamers, sgc8c targeting PTK7 and TD05.1 targeting membrane-bound IgM, were attached to keto-Fc using the two approaches shown in Figure 1. (a) Structure of hydrazide- and aminophenol-DNA oligonucleotides used for hydrazone formation and the oxidative coupling reaction, respectively. (b) SDS-PAGE analysis under non-reducing conditions showed the formation of Fc hybrids using either hydrazone formation (labeled as 'h', lanes 1-3) or oxidative coupling ('o', lanes 4-6). Single aptamer conjugates were the major products, along with lesser amounts of doubly-labeled conjugated species. (c) Anion exchange-HPLC purification of Fc-TD05.1 adduct following the oxidative coupling reaction. Integration of each peak also indicates the relative quantities of Fc, Fc-DNA, and Fc-$(DNA)_2$. (d) SDS-PAGE analysis of Fc-DNA contructs after anion exchange HPLC purification. Fractions at various time points of the HPLC runs were collected every 1/3 min, and small amounts were used for SDS-PAGE analysis to visualize the collected Fc-DNA specices. The combined fractions are outlined by the red dotted lines. (e) SDS-PAGE analysis (non-reducing) of the purified Fc-aptamer conjugates used for cell binding analysis. (Figure adapted from Ref. [1]).

2.3.4 Biological properties

2.3.4.1 Cell binding specificities

The specificities of Fc-sgc8c, Fc-TD05.1, and Fc-M2M2 hybrid constructs generated from both the hydrazone and the oxidative coupling strategies were next evaluated for selective cell binding using flow cytometry. Jurkat cells, a T-cell leukemia cell line overexpressing PTK7, were used as the targeted cells for the Fc-sgc8c constructs. Ramos cells, a Burkitt's lymphoma cell line overexpressing mIgM, were used as target cells for Fc-TD05.1. U266 cells, a B-cell line overexpressing neither membrane protein, were chosen as a negative control sample. The binding assay was conducted as outlined in Figure 2.7a, with detection of the cell-bound Fc conjugates using fluorescently labeled anti-human IgG1. Only Jurkat cells were bound by Fc-sgc8c, and only Ramos cells were recognized by Fc-TD05.1 (Figure 2.7b). Neither cell line was recognized by Fc-M2M2. Moreover, the U266 negative control cell line did not bind to any of the Fc-aptamer constructs. In addition to confirming that the aptamers retained their specificity after attachment to the Fc domains, these results also indicated that the Fc region retained its proper folding and thus could still be recognized by the fluorescent secondary antibodies.

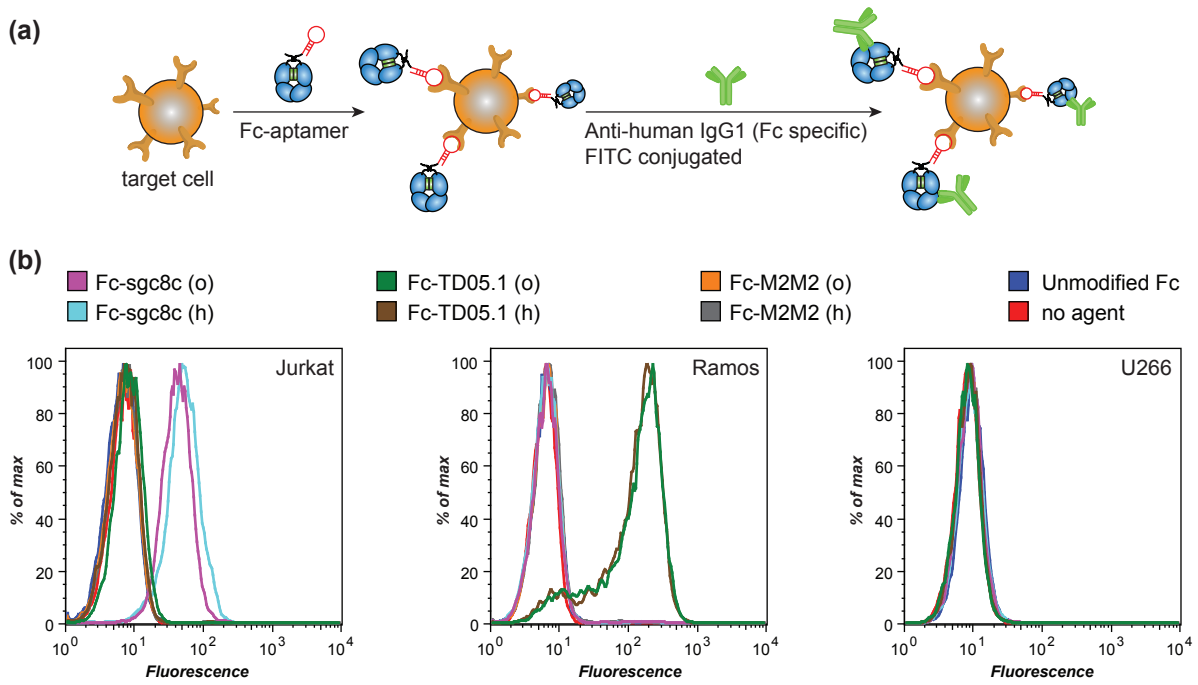

Figure 2.7. Cell binding specificity of Fc-aptamer conjugates. (a) The general cell binding analysis scheme is shown. The cells were incubated with Fc-aptamer samples, which were subsequently detected using FITC-labeled secondary antibodies specific for Fc of human IgG1. (b) Flow cytometry data are shown for the binding of Fc-aptamer conjugates to Jurkat cells (overexpressing PTK7, the target of the sgc8c aptamer), Ramos cells (overexpressing membrane-bound IgM, the target for the TD05.1 aptamer), and U266 cells as a negative control. All Fc-sgc8c and Fc-TD05.1 conjugates retained their targeting specificity, whether they were generated using hydrazone formation (labeled 'h') or oxidative coupling (labeled 'o'). Unmodified Fc proteins and an Fc-M2M2 conjugate (bearing a non-specific 41-base oligonucleotide) did not bind to any cell lines. (Figure adapted from Ref. [1]).

2.3.4.2 Binding to immunologically relevant proteins

A key feature associated with the toxicity of many antibodies is the recruitment of complement proteins found in blood serum. We therefore evaluated the ability of the modified Fc proteins to bind to the C1q complement protein using ELISA [62]. Briefly, varying concentrations of the Fc conjugates were bound to a polystyrene 96-well plate, after which a 2 μg/mL solution of human C1q was added. Binding ability was confirmed using an anti-C1q antibody conjugated to horseradish peroxidase (HRP). These results showed that the PLP-treated Fc and Fc-aptamer constructs still retained their ability to bind to C1q with similar affinities. This suggests that the bulk of the immunological activating properties of the Fc domains remained intact following the modification process (Figure 2.8). Similarly, we also evaluate the binding of Fc-aptamer conjugates to Fc receptors (FcRs) using ELISA. The binding affinities of unmodified Fc and different Fc-aptamers to activating FcRs (FcRIIa and IIIa) are within the same order of magnitude to each other, indicating that the attachment of aptamers does not interfere with the ability of Fc to bind to FcRs (Figure 2.9).

2.3.4.3 Phagocytosis with neutrophils

To examine whether the Fc-DNA conjugates can still be recognized by immune cells, we established a collaboration with the Heinrich Group at UC Davis. Here, we used beads as a mimic of target cells and coated the beads with our Fc-DNA constructs from both the hydrazone forma-

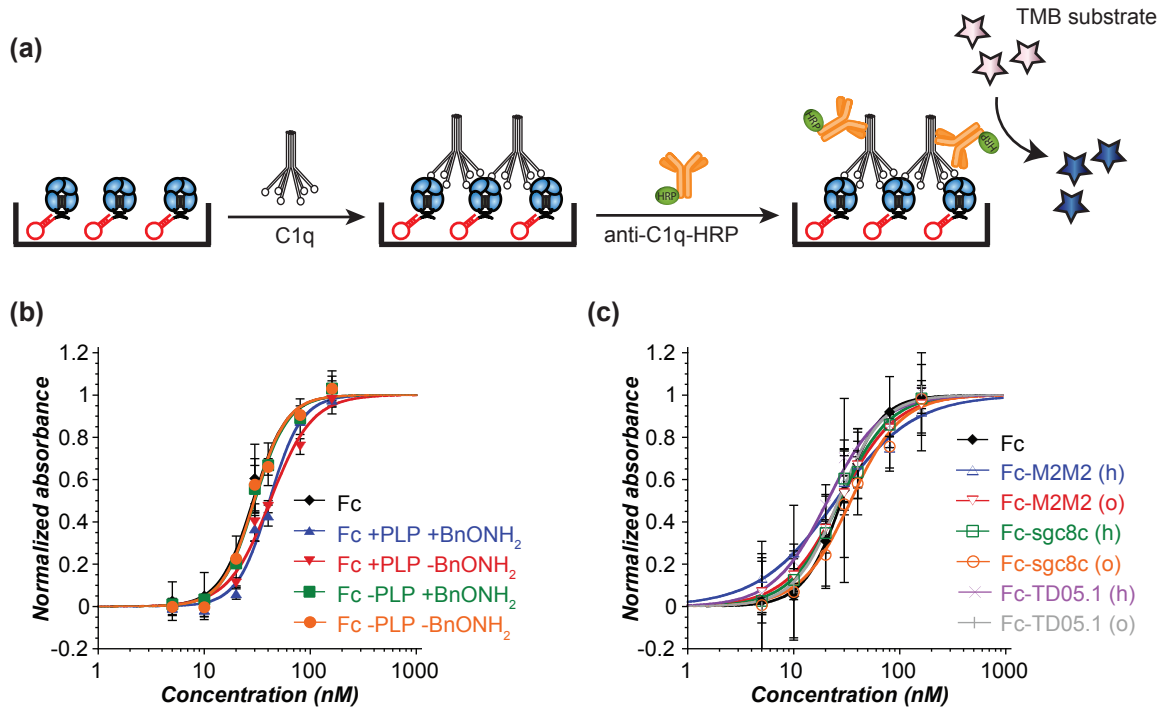

Figure 2.8. C1q binding of Fc-aptamer conjugates. (a) Scheme shows the experimental set up for ELISA. Various concentrations of modified and unmodified Fc were bound to a 96-well plate, followed by incubation with 2 μg/mL human C1q. The bound C1q were then detected by anti-human C1q HRP conjugated antibody. (b) ELISA data are shown for C1q binding to unmodified Fc, PLP-treated Fc, and Fc after oxime formation with $BnONH_2$. The binding of all the agents are similar, suggesting that transamination or attachment of $BnONH_2$ did not appreciably interrupt the binding of Fc to C1q. (c) ELISA data are shown for C1q binding to the Fc-aptamer conjugates. All the Fc-DNA conjugates retained similar C1q binding to unmodified Fc. (Figure adapted from Ref. [1]).

tion and the oxidative coupling strategy, as portrayed in Figure 2.10a. The Fc-DNA coated beads, together with negative controls (plain and DNA-coated beads), were then subjected to polymorphonuclear leukocytes (PMNs), mostly comprised of neutrophils isolated from human blood, and phagocytotic events were imaged and analyzed by flow cytometry (Figure 2.10b,c). Only Fc-DNA beads were phagocytosed by PMNs, suggesting that Fc modified with DNA oligonucleotides using our two strategies can still be recognized by immune cells. Even though only 30-50% of PMNs contained the Fc-DNA coated beads, this could be due to low density of Fc-DNA on the beads, and the assay can be further optimized.

2.4 Conclusions and Future Prospects

In this chapter, we have developed two new approaches for the site-specific modification of antibody Fc domains. We also further demonstrated the utility of these strategies to make antibody mimics through the generation of a new class of Fc-aptamer conjugates, in which the aptamers served as targeting molecules replacing Fab fragments. These hybrid agents still retain the binding specificity of the original aptamers while adding the ability of the Fc domain to be recognized by complement proteins and FcRs. The strategy developed here could be readily adapted for the attachment of other classes of synthetic molecules, such as peptoids or small molecules, to Fc domains for *in vivo* applications.

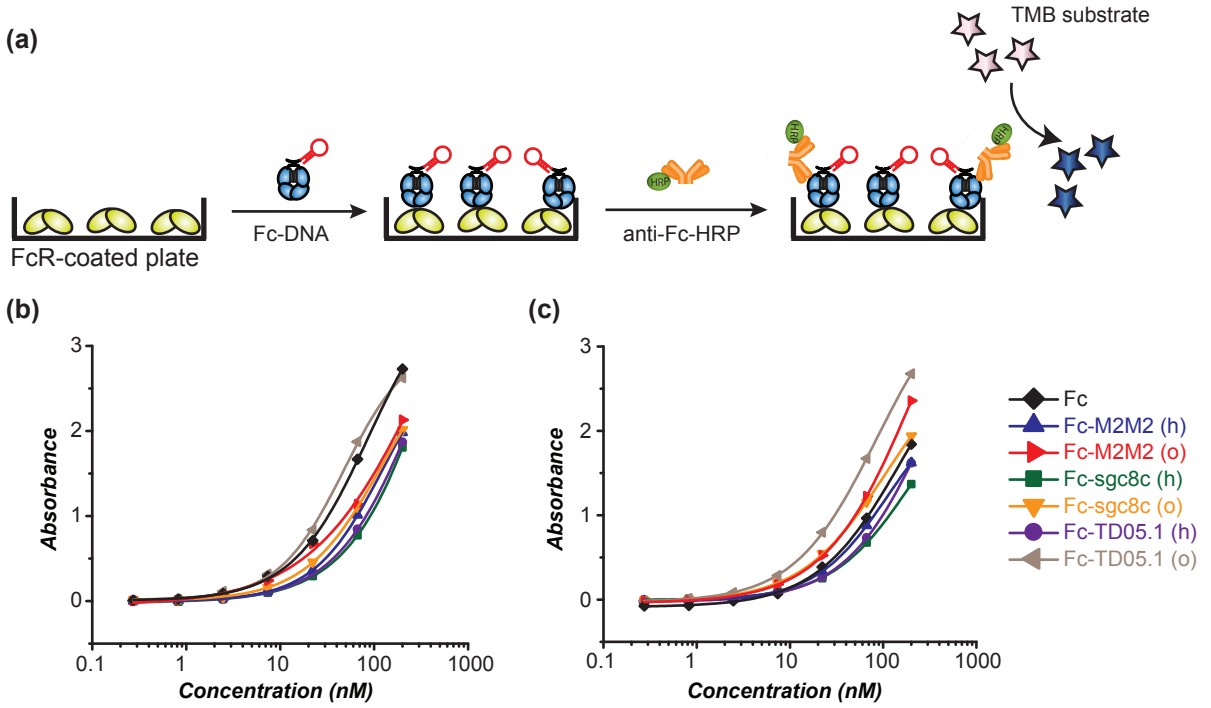

Figure 2.9. FcRs binding of Fc-aptamer conjugates. (a) Scheme shows the experimental set up for ELISA. FcRIIa and FcRIIIa (2 µg/mL) were bound to 96-well plate, followed by incubation with various concentrations of unmodified Fc and Fc-aptamer conjugates. The bound Fc conjugates were then detected by anti-human Fc HRP conjugated $F(ab')_2$ fragment. (b) ELISA data are shown for FcRIIa binding to unmodified Fc and Fc-DNA conjugates. The binding of all the agents are similar, suggesting that Fc-aptamers still retained their binding to FcRIIa. (c) ELISA data are shown for FcRIIIa binding to the Fc-aptamer conjugates. Similar to results in (b), all the Fc-DNA conjugates and unmodified Fc retained similar binding to FcRIIIa. Estimated K_d from these curves were also within the same order of magnitude (data not shown). However, the binding affinity of Fc to both FcRIIa and IIIa are low and the samples used in these experiments were not concentrated enough to reach the binding saturation. Therefore, the binding to FcRs may need further investigation to confirm the retention in FcR binding affinity.

The idea of making antibody mimics can also be expanded to the development of synthetic molecules mimicking the Fc protein itself. So we can imagine having a mix and match between each portion of antibody and the synthetic counterparts or even have a completely synthetic antibody mimics. Unlike the Fab fragments, whose main function is to bind target receptors, the Fc has many characteristics: (1) binding to FcRs to initiate ADCC and/or ADCP, (2) binding to complement proteins to initiate CDC, and (3) binding to FcRn for plasma half-life extension. The FcRs and complement proteins interact with the Fc at around the same site close to the hinge region, whereas FcRn binds at the junction of the C_H2 and C_H3 domains [9,78,83,84]. Even though it may be possible to create an Fc mimic that includes all of these properties, a much simpler and more systematic approach would be to mimic one property at a time, especially when the synthetic molecule mimic is much smaller and less complex than a 50 kDa Fc domain. As an initial attempt, we decided to create an FcRn binding peptoid in collaboration with the Kodadek group at Scripps, Florida. Peptoids (peptide mimics) have several advantages over peptides, including facile synthesis and proteolytic stability, while still retaining as large, if not larger, diversity as peptides [85].

We designed a one-bead-one-peptoid library with the size of ~500,000 members for our initial screen, which corresponds to a 5-mer peptoid with 14 different monomers. The interaction between Fc and FcRn is also pH dependent — FcRn binds to Fc inside lysosomes that have low pH (pH 6) and protect antibodies from degradation, and antibodies get released at physiological

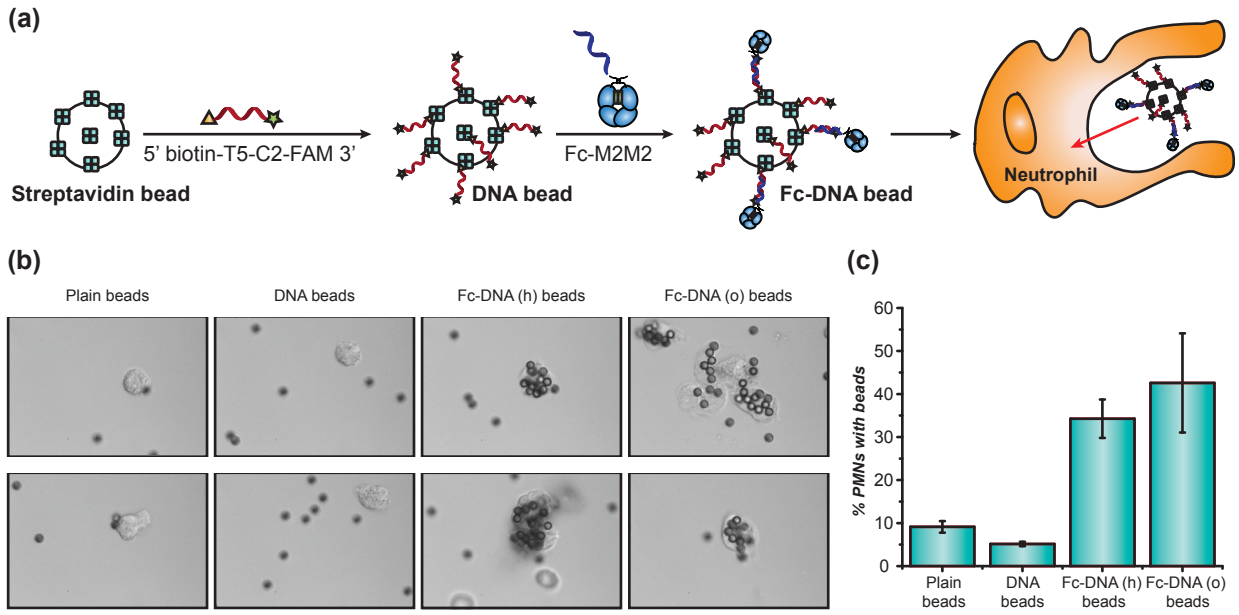

Figure 2.10. Phagocytosis of Fc-DNA conjugates. (a) Scheme shows experimental procedure of the phagocytosis experiment of beads coated with Fc-DNA conjugates. First, streptavidin beads ("plain beads") were coated with complementary oligonucleotides to yield "DNA beads," followed by incubation with the Fc-DNA conjugates from both hydrazone (h) and oxidative coupling (o) strategy, which readily formed double stranded complexes, resulting in Fc coated beads or "Fc-DNA beads." Plain, DNA, Fc-DNA (h), and Fc-DNA (o) beads were then incubated with polymorphonuclear leukocytes (PMNs), mostly comprising neutrophils, isolated from human blood. (b) Images of neutrophils after incubation with different types of beads. Only the Fc-coated beads were phagocytosed. (c) Flow cytometry analysis of fluorescent beads prepared similarly to scheme (a) showed that only Fc-DNA beads were phagocytosed by PMNs. Also, Fc-DNA from both hydrazone formation and oxidative coupling resulted in similar extent of phagocytosis. These results confirmed that Fc modified with DNA oligonucleotides can still be recognized by immune cells.

pH (pH 7.4) at the cell surface. A crystal structure of an FcRn/heterodimeric Fc complex reveals the amino acid residues on the Fc that is interacting with FcRn and these include 3xHis, Ile, Leu, Lys, Ser, and Tyr [84]. Having three histidines in the Fc-FcRn interface results in the pH dependent binding property. When we designed our library, we selected six of the 14 monomers to have side chains with pKa in the range of 5 to 7, similar to His. These side chains are derivatives of imidazole, pyridine, and quinoline (Figure 2.11). The rest of the library monomers include one Lys mimic, non-charged polar, and non-polar side chains (Figure 2.11). To conduct the library screen, we plan to follow on-bead two-color (OBTC) cell screen protocol established by Udugamasooriya *et al*, using human FcRn-expressing HEK293 cells (gift from Prof. Roopenian) as positive control cells and HEK293 can then be used as negative. If successful, this project can be beneficial in various applications including plasma half-life extenstion of various therapeutics and nanoscale delivery vehicles by attachment of FcRn-binding peptoids. Moreover, these conjugates may be considered for pulmonary delivery due to expression of FcRn in lung epithelial cells[13] and for vaccine application as antigen-presenting cells also highly express FcRn [86].

Alternatively, we may be able to use the same library to screen for an pH-dependent Fc binder for antibody purification purposes. The most widely used method for antibody purification is protein A or G affinity chromatography. However, these techniques require a harsh elution step using low pH (pH 2-3) elution buffer. An alternative Fc binder that can be switched on/off in milder conditions (e.g., pH 5-6) will prove useful for future purification of antibodies and perhaps other proteins.

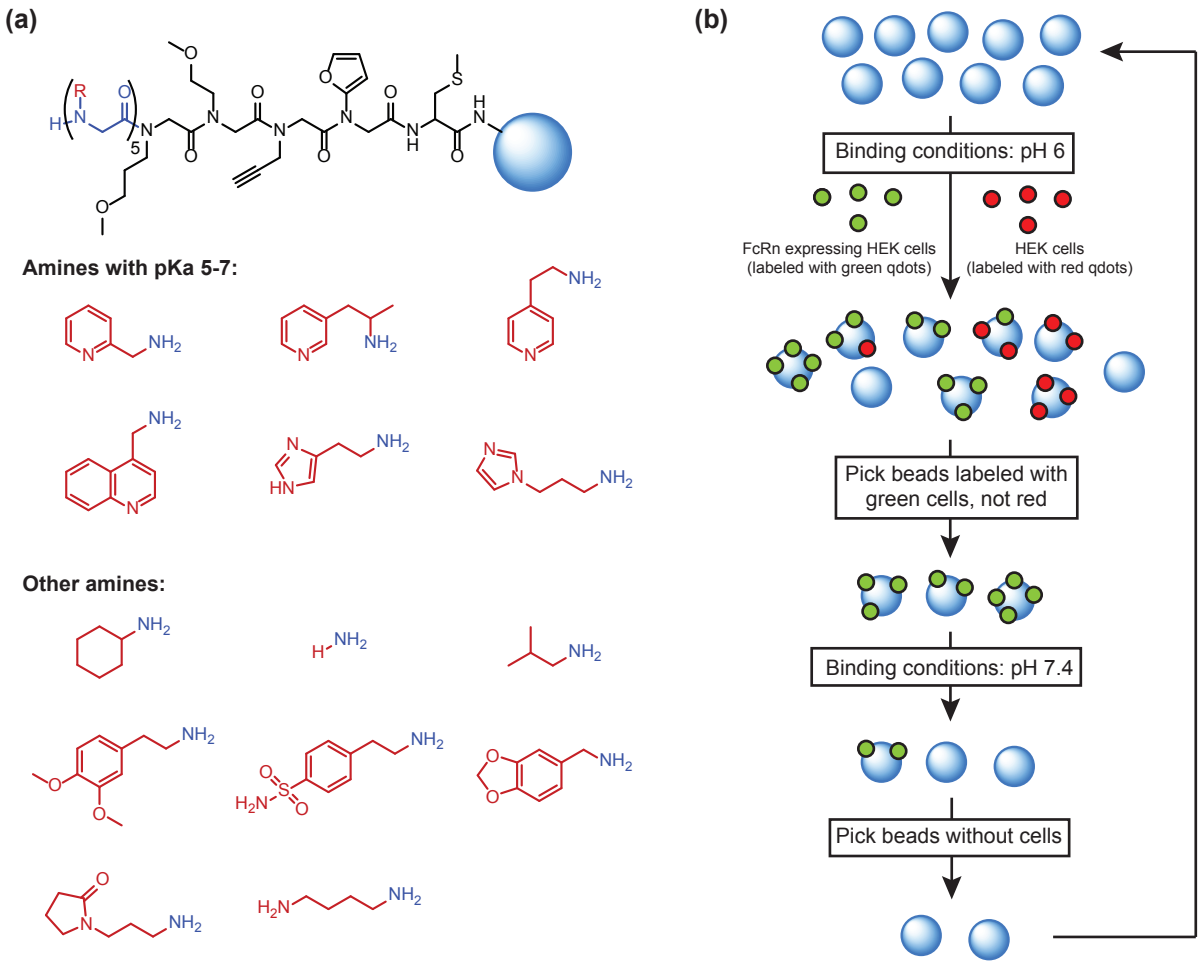

Figure 2.11. One- bead-one-peptoid library and screening assay design. (a) Structure of the peptoid library employed in the screen. Top: general structure of the compounds in the library. Five residues at the C-terminus serve as a spacer, comprising of methionine and four non-interfering amines (furfurylamine, propagylamine, methoxyethylamine (Nmea), and methoxypropylamine (Nmpa)), and the remaining five residues (drawn in blue) were diversified (side chains represented by "R,"drawn in red). Bottom: the 14 amines employed to make the library. Six of these amines are those with pKa in the range of 5 to 7, mimicking His residue. The nitrogen shown in blue becomes the main chain nitrogen in the peptoid. The library size is 5^{14} or ~500,000. (b) Design of the screening assay. The assay was designed to bind to FcRn at pH 6 but not at pH 7.4, mimicking the nature of Fc binding to FcRn. First, the beads were incubated with FcRn expressing HEK cells labeled wtih green quantum dots and regular HEK cells labeled with red quantum dots (negative control) in pH 6 binding buffer. Only the beads binding to FcRn expressing cells will be picked, followed by incubating these selected beads in pH 7.4 binding buffer. If the peptoids contain the pH dependent binding, the beads should be released from FcRn expressing cells and these beads will go through the same cycle for 2-3 more times.

2.5 Materials and Methods

2.5.1 General experimental procedures and materials

Unless otherwise noted, all chemicals and solvents were of analytical grade and used as received from commercial sources. Water (dd-H_2O) used in biological procedures or as the reaction solvent was deionized using a NANOpure purification system (Barnstead, USA). All oligonucleotides were obtained from Integrated DNA Technologies (Coralville, IA). All cell culture reagents were obtained from Gibco/Invitrogen Corp. (Carlsbad, CA) unless otherwise noted. Cell culture

was conducted using standard techniques. Jurkat and Ramos cells were grown in T-25 or T-75 culture flasks (Corning) in RPMI Medium 1640 supplemented with 10% (v/v) fetal bovine serum (FBS, Omega Scientific) and 1% penicillin/streptomycin (P/S, Sigma). U266 cells were grown in T-25 or T-75 culture flasks (Corning) in RPMI Medium 1640 supplemented with 15% (v/v) FBS and 1% P/S.

2.5.2 Construction of the plasmids for the expression of Fc domains

To express the Fc substrates, the pInFuse-hIgG1-Fc2 (InvivoGen, San Diego, CA) plasmid, which contained the human IgG1-Fc gene with its introns and an IL2 signal sequence, was used. A short intron was present between each region: one intron was located between the hinge and the C_H2 domain and one intron was located between C_H2 and C_H3 (Figure 2.12). The Fc protein expressed from this plasmid was comprised of the C_H2 and C_H3 domains of the human IgG1 heavy chain. Intracellular cleavage of this sequence occurs after Ser20 and leads to the secretion of the protein to the extracellular medium (Figure 2.12). As in the sequence shown in Figure 2.12, Ile-Ser-Ala remains at the N-terminus of the secreted Fc protein after the IL2 signal sequence is cleaved. The DNA sequence ATATCGGCC encoding Ile-Ser-Ala at the N-terminus was replaced with GCAAAGACC, encoding Ala-Lys-Thr (the optimized sequence for PLP-mediated transamination) using a Quikchange site-directed mutagenesis kit (Stratagene, La Jolla, CA). Moreover, the ATG following these 9 bases was also changed to ACG to eliminate the potential of having another translation initiation site. This was accomplished via two rounds of Quikchange site-directed mutagenesis: the first round mutated ISA to AKT and the second mutated M to T. The sequences of

Figure 2.12. Sequence of IL2ss and human IgG1 Fc in expression vector from InVivogen. The sequence of the IL2ss (grey) and human IgG1 Fc (upper case letters) is shown with introns (lower case letters) inserted between hinge and C_H2 and between C_H2 and C_H3 (red). The mutated region is in bold. (Figure adapted from Ref. [1]).

mutagenic and sequencing primers used in this study are listed in Table 2.

The polymerase chain reaction (PCR) mixture was composed of 1 μL of 50 ng/μL plasmid template, 5 μL of each primer (25 ng/μL), 1 μL of dNTP mixture, 5 μL of 10x buffer, 1 μL of Pfu-Turbo DNA polymerase (2.5 units/μL) and 33 μL of dH_2O. The reaction was started with 2 min at 95 °C to predenature the template, followed by 18 cycles of 30 sec at 95 °C, 1 min at 55 °C and 6 min at 70 °C. The PCR ended with final polymerization at 70 °C for 10 min, and the reaction mixture was left at 10 °C until the next step. After the PCR, 1 μL of DpnI (10 units/μL) was added and the mixture was incubated at 37 °C for 2 h to degrade the original unmodified plasmid templates. After DpnI digestion, 2 μL of the mixture was used to transform *E. coli* XL1-Blue competent cells by heat-shock following the manufacturer's protocol. The transformed *E. coli* XL1-Blue was spread on LB plates containing Zeocin (Fast-Media Zeo Agar, InvivoGen) and incubated at 37 °C overnight (~16 h). Colonies were selected and grown in 5 mL terrific broth (TB) media containing

Table 2. Primer sequences used for construction of plasmid expressing AKT-Fc and sequencing primers.

Purpose	Primers*
Mutating ISA to AKT	5'-GCACTAAGTCTTGCACTTGTCACGAATTCG**GCAAAGACC**ATGGTTAGATCTGACAAAACT-3'
	5'-ATGTGTGAGTTTTGTCAGATCTAACCAT**GGTCTTTGC**CGAATTCGTGACAAGTGCAAGAC-3'
Mutating M to T	5'-TGTCACGAATTCGGCAAAGACC**ACG**GTTAGATCTGA-3'
	5'-AGTTTTGTCAGATCTAAC**CGT**GGTCTTTGCCGAATTC-3'
Sequencing	5'-TGCTTGCTCAACTCTACGTC-3'
	5'-TTGCAGCTTATAATGGTTACAAA-3'

*The mutated sites are in bold.

Zeocin (Fast-Media Zeo TB, InvivoGen) at 37 °C overnight (12-16 h). Plasmid DNA was isolated using a QIAprep Spin Miniprep Kit (Qiagen). The DNA sequences were confirmed by gene sequencing. The sequences of the primers used for sequencing are listed in Table 2.

2.5.3 General procedure for expression of AKT-Fc

The plasmids expressing AKT-Fc constructed above were transiently transfected into human embryonic kidney (HEK) 293T cells using Lipofectamine 2000 (Invitrogen) in Opti-MEM medium following the protocol from Invitrogen. The cells were incubated at 37 °C in 5% CO_2. After 2 days, media were collected, and secreted antibodies were purified using protein G affinity chromatography, according to the procedure from the manufacturer (Pierce). Fresh media was added, and cultures were grown for additional 3 days, after which additional antibodies were harvested and purified as above. Purified protein was buffer exchanged into PBS using Amicon Ultra 4 mL 10 kDa MWCO (Millipore) centrifugal ultrafiltration membranes. Purity was evaluated by SDS-PAGE with Coomassie staining (Figure 2.13).

2.5.4 General procedure for PLP transamination

The 2x protein stock solutions were prepared at 10-40 μM using 25 mM phosphate buffer at pH 6.5. The 2x (200 mM) PLP stock solutions were prepared in 25 mM phosphate buffer and the pH of the solution was adjusted to 6.5 using NaOH solution. Protein and PLP stock solutions were mixed in equal volumes. The reaction mixture was briefly agitated to ensure mixing and then incubated without further agitation at 37 ˚C for 1 h. After incubation, the PLP was removed using NAP Sephadex size exclusion columns (GE Healthcare). The resulting keto-Fc solution was then

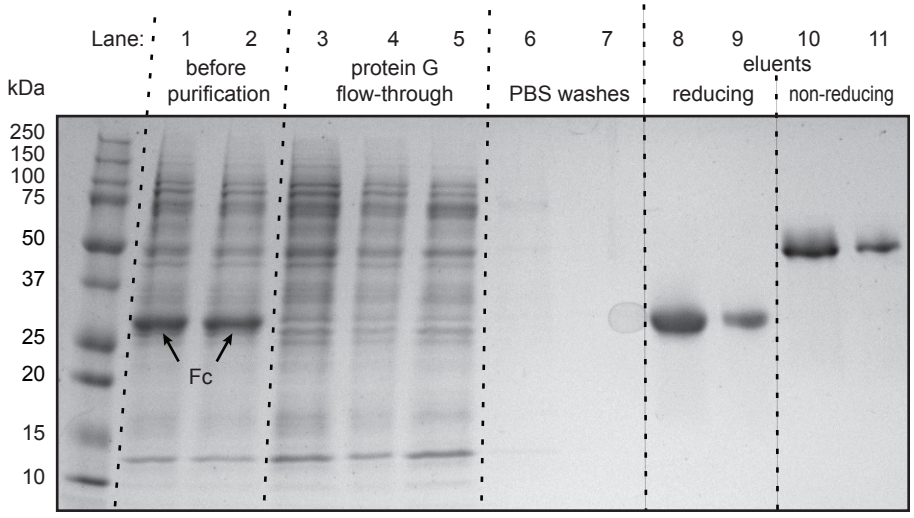

Figure 2.13. SDS-PAGE analysis of the Fc protein collected and purified using a protein G column. Lanes 1 and 2 represent all secreted proteins collected before protein G purification. Lanes 3-7 are the flow-through and PBS wash fractions from the protein G column. These fractions contained all other proteins except the Fc (~30 kDa). Lanes 8 and 9 were the eluent from protein G column, analyzed under reducing conditions. The reduced Fc monomers appear at ~30 kDa. Lanes 10 and 11 were the same samples as lanes 8 and 9, but were run under non-reducing conditions. Fc dimers are evident at ~ 55 kDa. Samples in all lanes except 10 and 11 were prepared with a reducing loading buffer (β-mercaptoethanol). (Figure adapted from Ref. [1]).

concentrated and buffer exchanged with 25 mM phosphate buffer (pH 6.5), using Millipore 0.5 or 4 mL spin concentrators (MWCO 10 kDa), following the protocol from the manufacturer.

2.5.5 General procedure for hydrazone and oxime formation

The reaction was performed with 10-40 μM keto-Fc and $RONH_2$ or $R(CO)NHNH_2$ at varied concentrations. For the analysis of PLP transamination efficiency, $BnONH_2$ and AlexaFluor 488-ONH_2 were added to keto-Fc to a final concentration of 100 mM and 80 μM, respectively. For the attachment of an oxidative coupling partner, aniline-ONH_2 was added to a final concentration of 25 mM. To make Fc-aptamer constructs, keto-Fc was mixed with the hydrazide-aptamer (aptamer sequences shown in table 3) at a final concentration of 100 μM in the presence of 100 mM aniline, which is known to enhance the rate of hydrazone formation [76]. The reaction mixture was incubated at RT for 18-50 h. All the reactions were carried out in 25 mM phosphate buffer (pH 6.5), except for oxime formation with aniline-ONH_2, which was done in 25 mM phosphate buffer (pH 5). Following the reaction, the small molecules were removed using NAP Sephadex size exclusion columns (GE Healthcare) and the resulting product mixtures were concentrated using Millipore 0.5 or 4 mL spin concentrators (MWCO 10 kDa), following the protocol from the manufacturer. The percent reaction conversion for the Fc samples with small molecules was analyzed using LCMS and the modification with large molecules was analyzed using SDS-PAGE with Coomassie staining.

Table 3. Sequence of DNA oligonucleotides used in the protein modification.

DNA oligonucleotides	Sequence
Sgc8c (41-mer)	5'-ATCTAACTGCTGCGCCGCCGGGAAAATACTGTACGGTTAGA-3'
TD05.1 (37-mer)	5'-AGGAGGATAGTTCGGTGGCTGTTCAGGGTCTCCTCCT-3'
M2M2 (41-mer)	5'-CCCTAGAGTGAGTCGTATGACCCTAGAGTGAGTCGTATGAA-3'

2.5.6 General procedure for oxidative coupling

To a solution of 10-40 μM Fc-aniline (**9**) in 25 mM phosphate buffer (pH 6.5) was added a solution of aminophenol-2k PEG (**10a**) or aminophenol-aptamer (**10b**) (aptamer sequences shown in table 3) to a final concentration of 100 μM. Sodium periodate (Sigma-Aldrich) was dissolved to a concentration of 10 mM in 25 mM phosphate buffer (pH 6.5). The sodium periodate was then added to the reaction mixture to reach a final concentration of 1 mM, and the reaction was allowed to proceed for 2 min at RT. In some cases, a solution of mannose was also added to a final concentration of 10 mM or 100 mM before addition of the periodate solution. The resulting protein samples were purified on NAP Sephadex size exclusion columns (GE Healthcare) and concentrated using Millipore 0.5 or 4 mL spin concentrators (MWCO 10 kDa), following the protocol from the manufacturer.

2.5.7 Purification of Fc-aptamer constructs

The resulting Fc-DNA conjugates from both hydrazone formation and oxidative coupling were purified from unreacted Fc and DNA using anion exchange HPLC with a 20-min gradient of 100 % buffer A to 5% buffer A 95% buffer B, where buffer A is 25 mM sodium phosphate buffer pH 6.5 and buffer B is 25 mM sodium phosphate buffer pH 6.5 with 1 M NaCl. The fractions collected were analyzed using SDS-PAGE and those containing Fc-DNA constructs were combined and concentrated using Millipore 0.5 mL spin concentrators (MWCO 10 kDa).

2.5.8 Flow cytometry analysis for cells binding specificities

Flow cytometry was used to determine the binding ability of all the Fc-aptamer constructs. All experiments were carried out in triplicate. For all samples, 100 μL of $3x10^6$ cells/mL of Jurkat, Ramos, and U266 were used, suspended in binding buffer (4.5 g/L glucose, 5 mM $MgCl_2$, 0.1 mg/mL yeast tRNA (Sigma) and 1 mg/mL BSA (Fisher) in Dulbecco's PBS with calcium chloride and magnesium chloride (Invitrogen)). To these cells were added 10 μL of a series of 400 nM Fc-aptamer construct solutions. The samples were then incubated on ice for 1 h. The resulting cells were washed with 500 μL of binding buffer and resuspended in an additional 100 μL of binding buffer. Anti-human IgG1 antibody (specific for the Fc domain) with FITC conjugated (Sigma) was then added to a final concentration of ~ 0.30 μM. Cells were incubated for 1 h on ice in the dark, washed with 500 μL of binding buffer, and resuspended in 200 μL of binding buffer. The cells were analyzed by flow cytometry (Becton Dickinson FACScalibur) to determine the amount of FITC fluorescence. For each sample, 10,000 cells were counted. A FACSCalibur flow cytometer (BD Biosciences, USA) equipped with 488 and 633 nm lasers were used for all flow cytometry measurements, usage courtesy of Prof. Carolyn Bertozzi (UC Berkeley). Data was analyzed using FlowJo 8.0 (TreeStar, Ashland, OR).

2.5.9 ELISA for C1q binding

The binding of human C1q to AKT-Fc, chemically-modified Fc, and Fc-DNA conjugates was assessed by an ELISA binding assay, adjusted from a published procedure [78]. High binding Costar 96-well plates (Corning, NY) were coated with varying concentrations of Fc samples in coating buffer (0.05 M sodium carbonate buffer, pH 9) overnight at 4 °C. All samples were run in duplicate. The plates were washed three times after each incubation step with 300 μL of PBST buffer (PBS, containing 0.05% Tween 20, pH 7.4). After coating, the plates were blocked with 200 μL of ELISA diluent (0.1 M Na_3PO_4, 0.1 M NaCl, 0.1% gelatin, 0.05% Tween 20, 0.05% Pro-

Clin300) for 1 h at RT, followed by incubation with 100 µL of 2 µg/mL human C1q (Quidel, San Diego, CA) in ELISA diluent for 2 h. Then, 100 µL of a 1:400 dilution of sheep anti-human C1q peroxidase-conjugated antibody (Abcam) in ELISA diluent was added and incubated at RT for 1 h. The plates were developed with 100 µL of 3,3',5,5'-tetramethylbenzidine (TMB) substrate buffer (Sigma) at RT for 15 min. The reaction was stopped upon the addition of 100 µL of stop reagent for TMB substrate (Sigma), and the absorbance at 450 nm was measured using a Spectramax M3 microplate reader (Molecular Devices, Sunnyvale, CA). The obtained Hill plots displayed different amplitudes for the binding curves, which were taken to arise from different amounts of Fc samples binding to the wells. The plots were therefore normalized based on their maximum overall absorbance.

2.5.10 ELISA for FcR binding

The binding of human FcRIIa and FcRIIIa to unmodified Fc and Fc-DNA conjugates was assessed by an ELISA binding assay, adjusted from a published procedure [79]. High binding Costar 96-well plates (Corning, NY) were coated with 100 µL of 2 µg/mL FcRIIa or FcRIIIa in PBS overnight at 4 °C or for 2 h at RT. The plates were washed three times after each incubation step with 200 µL of PBST buffer. After coating, the plates were blocked with 200 µL of PBS+3% BSA (w/v) overnight at 4 °C or for 2 h at RT, followed by 2 h incubation at RT with 100 µL of 3-fold serial dilution in PBST buffer of unmodified Fc or Fc-DNA samples, starting from 200 nM. Then, 100 µL of a 1:2000 dilution of HRP-conjugated $F(ab')_2$ fragment of anti-human Fc (Jackson Immunoresearch) in PBST buffer was added and incubated at RT for 1 h. The plates were developed with 100 µL of 3,3',5,5'-tetramethylbenzidine (TMB) substrate buffer (Sigma) at RT until blue color was developed. The reaction was stopped upon the addition of 100 µL of stop reagent for TMB substrate (Sigma), and the absorbance at 450 nm was measured using a Spectramax M3 microplate reader (Molecular Devices, Sunnyvale, CA). The obtained Hill plots were calculated using Origin 8.0.

2.5.11 Generation of Fc-DNA coated beads

Streptavidin-coated green fluorescent polystyrene beads or Streptavidin Fluoresbrite® YG Microspheres (Polysciences, Warrington, PA) were washed three times with binding buffer (0.1 M phosphate buffer, 0.15 M NaCl, 10 mg/mL BSA, pH 7.4) and then resuspended into binding buffer to the density of $5x10^8$ particles/mL. To the beads solution, the biotin-5T-C2 oligonucleotides (complementatry strand of M2 sequence with biotin functionalized at the 5' end and five thymines spacer in between) were added to a final concentration of 2 µM and incubated at 4 °C for 30 min on a rotator. The beads were washed three times with binding buffer and then resuspended in PBS containing 10 mg/ mL BSA and 0.1% v/v Tween-20. The Fc-DNA was added to the final concentration of 100 nM and incubated overnight at 4 °C or for 30 min at RT on a rotator. The beads were washed three times in Hanks' balanced salt solution (HBSS without calcium or magnesium; Sigma-Aldrich, St Louis, MO) and used in phagocytosis experiment.

2.5.12 Neutrophils phagocytosis

Neutrophils were isolated from human blood according to the published protocol [82] on the day of use and resuspended in HBSS with calcium. Neutrophils were then incubated with Fc-DNA coated beads and also the negative controls (plain beads and beads coated with DNA only) in a ratio of 1:5 of cells:beads with end-over-end rotation for 1 h at RT. The cells were washed twice

to remove unbound beads. Each cell washing step involved spinning down at 200 x*g* for 6 min for cells to pellet, discarding the supernatant, and resuspending cells in PBS. The neutrophils were fixed by incubation with 2% formaldehyde for 10 min at RT, followed by a cell washing step, and then characterized by flow cytometry and microscopy. This experiment was done in collaboration with The Heinrich Lab at UC Davis.

2.5.13 Synthesis of hydrazide-DNA (5)

The synthesis of hydrazide-DNA (**5**) is outlined in Figure 2.14. The 5' thiol DNA oligonucleotide supplied by IDT was reduced in 40 mM TCEP in PBS, pH 7.4 for 2 h at RT. The TCEP was removed using NAP Sephadex size exclusion columns (GE Healthcare). Ten equivalents of 3, 3'-*N*-(ε-maleimidocaproic acid) hydrazide, trifluoroacetic acid salt (EMCH, Pierce), were added to a sample of reduced 5' thiol oligonucleotide in PBS, pH 7.4. The reaction mixture was incubated for 2.5 h at RT. The resulting hydrazide-DNA (**5**) was purified using NAP Sephadex size exclusion columns (GE Healthcare), followed by spin concentration with Millipore 0.5 mL spin concentrators (MWCO 10 kDa).

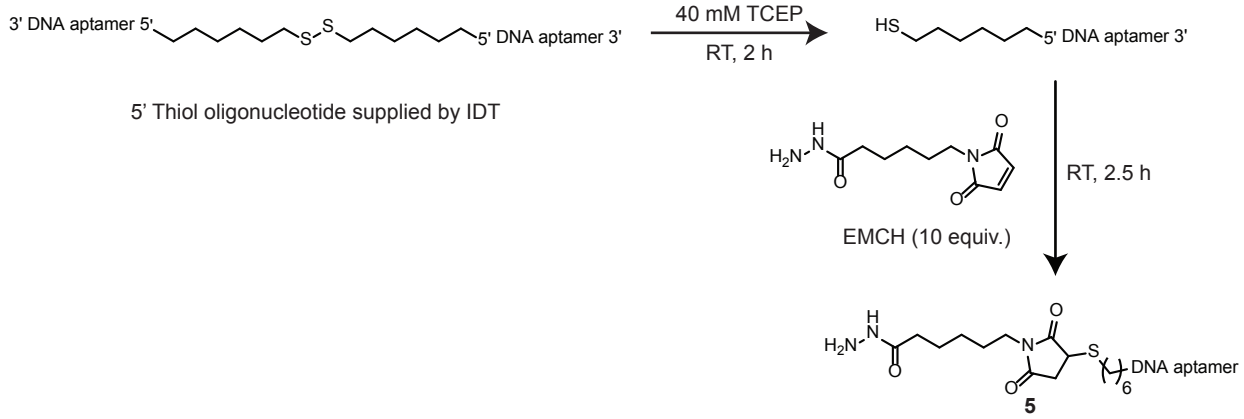

Figure 2.14. Scheme for the synthesis of hydrazide-DNA oligonucleotide **5**. (Figure adapted from Ref. [1]).

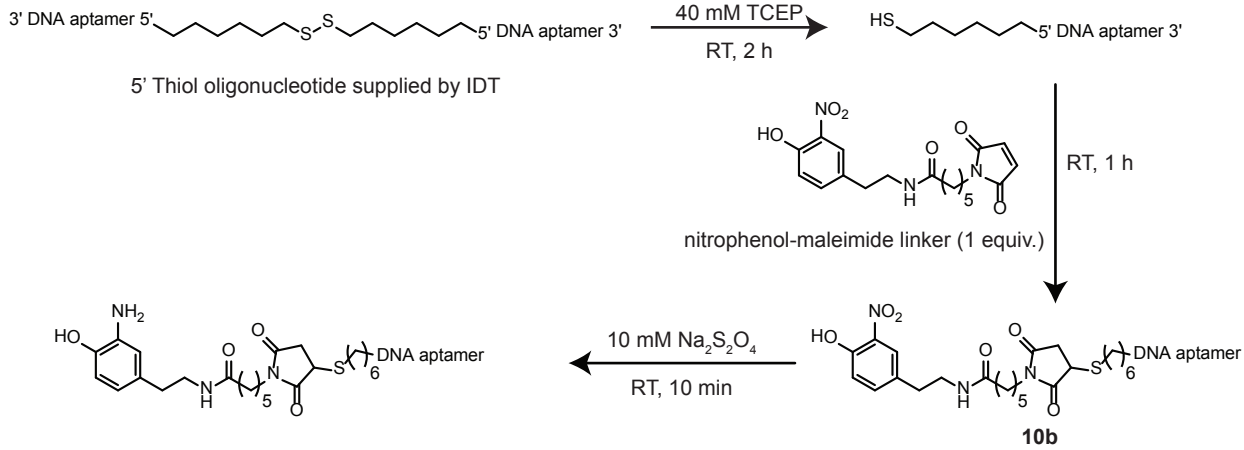

Figure 2.15. Scheme for the synthesis of aminophenol-DNA oligonucleotide **10b**. (Figure adapted from Ref. [1]).

2.5.14 Synthesis of aminophenol-DNA (10b)

The synthesis of aminophenol-DNA (**10b**) is outlined in Figure 2.15. The 5' thiol DNA oligonucleotide supplied by IDT was reduced in 40 mM TCEP in PBS, pH 7.4 for 2 h at RT. The TCEP was removed using NAP Sephadex size exclusion columns (GE Healthcare). The resulting product was buffered exchanged into 25 mM phosphate buffer at pH 8 by spin concentration with Millipore 0.5 mL spin concentrators (MWCO 10 kDa). Approximately one equivalent of a nitrophenol-maleimide linker was added to the reduced 5' thiol DNA oligonucleotide and the reaction was carried out in 25 mM phosphate buffer pH 8 at RT for 1 h. The resulting nitrophenol-DNA was then purified using NAP Sephadex size exclusion columns (GE Healthcare), followed by spin concentration with Millipore 0.5 mL spin concentrators (MWCO 10 kDa) into PBS. The nitro group was reduced to the corresponding aniline in the presence of 10 mM sodium dithionite at RT for 10 min. The final product aminophenol-DNA was purified using NAP Sephadex size exclusion columns (GE Healthcare), followed by spin concentration with Millipore 0.5 mL spin concentrators (MWCO 10 kDa) into 25 mM phosphate buffer pH 6.5 for subsequent conjugation with Fc proteins.

2.5.15 Synthesis of aniline-ONH_2 (8)

To (Boc-aminooxy)acetic acid (280 mg, 1.5 mmol) dissolved in methylene chloride was added dicyclohexylcarbodiimide (362 mg, 1.7 mmol) and *N*-hydroxysuccinimide (168 mg, 1.5 mmol). After 15 min with stirring, the precipitate was filtered through Celite, followed by a 0.22 µm PVDF syringe filter. To the remaining solution was added 2-(4-aminophenyl)ethylamine (200 mg, 1.5 mmol) and triethylamine (400 mg, 4 mmol). After 1 h of stirring the solution was concentrated under reduced pressure and applied to a silica gel column. Purification using ethyl acetate as the mobile phase afforded approximately 200 mg of the desired product (45% yield). ^{1}H NMR (400 MHz, $CDCl_3$) δ 1.4 (s, 9H), 2.7 (t, 2H), 3.4 (q, 2H), 3.5 (br s, 2H), 4.2 (s, 2H), 6.6 (d, 2H), 7.0 (d, 2H), 8.1 (br s, 1H), 8.5 (s, 1H). The Boc group was removed via exposure to 1:1 trifluoroacetic acid:methylene chloride for 10 min, after which the solvent was removed under a stream of nitrogen. The resulting oil was placed under high vacuum overnight, dissolved to 100 mM in water, and stored frozen until used. To avoid precipitation of protein, it was necessary to neutralize the residual trifluoroacetic acid by adding phosphate buffer before addition to protein-containing solutions.

2.5.16 Synthesis of 2k PEG-aminophenol (10a)

2k PEG-aminophenol (**10a**) was synthesized according to a published protocol [52].

2.5.17 Synthesis of nitrophenol-maleimide linker

To tyramine was added dropwise one equivalent of fuming nitric acid at 4 °C using trifluoroacetic acid as the solvent, resulting in quantitative conversion to *o*-nitrotyramine. The resulting *o*-nitrotyramine (50 mg, 0.27 mmol) was dissolved in 10 mL DMF and treated with one equivalent of succinimidyl-6-*N*-maleimidohexanoate [81] along with sufficient triethylamine to reach pH 8. Multiple equivalents of triethylamine were required due to residual trifluoroacetic acid from the nitration step. After 45 min, 20 mL of 0.1 M $NaHSO_4$ were added to the reaction. The product was extracted with methylene chloride, dried over Na_2SO_4, and purified on a silica column using ethyl acetate as the mobile phase. The isolated yield was 33%. ^{1}H NMR (300 MHz, $CDCl_3$) δ 1.2 (m, 2H), 1.6 (m, 4H), 2.1 (t, 2H), 2.8 (t, 2H), 3.5 (t, 4H), 5.6 (br s, 1H), 6.6 (s, 2H), 7.0 (d, 1H), 7.5 (d,

1H), 8.0 (s, 1H), 10.5 (br s, 1H).

2.5.18 Instrumentation and sample analysis

2.5.18.1 Liquid chromatography mass spectrometry (LCMS)

Fc protein bioconjugates were analyzed using an Agilent 1200 liquid chromatograph (LC; Santa Clara, CA) that was connected in-line with an LTQ Orbitrap XL hybrid mass spectrometer equipped with an electrospray ionization source (ESI; Thermo Fisher Scientific, Waltham, MA), located in the QB3/Chemistry Mass Spectrometry Facility at UC Berkeley. The LC was equipped with a reversed-phase C8 column (100 mm x 1.0 mm, 5 μm particles, Restek, Bellefonte, PA). Solvent A was 0.1% formic acid/99.9% water and solvent B was 0.1% formic acid/99.9% acetonitrile (v/v). For each sample, approximately 200 picomoles of protein analyte were injected onto the column. Following sample injection, analyte trapping was performed for 5 min with 99.5% A. The elution program consisted of a linear gradient from 30% to 95% B over 19.5 min, isocratic conditions at 95% B for 5 min, a linear gradient to 0.5% B over 0.5 min, and then isocratic conditions at 0.5% B for 9.5 min. Solvent (Milli-Q water) blanks were run between samples, and the autosampler injection needle was rinsed with Milli-Q water after each sample injection, to avoid cross-contamination between samples. Mass spectra were recorded in the positive ion mode over the range m/z = 450-2000. Raw mass spectra were processed using Xcalibur software (version 2.0.7 SP1, Thermo) and protein charge state distributions were deconvoluted using ProMass software (version 2.5 SR-1, Novatia, Monmouth Junction, NJ).

2.5.18.2 High Performance Liquid Chromatography (HPLC)

HPLC was performed on an Agilent 1100 Series HPLC System (Agilent Technologies, USA). Sample analysis for all HPLC experiments was achieved with an inline diode array detector (DAD). Anion exchange HPLC of Fc-DNA conjugates was accomplished using a Biosep-DE-AE-PEI column (Phenomenex).

2.5.18.3 Gel Analyses

For protein analysis, sodium dodecyl sulfate-polyacrylamide gel electrophoresis (SDS-PAGE) was carried out on a Mini-Protean apparatus from Bio-Rad (Hercules, CA), following the protocol of Laemmli [80]. The reducing protein electrophoresis samples were heated for 10 min at 95 °C in the presence of β-mercaptoethanol to ensure reduction of any disulfide bonds. Gels were run for 40 min at 200 V to allow good separation of bands. Commercially available markers (Fisher) were applied to at least one lane of each gel for assignment of apparent molecular masses. Visualization of protein bands was accomplished by staining with Coomassie Brilliant Blue R-250 (Bio-Rad). For fluorescent protein conjugates, visualization was accomplished on a Typhoon 9410 (Amersham Biosciences).

2.6 References

1. Netirojjanakul, C.; Witus, L. S.; Behrens, C. R.; Weng, C. H.; Iavarone, A. T.; Francis, M. B. *Chem. Sci*. **2013**, *4*, 266–272.
2. Walsh, G. *Nat. Biotechnol.* **2010**, *28*, 917–924.
3. Carter, P. *J. Exp. Cell Research* **2011**, *317*, 1261–9.
4. Huang, C. *Curr. Opin. Biotechnol.* **2009**, *20*, 692–699.
5. Roopenian, D. C.; Akilesh, S. *Nat. Rev. Immunol.* **2007**, *7*, 715–725.
6. Ghetie, V.; Ward, E. S. *Ann. Rev. Immunol.* **2000**, *18*, 739–766.
7. Iannello, A.; Ahmad, A. *Cancer Metastasis Rev.* **2005**, *24*, 487–499.
8. Gelderman, K. A.; Tomlinson, S.; Ross, G. D.; Gorter, A. *Trends in Immunology* **2004**, *25*, 158–164.
9. Shields, R. L.; Namenuk, A. K.; Hong, K.; Meng, Y. G.; Rae, J.; Briggs, J.; Xie, D.; Lai, J.; Stadlen, A.; Li, B.; Fox, J. A.; Presta, L. G. *J. Biol. Chem.* **2001**, *276*, 6591–6604.
10. Clynes, R. A.; Towers, T. L.; Presta, L. G.; Ravetch, J. V. *Nat. Med.* **2000**, *6*, 443–446.
11. Yokota, T.; Milenic, D. E.; Whitlow, M.; Schlom, J. *Cancer Res.* **1992**, *52*, 3402–3408.
12. Hicke, B. J.; Stephens, A. W.; Gould, T.; Chang, Y.-F.; Lynott, C. K.; Heil, J.; Borkowski, S.; Hilger, C.-S.; Cook, G.; Warren, S.; Schmidt, P. G. *J. Nucl. Med.* **2006**, *47*, 668–678.
13. Low, S. C.; Nunes, S. L.; Bitonti, A. J.; Dumont, J. A. *Hum. Reprod.* **2005**, *20*, 1805–1813.
14. Bitonti, A. J.; Dumont, J. A.; Low, S. C.; Peters, R. T.; Kropp, K. E.; Palombella, V. J.; Stattel, J. M.; Lu, Y.; Tan, C. A.; Song, J. J.; Garcia, A. M.; Simister, N. E.; Spiekermann, G. M.; Lencer, W. I.; Blumberg, R. S. *Proc. Natl. Acad. Sci. U.S.A.* **2004**, *101*, 9763–9768.
15. Wuellner, U.; Gavrilyuk, J. I.; Barbas III, C. F. *Angew. Chem. Int. Ed. Engl.* **2010**, *49*, 5934–5937.
16. Rader, C.; Sinha, S. C.; Popkov, M.; Lerner, R. A.; Barbas III, C. F. *Proc. Natl. Acad. Sci.* **2003**, *100*, 5396–5400.
17. Ellington, A. D.; Szostak, J. W. *Nature* **1990**, *346*, 818–822.
18. Tuerk, C.; Gold, L. *Science* **1990**, *249*, 505–510.
19. Zuckermann, R. N.; Kodadek, T. *Curr. Opin. Mol. Ther.* **2009**, *11*, 299–307.
20. Thayer, A. M. *Chem. Eng. News*. **2011**, *89*, 13–20.
21. Henchey, L. K.; Jochim, A. L.; Arora, P. S. *Curr. Opin. Chem. Biol.* **2008**, *12*, 692–697.
22. Boohaker, R. J.; Lee, M. W.; Vishnubhotla, P.; Perez, J. M.; Khaled, A. R. *Curr. Med. Chem.* **2012**, *19*, 3794–804.
23. Schafmeister, C. E.; Po, J.; Verdine, G. L. *J. Am. Chem. Soc.* **2000**, *122*, 5891–5892.
24. Walensky, L. D.; Kung, A. L.; Escher, I.; Malia, T. J.; Barbuto, S.; Wright, R. D.; Wagner, G.; Verdine, G. L.; Korsmeyer, S. J. *Science.* **2004**, *305*, 1466–1470.

25. Verdine, G. L.; Hilinski, G. J. *Meth. Enzymology* **2012**, *503*, 3–33.

26. Heinis, C.; Rutherford, T.; Freund, S.; Winter, G. *Nat. Chem. Biol.* **2009**, *5*, 502–507.

27. Shaunak, S.; Godwin, A.; Choi, J.; Balan, S.; Pedone, E.; Vijayarangam, D., Heidelberger, S.; Teo, I.; Zloh, M.; Brocchini, S. *Nat. Chem. Biol.* **2006**, *2*, 312–313.

28. Junutula J. R., Raab, H.; Clark, S.; Bhakta, S.; Leipold, D. D.; Weir, S.; Chen, Y.; Simpson, M.; Tsai, S. P.; Dennis, M. S.; Lu, Y.; Meng, Y. G.; Ng, C.; Yang, J.; Lee, C. C.; Duenas, E.; Gorrell, J.; Katta, V.; Kim, A.; McDorman, K.; Flagella, K.; Venook, R.; Ross, S.; Spencer, S. D.; Wong, W. L.; Lowman, H. B.; Vandlen, R.; Sliwkowski, M. X.; Scheller, R. H.; Polakis, P.; and Mallet, W. *Nat. Biotech.* **2008**, *26*, 925–932.

29. Xiao, J.; Chen, R.; Pawlicki, M. A.; Tolbert, T. J. *J. Am. Chem. Soc.* **2009**, *131*, 13616–13618.

30. Wu, P., Shui, W.; Carlson, B. L.; Hu, N.; Rabuka, D.; Lee, J.; Bertozzi, C. R. *Proc. Nat. Acad. Sci. USA.* **2009**, *106*, 3000–3005.

31. Hofer, T; Thomas, J. D.; Burke, T. R.; Rader, C. Hofer, T.; Thomas, J. D.; Burke, T. R.; Rader, C. *Proc. Nat. Acad. Sci. USA.* **2008**, *105*, 12451–12456.

32. Hutchins, B. M.; Kazane, S. A.; Staflin, K.; Forsyth, J. S.; Felding-Habermann, B.; Schultz, P. G.; Smider, V. V. *J. Mol. Biol.* **2011**, *406*, 595-603.

33. Hutchins, B. M.; Kazane, S. A.; Staflin, K.; Forsyth, J. S.; Felding-Habermann, B.; Smider, V. V.; Schultz, P. G. *Chem. Biol.* **2011**, *18*, 299–303.

34. Tian, F.; Lu, Y.; Manibusan, A.; Sellers, A.; Tran, H.; Sun, Y.; Phuong, T.; Barnett, R.; Hehli, B.; Song, F.; Deguzman, M. J.; Ensari, S.; Pinkstaff, J. K.; Sullivan, L. M.; Biroc, S. L.; Cho, H.; Schultz, P. G.; Dijoseph, J.; Dougher, M.; Ma, D.; Dushin, R.; Leal, M.; Tchistiakova, L.; Feyfant, E.; Gerber, H.-P.; Sapra, P. *Proc. Natl. Acad. Sci. U. S. A*. **2014**, *111*, 1766–1771.

35. Salfeld, J. G. *Nat. Biotechnol*. **2007**, *25*, 1369–1372.

36. Correia, I. R. *mAbs*. **2010**, *2*, 221–232.

37. Murphy, K. P.; Travers, P.; Walport, M.; Janeway, C. *Janeway's immunobiology.* **2008**. Garland Science.

38. Tong, G. J.; Hsiao, S. C.; Carrico, Z. M.; Francis, M. B. *J. Am. Chem. Soc.* **2009**, *131*, 11174–11178.

39. Gilmore, J. M.; Scheck, R. A.; Esser-Kahn, A. P.; Joshi, N. S.; Francis, M. B. *Angew. Chem. Int. Ed.* **2006**, *45*, 5307–5311.

40. Scheck, R. A.; Francis, M. B. *ACS Chem. Biol.* **2007**, *2*, 247–251.

41. Scheck, R. A.; Dedeo, M. T.; Iavarone, A. T.; Francis, M. B. *J. Am. Chem. Soc.* **2008**, *130*, 11762–11770.

42. Witus, L. S.; Moore, T.; Thuronyi, B. W.; Esser-Kahn, A. P.; Scheck, R. A.; Iavarone, A. T.; Francis, M. B. *J. Am. Chem. Soc.* **2010**, *132*, 16812–16817.

43. Snell, E. E. *J. Am. Chem. Soc.* **1945**, *67*, 194–197.

44. Dixon, H. B. F. *J. Protein Chem.* **1984**, *3*, 99–108.

45. Dixon, H. B. F.; Fields, R. *Methods Enzymol.* **1972**, *25*, 409–419.

46. Witus, L.S.; Netirojjanakul, C.; Palla, K.S.; Muehl, E.M.; Weng, C.H.; Iavarone, A.T.; Francis, M.B. *J. Am. Chem. Soc*. **2013**, *135*, 17223–17229.

47. Jencks, W. P. *J. Am. Chem. Soc.* **1959**, *81*, 475–481.

48. Cornish, V. W.; Hahn, K. M.; Schultz, P. G. *J. Am. Chem. Soc.* **1996**, *118*, 8150–8151.

49. Mahal, L. K.; Yarema, K. J.; Bertozzi, C. R. *Science* **1997**, *276*, 1125–1128.

50. Kalia, J.; Raines, R. *Angew. Chem. Int. Ed.* **2008**, *47*, 7523–7526.

51. Hooker, J. M.; Esser-Kahn, A. P.; Francis, M. B. *J. Am. Chem. Soc.* **2006**, *128*, 15558–15559.

52. Behrens, C. R.; Hooker, J. M.; Obermeyer, A. C.; Romanini, D. W.; Katz, E. M.; Francis, M. B. *J. Am. Chem. Soc.* **2011**, *133*, 16398–16401.

53. Obermeyer, A. C.; Jarman, J. B.; Netirojjanakul, C.; El Muslemany, K.; Francis, M. B. *Angew. Chem. Int. Ed. Engl*. **2014**, *53*, 1057–1061.

54. Smyth, D. S.; Utsumi, S. *Nature*. **1967**, *216*, 332–335.

55. Moorhouse, K. G.; Nashabeh, W.; Deveney, J.; Bjork, N. S.; Mulkerrin, M. G.; Ryskamp, T. *J. Pharm. Biomed. Anal*. **1997**, *16*, 593–603.

56. Lau, H.; Pace, D.; Yan, B.; McGrath, T.; Smallwood, S.; Patel, K.; Park, J.; Park, S. S.; Latypov, R. F. *J. Chromatography B*. **2010**, *878*, 868–876.

57. Watt, G. M.; Lund, J.; Levens, M.; Kolli, V. S. K.; Jefferis, R.; Boons, G.-J. S. *Chem. Biol*. **2003**, *10*, 807–814.

58. Wei, Y.; Li, C.; Huang, W.; Li, B.; Strome, S.; Wang, L.-X. *Biochemistry*. **2008**, *47*, 10294–1304.

59. Shinkawa, T., *et al*. *J. Biol. Chem*. **2003**, *278*, 3466–3473.

60. Shields, R. L., *et al*. *J. Biol. Chem*. **2002**, *277*, 26733–26740.

61. Li, H., *et al*. *Nat. Biotechnol*. **2006**, *24*, 210–215.

62. Kleemann, G. R.; Beierle, J.; Nichols, A. C.; Dillon, T. M.; Pipes, G. D.; Bondarenko, P. V. *Anal. Chem*. **2008**, *80*, 2001–2009.

63. Fang, X.; Tan, W. *Acc. Chem. Res.* **2010**, *43*, 48–57.

64. Jayasena, S. D. *Clin. Chem.* **1999**, *45*, 1628–1650.

65. Nimjee, S. M.; Rusconi, C. P.; Sullenger, B. A. *Ann. Rev. Med.* **2005**, *56*, 555–583.

66. Bouchard, P. R.; Hutabarat, R. M.; Thompson, K. M. *Ann. Rev. Pharm. Tox.* **2010**, *50*, 237–257.

67. Shangguan, D.; Li, Y.; Tang, Z.; Cao, Z. C.; Chen, H. W.; Mallikaratchy, P.; Sefah, K.; Yang, C. J.; Tan, W. *Proc. Natl. Acad. Sci.* **2006**, *103*, 11838–11843.

68. Shangguan, D.; Tang, Z.; Mallikaratchy, P.; Xiao, Z.; Tan, W. *Chembiochem* **2007**, *8*, 603–606.

69. Shangguan, D.; Cao, Z.; Meng, L.; Mallikaratchy, P.; Sefah, K.; Wang, H.; Li, Y.; Tan, W. *J. Proteome Res.* **2008**, *7*, 2133–2139.

70. Mallikaratchy, P.; Tang, Z.; Kwame, S.; Meng, L.; Shangguan, D.; Tan, W. *Mol. Cell. Proteomics* **2007**, *6*, 2230–2238.

71. Mallikaratchy, P. R.; Ruggiero, A.; Gardner, J. R.; Kuryavyi, V.; Maguire, W. F.; Heaney, M. L.; McDevitt, M. R.; Patel, D. J.; Scheinberg, D. A. *Nucl. Acids Res.* **2011**, *39*, 2458–2469.

72. Shi, H.; He, X.; Wang, K.; Wu, X.; Ye, X.; Guo, Q.; Tan, W.; Qing, Z.; Yang, X.; Zhou, B. *Proc. Natl. Acad. Sci. U.S.A.* **2011**, *108*, 3900–3905.

73. Douglas, S. M.; Bachelet, I.; Church, G. M. *Science* **2012**, *335*, 831–834.

74. Luo, Y.-L.; Shiao, Y.-S.; Huang, Y.-F. *ACS Nano* **2011**, *5*, 7796–7804.

75. Stephanopoulos, N.; Tong, G. J.; Hsiao, S. C.; Francis, M. B. *ACS Nano* **2010**, *4*, 6014–6020.

76. Dirksen, A.; Hackeng, T. M.; Dawson, P. E. *Angew. Chem. Int. Ed.* **2006**, *45*, 7581–7584.

77. Dirksen, A.; Dirksen, S.; Hackeng, T. M.; Dawson, P. E. *J. Am. Chem. Soc.* **2006**, *128*, 15602–15603.

78. Idusogie, E. E.; Presta, L. G.; Totpal, K.; Wong, P. Y.; Meng, Y. G.; Mulkerrin, M. G.; Alerts, E. *J. Immunol.* **2000**, *164*, 4178–4184.

79. Shields, R. L.; Namenuk, A. K.; Hong, K.; Meng, Y. G.; Rae, J.; Briggs, J.; Xie, D.; Lai, J.; Stadlen, A.; Li, B.; Fox, J. A.; Presta, L. G. *J. Biol. Chem.* **2001**, *276*, 6591–6604.

80. Laemmli, U. K. *Nature*. **1970**, *227*, 680–685.

81. Nielsen, O.; Buchardt, O. *Synthesis*. **1991**, *10*, 819–821.

82. Lee, C.-Y.; Herant, M.; Heinrich, V. *J. Cell Sci*. **2011**, *124*, 1106–1114.

83. Sondermann, P.; Huber, R.; Oosthuizen, V.; Jacob, U. *Nature*. **2000**, *406*, 267–273.

84. Martin, W. L.; West, A. P.; Gan, L.; Bjorkman, P. J. *Mol. Cell*. **2001**, *7*, 867–877.

85. Zuckermann, R. N. *Biopolymers* **2011**, *96*, 545–555.

86. Czajkowsky, D. M.; Hu, J.; Shao, Z.; Pleass, R. J. *EMBO Mol. Med*. **2012**, *4*, 1015–1028.

Chapter 3

Generation of Antibody-DNA conjugates for Application as Bispecific Antibodies

Abstract

This chapter describes the design and development of antibody-DNA (Ab-DNA) conjugates, which have been widely used in many applications, such as immuno PCR, proximity ligation, and DNA barcoding. Here, we describe our chemical approaches in generating these conjugates and propose their application as bispecific antibodies. First, antibodies were installed with an aniline oxidative coupling partner either site-specifically at the N-termini via transamination or at lysine residues via NHS ester chemistry. These anilines can then be coupled to aminophenol-containing DNA aptamers to produce the Ab-DNA aptamer conjugates. In the N-terminally modified conjugates, we also provide strategies to achieve chain-specific Ab modifiction using pyridoxal 5′-phosphate (PLP) or Rapoport's salt (RS) mediated N-terminal transamination reaction. The binding specificity and affinity of Ab-aptamer conjugates were demonstrated. In addition, the feasibility of using these conjugates to improve binding affinity of Ab and to redirect immune effector cells to target cells was preliminarily studied.

The RS-mediated N-terminal modification studies described in this chapter have been reported in a separate publication [1].

3.1 Introduction

Antibody-DNA (Ab-DNA) conjugates have proven useful in many applications, including immuno PCR (using traditional PCR [2-7], T7 RNA polymerase [8], rolling circular amplification (RCA) [9]), proximity ligation assays (PLA) [10-12], DNA barcoding [13], and DNA-encoded antibody library (DEAL) techniques [14] that rely on the high affinity and specificity of antibodies, in combination with unique properties of DNA, such as hybridization, PCR amplification, etc. Previous efforts for coupling oligonucleotides to antibodies have taken advantage of the strong binding between biotin and streptavidin [2-6], crosslinking amino groups on the antibodies and oligonucleotides with glutaraldehyde [8], reacting sulfhydryl group-containing oligonucleotides with maleimide-modified antibodies [7,9], and conjugating modified oligonucleotides and antibodies via hydrazone formation [15]. A more recent development incorporated non-natural amino acids into Fab fragments for site-selective attachment of oligonucleotides [16]. In this chapter, we demonstrate a new method for generating Ab-DNA conjugates, site-selectively and non-site-selectively. An oxidative coupling reaction, a highly efficient bioconjugation reaction requiring mild conditions and short reaction time [17-19], was used to covalently connect the two large biomolecules – antibodies and DNA oligonucleotides. First, Ab and DNA were decorated with oxidative coupling partners: aniline and aminophenol moieties, respectively. The aniline-Ab and aminophenol-DNA can be produced in large batches and stored under appropriate conditions. Once needed, these two reagents can be covalently coupled at room temperature in less than 5 min. The site-selectivity was achieved using pyridoxal 5'-phosphate (PLP)- or Rapoport's salt (RS)-mediated N-terminal transamination [1,20-25]. Moreover, due to N-terminal sequence preferences of these two reagents, chain specific modification on the Ab can be demonstrated by altering the N-terminal sequences of the wild-type Ab to match the preferences of each reagent (Figure 3.1). The non-site-selective approach used was via lysine modification for applications that do not require site-selectivity (Figure 3.1). Using NHS ester chemistry, a higher number of aniline coupling partners can be appended onto Ab, and no sequence alteration is necessary.

Despite many other applications shown in prior works, we proposed the use of these conjugates in therapeutic applications, including bispecific antibodies, antibody-derived proteins with the ability to bind to two different epitopes. Dual targeting strategies can be (1) those that directly act on target structures, e.g., cell surface receptors or soluble factors and (2) those that use dual targeting for delivery (retargeting) of a therapeutically active moiety, e.g., effector molecules and effector cells [26-28]. Even though the concept of bispecific antibodies (bsAb) has existed for several decades, they have become increasingly important as our knowledge of the potential efficacy of antibody-based therapeutics expands. The first bsAb in the market was catumaxomab (anti-EpCAM x anti-CD3), approved in the European Union for the treatment of malignant ascites [29]. It was produced from a mouse/rat quadroma cell line, a fusion of two different hybridoma cell lines. Another approach to generate bsAb is chemical conjugation focusing on the use of homo- or hetero- bifunctional crosslinking reagents [26,30]. The difficulty in generating bsAbs and batch-to-batch variation using quadromas and chemical cross-linking has depopularized the use of these techniques [26-28,30]. Instead, the significant improvements in recombinant antibody technologies has led to the development of many new bsAb formats (45 formats in the past two decades) [26]. However, employing the recombinant techniques, the targeting agents would be limited to the use of proteins or peptides.

In this work, we aimed to expand the class of bsAb to include Ab-synthetic molecule hybrids. Our first attempt involved the attachment of DNA (or potentially RNA) aptamers to full-

sized antibodies. The new hybrid constructs combine the binding ability of the two agents and should increase the affinity and specificity to target cells that express two target receptors. In this particular case, the N-terminal modification became attractive due to the proximity of the Ab binding site and the newly introduced targeting agent. We compared the properties of the N-terminally modified constructs with the lysine modified ones. Preliminary results showed that the enhancement in binding affinity of Ab-aptamer constructs depends on the selected pair of targeted receptors. Much further investigation is necessary to establish the use of these constructs as bispecifics. However, our studies offer an alternative route for the generation of Ab-DNA conjugates, not only to expand the class of bispecific antibodies, but also to be used in many other applications. Moreover, these methods can be applied to attaching other classes of synthetic molecules to full-sized antibodies, antibody fragments, or even other types of proteins.

3.2 Design and Strategy

Building on the success of site-selective modification of Fc fragments, we used the sequence preference for PLP-mediated N-terminal transamination to achieve chain-selective modification of antibodies. Through peptide library screening, previous work in the lab has identified optimal seqences for transamination by PLP, as well as sequences that have lower transamination yields. The alanine-lysine-threonine (AKT) sequence was one of the highest yielding sequences, while leucine-glutamine-threonine (LQT) was identified as one of the lowest transamination-yielding sequences [22,23,31]. To build antibodies with only modified light chains, we then engineered the light chain to contain highly-modifiable N-terminal sequences and heavy chain with low yielding sequences, resulting in antibodies with two modification sites available (Figure 3.1c). However, when modification of all four N-terminal sites is desired, both light chains and heavy chains were engineered to contain the sequence with optimal yields (Figure 3.1c). To minimize the interferance with protein folding, the three residue sequences were appended at the N-termini, instead of replacing the natural sequences. The extension would also increase the solvent and reagent accessibility, resulting in the higher likelihood of being modified.

While the effort on PLP modification is ongoining, Rapoport's salt (RS) or *N*-methylpyridinium-4-carboxaldehyde was identified as another N-terminal transamination reagent, together with another set of highly reactive sequences (glutamate terminal), through library screening. In collaboration with Dr. Leah Witus, we elected to demonstrate the application of RS via antibody modification as >50% of human IgG1 (the most common isotype for therapeutics) contain glutamate terminal heavy chains [32-34]. In addition, we designed antibodies with N-termini containing glutamate-glutamate-serine (EES) and proline-glutamate-serine (PES), one of the most optimal and least optimal sequences, respectively (Figure 3.1c).

3.3 Results and Discussion

3.3.1 Antibody engineering and expression

To achieve chain-selective modifications, the alanine-lysine-threonine (AKT), one of the optimal sequences for PLP-mediated transamination, was appended to the N-termini of the chains on which modification was desired (in this case light chains), while leucine-glutamine-threonine (LQT), identified as one of the lowest transamination-yielding sequences, was appended to the

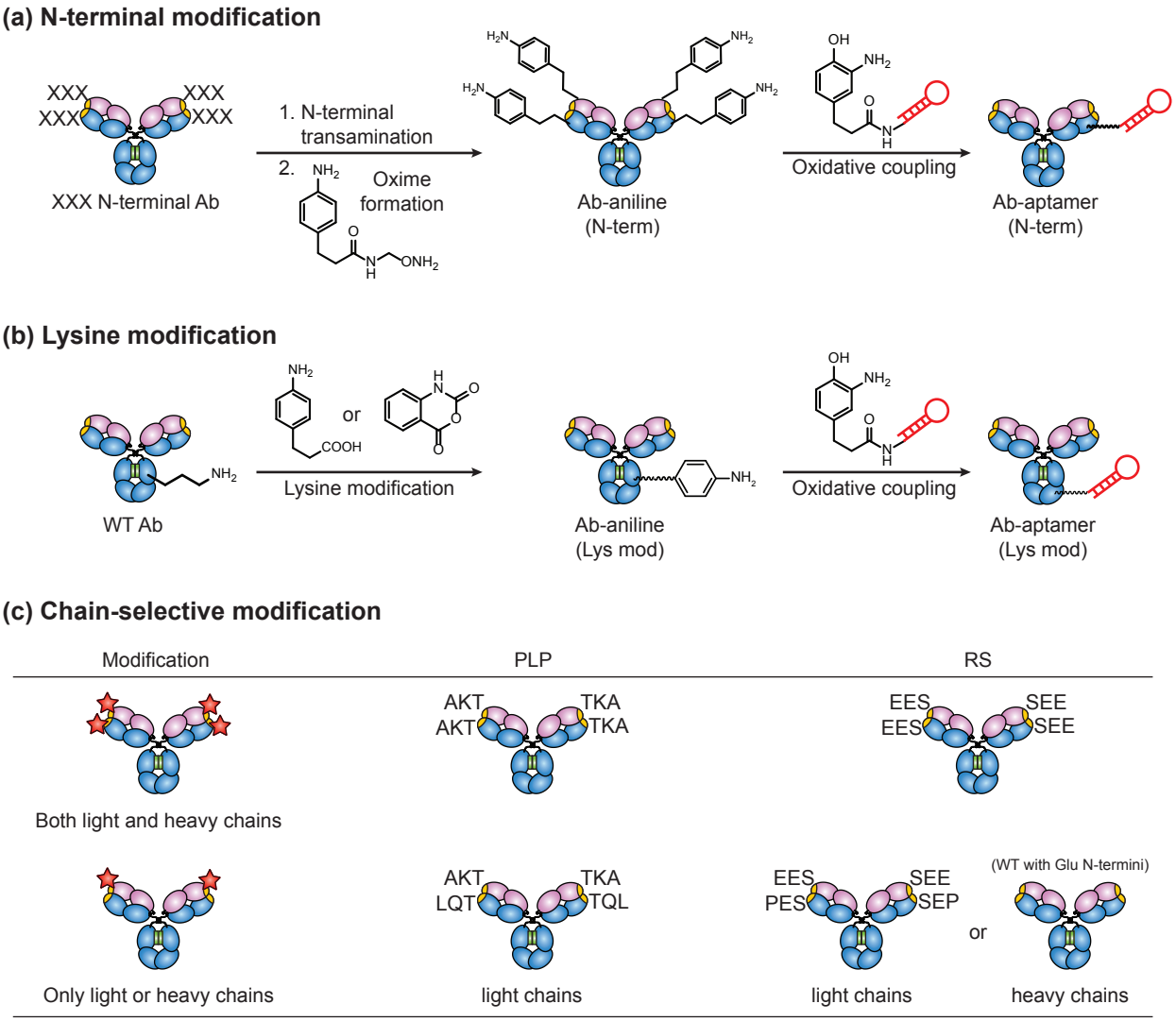

Figure 3.1. Design of antibody-DNA conjugates. Among many approaches that can be used to modify antibodies, we selected two strategies for the attachment of DNA oligonucleotides: (a) site-selective N-terminal modification and (b) lysine modification. Further, we used oxidative coupling, a highly efficient ligation, as a main strategy for the conjugation of two large biomolecules. First, we appended the oxidative coupling partners to antibodies and oligonucleotides. Previously, we found that aminophenols, the more reactive partner, can crosslink the two chains of antibodies if two aminophenol groups are in the same vicinity (data not shown). Therefore, anilines were added to the antibodies, and aminophenols were on DNA strands. For N-terminal modification of antibodies, we used PLP or RS to transaminate the N-termini of antibodies on either or both chains. Using these two reagents, we achieved chain-selective modification by varying the sequence at the N-termini as shown in (c). The Ala-Lys-Thr (AKT) and Leu-Gln-Thr (LQT) were chosen as a reactive and an unreactive sequence for PLP-mediated reaction, and the Glu-Glu-Ser (EES) and Pro-Glu-Ser (PES) were a reactive and an unreactive sequence for RS-mediated modification, respectively. Moreover, we also found that the wild-type human IgG1 with Glu at the N-termini of the heavy chain were selectively modified with no modification on the light chains (Asp N-terminal). After transamination, the ketone groups can then be attached to aniline via oxime formation. For lysine modification in (b), we attached aniline groups via NHS ester chemistry or via amide bond formation with isatoic anhydride. The final step was to conjugate antibody-aniline conjugates to aminophenol-DNA via oxidative coupling, using sodium periodate or newly found potassium ferricyanide as oxidants.

heavy chains. When modification of all chains was desired, an AKT sequence was added to the N-termini of both heavy and light chains. As a proof of concept, we chose humanized anti-HER2 monoclonal antibody (known under the trade name Herceptin) as our modification platform. The sequences of the variable domains of the light chain (V_L) and variable and constant region 1 of

the heavy chains (V_H and C_H1) of the anti-HER2 antibody were obtained from the literature [35] and assembled into gene inserts. The plasmids for light and heavy chains were then constructed separately using plasmid backbones containing light chain constant region C_L1 and heavy chain constant regions C_H2 and C_H3 from InVivogen (Figure 3.2 and S3.1). IL2 signal sequences were used as secretion signal to achieve higher expression yields.

Similarly, we also explored the possibility of using RS as a transamination reagent. We used both mutants and wild-type of anti-HER2 antibodies as >50% of the wild-type heavy chain sequences contain Glu termini. For the mutants, the EES and PES were chosen as one of the most reactive sequences and least reactive sequences for RS-mediated N-terminal transamination, respectively. To obtain antibodies with EES and/or PES N-termini, the Quikchange mutagenesis technique was used to alter the sequence at the AKT and/or LQT sites.

To optimize the expression of monoclonal antibodies (mAbs), various ratios of light to heavy chain plasmids were transfected into the HEK293T cell expression system (Figure 3.2). The 3:2 ratio of light and heavy chains was found to give the highest yield of anti-HER2 mAbs. These antibodies were then purified using protein A or G columns. While expressed, miscleavage of IL2ss caused the chains with LQT and EES to contain two species (Figure S3.2, S3.3). The EES/PES antibodies were not expressed in high enough yields for further studies.

3.3.2 Antibody modification

3.3.2.1 N-terminal modification of engineered anti-HER2 antibody

Anti-HER2 antibodies with AKT appended to both light and heavy chains (AKT/AKT) and with AKT appended to the light chains and LQT to heavy chains (AKT/LQT) were incubated with 100 mM PLP at 37 °C for 1 h, followed by oxime formation with aniline-ONH_2. More than 90% of all the chains containing AKT at the N-termini, translating to both light and heavy chains of AKT/AKT antibodies and only the light chain of AKT/LQT antibodies, were modified, while the modification of LQT termini was much less (Figure 3.3). However, using LQT, we were not able to fully suppress the modification. We also observed chain-selective modification in the subsequent oxidative coupling of antibody-aniline conjugates and aminophenol-containing PEG (2 kDa and 5 kDa). Both chains of the AKT/AKT antibodies were modified to ~40-50% yields, while only the light chains of AKT/LQT ones were conjugated to aminophenol-PEG to the same extent (Figure S3.4). The LQT heavy chains were <10% modified. Note that we have observed previously that most protein reactions with PEG stopped at ~50% yields, not reflecting the extent of modification seen in attachment of small molecules. We hypothesized that this results from the steric hindrance caused by large size of PEG. As shown in previous studies [37], up to 10 mM mannose can be added to the oxidative coupling reaction to prevent oxidation of glycans without sacrificing the yield of the products (Figure S3.4). Higher concentrations of mannose (e.g., 100 mM) resulted in loss of product yields.

Exploring another transamination reagent, Rapoport's salt (RS) or *N*-methylpyridinium-4-carboxaldehyde, wild-type anti-HER2 antibodies and those containing EES on both light and heavy chains (EES/EES) were incubated with 100 mM RS at 37 °C for 1 h. Unfortunately, EES/PES antibodies did not get expressed in high enough yields; therefore, they were omitted from these studies. Following oxime formation with $BnONH_2$, LCMS was used to analyze the extent of modification. The heavy chain wild-type sequence provided 67% conversion to the oxime product, in which 15% also included the RS adduct (Figure 3.3, S3.3). In contrast, no modification

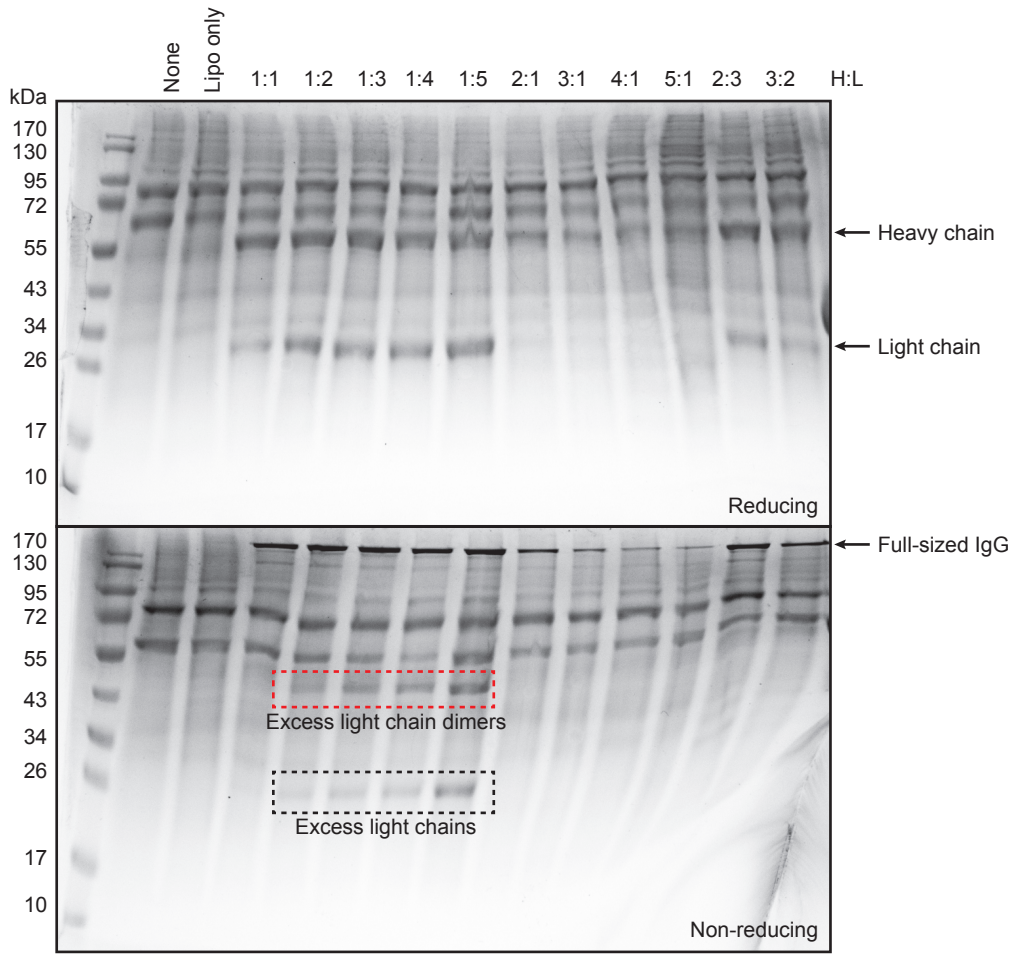

Figure 3.2. Optimization of anti-HER2 human IgG1 expression. Genes for variable regions of light and heavy chains were constructed and cloned into two seperate expression vectors from Invivogen (see scheme in Figure S3.1). Using Lipofectamine2000, both plasmids were transfected into HEK293T cells in various ratios to find one that yielded the highest expression level. SDS-PAGE analysis under reducing conditions (top) and non-reducing conditions (bottom) was used to detect proteins that were expressed and secreted from HEK293T. The first two lanes were negative controls (lane 1: neither plasmids nor Lipofectamine was added; lane 2: only Lipofectamine was added) showing proteins in the media or naturally expressed. We found that the expression of IgGs was highest when light chain plasmids were in excess compared to heavy chain plasmids (H:L = 1:2, 1:3, 1:4, 1:5, and 2:3). However, the more light chain plasmids were transfected, the more excess light chains that did not pair with heavy chains were expressed. We hypothesized that proteins in red dotted box were excess light chains that formed dimers with each other, and those in black dotted box were the monomers. A ratio of 2:3 of heavy to light chain plasmids (H:L) was chosen as the most optimized for scale-up expression.

was observed for the light chain (Figure 3.3, S3.3). This is likely because the steric environment of the folded protein reduces the accessibility of the already less-reactive substrate (DIQ terminal sequence). The complete lack of modification also clearly demonstrated that RS does not react with lysine side chain amines or other residues. The net result of this experiment is that RS-mediated transamination of the wild-type sequence allowed the selective modification of only the heavy chain [1]. The EES/EES antibodies were modified on both the light and the heavy chains (56% and 68%, respectively). During the expression of this mutant, we observed some improper cleavage of the IL2 signal sequences, which led to the production of a small proportion of light and heavy chains that lacked the N-terminal EE groups. The resulting serine-terminal analogs were not modified to the same extent as the EES sequence on the heavy chain, and we observed no modifi-

cation for the serine-terminal light chain (Figure S3.3).

3.3.2.2 Lysine modification of wild-type anti-HER2 antibodies

To attach aniline onto lysine side chains, we first explored and optimized the reaction with isatoic anhydride (Figure 3.4c). Incubation of antibodies with 1 mM isatoic anhydride at RT for 1 h seemed to give us good modification on both light and heavy chains (average of two anilines per light chain and four anilines per heavy chain). However, the yields of antibody-DNA conjugates following oxidative coupling was not as high as expected. Another route coupling 3-(4-amino-phenyl) propionic acid (aniline-COOH) to the lysine side chains via NHS/EDC-mediated amide bond formation was investigated on a model protein substrate lysozyme. Even though the number of anilines attached to proteins was similar, the subsequent oxidative coupling of aniline from

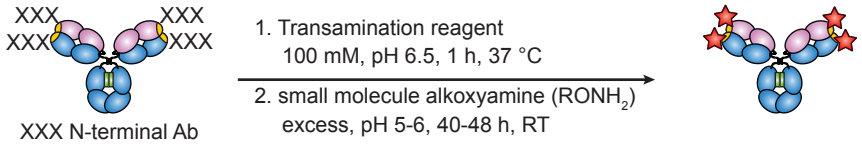

Transamination reagent	Mutant:	Chain (N-terminal sequence):	% Oxime yield:	Chains modified:
PLP	AKT/LQT	light (AKT) heavy (LQT)	90 22	
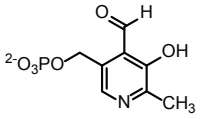	AKT/AKT	light (AKT) heavy (AKT)	89 >95	
RS	wild type	light (DIQ) heavy (EVQ)	0 67	
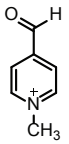	EES/EES	light (EES) heavy (EES)	56 68	

Figure 3.3. Transamination efficiency of PLP and RS and the use towards chain-selective antibody modification. Previous studies have shown that transamination reagents such as PLP and RS are more reactive towards certain amino acid sequences at the N-termini. In this work, we demonstrated this principle by extending heavy and light chain of anti-HER2 human IgG1 with the following sequences: (1) Ala-Lys-Thr (AKT), (2) Leu-Gln-Thr (LQT), and (3) Glu-Glu-Ser (EES). AKT and LQT were found to be one of the most and least reactive sequences, respectively, for PLP, and EES was one of the most reactive sequences for RS. Different combinations of N-terminal sequences were analyzed by LCMS of the products from transamination, followed by oxime formation with small molecule alkoxyamines. When treated with PLP, antibodies with AKT on both chains achieved the highest yield of modification (89% on light and >95% on heavy); however, when the AKT N-terminal sequence was replaced with LQT, the yield dropped to only 22% on the heavy chains. For RS, which is highly reactive to Glu N-terminal residue, wild-type N-terminal sequences of anti-HER2 antibodies, containing EVQ N-terminal sequence on the heavy chains, were tested and found to achieve site-selective modification as only the heavy chains were modified. The light chain with DIQ N-terminal sequence did not yield any transaminated product. While this result show that Glu is a more reactive terminal residue, lack of modification on the light chain can also be due to buried N-termini. To achieve transamination on both light and heavy chains using RS, the EES sequences were appended, and ~60-70% modification on both chains were obtained. The LCMS traces of this analysis are shown in Figure S3.2 and S3.3. (Figure adapted from Ref. [1]).

aniline-COOH gave much higher yields, indicating that the aniline yielded from aniline-COOH/NHS/EDC coupling was more reactive towards oxidative coupling (Figure 3.4). The carbonyl conjugated to the aniline after isatoic anhydride reacted with lysine reduced the nucleophilicty of the aniline, resulting in less reactivity. Therefore, aniline-COOH/NHS/EDC coupling was chosen. In both case, the aminophenol-PEG also reacts with the proteins in the absence of aniline group (Figure 3.4d,e, lane 2-3), suggesting the reactivity of native amino acid residues in the presence of oxidants, either $NaIO_4$ or $K_3Fe(CN)_6$. This was later explored by Obermeyer *et al.* and found to be amine groups at the N-termini [36]. Lanes 4-7 in Figure 3.4d also showed a small amount of

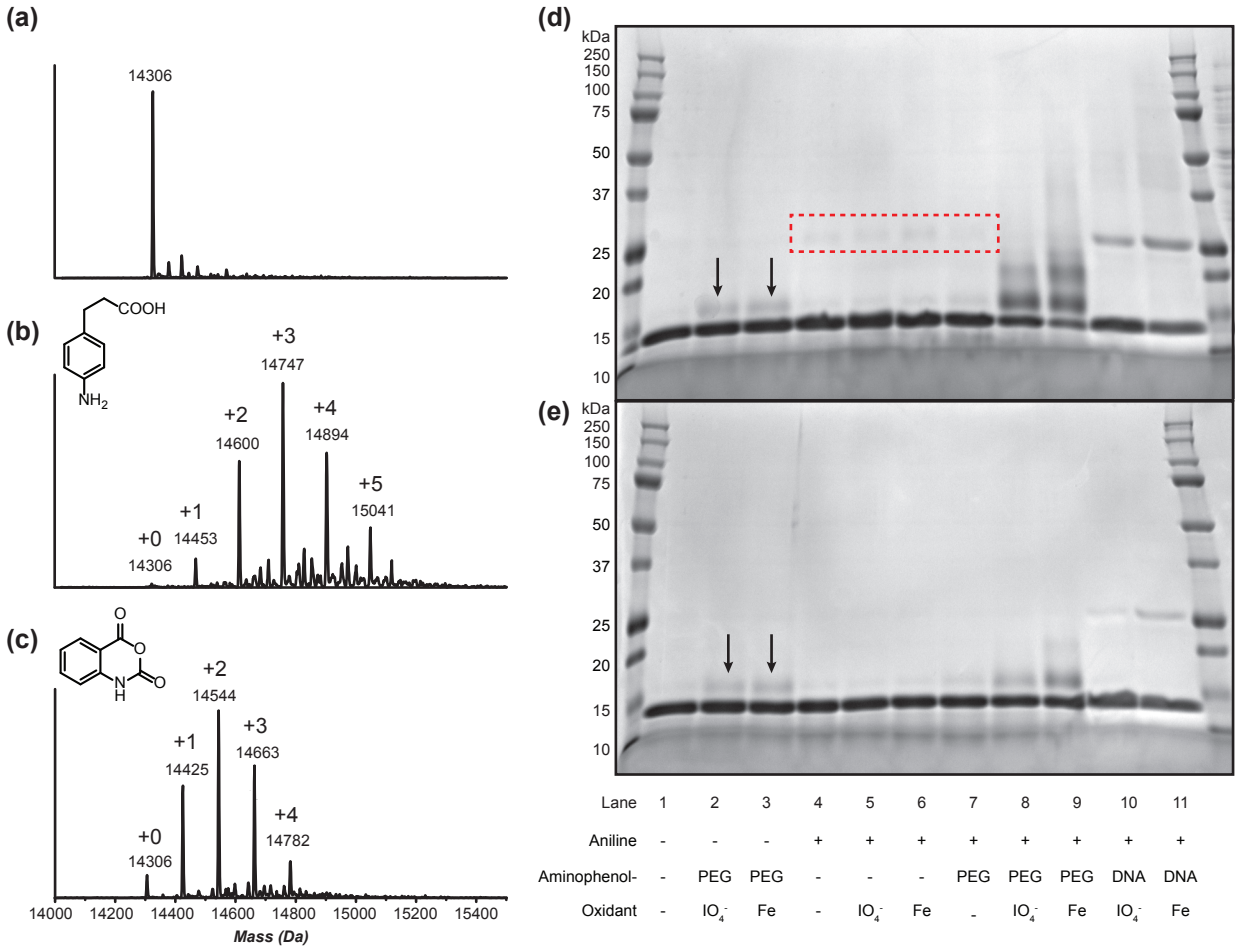

Figure 3.4. LCMS of lysozyme after attachment of aniline groups using aniline-COOH/NHS/EDC and isatoic anhydride, and SDS-PAGE analysis of lysozyme-aniline after oxidative coupling. Lysozyme was used as a model protein to compare the reactivity of aniline from attachment using aniline-COOH/NHS/EDC (+147) and isatoic anhydride (+119). LCMS analysis showed an average of three anilines per lysozyme for aniline-COOH/NHS/EDC coupling (b) and two anilines per lysozyme for isatoic anhydride coupling (c). Figure 3.4a displays an MS of unmodified lysozyme. (d) and (e) show SDS-PAGE analysis of oxidative coupling reaction of lysozyme-aniline from aniline-COOH/NHS/EDC coupling (d) and isatoic anyhydride coupling (e). The lysozyme-aniline conjugates obtained from both methods were oxidative coupled with aminophenol-PEG (2k) and aminophenol-DNA (47-mer). Despite similar number of anilines attached on to lysozyme via both methods, the aniline from aniline-COOH/NHS/EDC coupling were more reactive towards oxidative coupling. Two oxidants, $NaIO_4$ and $K_3Fe(CN)_6$ (abbreviated as Fe in the figure), were explored. In the reaction conditions used (2 min at RT for $NaIO_4$ and 15 min at RT for $K_3Fe(CN)_6$), oxidative coupling using $K_3Fe(CN)_6$ (lane 9 and 11) seemed to give slight higher yields than the ones using $NaIO_4$ (lane 8 and 10). We also noticed background coupling reaction between native amino acid residues and oxidized aminophenol-PEG in the absence of aniline (lane 2-3, arrow pointed). In addition, lane 4-7 of Figure 3.4d showed slight amount of lysozyme dimers from self-coupling (red dotted box), which was later prevented by adjusting the ratio of aniline-COOH:NHS:EDC used in the reaction to 1:1:1.

cross-linked proteins as a results of excess EDC and NHS (the ratio of aniline-COOH:NHS:EDC used was 1:2:2 as obtained from Behrens *et al*. [18]). The amount of cross-linked proteins became even more significant when the reaction was pursued on antibodies, as light and heavy chains of antibodies are close in space to each other (Figure 3.5a, lane 4-7). In an effort to optimize the reaction further, we adjusted the ratio of aniline-COOH:NHS:EDC to 1:1:1 to reduce the amount of excess NHS/EDC and prevent cross-linking (Figure 3.5b, lane 1-2). Imidazole was also added to the reaction conditions, as it was found to minimize the side reaction with native N-termini. Even though the side reactions should not interfere with our applications, the addition of imidazole up

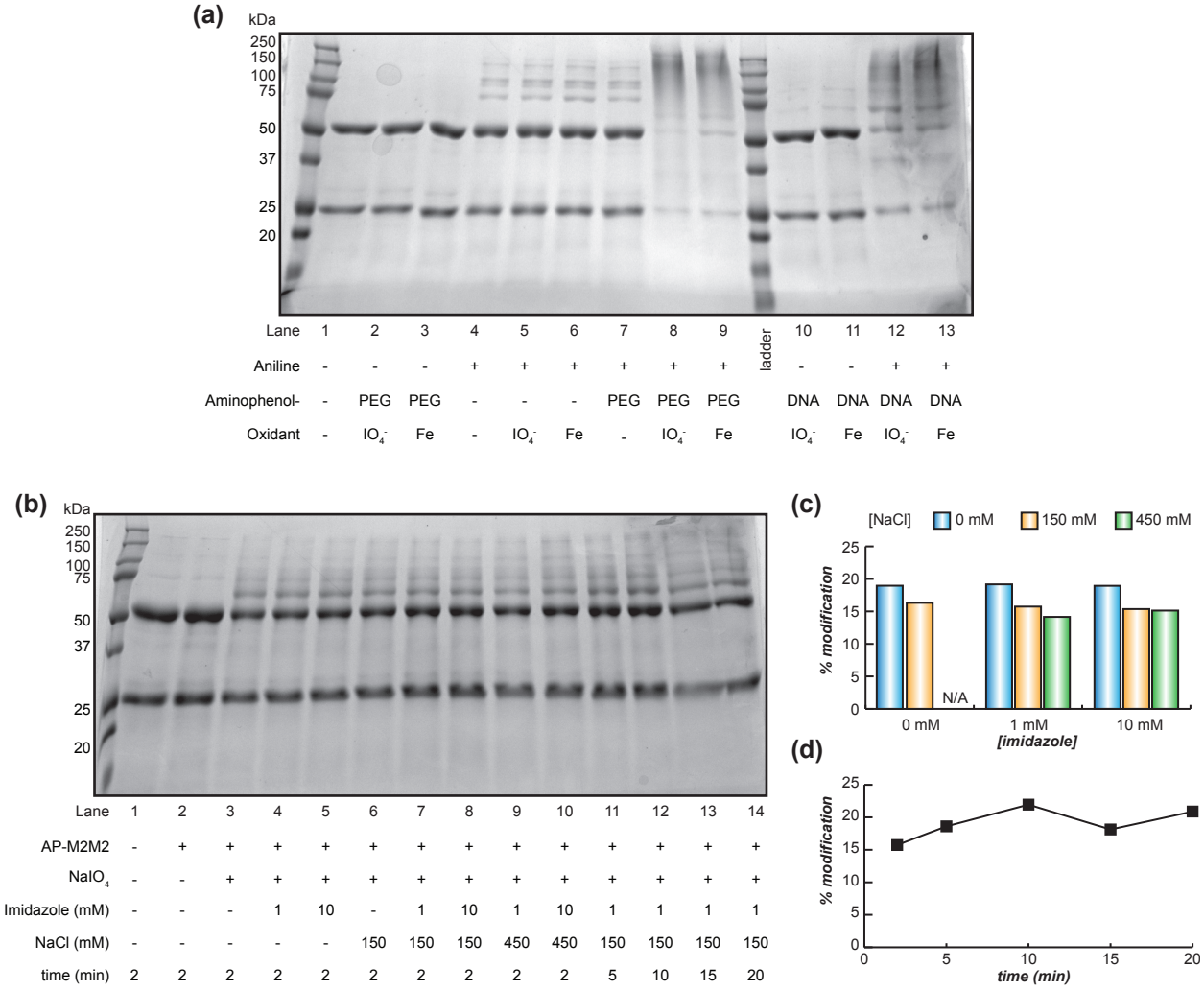

Figure 3.5. SDS-PAGE analysis of oxidative coupling reaction of aniline-antibody and aminophenol-DNA oligonucleotides. After lysine modification using aniline-COOH/NHS/EDC coupling, the resulting antibody-aniline conjugates were subjected to oxidative coupling with aminophenol-PEG (5 kDa) and aminophenol-DNA to test the efficiency of the reaction using $NaIO_4$ and $K_3Fe(CN)_6$ (abbrev. as Fe in the figure) as oxidants. The SDS-PAGE analysis of the products from these reactions is shown in (a). The two oxidants used gave similar product yields. While $NaIO_4$ requires less time, $K_3Fe(CN)_6$ is a milder oxidant that was found to not oxidize oligosaccharides. The use of these two oxidants would depend on the presence and the importance of glycans for each protein substrates. Figure (b) displays the optimization of $NaIO_4$-mediated oxidative coupling between antibody-aniline and aminophenol-DNA by varying [NaCl], [imidazole], and reaction time. We found that none of these factors affected the reaction yields. In this experiment, we also reduced the ratio of aniline-COOH:NHS:EDC to 1:1:1 in Lys modification to generate the antibody-aniline conjugates from 1:2:2 in (a). Lane 1-2 in figure (b) show fewer crosslinked chains as compared to lane 4-7 in figure (a).

to 10 mM did not affect the yield of the antibody-DNA conjugates. Various amounts of NaCl were added to shield the negative charges on DNA oligonucleotides; however, the reaction yield did not increase even after 450 mM was added (Figure 3.5b,c). Finally, reaction time was varied and again a longer reaction time did not result in higher yield (Figure 3.5b,d). This is perhaps because oxidative coupling using $NaIO_4$ is highly efficient, and the reaction is normally complete in 2 min or less. In fact, the most important factor we found for oxidative coupling of two large biomolecules is the number of equivalents of the aminophenol coupling partners. The larger the molecules desired to attach, the higher number of equivalents required. For example, ~10 equivalents of 5 k-PEG were required to achieve significant modification yields, while at least 30-50 equivalents of 50-mer DNA oligonucleotides were necessary to reach similar yields (Figure S3.5).

3.3.3 Generation of antibody-DNA aptamer conjugates for improvement in binding affinity

In order to generate bispecific antibodies from antibody-DNA aptamer conjugates, we explored two different routes: (1) site-specific N-terminal modification and (2) non-specific lysine modification. Oxidative coupling was chosen as the secondary conjugation reaction due to its high efficiency. For the N-terminal modification, AKT/AKT anti-HER2 antibodies gave us the highest percent modification of aniline conjugates. For the lysine modification, aniline-COOH/NHS/EDC coupling yielded the more reactive aniline. Thus, we decided to pursue further modification with these constructs.

We first explored the modification of anti-HER2 antibodies with sgc8c, an anti-PTK7 aptamers, and TD05.1, an anti-mIgM aptamer [38-42]. These two constructs were successfully generated via the two routes as analyzed by SDS-PAGE (Figure 3.6a). The Ab-aptamer conjugates were purified away from excess DNA aptamers by size exclusion FPLC (Figure 3.6c,d). Other purification methods such as protein A or G were also explored. The acidic elution conditions were avoided by instead using Gentle Ag/Ab Elution Buffer, pH 6.6 from Pierce. The Ab-DNA could also be successful obtained via this approach (Figure 3.6b). However, there is still a significant amount of Ab-DNA left in the flow-through (Figure 3.6b). Thus, the size exclusion FPLC was a more efficient purification method and was used to seperated up to 50-mer DNA from its Ab-DNA conjugates. Note that we did not attempt to separate antibodies with one, two, and/or three aptamers attached. Therefore, the final solution remained a mixture of all possible constructs.

The concentration of Ab-sgc8c and Ab-TD05.1 conjugates were quantified using BCA assays[1] for protein quantification, and their binding properties were assessed on Jurkat and Ramos, target cells for sgc8c and TD05.1, respectively, using flow cytometry. The results show specific binding of both constructs to their target cells at low concentration (2 nM) (Figure 3.7). However, at higher concentrations (20 and 200 nM), the results showed slight increase in non-specific binding of Ab-aptamer conjugates to the negative control cell lines (Figure 3.7). This non-specific binding could result from the conjugates with more than one aptamers attached. The binding of Ab-DNA to a HER2-positive cell line, MCF7 clone 18, suggested that the antibodies did not lose their binding properties to the original target at least at a high concentration (200 nM) tested.

To test the whether dual targeting can increase the binding affinity, we selected HCC1954 and MCF7 clone 18 to be the target cells. In previous studies, sgc8c aptamer was found to bind protein tyrosine kinase 7 overexpressed in T-cell leukemia [38-40]. We also screened binding

[1] The BCA assay was conducted without using unmodified antibodies of known concentrations as positive controls. Therefore, even though the concentrations obtained should still be accurate within the same order of magnitude, the uncertainty in concentrations of Ab-DNA conjugates may become crucial in the binding studies.

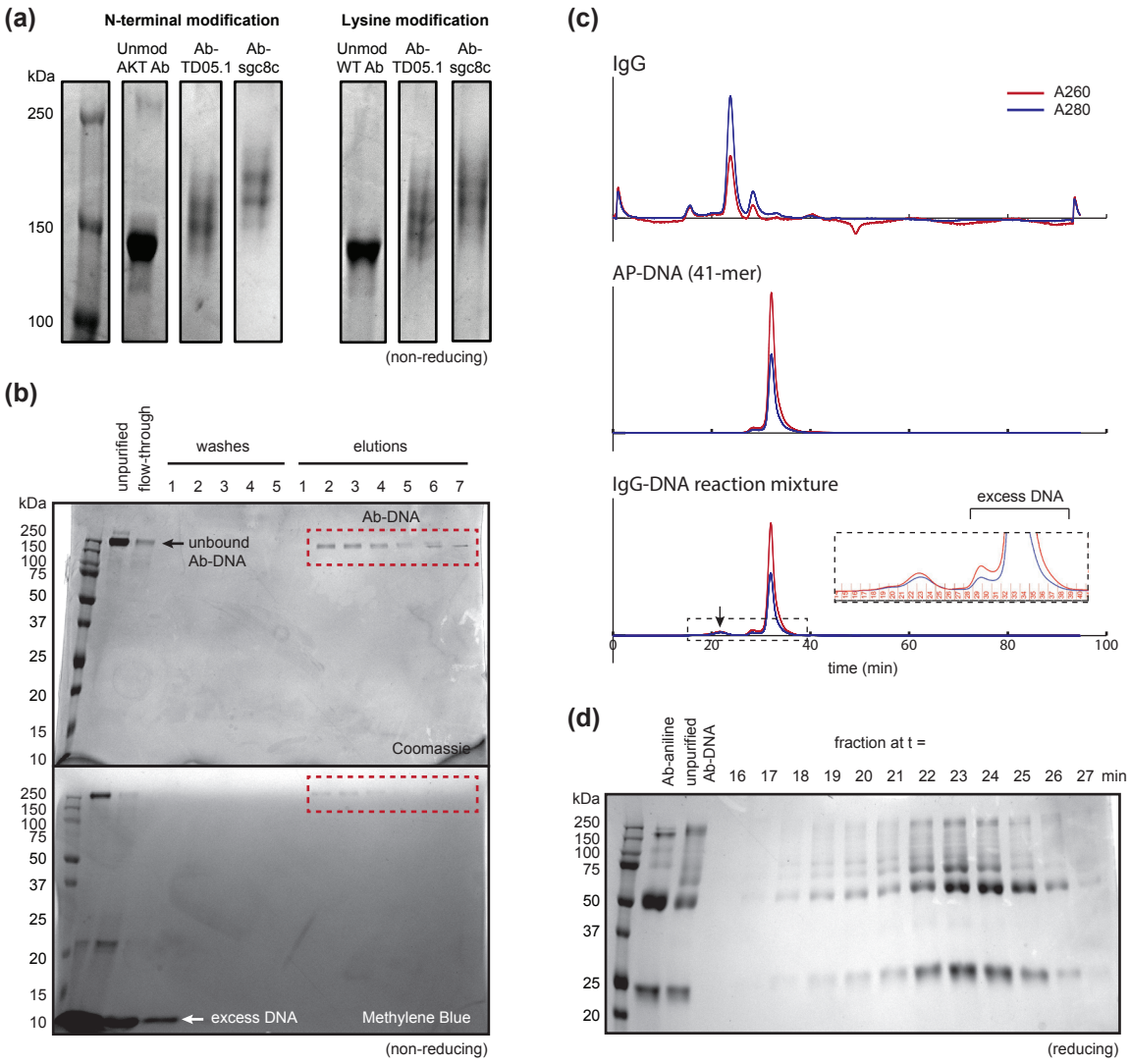

Figure 3.6. SDS-PAGE analysis and purification of antibody-DNA aptamer conjugates from N-terminal and lysine modification strategies. Two DNA aptamers, sgc8c (targeting protein tyrosine kinase 7, PTK7) and TD05.1 (targeting membrane-bound IgM, mIgM), were chosen to attach to anti-HER2 human IgG1s and the oxidative coupling products were analyzed by 5% Tris-HCl SDS-PAGE gel (under non-reducing conditions) to visualize the full-sized antibodies. The conjugates were shown in figure (a) to be successfully prepared in good yields with almost no trace of unmodified antibodies. The antibody-DNA conjugates can be purified from excess aminophenol-DNA by using protein G columns or size exclusion FPLC. Figure (b) shows the SDS-PAGE analysis (10-20% Tris-HCl gel under non-reducing conditions) of flow-through, washes, and eluents from protein G columns using Coomassie stain (top) to visualize protein and Methylene Blue stain (bottom) to visualize single-stranded DNA. This method can be used to separate Ab-DNA conjugates from excess DNA; however, there is still a significant amount of Ab-DNA, which did not bind to the column, left in the flow-through. Figure (c) shows the absorbance traces at 260 nm and 280 nm from the size exclusion FPLC purification. Ab-DNA conjugates were eluted from the colum slightly earlier than the DNA oligonucleotides itself. Thus, Ab-DNA can be successfully purified and SDS-PAGE analysis (10-20% Tris-HCl gel under reducing conditions) of the Ab-DNA peak is shown in (d). The size exclusion FPLC was a more efficient purification method and was used to seperated up to 50-mer DNA from its Ab-DNA conjugates.

of sgc8c aptamers to other cancer cell lines and found that it binds to several others, such as HCC1954, MDA-MB-453, MCF7 clone18, and L3.6pl (Figure S3.6). Subsequent studies of PTK7 expression on HCC1954 and MCF7 clone 18 suggested that the binding of sgc8c on these cell lines was likely through PTK7 receptors as these cell lines show high expression level of PTK7, especially in HCC1954 which seemed even higher than that of Jurkat, a T-cell leukemia in the original

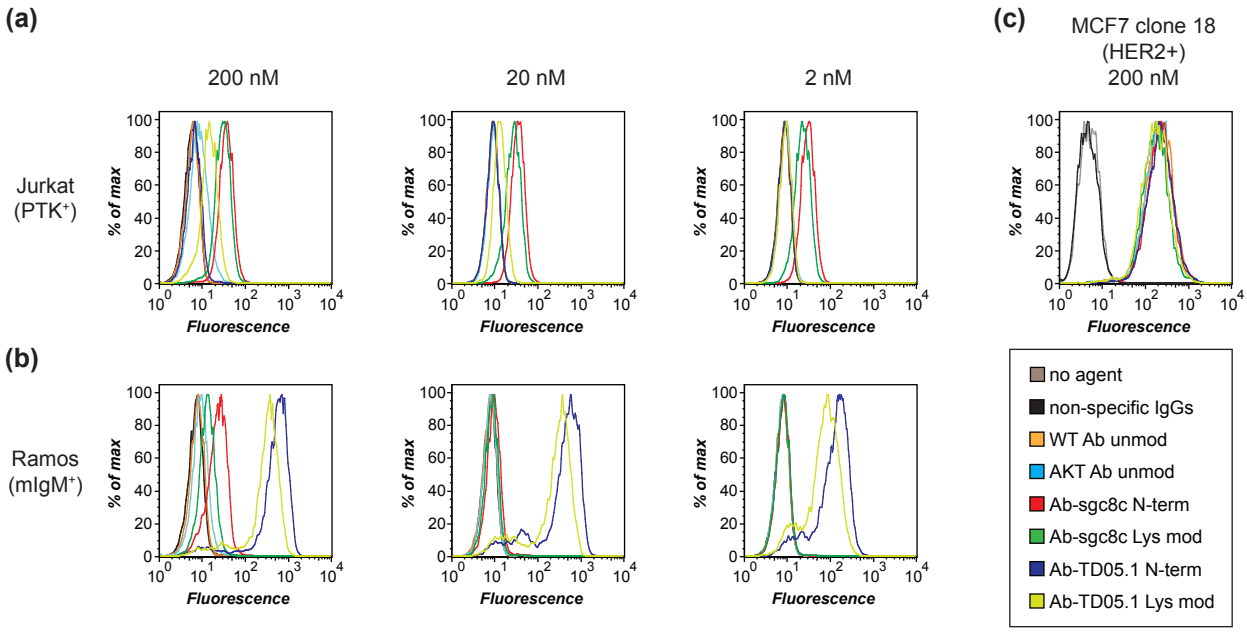

Figure 3.7. Flow cytometry analysis of Ab-DNA conjugates. The binding of anti-HER2 Ab-sgc8c and anti-HER2 Ab-TD05.1 conjugates from N-terminal and lysine modification were tested on their target cells, Jurkat (a) and Ramos (b), respectively. Since these two aptamers do not cross talk, they are also negative controls of each other. Unmodified wild-type and AKT antibodies, as well as non-specific human IgGs isolated from myeloma, were used as negative controls agents. At high concentration (200 nM), there is some background binding of Ab-aptamer conjugates to the non-target cell lines. Since normally these two aptamers by themselves do not show non-specific binding at 200 nM, this observed background binding could be due to the Ab-DNA conjugates containing more than one aptamer. At lower concentrations, we observed less non-specific binding and none at all at 2 nM. The binding of the Ab-DNA conjugates was also tested on MCF7 clone 18 cells, which overexpress HER2, as shown in figure (c). The modification did not seem to interfere with binding when high concentration (200 nM) of agents was present.

studies. HCC1954 and MCF7 clone 18 were then chosen for further studies of HER2/ PTK7 dual targeting purpose.

Binding of Ab-sgc8c from both the N-terminal and lysine modifications at different concentrations were assessed using flow cytometry. However, instead of an increase in affinity, Ab-DNA seemed to lose their binding affinity as compared to the unmodified Ab (Figure 3.8a,b). The estimated K_d obtained from Hill curve fit showed at least 10-fold decrease in binding and the two different DNA aptamers appeared similar in K_d, indicating that the attached aptamers did not play a role in binding. Instead, these DNA oligos somehow blocked the binding of Ab to its target. The different attachment sites (N-termini vs. lysine) also showed no difference in binding (both decreased from the unmodified).

We further tested another construct of Ab-aptamer by generating anti-CD20-TD05.1 conjugates via lysine modification. The preliminary binding studies to Ramos cell line, expressing both CD20 and mIgM, showed improvement in binding affinity of anti-CD20-TD05.1 over unmodified anti-CD20 antibodies (Figure 3.8c). These results suggested that whether the binding of the Ab and synthetic molecules will have synergistic effects may depend on the target receptors. Therefore, we may be able to use the Ab-synthetic conjugates to improve binding to target cells only in some cases while in others, they may have negative effects.

3.3.4 Generation of antibody-DNA aptamer conjugates for redirecting effector cells

Another widespread application of bispecific antibodies is to redirect immune effector cells

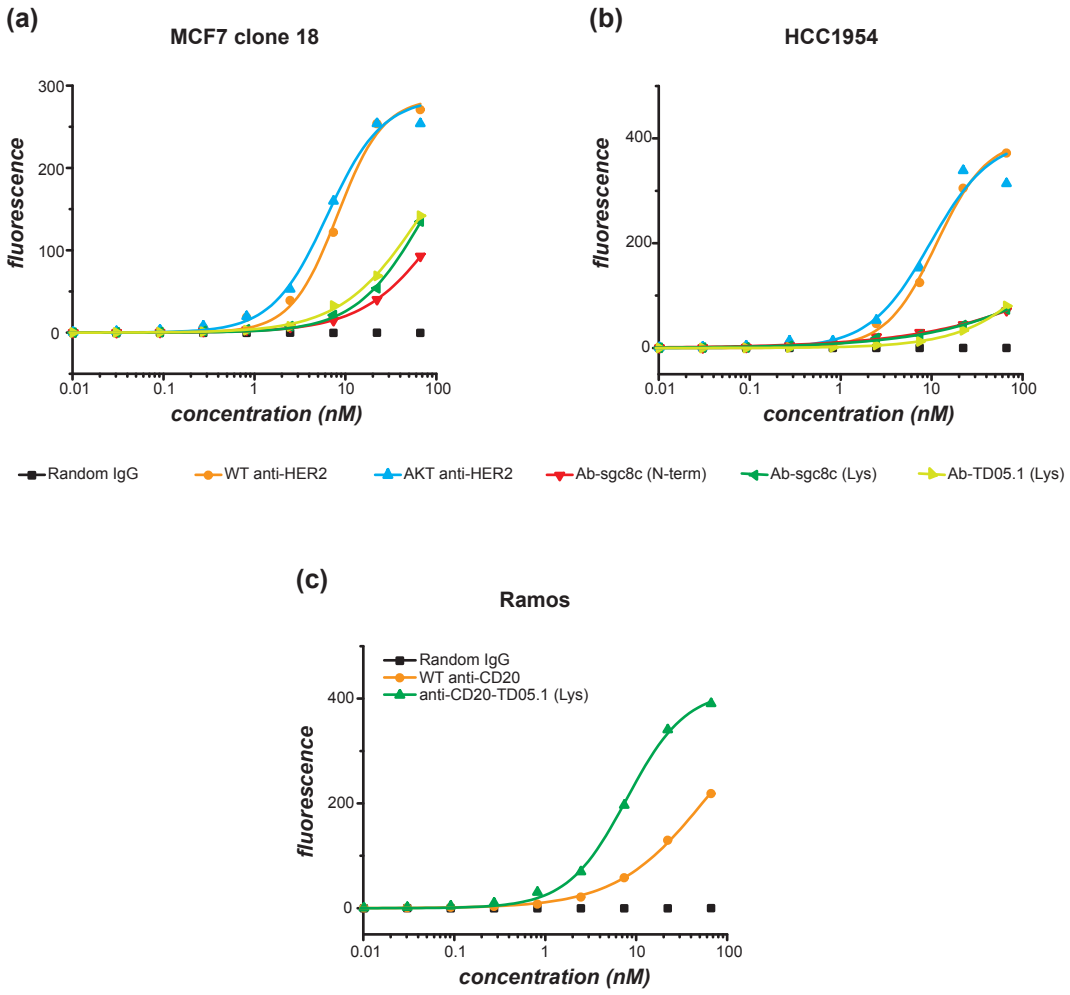

Figure 3.8. Binding studies of Ab-DNA in comparison to unmodified Ab. Flow cytometry analysis was used to construct binding curves of Ab-DNA from N-terminal and lysine modification in comparison to the unmodified Ab (wild-type and AKT mutants) on MCF7 clone 18 (a) and HCC1954 (b), both overexpress HER2 and PTK7, targets of anti-HER2 Ab and sgc8c aptamer. Our hypothesis was that dual binding of anti-HER2 Ab-sgc8c conjugates would increase their binding affinities to the target as compared to the unmodified Ab. However, we found that the binding affinities of these Ab-sgc8c conjugates decrease and appeared similar to the Ab-TD05.1, whose targets are present on neither MCF7 clone 18 nor HCC1954. Therefore, it is likely that the attachment of DNA aptamers in this case, irrespective of sites of attachment, interfere with the binding of the anti-HER2 Ab to the HER2 target antigens on these cell surfaces. Another combination of antibody and DNA aptamers, anti-CD20 Ab-TD05.1 conjugate by Lys modification, was examined. The preliminary binding studies showed an improvement in binding affinity of this pair, as shown in (c).

to induce cytotoxic effects on the target cells. One of the most successful strategies was "bispecific T-cell engager" or BiTE antibodies [43-46]. This technology recombinantly links two single-chian variable fragments (scFv), one of which is an anti-CD3 scFv having the ability to bind and activate $CD3^{+}CD8^{+}$ cytotoxic T-cells and the other can be specific to a target antigen [43-48]. In this case, we applied a similar concept to the Ab-aptamer construct by appending the TD05.1 aptamer, which is specific to mIgM, over expressed in Burkitt lymphoma, to UCHT1 mouse IgG1, which specifically binds the ε-chain of the CD3/TCR complex. The lysine modification scheme was applied to generating UCHT1-TD05.1 conjugates, and flow cytometry analysis of the construct confirms the bispecificity of the hybrid to both target Burkitt's lymphoma cell line, Ramos, and also the T

lymphocyte cell line, Jurkat (Figure 3.9). Further studies need to be conducted to demonstrate the ability to recruite primary cytotoxic T lymphocytes, which can be obtained from peripheral blood mononuclear cells (PBMCs), to kill the target cells. However, we hypothesized that similar to other anti-CD3-based bispecific antibodies, such a construct would be able to activate and recruit cytotoxic T-cells to target tumor cells and induce subsequent lysis of the target cells. In this particular case, one of the major advantages of using the TD05.1 aptamer as a targeting agent is the ability to bind specifically to only the mIgM and not the circulating IgM [42]. Other anti-Ig antibodies that have been developed as therapeutic vehicles for the treatment of lymphoma also interact with the soluble Ig in serum, which is found in high concentration. The interaction with soluble Ig also leads to immune complexes that are cleared, thus resulting in limited binding to tumor targets [42]. This work may demonstrate significance in expanding the class of antibody-based therapeutics to include antibody-synthetic molecule conjugates.

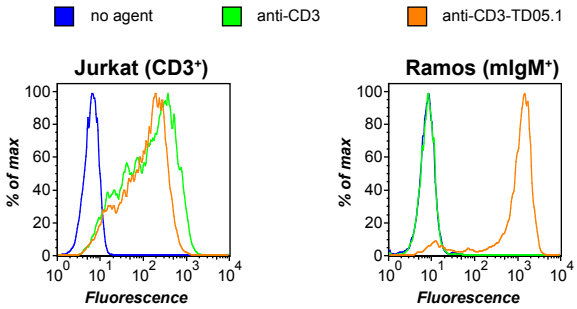

Figure 3.9. Flow cytometry analysis of anti-CD3-TD05.1 conjugate. The binding of anti-CD3-TD05.1 conjugates from lysine modification were tested on Jurkat, a $CD3^+$ T lymphocyte cell line (left), and Ramos, a model Burkitt's lymphoma cell line (right). Both cells were treated with 60 nM unmodified anti-CD3 and anti-CD3-TD05.1 conjugate on ice for 1 h, followed by detection using AlexaFluor 488 conjugated anti-mouse secondary antibodies. The anti-CD3-TD05.1 conjugate still retained similar binding specificity and affinity to the unmodified one. In addition, the Ab-aptamer conjugate were able to bind the target Ramos cell line, while the unmodified Ab remained unbound.

3.4 Conclusions and Future Prospects

In this chapter, we demonstrated the use of chemically-based bioconjugation techniques in creating Ab-DNA conjugates. The Ab can be site-selectively modified with aniline, an oxidative coupling partner, at the N-termini using either PLP or RS as transaminating reagents. Chain-selectivity can also be achieved by altering the N-terminal sequences of heavy and/or light chains to those preferred or unpreferred by PLP or RS. For application requiring no site-selectivity, standard lysine modification can be used to attach aniline groups to Ab. The aminophenol-containing oligonucletides can be conjugated to aniline-Ab via the highly efficient oxidative coupling reactions, using either $NaIO_4$ or $K_3Fe(CN)_6$ as oxidants. Ab-DNA conjugates can be synthesized in high yields with almost no trace of unmodified Ab and purified using SEC FPLC. To separate Ab with different numbers of oligonucleotides attached, anion-exchange chromatography can also be employed.

Upon attaching DNA aptamers, the antibodies can be redirected to new target cell lines. However, depending on the original targets of the Ab and perhaps the Ab sequences, the Ab may lose its binding affinity to the original targets. This could be due to the chemical alteration and also the attachment of a large DNA oligonucleotides. We also further showed that the loss in binding

affinity could be case specific to each pair of target antigens. In some others, the binding of aptamers and antibodies can be synergistic, as seen in the increase in binding of anti-CD20-TD05.1 conjugates.

To demonstrate the use of these Ab-DNA aptamer conjugates as bsAbs for retargeting effector cells, future studies of the constructs, such as anti-CD3-aptamers or anti-CD16-aptamers for for redirecting cytotoxic T-cells and NK cells, may be conducted. This approach will expand the use of the bsAb concept to include other targets that may not have been reached by antibodies, antibody fragments, or peptides. The use of other types of synthetic molecules, such as small molecules, peptoids, or chemically modified peptides, can also be used instead of DNA or RNA aptamers. As such, the targets of Ab-synthetic molecule conjugates also should not be limited to cell surface receptors but include other ligands or soluble factors, both for activiating and/or neutralizing effects of any ligand-receptor targets.

3.5 Materials and Methods

3.5.1 General experimental procedures and materials

Unless otherwise noted, all chemicals and solvents were of analytical grade and used as received from commercial sources. Water (dd-H_2O) used in biological procedures or as the reaction solvent was deionized using a NANOpure purification system (Barnstead, USA). *N*-methylpyridinium-4-carboxaldehyde benzenesulfonate salt (Rapoport's salt, RS) was obtained from Alfa Aesar. Pyridoxal 5'-phosphate monohydrate was obtained from Aldrich. Wild-type anti-HER2 human IgG1 monoclonal antibodies were obtained from Eureka Therapeutics (Emeryville, CA). Mouse anti-human CD3 antibodies clone UCHT1 were obtained from Southern Biotech (Birmingham, AL). Goat anti-human IgG (Fcγ specific) PerCP-conjugated $F(ab')_2$ fragments were purchased from Jackson ImmunoResearch Laboratories (West Grove, PA). Anti-human IgG1 (Fc specific) FITC-conjugated purified mouse IgG clone 8c/6-39 and non-specific IgG1 kappa isolated from human myeloma were purchased from Sigma (St. Louis, MO). Anti-mouse IgG AlexaFluor 488-conjugated antibodies were purchased from Life Technologies (Grand Island, NY). All oligonucleotides were obtained from Integrated DNA Technologies (Coralville, IA). All cell culture reagents were obtained from Gibco/Invitrogen Corp. (Carlsbad, CA) unless otherwise noted. Cell culture was conducted using standard techniques. Jurkat, Ramos, and HCC1954 cells were grown in culture-treated flasks (Corning) in RPMI Medium 1640 supplemented with 10% (v/v) fetal bovine serum (FBS, Omega Scientific) and 1% penicillin/streptomycin (P/S, Sigma). HEK293T, MCF7, MCF7 clone 18, L3.6pl, and MDA-MB-231 cells were grown in culture-treated flasks (Corning) in Dulbecco's Modified Eagle Medium (DMEM) supplemented with 10% (v/v) FBS and 1% P/S. MDA-MB-453 cells were grown in culture-treated flasks (Corning) in L-15 media supplemented with 10% (v/v) FBS and 1% P/S.

3.5.2 Construction of light chain anti-HER2 human IgG1 expression plasmids

To clone a plasmid for the expression of the anti-HER2 human IgG1 light chain, the sequence for the variable domain of the light chain (V_L) was obtained from the literature [35] with an additional GCTAAAACT added to the 5' end in order to create a three residue N-terminal extension Ala-Lys-Thr (AKT). Gene2Oligo [49] was used to generate the following set of oligonucleotides for gene assembly from the V_L sequence. An IL2 signaling sequence was also included

in the N-terminal region: (The bases in lower case were added by the Gene2Oligo program and did not belong to the input sequence):

R0 ACCTTTTTTTacattgaagtgcag
F0 ctgcacttcaatgtAAAAAAAGGTCACCATGTACAGGATGCA
R24 GCAATGCAAGACAGGAGTTGCATCCTGTACATGGTG
F42 ACTCCTGTCTTGCATTGCACTAAGTCTTGCACTTGTCA
R60 TCAGTCTTAGCCGAATTCGTGACAAGTGCAAGACTTAGT
F80 CGAATTCGGCTAAGACTGACATCCAAATGACTCAGAGCC
R99 GCGCTCAGGGAACTGGGGCTCTGAGTCATTTGGATG
F119 CCAGTTCCCTGAGCGCTTCCGTAGGGGACAGG
R135 GCCCGACATGTTATTGTCACCCTGTCCCCTACGGAA
F151 GTGACAATAACATGTCGGGCTAGCCAGGATGTCAATACAG
R171 CTGGTACCAAGCGACAGCTGTATTGACATCCTGGCTA
F191 CTGTCGCTTGGTACCAGCAAAAGCCCGGAAAGGC
R208 GCTGTATATAAGAAGCTTTGGCGCCTTTCCGGGCTTTTG
F225 GCCAAAGCTTCTTATATACAGCGCCAGTTTCCTCTATTCTGG
R247 GAACCTGCTCGGCACGCCAGAATAGAGGAAACTGGC
F267 CGTGCCGAGCAGGTTCTCTGGATCTCGGTCCG
R283 TCAGTGTGAAATCGGTCCCGGACCGAGATCCAGA
F299 GGACCGATTTCACACTGACCATTAGTTCTCTGCAGCC
R317 TAGTATGTTGCAAAGTCCTCTGGCTGCAGAGAACTAATGG
F336 AGAGGACTTTGCAACATACTACTGCCAGCAGCACTAT
R357 AGGTTGGGGGTGTGGTATAGTGCTGCTGGCAG
F373 ACCACACCCCCAACCTTTGGTCAGGGCACGAA
R389 CGTACGCTTGATTTCCACCTTCGTGCCCTGACCAA
F405 GGTGGAAATCAAGCGTACGAAAAAAAcccccaactttgt
F424 acaaagttgggggTTTTTTT

These DNA sequences were assembled into a gene by PCR (see detailed protocol in supplementary information), then cloned into a plasmid containing the light chain constant region. The resulting V_L gene was inserted into a vector at BsiWI and BstEII restriction sites using standard cloning techniques. The vector used, pFUSE2-CLIg-hk from Invivogen (San Diego, CA), already contained the constant region of the kappa light chain (Figure S3.1). A Quikchange site-directed mutagenesis kit (Stratagene, La Jolla, CA) was used to generate plasmids for the desired N-terminal Glu-Glu-Ser (EES) mutant. Incorporation of these mutations was verified by sequencing.

3.5.3 Construction of heavy chain anti-HER2 human IgG1 expression plasmids

A plasmid for the expression of the anti-HER2 heavy chain was cloned in a similar fashion to that of light chain. In brief, the variable and constant region 1 of heavy chain (V_H and C_H1) was constructed from the following set of oligonucleotides with additional bases (CTCCAAACA) at the 5' end, corresponding to three N-terminal residues, Leu-Gln-Thr (LQT).

R0 TTTTTTTcttagctgctttga
F0 tcaaagcagctaagAAAAAAAGAATTCGCTCCAAACAG
R21 CGACGAGTTGGACTTCTGTTTGGAGCGAATTC
F38 AAGTCCAACTCGTCGAAAGCGGAGGTGGC

R53 CCAGGCTGAACCAGGCCACCTCCGCTTT
F67 CTGGTTCAGCCTGGCGGAAGCCTGCGC
R81 GCAGCACAGCTCAAGCGCAGGCTTCCG
F94 TTGAGCTGTGCTGCCTCCGGATTTAATATCAAAGA
R108 CGAACCCAGTGTATATAAGTATCTTTGATATTAAATCCGGAG
F129 TACTTATATACACTGGGTTCGCCAGGCTCCTGGA
R150 CCACTCCAGACCCTTTCCAGGAGCCTGG
F163 AAGGGTCTGGAGTGGGTGGCGAGAATCTACC
R178 GGGTATAACCATTGGTTGGGTAGATTCTCGCCAC
F194 CAACCAATGGTTATACCCGCTATGCAGACAGCG
R212 GTAAACCGCCCTTTCACGCTGTCTGCATAGC
F227 TGAAAGGGCGGTTTACAATTAGTGCCGACACA
R243 GGTAAGCGGTATTTTTAGATGTGTCGGCACTAATT
F259 TCTAAAAATACCGCTTACCTCCAGATGAACTCTCTG
R278 TGTCCTCGGCCCTCAGAGAGTTCATCTGGA
F295 AGGGCCGAGGACACGGCTGTGTATTATTGC
R308 CACCCCACCGGCTGCAATAATACACAGCCG
F325 AGCCGGTGGGGTGGAGACGGATTCTATGCT
R338 TGACCCCAATAGTCCATAGCATAGAATCCGTCTC
F355 ATGGACTATTGGGGTCAGGGCACTCTCGTCA
R372 TGGCACTGCTTACAGTGACGAGAGTGCCC
F386 CTGTAAGCAGTGCCAGCACAAAGGGGCC
R401 CAAGGGGAAAGACACTAGGCCCCTTTGTGC
F414 TAGTGTCTTTCCCCTTGCTCCATCTAGCAAATCTAC
R431 GGTGCCCCCGCTGGTAGATTTGCTAGATGGAG
F450 CAGCGGGGGCACCGCCGCCCTGGGAT
R463 GTCCTTGACCAGGCATCCCAGGGCGGC
F476 GCCTGGTCAAGGACTATTTTCCTGAGCCAGT
R490 TCCAGGACACGGTGACTGGCTCAGGAAAATA
F507 CACCGTGTCCTGGAATAGTGGCGCCTTGA
R521 TGTGTGAACACCAGAAGTCAAGGCGCCACTAT
F536 CTTCTGGTGTTCACACATTTCCCGCCGTCC
R553 CAGCCCACTAGATTGAAGGACGGCGGGAAA
F566 TTCAATCTAGTGGGCTGTACTCTCTCTCCAGTGT
R583 TGGGTACCGTCACCACACTGGAGAGAGAGTA
F600 GGTGACGGTACCCAGTTCAAGCTTGGGCA
R614 TGCAGATATAGGTCTGTGTGCCCAAGCTTGAAC
F629 CACAGACCTATATCTGCAATGTGAACCACAAGCC
R647 CCACCTTTGTATTGCTGGGCTTGTGGTTCACAT
F663 CAGCAATACAAAGGTGGACAAAAAAGTCGAGCCT
R680 TGTCACAGCTCTTTGGAGGCTCGACTTTTTTGT
F697 CCAAAGAGCTGTGACAAAACTCACACATGCCC
R713 TACCTGGGCACGGTGGGCATGTGTGAGTTT
F729 ACCGTGCCCAGGTAAGCCAGCCCAGGC
R743 ccccattgactTTTTTTTAGGCCTGGGCTGGCT

R756 CTAAAAAAAagtcaatgggg

The BglII site was introduced using PCR with forward primer F0 and a reverse primer containing a BglII restriction site (sequences shown below).

Forward: tcaaagcagctaagAAAAAAAGAATTCGCTCCAAACAG

Reverse: ttttttAGATCTCTTTGGAGGCTCGACTTTTTTGT

The gene encoding V_H and C_H1 was inserted into a vector comprising the crystallizable fragment (Fc) domain (i.e., C_H2 and C_H3 domains) of human IgG1 heavy chain (pINFUSE-hIgG1-Fc2 from Invivogen) at the EcoRI and BglII restriction sites (Figure S3.1). A Quikchange site-directed mutagenesis kit was used to generate plasmids for the desired N-terminal Ala-Lys-Thr (AKT), Pro-Glu-Ser (PES), and Glu-Glu-Ser (EES) mutants. Incorporation of these mutations was verified by sequencing.

3.5.4 General procedure for expression and purification of mutant antibodies

The plasmids for the light and heavy chains of the anti-HER2 antibody were transiently co-transfected into human embryonic kidney (HEK) 293T cells in a 3:2 ratio using Lipofectamine 2000 (Invitrogen, Grand Island, NY) in Opti-MEM medium following the protocol from Invitrogen. The ratio used was found to be one of the highest yielding from the optimization process in which various ratios of heavy to light chain plasmids were used. The cells were incubated at 37 °C in 5% CO_2. After two days, the media was collected and the secreted antibodies were purified using protein G affinity chromatography, according to the procedure from the manufacturer (Pierce, Rockford, IL). The media was replaced and cultures were grown for an additional 3 days, after which the additional antibodies were harvested and purified as above. Purified protein was buffer exchanged into PBS using Amicon Ultra 4 mL 10 kDa MWCO (Millipore) centrifugal ultrafiltration membranes. Purity was evaluated by SDS-PAGE with Coomassie staining.

3.5.5 General procedure for PLP or RS-mediated transamination of antibody substrates

Protein, PLP, and RS stock solutions were prepared at twice the desired final concentration and mixed in equal volumes in a 1.7 mL Eppendorf tube. The 2x antibody stock solutions were prepared at 0.5 - 1 mg/mL in 25 mM phosphate buffer at pH 6.5. The 2x PLP or RS stock solution (200 mM) was freshly prepared before each reaction in 25 mM phosphate buffer (with 0.02% NaN_3), pH 6.5 from solid stocks of PLP (pH adjustment using 1-5 M NaOH solution is necessary for the solubility of PLP in buffer) [50] or RS (recrystallized from acetonitrile). The reaction mixture was briefly agitated to ensure mixing and then incubated without further agitation at 37 °C for 1 h. Following the reaction, the excess aldehyde was removed using NAP Sephadex size exclusion columns (GE Healthcare, USA). The resulting keto-protein solution was then concentrated and buffer exchanged using 0.5 mL spin concentrators with a MWCO of 10 kDa (Millipore, Billerica, MA). The buffer exchange first involved the dilution of each sample to 500 µL with 25 mM phosphate buffer (pH 6.5). Each sample was then concentrated to ~50 µL, and the process was repeated 3 times. The resulting keto-protein was then treated with 125 mM $BnONH_2$ (in water with the pH adjusted to 5.5) in a 1.7 mL Eppendorf tube and incubated at RT for 48 h to analyze the transamination efficiency. After oxime formation, the NAP column and buffer exchange steps were again repeated to remove the excess alkoxyamine to stop the reaction. The reduction and capping of antibody chains for mass spectrometry analysis of modification of the heavy and light

chains is described as followed.

3.5.6 General procedure for generating antibody-aniline conjugates via N-terminal transamination

First, the Ala-Lys-Thr (AKT) mutant of anti-HER2 antibodies was subjected to PLP-mediated N-terminal transamination as described above. The aniline group was attached at the N-termini via oxime formation of transaminated products and aniline-ONH_2 (synthesis of this small molecule was described in chapter 2 and also in Ref. 37). The oxime formation was conducted in 25 mM phosphate buffer pH 5 at RT for 40-48 h. Under these conditions, we believe that the ketone generated from transamination would form oxime products.

3.5.7 General procedure for generating antibody-aniline conjugates via lysine modification using aniline-COOH/NHS/EDC

Aniline-NHS ester was pre-formed by mixing 3-(4-aminophenyl) propionic acid (aniline-COOH), *N*-hydroxysuccinimide (NHS), and 1-ethyl-3-(3-dimethylaminopropyl)carbodiimide (EDC) in a 1:1:1 ratio at a final concentration of 50 mM in DMF for 10 mM at RT. An example of the mixture is shown below.

Reagent	Stock conc.	Vol (μL)	Final conc.
Aniline-COOH	100 mM	50	50 mM
NHS	0.5 M	10	50 mM
EDC	125 mM	40	50 mM

In the meantime, the antibody was buffer exchanged into 25 mM phosphate buffer pH 8 by spin concentration 3-6 times using Amicon-0.5 mL spin concentrators with a MWCO of 10 kDa (Millipore, Billerica, MA). For a 100 uL reaction, 5 uL of aniline-COOH/NHS/EDC mixture was added to 95 uL of ~ 1mg/mL Ab (scale up as appropriate). The reaction was incubated at RT for 1 h and quenched by adding 10 μL of 110 mM NH_2-OH (final conc. = 10 mM) to reverse any transient amide bond formation. The small molecules were then removed from the reaction mixture by using NAP Sephadex size exclusion columns (GE Healthcare, USA) equilibrated with 25 mM phosphate buffer pH 6.5. Further spin concentration using Amicon-0.5 mL spin concentrators with a MWCO of 10 kDa up to 6 times with 25 mM phosphate buffer pH 6.5 was conducted to ensure all aniline-COOH was removed. The Ab-aniline conjugates can be stored at 4 °C. An example of a detailed protocol is in the supplementary information of this chapter.

3.5.8 General procedure for generating aminophenol DNA oligonucleotides

The procedure for generating aminophenol-DNA (AP-DNA) was previously published [51,52]. Briefly, the stock solution of 1 mM amine-DNA (DNA oligonucleotides with amine ($C6NH_2$) functional group at the 5' end) in 50 mM phosphate buffer pH 8 was mixed with 38 mM nitrophenol-NHS ester (NP-NHS) in DMF in a 1:1 ratio. The reaction mixture was incubated for 1.5 h at RT. Any precipitate may be filtered out using 0.22 uM spin filter. Excess NP-NHS was then removed by NAP Sephadex size exclusion columns (GE Healthcare, USA) equilibrated with ddH_2O. The resulting nitrophenol-DNA conjugates were collected in 1 mL ddH_2O (if NAP5 was used). Sodium dithionite ($Na_2S_2O_4$) was added to the final concentration of ~ 5 mM and incubated

with NP-DNA for 15 min at RT to reduce the nitrophenol to the aminophenol. The reaction mixture was then subjected to three NAP columns (equilibrated with ddH_2O) to ensure the removal of all excess small molecules which can affect subsequent bioconjugation steps. The resulting AP-DNA solution was frozen and then lyophilized o/n. It could be stored in lyophilized form or resuspended in 50 µL 50 mM phosphate buffer pH 7.2 and stored at -20 °C. An example of a detailed protocol is in the supplementary information of this chapter.

3.5.9 General procedure for conjugating antibody-aniline and aminophenol DNA

The antibody-DNA conjugates were generated via oxidative coupling of antibody-aniline and aminophenol-DNA using sodium periodate as an oxidant. However, potassium ferricyanide, the newly reported oxidant from the Francis group, may also be used following this similar procedure, as a milder alternative that does not oxidize glycans [19]. To the reaction mixture, the reagents in the table shown below were added (reaction can be scaled up or down as necessary) and left incubated at RT for 2-5 min.

Reagent	Stock conc.	Vol (µL)	Final conc.	# equivalents
Antibody-aniline	1-3 mg/mL (18-30 µM)	30	1-4 µM	1
AP-DNA	1 mM	15	100 µM	25-100
$NaIO_4$	10 mM	15	1 mM	
Imidazole	100 mM	15	10 mM	
PB pH 6.5	25 mM	75		
Total		150		

The excess small molecules were removed by NAP Sephadex size exclusion columns (GE Healthcare, USA) equilibrated with phosphate buffered saline (PBS). Antibody-DNA conjugates were purified from excess AP-DNA by AKTA FPLC system on Superdex 200 10/300 GL SEC column. All the fractions containing Ab-DNA were combined and spin concentrated with PBS using Amicon-4 mL or Amicon-0.5 mL spin concentrators with a MWCO of 10 kDa. The concentration of Ab-DNA was measured using BCA assay (Pierce). An example of a detailed protocol is in the supplement info of this chapter.

3.5.10 General procedure for antibody disulfide reduction and cysteine capping for mass spectrometry analysis

To prepare the antibody mutants for mass spectrometry analysis, first the oligosaccharides were removed via treatment with Peptide-N-Glycosidase F (PNGase F) following the protocol from the manufacturer (New England Biolabs, Ipswich, MA). Briefly, a buffer exchange into PBS was performed on the antibody samples. In a 1.7 mL Eppendorf tube, 35 µL of protein (~1 mg/mL) was mixed with 5 µL of G7 reaction buffer, 2 µL PNGase, and additional PBS to a total volume of 50 µL. The mixture was then incubated at 37 °C overnight. Immediately following treatment with PNGase, buffer exchange was performed into 100 mM Tris buffer, pH 8. Dithiothrietol (DTT) and ethylenediaminetetraacetic acid (EDTA) were then added to a final concentration of 10 mM each, and the reaction was incubated at room temperature for 20 min. After the reduction, iodoacetamide was added to a final concentration of 50 mM and the mixture was incubated at 37 ºC for 30

min. The samples were then subjected to buffer exchange into 10 mM Tris buffer pH 8 for mass spectrometry analysis.

3.5.11 Flow cytometry analysis of antibody bioconjugates

For the binding experiment, adherent cell lines (HCC1954, MCF7, MCF7 clone 18, L3.6pl, MDA-MB-231, and MDA-MB-453 cells) were first trypsinized at 37 °C for 5 min, followed by the addition of complete media (L-15 + 10% FBS in the case of MDA-MB-453, RPMI + 10% FBS in the case of HCC1954, or DMEM + 10% FBS for all the other cell lines) to stop trypsinization. For suspension cell lines (Jurkat and Ramos cells), the overnight culture were used without further treatment. Cells were then pelleted and resuspended in binding buffer (Dulbecco's phosphate buffered saline (DPBS) containing 1% FBS) to the density of 2-3 x10^6 cells/mL. Aliquots of 100 µL containing 2-3 x10^6 cells/mL of cells were incubated with antibody conjugate samples at specified final concentration for 45-60 min on ice. The cells were then washed twice with 150 µL of binding buffer (or once with 500 µL) and resuspended in 100 µL of binding buffer containing 1:1000 dil. anti-human IgG (Fcγ specific) PerCP-conjugated goat F(ab')$_2$ fragments or anti-mouse IgG AlexaFluor 488-conjugated antibodies (Life Technologies). Another secondary Ab used was anti-human IgG1 (Fc specific) FITC-conjugated purified mouse IgG clone 8c/6-39 (Sigma) at 0.15 µM final concentration. The cells were incubated for 30 min on ice in the dark, then washed twice with 150 µL of binding buffer (or once with 500 µL) and resuspended in 200 µL of binding buffer. The cells were analyzed by flow cytometry to determine the amount of FITC or PerCP fluorescence. For each sample, 10,000 cells were counted. A FACSCalibur flow cytometer (BD Biosciences, USA) equipped with 488 and 633 nm lasers were used for all flow cytometry measurements, usage courtesy of Prof. Carolyn Bertozzi (UC Berkeley). Data was analyzed using FlowJo 8.0 (TreeStar, Ashland, OR).

3.5.12 Instrumentation and sample analysis

3.5.12.1 Liquid chromatography mass spectrometry (LCMS) analysis of reduced antibody bioconjugates

Acetonitrile (Fisher Optima grade, 99.9%), formic acid (Pierce, 1 mL ampules, 99+%), and water purified to a resistivity of 18.2 MΩ·cm (at 25 °C) using a Milli-Q Gradient ultrapure water purification system (Millipore, Billerica, MA) were used to prepare mobile phase solvents for LCMS. Electrospray ionization mass spectrometry (ESI-MS) of proteins was performed using an Agilent 1260 series liquid chromatograph outfitted with an Agilent 6224 Time-of-Flight (TOF) LCMS system (Santa Clara, CA). The LC was equipped with a Poroshell 300SB-C18 (5 µm particles, 1.0 mm × 75 mm, Agilent, Santa Clara, CA) analytical column. Solvent A was 99.9% water/0.1% formic acid and solvent B was 99.9% acetonitrile/0.1% formic acid (v/v). For each sample, approximately 15 to 30 picomoles of analyte was injected onto the column. Following sample injection, a 20-100% B elution gradient was run at a flow rate of 0.55 mL/min for 7 min. Data was collected and analyzed using Agilent MassHunter Qualitative Analysis B.05.00.

3.5.12.2 Fast protein liquid chromatography (FPLC)

FPLC was performed on an AKTA Pure M System (GE Healthcare, USA). Size exclusion FPLC of Ab-DNA conjugates was accomplished using Superdex 200 10/300 GL column (GE Healthcare, USA) with 50 mM phosphate buffer, pH 7.0 in the presence of 150 mM NaCl and

0.02% NaN_3 as elution buffer at 0.5 mL/min flow rate.

3.5.12.3 Gel analyses

For protein analysis, sodium dodecyl sulfate-polyacrylamide gel electrophoresis (SDS-PAGE) was carried out on a Mini-Protean apparatus from Bio-Rad (Hercules, CA), following the protocol of Laemmli [53]. The reducing protein electrophoresis samples were heated for 10 min at 95 °C in the presence of β-mercaptoethanol to ensure reduction of any disulfide bonds. Gels were run for 60 min at 150 V to allow good separation of the bands. Commercially available markers (Bio-Rad) were applied to at least one lane of each gel for assignment of apparent molecular masses. Visualization of protein bands was accomplished by staining with Coomassie Brilliant Blue R-250 (Bio-Rad). For fluorescent protein conjugates, visualization was accomplished on a Typhoon 9410 (Amersham Biosciences). For visualizing single-stranded DNA, 0.02% Methylene Blue stain (for 50 mL, 10 mg Methylene Blue + 1 mL 5x TBE buffer + 49 mL ddH_2O) was used.

3.6 Supplementary Information

3.6.1 Design and assembly of synthetic DNAs

Design DNA:

1. Use GeneDesigner (DNA 2.0) to back-translate the protein sequence to a DNA sequence
2. Make sure to add a stop codon at the end of your gene
3. Check boxes for restriction sites you would like to avoid
4. Typical codon usage for protein expression in *E. coli* is Class II (highly-expressed during exponential growth) with a cut-off of 10%
5. Make sure the smallest repeat sequence is only 6-8 bp
6. Add any regulatory sequences (rbs, promoter) and cloning sequences (restriction sites, purification tags)
7. Back translate sequence

Design oligos for assembly:

1. Use Gene2Oligo (http://berry.engin.umich.edu/gene2oligo) to generate a set of oligos for the assembly
2. If default conditions do not succeed try lowering the hybridization length or the Tm
3. Design rescue primers for the 5' and 3' ends of the gene for PCR amplification and sub cloning (can just use the ones with lower case letters)

PCR Assembly of the Synthetic DNA:

1. Resuspend all of the primers to 100 µM in Buffer EB (or water)
2. Mix 5 µl of each of the primers to make a master mix (leaving out the rescue primers) and calculate the concentration of each primer in this solution
3. Dilute the master mix to 1 µM of each oligo
4. Make a serial dilution using this master mix with the final concentrations of each primer being 500, 250, 100, 50, and 25 nM
5. Set up the PCR using the following conditions:

Reaction: (in order of addition)

37.6 µL water
5 µL Pfu Turbo Reaction Buffer
1 µL dNTPs (10 mM each)
5 µL primer mix (1 uM to 25 nM in each oligo)
0.2 µL Forward Rescue Primer (100 uM)
0.2 µL Reverse Rescue Primer (100 uM)
1 µL Pfu Turbo
total volume = 50 µL

Thermocycler Conditions:

initial cycle:	95 °C, 5 min; 55 °C, 2 min; 72 °C, 1 min
25 cycles:	95 °C, 0.5 min; 55 °C, 0.5 min; 72 °C, 3-5 min
final extension:	72 °C, 10 min; 10 °C, infinity

6. Gel purify your fragment
7. (optional) PCR amplify your gene using the same rescue primers and your PCR program of choice

3.6.2 Sample protocol for generating antibody-aniline conjugates

Materials

1. 100 mM 3-(4-aminophenyl) propionic acid (aniline-COOH) (Sigma # 560251)
   (16.52 mg in 1 mL DMF) *Make fresh before use*
2. 0.5 M NHS (Sigma # 130672)
   (5.755 mg in 100 µL DMF) *Make fresh before use*
3. 125 mM EDC (Sigma # 03450)
   (2.4 mg in 100 µL DMF) *Make fresh before use*
4. 110 mM hydroxylamine HCl (NH_2-OH) (Sigma # 255580)
   (7.6 mg in 1 mL 50 mM phosphate buffer pH 8) *Make fresh before use*

Protocol

1. Buffer exchange antibody into 25 mM phosphate buffer pH 8 using Amicon-0.5 -10k 3-6 times
2. Mix aniline-COOH, NHS, and EDC (scale up as necessary)

Reagent	Stock conc.	Vol (µL)	Final conc.
Aniline-COOH	100 mM	50	50 mM
NHS	0.5 M	10	50 mM
EDC	125 mM	40	50 mM

   Incubate at RT for 10 min
3. Add 5 µL of aniline-COOH/NHS/EDC mixture to 95 uL of ~ 1 mg/mL Ab (buffered ex-

change in step 1) (Scale up as necessary)
4. Incubate at RT for 1 h
5. Quench reaction by adding 10 µL of 110 mM NH_2-OH (final conc = 10 mM)
6. NAP5 with 25 mM phosphate buffer pH 6.5 to remove excess small molecules
7. Spin concentrate using Amicon-0.5-10k 6 times with 25 mM phosphate buffer pH 6.5 (to make sure all aniline-COOH is removed)
8. Store Ab-aniline at 4 °C

3.6.3 Sample protocol for generating aminophenol-DNA

Material

1. 5 mM Amine-DNA in 50 mM phosphate buffer pH 8
2. 0.4 M nitrophenol-NHS (NP-NHS) in DMSO
   (0.123 g in 1 mL DMSO) *Can be stored as solution at -20 °C*
3. 100 mM $Na_2S_2O_4$ (Sigma, # 157953) in 0.2 M phosphate buffer pH 6.5
   (17.4 mg in 1 mL of 0.2 M PB pH 6.5) *Make fresh before use*

Protocol

1. Mix 50 µL of 5 mM amine-DNA with 200 µL of 50 mM phosphate buffer pH 8
2. Mix 24 µL of 0.4 M NP-NHS with 226 µL DMF
3. Mix solution from step 1 and 2. Incubate for 1.5 h at RT
4. If there is any precipitate, filter it out using 0.22 um spin filter
5. Remove excess NP-NHS using NAP 5 pre-equilibrated with ddH_2O (add 500 µL rxn mixture, then elute with 1 mL ddH_2O)
6. Add 53 uL of 100 mM $Na_2S_2O_4$ to the 1 mL from step 5
7. Incubate at RT for 15 min
8. NAP 10 pre-equilibrated with ddH_2O (1 mL rxn mixture, elute with 1.5 mL ddH_2O)
9. NAP25 pre-equilibrated with ddH_2O (1.5 mL from above, then 1 mL ddH_2O, elute with 2.5 mL ddH_2O)
10. NAP25 pre-equilibrated with ddH_2O (2.5 mL from above, elute with 3.5 mL ddH_2O)
    NOTE: These three NAP steps (8-10) may be eliminated by doing HPLC or FPLC purifi cation instead.
11. Freeze then lyophilize o/n
12. Resuspend in 50 uL 50 mM phosphate buffer pH 7.2
13. Measure A260 using Nanodrop. Then adjust concentration to 1 mM (keep stock at -20 °C)

3.6.4 Sample protocol for generating antibody-DNA conjugates

Materials

1. 1 mM Aminophenol-DNA (from above)
2. 3-5 mg/mL antibody-aniline (from above)
3. 10 mM $NaIO_4$ (Sigma # 311448) in 25 mM phosphate buffer pH 6.5

(2.1 mg in 1 mL 25 mM phosphate buffer pH 6.5) *Make fresh before use*

4. 100 mM imidazole pH 6.5

Protocol

1. Mix the following reagents:

Reagent	Stock conc.	Vol (µL)	Final conc.	# equivalents
Antibody-aniline	1-3 mg/mL (18-30 µM)	30	1-4 µM	1
AP-DNA	1 mM	15	100 µM	25-100
$NaIO_4$	10 mM	15	1 mM	
Imidazole	100 mM	15	10 mM	
PB pH 6.5	25 mM	75		
Total		150		

(Scale up or down as necessary)
Incubate at RT for 2-5 min

2. NAP5 with PBS to remove excess small molecules
3. Purify using AKTA system (Superdex 200 10/300 GL column, GE Healthcare)
   Elution buffer: 50 mM phosphate buffer + 150 mM NaCl + 0.02% NaN_3, pH 7.0
4. Combine all Ab-DNA fractions. Spin concentrate and buffer exchange into PBS using Amicon-4 mL or Amicon-0.5 mL spin concentrators with a MWCO of 10 kDa depending on the volume all the combined fractions and the final volume desired. For example, if starting volume is ~ 4 mL and the desired volume is ~100 uL, one approach is the following. Spin concentrate using Amicon-4-10k with PBS twice. Get all the liquid above membrane (rinse membrane with 200 uL PBS 3 times). Spin concentrate using Amicon-0.5-10k 2 times (14000 x*g*, 5-7 min). Flip (1000 x*g*, 2 min) then rinse the membrane with 50 µL PBS once. Obtain ~80-90 µL.
5. Measure the concentration of Ab-DNA using BCA assay

3.6.5 Supplementary figures

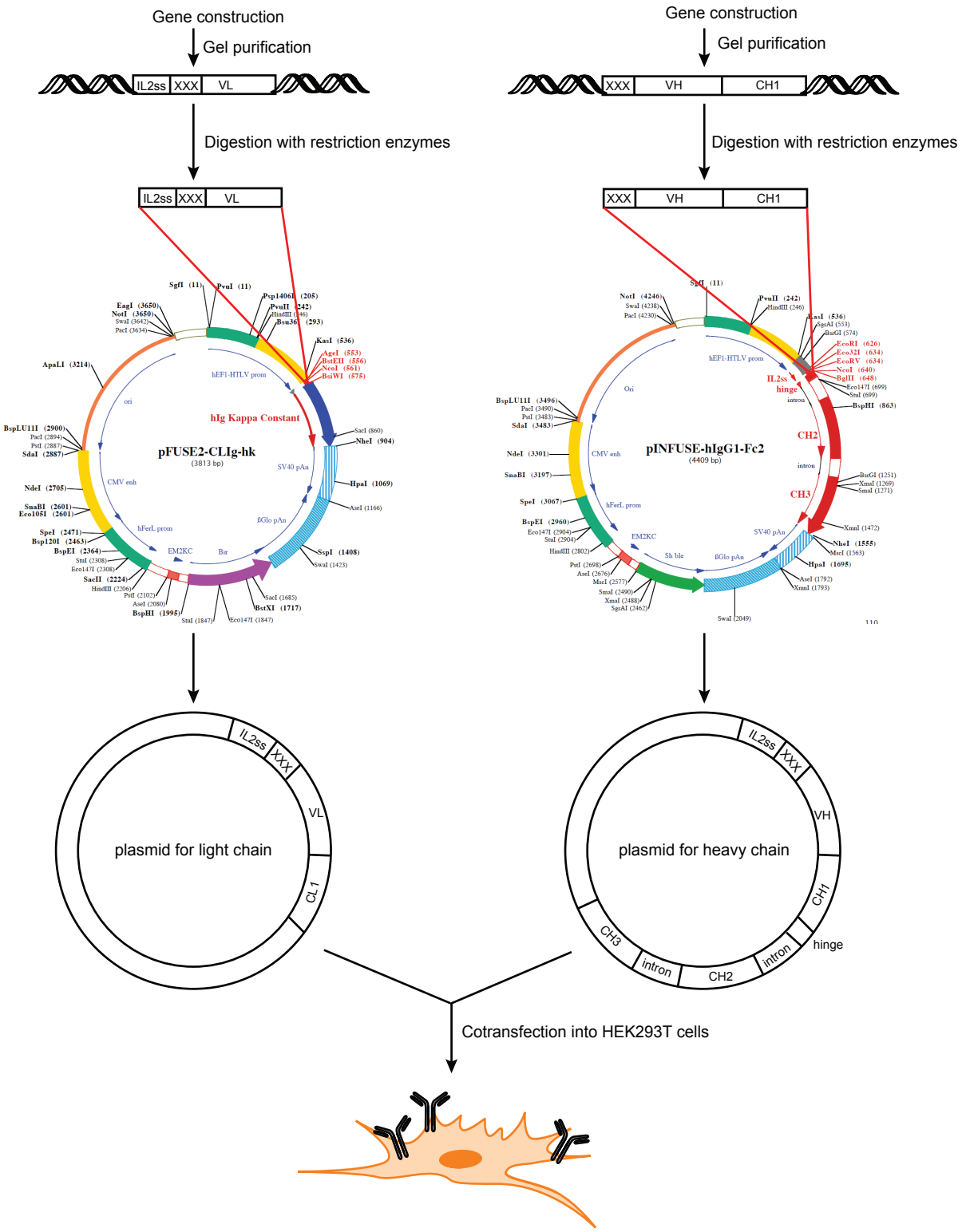

Figure S3.1. Scheme of antibody cloning and expression. The plasmid diagrams were obtained from the Invivogen catalog. "XXX" represents the three N-terminal residues that were extended in the mutant expressed to include the AKT, LQT, or EES motifs (Figure adapted from Ref. [1]).

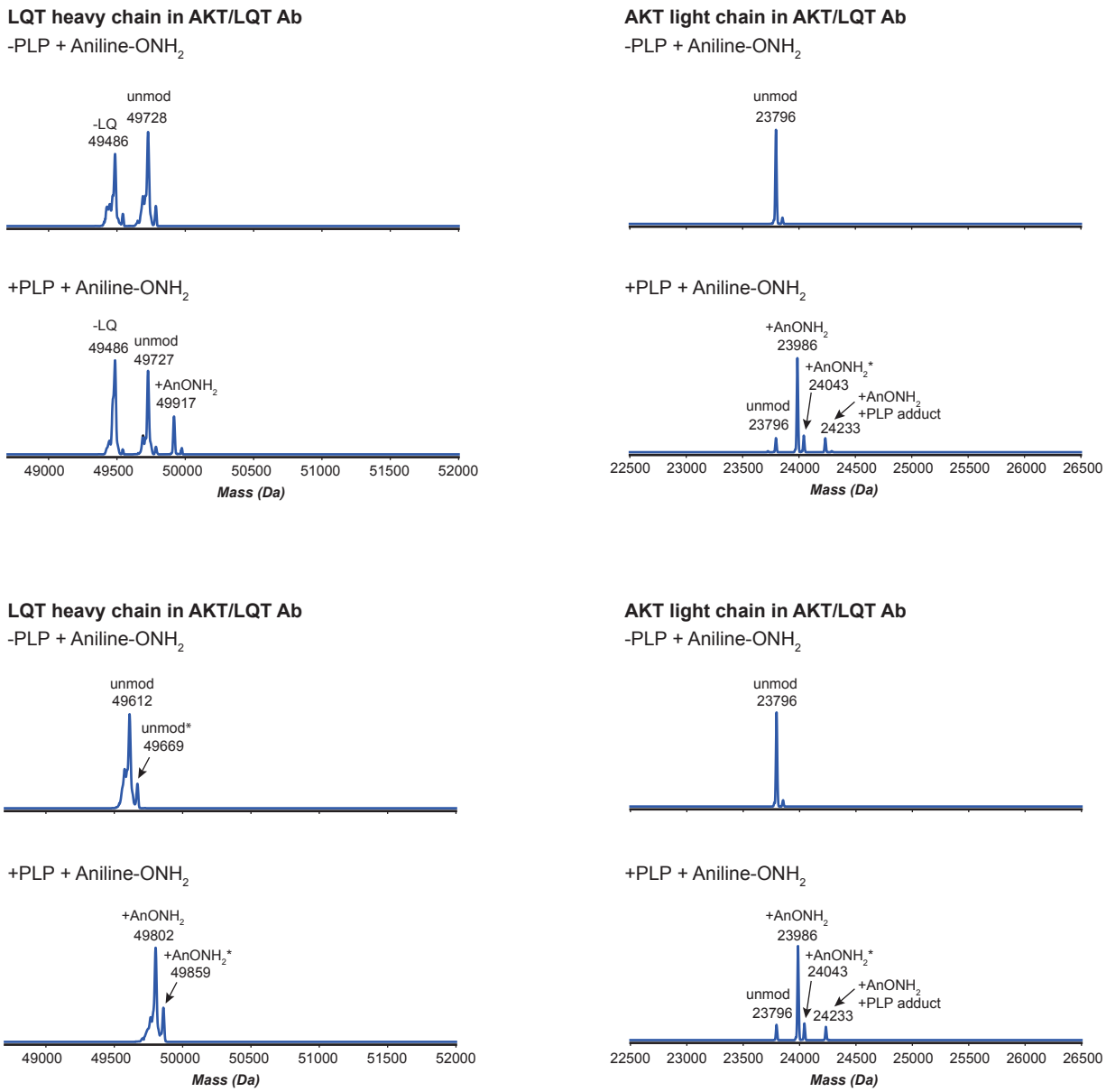

Figure S3.2. Deconvoluted LCMS spectra of the heavy and light chain of AKT/LQT and AKT/AKT anti-HER2 antibodies after transamination using PLP, followed by oxime formation with aniline-ONH_2 ($AnONH_2$). The full-sized antibodies were deglycosylated using PNGase F and reduced with DTT. The reduced cysteines were capped with iodoacetamide before LCMS analysis. The asterisk denotes peaks with an additional iodoacetamide attached to the proteins.

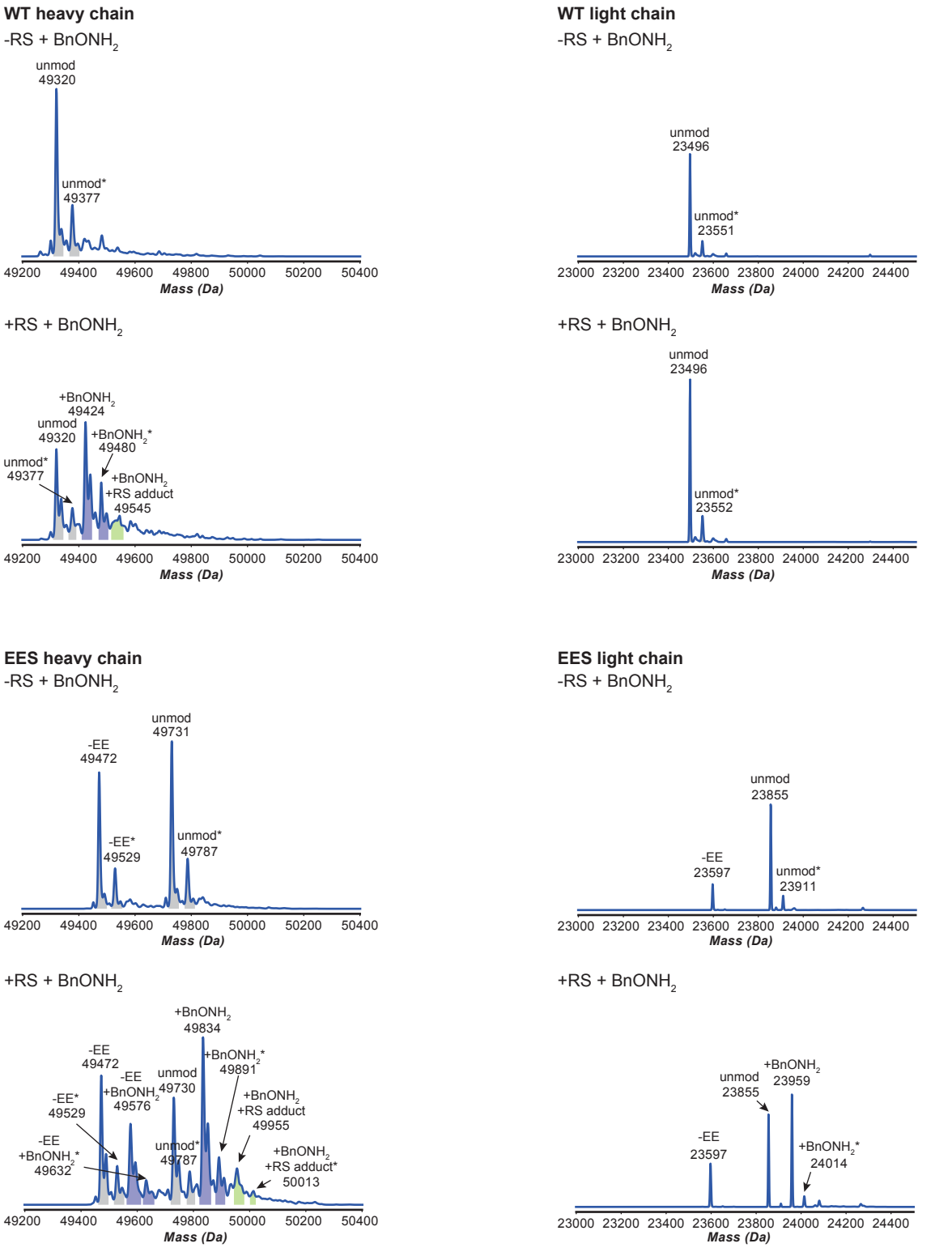

Figure S3.3. Deconvoluted LCMS spectra of the heavy and light chain of wild-type and EES/EES anti-HER2 antibodies after transamination using RS, followed by oxime formation with $BnONH_2$. The full-sized antibodies were deglycosylated using PNGase F and reduced with DTT. The reduced cysteines were capped with iodoacetamide before LCMS analysis. The asterisk denotes peaks with an additional iodoacetamide attached to the proteins. The shoulder peaks observed were 18 mass units from the main peak, and likely resulted from the addition of water. (Figure adapted from Ref. [1]).

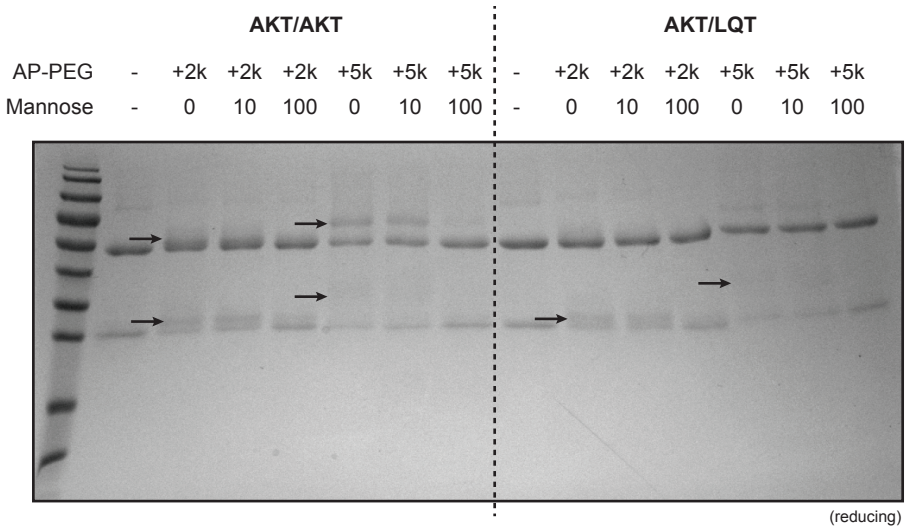

Figure S3.4. PEG shift analysis of oxidative coupling between aminophenol-PEG and antibody-aniline conjugates from N-terminal modification. Antibody-aniline conjugates from transamination of AKT/AKT and AKT/LQT Ab with PLP, followed by oxime formation with aniline-ONH_2, were subjected to oxidative coupling with aminophenol-PEG (2 kDa and 5 kDa). The AKT/AKT showed modification with PEG on both chains, while the LQT sequence on the heavy chain of the other sample greatly reduced the yield of aniline put on that chain, hence less oxidative coupling PEG products on the heavy chain of AKT/LQT Ab. Up to 10 mM of mannose can also be added to the reaction to suppress glycan oxidation without sacrificing the yield of oxidative coupling. At 100 mM mannose addition, the yield noticeably dropped. The analysis was performed on 10-20% Tris-HCl SDS-PAGE under reducing conditions.

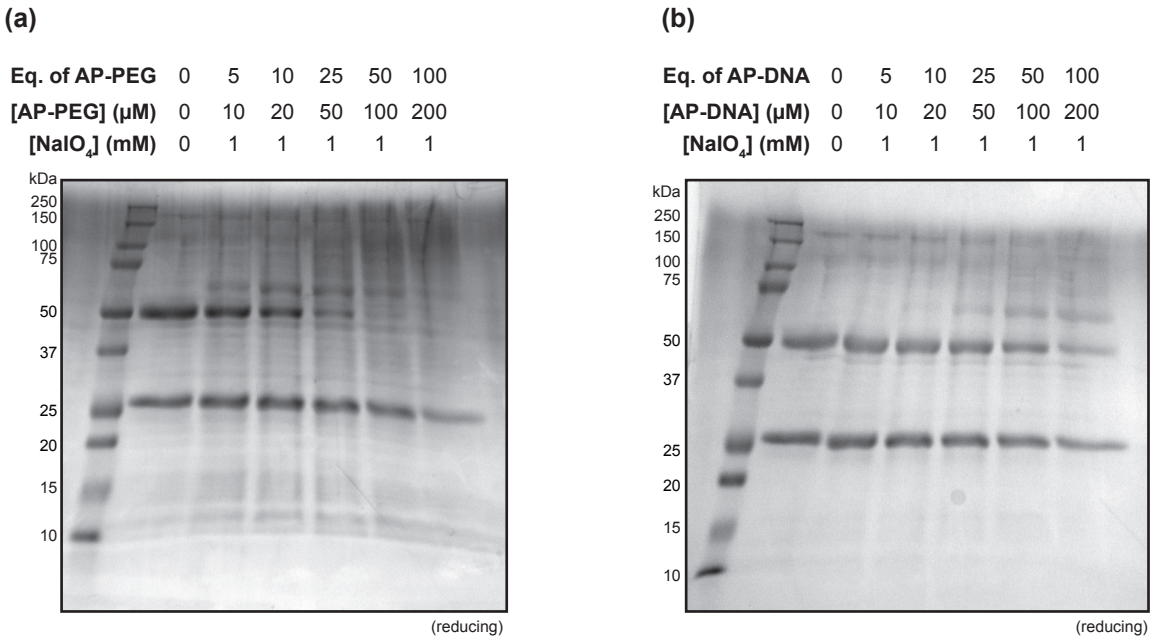

Figure S3.5. Equivalent screen of AP-5k PEG and AP-DNA (50-mer) in oxidative coupling with aniline-antibodies. The oxidative coupling reactions were performed with 2 μM aniline-antibodies in the presence of 1 mM $NaIO_4$ (except for the first lane which is a negative control), 10 mM imidazole, and various concentrations of aminophenol-5k PEG or 50-mer DNA at RT for 2 min. After 2 min, the reactions were quenched by adding 2 μL of 0.5 M TCEP and the reaction mixtures were analyzed by 10-20% Tris-HCl SDS-PAGE under reducing conditions.

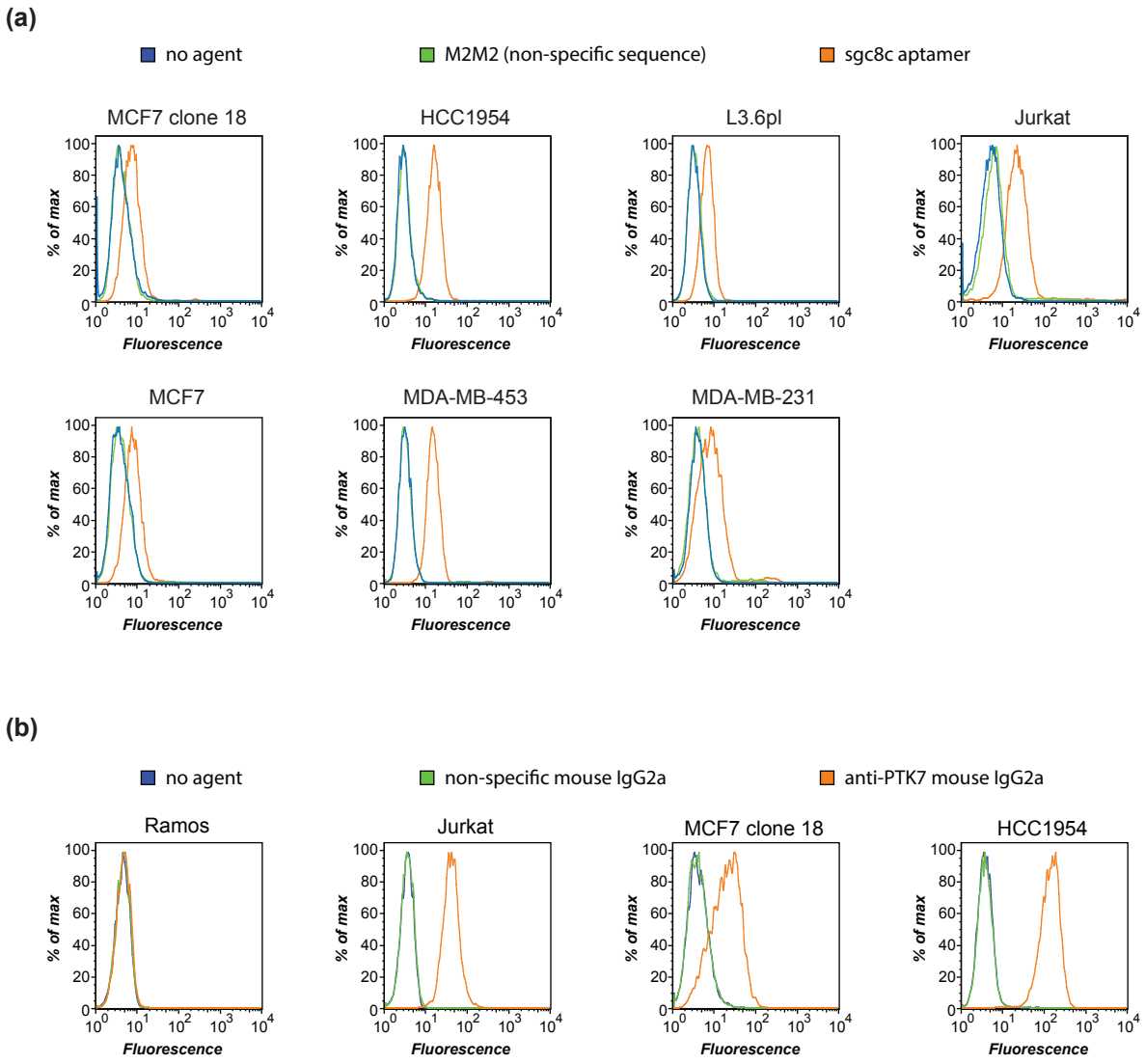

Figure S3.6. (a) Binding studies of sgc8c aptamers to various cancer cell lines. M2M2 was a non-specific 41-mer sequence, used as a negative control. (b) Expression level of PTK7 on MCF7 clone 18 and HCC1954, as compared to Jurkat (one of the original target cell lines for sgc8c aptamer), by flow cytometry analysis with anti-PTK7 mouse Ab. Non-specific mouse antibodies of the same isotype were used as a negative control.

3.7 References

1. Witus, L. S.; Netirojjanakul, C.; Palla, K. S.; Muehl, E. M.; Weng, C. H.; Iavarone, A. T.; Francis, M. B. *J. Am. Chem. Soc.* **2013**, *135*, 17223–17229.
2. Sano, T.; Smith, C. L.; Cantor, C. R. *Science*. **1992**, *258*, 120–122.
3. Niemeyer, C. M.; Sano, T.; Smith, C. L.; Cantor, C. R. *Nucl. Acids. Res*. **1994**, *22*, 5530–5539.
4. Niemeyer, C.; Adler, M.; Pignataro, B.; Lenhert, S.; Gao, S.; Lifeng, C.; Fuchs, H.; Dietmar, B. *Nucl. Acids. Res*. **1999**, *27*, 4553–4561.
5. Sugawara, K.; Kobayashi, D.; Saito, K.; Furuya, D.; Araake, H.; Yagihashi, A.; Yajima, T.; Hosoda, K.; Kamimura, T.; Watanabe, N. *Clin. Chim. Acta.* **2000**, *299*, 45–54.
6. Niemeyer, C. M.; Adler, M.; Wacker, R. *Nat. Protoc*. **2007**, *2*, 1918–1930.
7. Hendrickson, E. R.; Truby, T. M. H.; Joerger, R. D.; Majarian, W. R.; Ebersole, R. C. *Nucl. Acids. Res.* **1995**, *23*, 522–529.
8. Zhang, H. T.; Kacharmina, J. E.; Miyashiro, K.; Greene, M. I.; Eberwine, J. *Proc. Natl Acad. Sci. U.S.A*. **2001**, *98*, 5497–5502.
9. Schweitzer, B.; Wiltshire, S.; Lambert, J.; O'Malley, S.; Kukanskis, K.; Zhu, Z.; Kingsmore, S F.; Lizardi, P. M.; Ward, D. C. *Proc. Natl Acad. Sci. U.S.A.* **2000**, *97*, 10113–10119.
10. Fredriksson, S.; Gullberg, M.; Jarvius, J.; Olsson, C.; Pietras, K.; Gústafsdóttir, S. M.; Ostman, A.; Landegren, U. *Nat. Biotechnol.* **2002**, *20*, 473–477.
11. Fredriksson, S.; Dixon, W.; Ji, H.; Koong, A. C.; Mindrinos, M.; Davis, R. W. *Nat. Methods.* **2007**, *4*, 327–329.
12. Fredriksson, S.; Horecka, J.; Brustugun, O. T.; Schlingemann, J.; Koong, A. C.; Tibshirani, R.; Davis, R. W. *Clin. Chem.* **2008**, *54*, 582–589.
13. Agasti, S. S.; Liong, M.; Peterson, V. M.; Lee, H.; Weissleder, R. *J. Am. Chem. Soc.* **2012**, *134*, 18499–18502.
14. Fan, R.; Vermesh, O.; Srivastava, A.; Yen, B. K. H.; Qin, L.; Ahmad, H.; Kwong, G. A.; Liu, C.-C.; Gould, J.; Hood, L.; Heath, J. R. *Nat. Biotechnol.* **2008**, *26*, 1373–1378.
15. Kozlov, I. A.; Melnyk, P. C.; Stromsborg, K. E.; Chee, M. S.; Barker, D. L.; Zhao, C. *Biopolymers.* **2004**, *73*, 621–630.
16. Kazane, S. A.; Sok, D.; Cho, E. H.; Uson, M. L.; Kuhn, P.; Schultz, P. G., Smider, V. V. *Proc. Natl Acad. Sci. U.S.A.* **2012**, *109*, 3731–3736.
17. Hooker, J. M.; Esser-Kahn, A. P.; Francis, M. B. *J. Am. Chem. Soc.* **2006**, *128*, 15558–15559.
18. Behrens, C. R.; Hooker, J. M.; Obermeyer, A. C.; Romanini, D. W.; Katz, E. M.; Francis, M. B. *J. Am. Chem. Soc.* **2011**, *133*, 16398–16401.
19. Obermeyer, A. C.; Jarman, J. B.; Netirojjanakul, C.; El Muslemany, K.; Francis, M. B. *Angew. Chem. Int. Ed. Engl.* **2014**, *53*, 1057–1061.
20. Gilmore, J. M.; Scheck, R. A.; Esser-Kahn, A. P.; Joshi, N. S.; Francis, M. B. *Angew. Chem. Int. Ed.* **2006**, *45*, 5307–5311.

21. Scheck, R. A.; Francis, M. B. *ACS Chem. Biol.* **2007**, *2*, 247–251.

22. Scheck, R. A.; Dedeo, M. T.; Iavarone, A. T.; Francis, M. B. *J. Am. Chem. Soc.* **2008**, *130*, 11762–11770.

23. Witus, L. S.; Moore, T.; Thuronyi, B. W.; Esser-Kahn, A. P.; Scheck, R. A.; Iavarone, A. T.; Francis, M. B. *J. Am. Chem. Soc.* **2010**, *132*, 16812–16817.

24. Snell, E. E. *J. Am. Chem. Soc.* **1945**, *67*, 194–197.

25. Dixon, H. B. F. J. *Protein Chem.* **1984**, *3*, 99–108. (g) Dixon, H. B. F.; Fields, R. *Methods Enzymol.* **1972**, *25*, 409–419.

26. Kontermann, R. *mAbs*. **2012**, *4*, 182–197.

27. Byrne, H.; Conroy, P. J.; Whisstock, J. C.; O'Kennedy, R. J. *Trends. Biotech.* **2013**, *31*, 621–632.

28. Kontermann, R. E. (n.d.). *Bispecific Antibodies*. Springer **2011**; ISBN 978-3-642-20909-3.

29. Seimetz, D.; Lindhofer, H.; Bokemeyer, C. *Cancer. Treat. Rev.* **2010**, *36*, 458–467.

30. Parashar, A.; Sarkar, S. Ganguly, A.; Sharma, S.K.; Suresh, M. R. *Bispecific antibodies for diagnostic applications*. In *Bispecific Antibodies* (1st edn) (Kontermann, R.E., ed.), pp. 349–367, Springer **2011**.

31. Private discussion with Dr. Leah S. Witus.

32. Liu, H.; Gaza-Bulseco, G.; Faldu, D.; Chumsae, C.; Sun, J. *J. Pharm. Sci.* **2008**, *97*, 2426−2447.

33. Chelius, D.; Jing, K.; Lueras, A.; Rehder, D. S.; Dillon, T. M.; Vizel, A.; Rajan, R. S.; Li, T.; Treuheit, M. J.; Bondarenko, P. V. *Anal. Chem.* **2006** , *78*, 2370−2376.

34. Yu, L.; Vizel, A.; Huff, M. B.; Young, M.; Remmele, R. L., Jr.; He, B. *J. Pharm. Biomed. Anal.* **2006**, *42*, 455−463.

35. Cho, H.-S.; Mason, K.; Ramyar, K. X.; Stanley, A. M.; Gabelli, S. B.; Denney, D. W.; Leahy, D. J. *Nature* **2003**, *421*, 756–760.

36. Obermeyer, A.; Jarman, J. B.; Francis, M. B., *submitted*.

37. Netirojjanakul, C.; Witus, L. S.; Behrens, C. R.; Weng, C. H.; Iavarone, A. T.; Francis, M. B. *Chem. Sci*. **2013**, *4*, 266–272.

38. Shangguan, D.; Li, Y.; Tang, Z.; Cao, Z. C.; Chen, H. W.; Mallikaratchy, P.; Sefah, K.; Yang, C. J.; Tan, W. *Proc. Natl. Acad. Sci.* **2006**, *103*, 11838–11843.

39. Shangguan, D.; Tang, Z.; Mallikaratchy, P.; Xiao, Z.; Tan, W. *Chembiochem* **2007**, *8*, 603–606.

40. Shangguan, D.; Cao, Z.; Meng, L.; Mallikaratchy, P.; Sefah, K.; Wang, H.; Li, Y.; Tan, W. J. *Proteome Res.* **2008**, *7*, 2133–2139.

41. Mallikaratchy, P.; Tang, Z.; Kwame, S.; Meng, L.; Shangguan, D.; Tan, W. *Mol. Cell. Proteomics* **2007**, *6*, 2230–2238.

42. Mallikaratchy, P. R.; Ruggiero, A.; Gardner, J. R.; Kuryavyi, V.; Maguire, W. F.; Heaney, M.

L.; McDevitt, M. R.; Patel, D. J.; Scheinberg, D. A. *Nucl. Acids Res.* **2011**, *39*, 2458–2469.

43. Baeuerle, P. A.; Reinhardt, C. *Cancer Res*. **2009**, *69*, 4941–4944.
44. Mølhøj, M., Crommer, S.; Brischwein, K.; Rau, D.; Sriskandarajah, M.; Hoffmann, P.; Kufer, P.; Hofmeister, R.; Baeuerle, P. A. *Mol. Immunol*. **2007**, *44*, 1935–1943.
45. Lutterbuese, R., *et al*. *Proc. Natl Acad. Sci. U.S.A.* **2010**, *107*, 12605–12610.
46. Amann, M., *et al*. *Cancer Res*. **2008**, *68*, 143–151.
47. Zhu, Z.; Carter, P. *J. Immunol*. **1995**, *155*, 1903–1910.
48. Kim, C. H.; Axup, J. Y.; Dubrovska, A.; Kazane, S. A.; Hutchins, B. A.; Wold, E. D.; Smider, V. V.; Schultz, P. G. *J. Am. Chem. Soc*. **2012**, *134*, 9918–9921.
49. Rouillard, J.-M.; Lee, W.; Truan, G.; Gao, X.; Zhou, X.; Gulari, E. *Nucl. Acids Res.* **2004**, *32*, 176–180. To access Gene2Oligo, go to http://berry.engin.umich.edu/gene2oligo/.
50. Witus, L. S.; Francis, M. B. *Curr. Protoc. Chem. Biol.* **2010**, *2*, 125–134.
51. Tong, G. J.; Hsiao, S. C.; Carrico, Z. M.; Francis, M. B. *J. Am. Chem. Soc.* **2009**, *131*, 11174–11178.
52. Capehart, S. L.; Coyle, M. P.; Glasgow, J. E.; Francis, M. B. *J. Am. Chem. Soc.* **2013**, *135*, 3011–3016.
53. Laemmli, U. K. *Nature*. **1970**, *227*, 680–685.

Chapter 4

A New Strategy for Generation of MS2-Antibody Conjugates

Abstract

This chapter describes a new strategy for conjugating antibodies to MS2 viral capsids. Previous work in the Francis Group has shown successful uses of the MS2 viral capsid as a targeted delivery vehicle for imaging agents and therapeutics using peptides or DNA aptamers as targeting moieties. Here, we expand the classes of targeting groups to include antibodies, arguably the most widely used targeting agents to date. The oxidative coupling reaction was chosen to conjugate the two large protein molecules. The antibodies were modified with nitrophenol coupling partners, followed by reduction and oxidative coupling with *p*-aminophenylalanine-containing MS2 capsids. The biophysical and biological properties of the resulting MS2-Ab conjugates were assessed.

The studies described in this chapter were done in collaboration with Dr. Adel Elsohly, Ioana Aanei, and Dr. Michelle Farkas and will be a part of a peer-reviewed publication.

4.1 Introduction

Multivalent scaffolds, such as polymers [1,2], dendrimers [3,4], inorganic nanoparticles [5,6], and liposomes [7,8], have been useful in many applications, including research tools, drug delivery, and diagnostic imaging. In addition to these synthetic scaffolds, self-assembled multimeric biomolecule complexes, such as heat shock proteins [9-11] and viral capsids [12-17], have also shown great promise for development of next generation imaging and drug delivery agents. The interior cavities and multiple attachment sites of these protein cage scaffolds allow them to house a large amount of imaging or therapeutic agents, leading to the enhancement of the imaging intensity and ability to deliver multiple copies of drug molecules. However, in order to achieve specific detection or delivery, these vehicles have to be modified with targeting agents. Various chemical bioconjugation techniques have played crucial roles in the development of these targeted protein cage nanoparticles using different types of targeting groups, including small molecules [18,19], nucleic acid aptamers [15], peptides [10,20,21], glycans [22], or antibodies [10,23].

Work in our lab has established the use of bacteriophage MS2 as a multimeric scaffold. The 27 nm capsid can be expressed recombinantly and self-assembles from 180 protein subunits. We have engineered both the interior and exterior surface of these capsids to allow for loading small molecule cargos on the inside and targeting agents on the outside. First, a solvent-accessible cysteine residue was introduced to the interior surface for site-specific attachment of small molecules that can diffuse through thirty-two 2 nm pores of these capsids. Dyes [14,15], photodynamic agents [24], metal ion chelators [17,25], or even drug molecules [16] have been successfully installed. Second, a non-natural amino acid *p*-aminophenylalanine (*p*AF) residue was engineered onto the exterior surface. This residue is critical for allowing site-specific attachment of targeting agents via an oxidative coupling (O.C.) reaction, which allows conjugation of large biomolecules to proceed rapidly with high product conversion under mild conditions [15,20,26]. This reaction has been used previously to attach peptides [20] and DNA oligonucleotides [15,27] to the capsids.

In this chapter, we describe the use of these strategies to generate MS2-antibody (MS2-Ab) conjugates. Among the different types of targeting agents, antibodies have been the most widely used for a variety of applications due to their high specificity and affinity to targets. In fact, until now, more than 20 antibodies have been approved as therapeutic agents targeting specific ligands or receptors [28-30]. Even more have been used as research tools or developed into diagnostic or imaging agents. Our strategy is to combine the high specificity and affinity of antibodies with the signal enhancement property of the MS2 capsid. The work presented here broadens the use of bacteriophage MS2 to reach more targets for use in a wider range of applications.

4.2 Design and Strategy

Previous work in the Francis Group has demonstrated the concept of using MS2 viral capsids as delivery vehicles for imaging agents [17,25] and therapeutic drugs [16,24]. The capacity of MS2 to load up to 180 copies of small molecules inside the capsid make it particularly useful for enhancing the intensity of imaging agents or delivering multiple copies of drugs in one carrier. To direct these carriers to specific targets, we have employed several classes of targeting agents, including cyclic peptides [20], designed ankyrin repeat proteins (DARPins) (unpublished), and DNA aptamers [15]. Antibodies, one of the largest collection of targeting agents, are still untapped. In this chapter, we established a strategy for conjugating antibodies to MS2 viral capsids for mass cytometry (CyTOF) and *in vivo* positron emission tomography (PET) imaging applications. The

enhancement in signal intensity gained by the attachment of >100 copies of metal chelators in one agent could be particularly useful in both applications.

4.2.1 Interior design

MS2 viral capsids can be decorated with small molecules on the interior via diffusion of these molecules through 2 nm pores in the capsids. To achieve interior modification, prior effort in the lab has utilized site-directed mutagenesis to incorporate Cys at residue 87 (N87C mutation). With no other solvent exposed Cys residues in MS2, small molecules can then be attached to the interior surface via maleimide-thiol chemistry (Figure 4.1).

4.2.2 Exterior design

Due to large sizes of both Ab and the MS2 viral capsid, we used oxidative coupling as the conjugation reaction of choice. This reaction has been shown to couple two large biomolecules under mild conditions and with very short reaction times [15,20,26,31]. However, the biomolecules need to contain oxidative coupling partners, one bearing an aniline and the other bearing an aminophenol [20]. Aniline-containing MS2 viral capsids were obtained via non-natural amino acids incorporation of *p*-aminophenylalanine (*p*AF) on the exterior surface of the capsids [32]. Aminophenol was attached to the antibodies via non-site-specific lysine modification using a nitrophenol-NHS ester, followed by the reduction of the nitrophenol-conjugated products to the corresponding aminophenols. $NaIO_4$ was then used as the oxidant to couple the two partners (Figure 4.1). However, $K_3Fe(CN)_6$, a newly reported oxidant, can also be used [33].

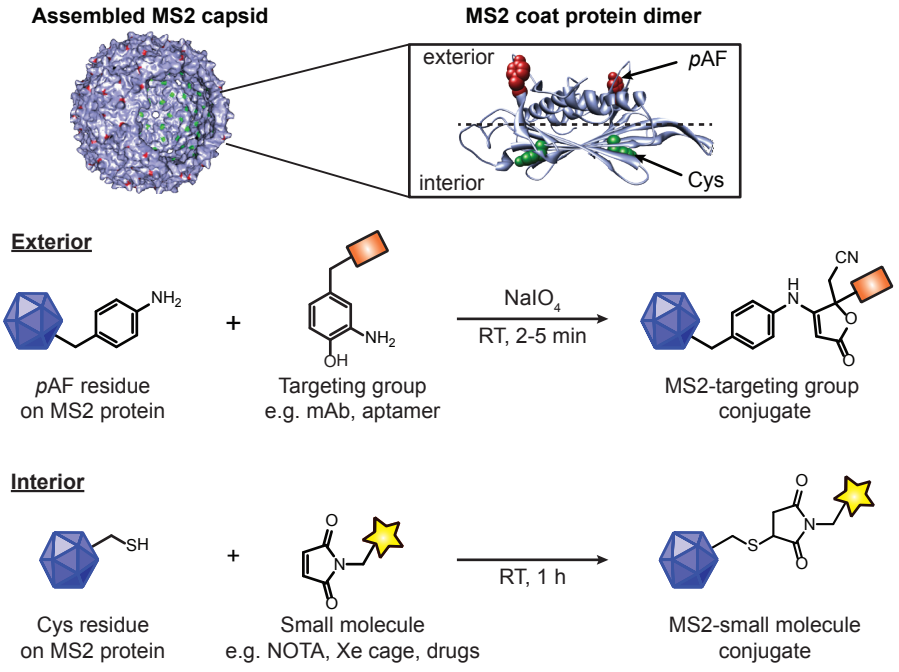

Figure 4.1. Site-specific dual surface modification of MS2 viral capsid. The exterior surface was introduced *p*-aminophenylalanine (*p*AF) residues for conjugation using oxidative coupling reaction. An Arg87 on the interior surface was mutated to a cysteine residue for an attachment with maleimide.

4.2.3 Linkers between antibody and MS2

We hypothesized that upon attachment, the conjugated antibodies may lie tangentially on the MS2 viral capsid surface; thus 5 kDa polyethylenenglycol (PEG) linkers were inserted as spacers between antibody (Ab) and MS2 capsid. The Ab would first be conjugated to nitrophenol-containing 5 kDa PEG-COOH (NP-PEG-COOH) via EDC coupling with lysine residues. Subsequent reduction would result in aminophenol-PEG-Ab (AP-PEG-Ab) conjugates, which can be oxidatively coupled to *p*AF MS2.

4.3 Results and Discussion

4.3.1 Antibody modification and attachment to MS2 viral capsids

First, antibodies were modified with nitrophenol-NHS ester (NP-NHS) at lysine residues, followed by reduction using $Na_2S_2O_4$ to obtain aminophenol-conjugated Ab (AP-Ab). The AP-Ab was then conjugated to the *p*AF residues on MS2 viral capsids via O.C. using $NaIO_4$ as the oxidant (Figure 4.2a). To investigate the possibility of generating MS2-Ab conjugates, we used an anti-human IgG mouse monoclonal antibody as a model substrate. To find the optimal number of aminophenol coupling partners to be attached to Ab, we varied the number of equivalents of NP-NHS from 5-100 equivalents in the first step. LCMS analysis revealed that with 5 equivalents of NP-NHS, ~30% of the light chains were modified with one NP and ~75% of the heavy chains had one, two, or three NPs (Figure 4.2b). More nitrophenol groups were appended on both the heavy and light chains as the number of NP-NHS increased. More than 10 nitrophenol groups were attached to the heavy chains and an average of 6 groups to the light chains when 100 equivalents of NP-NHS were added (Figure S4.1). However, even with only 5 equivalents of NP-NHS, the calculation of product distribution resulted in 98% of the full-sized Ab having at least one NP attached (Figure S4.2). After reducing the nitrophenol to aminophenol groups, these AP-Ab were then subjected to trial oxidative coupling reactions with *p*AF-MS2 in 3:1 and 5:1 antibody to capsid ratio. The high number of aminophenols on the Ab (after using 300 equivalents of NP-NHS) resulted in substantial amounts of inter-chain crosslinking of Ab light and heavy chains in the presence of $NaIO_4$ during the subsequent oxidative coupling step (Figure S4.3a, lane 2). Due to the nucleophilicity of aminophenol groups, they can easily couple to their oxidized counterparts when two of them are in close proximity. Lysine residues could also react with oxidized aminophenol groups, resulting in inter-chain crosslinks. Even though the crosslinking did not seem to affect the conjugation efficiency of AP-Ab to the MS2 viral capsids (Figure S4.3a, lane 3-4), using fewer equivalents (5-20 eq.) of NP-NHS substantially reduced the amount of Ab interchain crosslinking (Figure S4.3b-d, lane 2). Small amounts of crosslinked interchain products were still produced in the presence of $NaIO_4$ or even upon standing in solution (Figure S4.3b-d, lane 1-2). The lower numbers of aminophenol groups on the Ab did not seem to affect the MS2-Ab conjugation yields (Figure S4.3b-d, lane 3-4). Therefore, 5 equivalents of NP-NHS were used for the generation of AP-Ab in all the following experiments.

To optimize the ratio of Ab per capsid, we varied the number of anti-EGFR monoclonal Ab equivalents (3, 5, 10, and 20 equivalents) per capsid in the O.C. reaction with *p*AF MS2. The conjugation was confirmed by SDS-PAGE analysis (Figure 4.2c). For the 3:1 ratio, ~13% and ~9% of the light chains contained one and two MS2 monomers, respectively, and ~32% of the heavy chain were modified with one MS2 monomer, as analyzed by optical densitometry per-

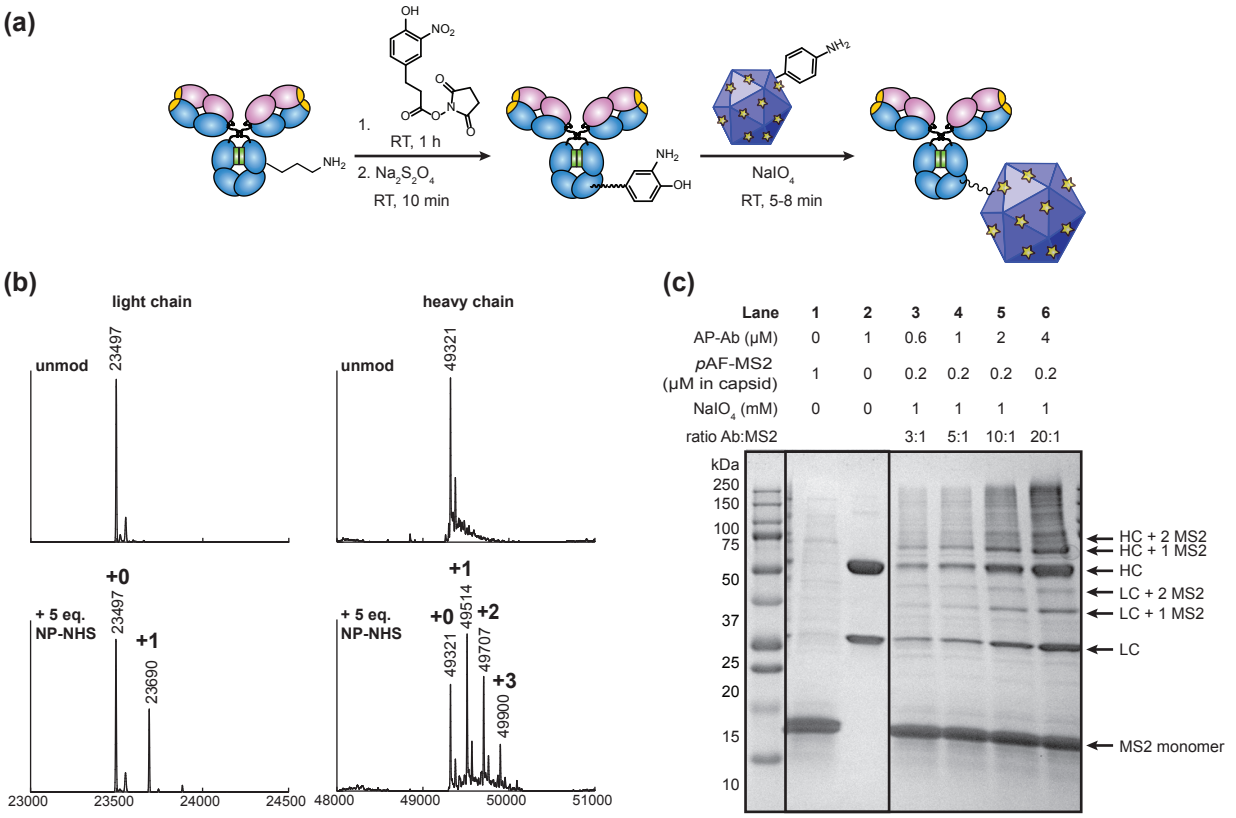

Figure 4.2. The generation of MS2-antibody conjugates. (a) General synthetic scheme of MS2-antibody conjugates. First, nitrophenol (NP) groups was attached to antibodies via lysine modification using NP-NHS. The nitrophenol groups were then reduced to yield aminophenol-Ab conjugates by addition of $Na_2S_2O_4$. The resulting AP-Ab was coupled to *p*AF MS2 via oxidative coupling using $NaIO_4$ as an oxidant. (b) LCMS analysis of antibodies after lysine modification with 5 equivalents of NP-NHS. The light chains were either unmodified (70%) or modified with one NP group (30%). The heavy chains were modified with 0 (22%), 1 (37%), 2 (29%), and 3 (12%) NP groups. (c) SDS PAGE analysis of MS2-Ab conjugates using 3, 5, 10, and 20 equivalents of Ab in excess of the MS2 capsid concentration. The gel showed conjugation of one or two MS2 monomers to the light and heavy chains of antibodies. The more equivalents of Ab, the higher intensity of the modified bands.

formed on SDS-PAGE gels. The higher degree of modification of heavy chain bands could not be accurately analyzed due to band diffusivity. For the 5:1 Ab:MS2 capsid ratio, ~19% and ~11% of the Ab light chains were modified with one and two MS2 monomers, respectively. For the 10:1 ratio of Ab:MS2 capsid, ~21% and ~9% of the Ab light chains were modified with one and two MS2 monomers, respectively. For the 20:1 ratio of Ab:MS2 capsid, ~22% and ~9% of Ab light chains were modified with one and two MS2 monomers, respectively. The heavy chains from all variations were modified in ~31-34% with one MS2 monomer (Table 4.1). The similar or slightly

Table 4.1. Percent modification of antibody light and heavy chains in MS2-Ab constructs analyzed by densitometry.

	% modification of light chains with # of MS2 monomers			% modification of heavy chains with # of MS2 monomers	
Ab:MS2 capsid ratio	0	1	2	0	1
3:1	78	13	9	68	32
5:1	70	19	11	66	34
10:1	70	21	9	67	33
20:1	69	22	9	69	31

higher percentage of modified light and heavy chains resulted in higher absolute number of modified Ab per capsid as the higher ratios of Ab:capsid were used.

To better understand the efficiency of these couplings, we performed size exclusion chromatography (SEC) to monitor the extent of the O.C. reactions containing 3, 5, 10, and 20 equivalents of Ab. Reaction mixtures generated before the addition of $NaIO_4$ (pre-O.C.) and with $NaIO_4$ added, followed by quenching with Na_2SO_3 (post-O.C.), were subjected to SEC high performance liquid chromatography (HPLC) to monitor the amount of unconjugated Ab remaining after the O.C. reactions (Figure 4.3). The reaction of MS2 with 3 equivalents of Ab left no trace of unmodified Ab, indicating that all the Ab were consumed in the reaction. While the reaction with 5 equivalents had only a trace of unmodified Ab, we found increased amounts of unmodified Ab remaining when 10 and 20 equivalents were added. The excess amount of unmodified Ab could be removed by performing spin concentration with molecular weight cutoff (MWCO) of 100 kDa. The MS2-Ab conjugates remained above the filter membrane, while Ab, which is much smaller in size, collected with the filtrate. The SEC HPLC after purification using spin concentrators showed that the unmodified Ab were removed.

We also found that the MS2-Ab conjugates derived from a higher number of Ab equivalents get eluted in shorter time, suggesting the increase in the size of MS2-Ab conjugate products due to higher numbers of antibodies attached to the MS2 capsids. The unmodified MS2-Oregon Green 488 (MS2-OG) conjugates were used as an internal standard to visualize the shift in elution time (Figure 4.4). The absorbance at 280 nm showed both the MS2-Ab conjugates after spin concentration purification and the MS2-OG internal standard. The absorbance at 488 nm was used to indicate the elution of MS2-OG by itself. In the light of these results, we chose the 3:1 Ab:MS2

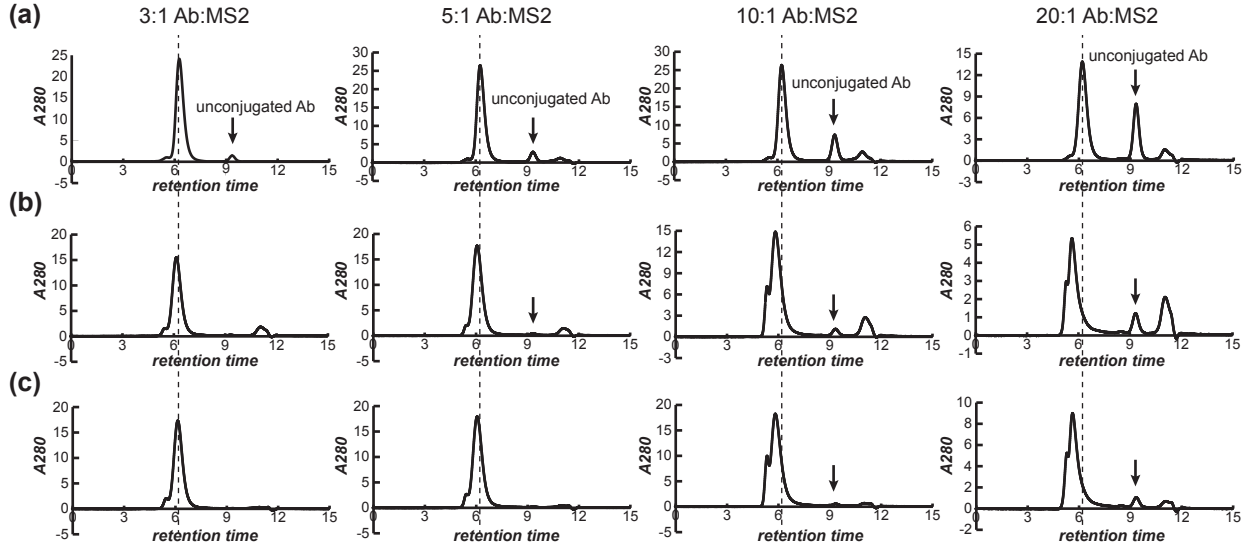

Figure 4.3. The extent of the oxidative coupling (O.C.) between aminophenol-Ab (AP-Ab) and *p*AF MS2 using varying ratios of the two starting materials. Size exclusion chromatography (SEC) HPLC was used to separate and analyze the components (MS2, Ab, and MS2-Ab products) of the O.C. reaction (a) before the reaction started, (b) after the reaction was complete, and (c) after purification using spin concentration. The AP-Ab and MS2 capsids were mixed in varying ratios: 3:1, 5:1, 10:1, and 20:1. The reaction was achieved in the presence of $NaIO_4$ for 6 min at RT. All the antibodies were consumed in the reaction using 3:1 Ab:MS2. Using a higher ratio of Ab:MS2 yielded the larger-sized MS2-Ab products, shown by the shorter retention times. In these samples, unconjugated AP-Ab was also present, indicating an incomplete reaction. However, a large portion of the unmodified Ab could be removed using 100 kDa MWCO spin concentrators. Peaks at 11 min retention time corresponded to small molecules, such as $Na_2S_2O_4$ remaining from the reduction step and Na_2SO_3 added to quenched excess $NaIO_4$.

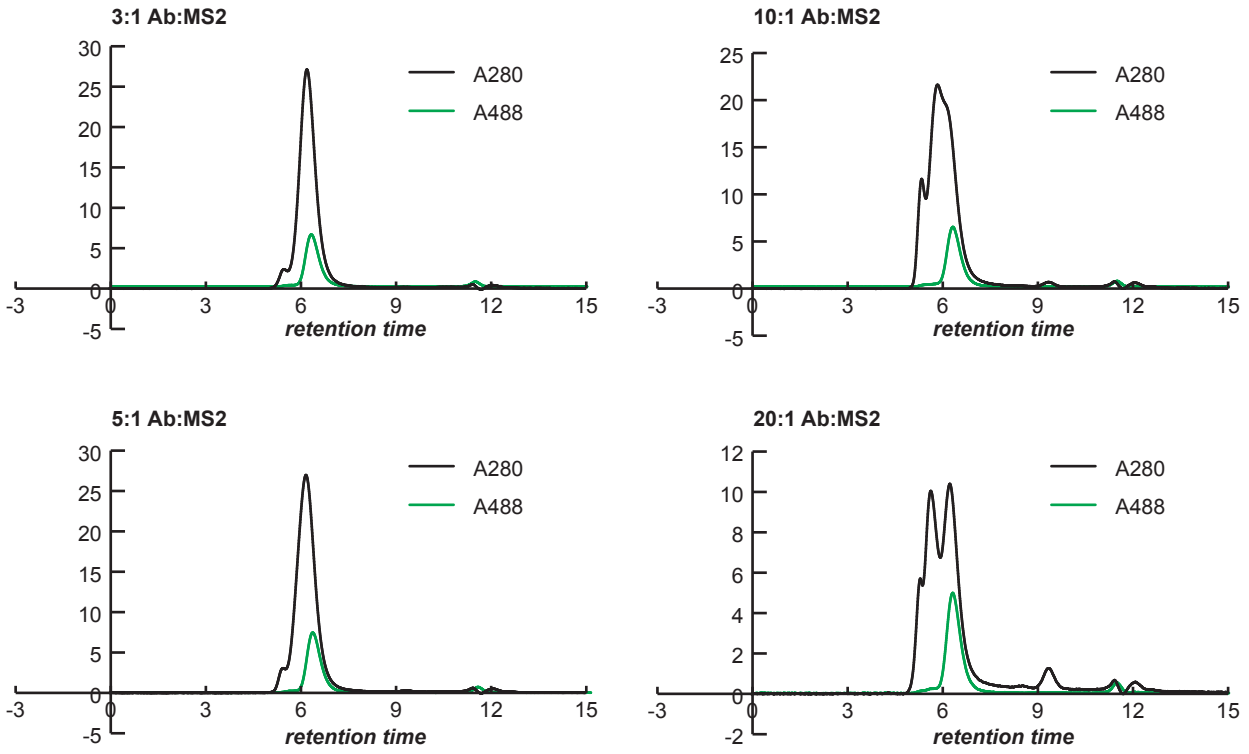

Figure 4.4. Identification of the MS2-Ab conjugates containing varying numbers of Ab. The spin concentration-purified products of the O.C. from varying ratios of Ab:MS2 starting materials were coinjected with Oregon Green 488-containing MS2 (MS2-OG) without exterior modification as an internal standard. MS2-OG represented the size and elution time of the unmodified MS2. As the higher ratio of Ab:MS2 used, we clearly see the emergence of a new species having lower retention time than the MS2-OG. These results confirmed that the conjugation between *p*AF MS2 and AP-Ab occured, and higher Ab:MS2 ratio led to larger constructs with more Ab attached.

ratio since statistically >95% of the conjugates would be expected to have at least one Ab appended per one viral capsid . This approach also requires no purification step as all the antibodies were consumed in the O.C. reaction with the MS2 capsid. However, more Ab can also be attached if a multivalency effect is desired.

4.3.2 Physical characterization of MS2-Ab conjugates

The sizes of the MS2-Ab conjugates were analyzed by dynamic light scattering (DLS). Using 3:1 ratio of Ab:MS2 capsid, the MS2-Ab conjugates appeared at the size of 30.73 ± 0.80 nm (Figure 4.5a). The MS2-Ab conjugates seemed to be only ~ 3 nm larger than the unmodified capsid, which measured 27.07 ± 1.16 nm, suggesting that the antibodies might attach tangentially, rather than perpendicularly, to the surface of the MS2 capsid (as modeled in Figure 4.5b). The higher the number of Ab attached to MS2, the larger the conjugates appeared (Figure 4.5a). Images from transmission electron microscopy (TEM) showed intact capsid after conjugation to Ab and supported our model of attachment as we observed a rather uniform surface of MS2 capsid even after conjugation with 3 equivalents of Ab (Figure 4.5c). The size of this conjugate was measured at 31 nm, consistent with the data obtained from DLS.

4.3.3 Biological assessment of MS2-Ab conjugates

To test the biological applicability of the MS2-Ab constructs, we first analyzed whether

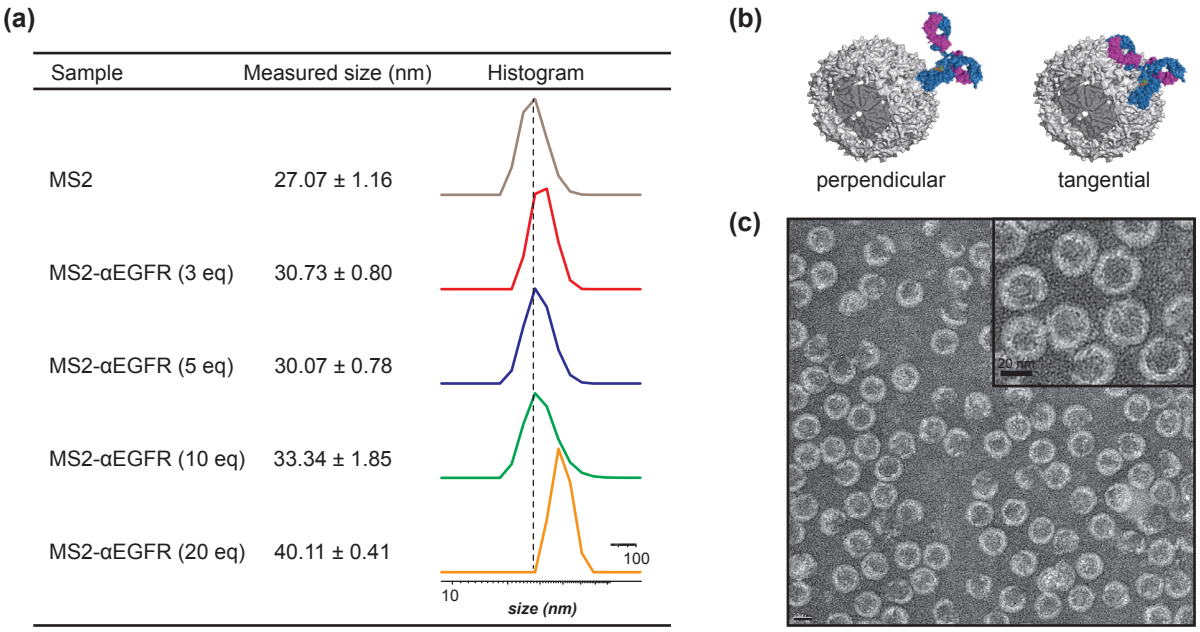

Figure 4.5. Biophysical analysis of MS2-Ab conjugates. (a) The size of MS2-Ab conjugates using varying numbers of equivalents of aminophenol-containing anti-EGFR antibodies as starting materials. Data plots were obtained from dynamic light scattering (DLS) measurements. Diameters were calculated from an average of three measurements, shown as size distribution by number, which weighs large and small particles equally. (b) Models for attachment of the antibodies to MS2 capsids. The attached antibodies can be oriented perpendicularly or tangentially to the surfaces of the capsids. (c) Transmission electron micrograph (TEM) images of MS2-Ab conjugates using 3 equivalents of AP-Ab. The capsids were shown to be intact, and their measured diameter was 31 nm. The scale bar represents 20 nm.

the specificity and affinity of the Ab was retained after conjugation to the MS2 capsid. First, we conjugated an anti-EGFR IgG1 monoclonal antibody, which targets epidermal growth factor receptor (EGFR), overexpressed in many types of cancers, to the Oregon Green 488-containing MS2 (MS2-OG) capsids. The Oregon Green 488 dyes were attached to the mutated Cys (N87C) residue on the interior of MS2 via thiol-maleimide chemistry (Figure S4.4). Using flow cytometry, we analyzed the binding specificity and affinity of MS2-anti-EGFR Ab conjugates in an EGFR-negative (MCF7 clone 18) and three EGFR-positive (MDA-MB-231, L3.6pl, and HCC1954) human-derived cancer cell lines. The MS2-anti-EGFR constructs only bound to the EGFR-positive cells (Figure 4.6). The MS2-OG by itself and MS2-OG conjugated to non-specific human IgG1 were used as negative controls, and neither of which exhibited binding to any of the cell lines tested. This result thus confirmed that the binding of MS2-anti-EGFR conjugates was specifically due to the EGFR/anti-EGFR Ab interaction. Live cell images from confocal microscopy after 1 h of incubation at 37 ºC with the agents also indicated the binding specificity of MS2-anti-EGFR conjugate to the target cells (Figure 4.6b). The images from confocal microscopy revealed several green fluorescent vesicles inside the cells, suggesting that the MS2-anti-EGFR conjugates might be internalized (Figure S4.6). EGFR has already been known to be internalized upon binding to a series of anti-EGFR antibodies, including cetuximab [34-38]. In fact, receptor downregulation and internalization is one of the main mechanisms of action of anti-EGFR therapeutic antibodies. A previous study from Tong *et al*. have shown internalization of MS2 conjugated to specific aptamers inside the target cells [15]. Further, we investigated the binding specificity of a few other MS2-Ab constructs, including anti-HER2, anti-CD3, and anti-CD20 (Figure S4.5). These results

confirm that the binding specificity of the all MS2-Ab conjugates we investigated was retained.

Next, we compared the binding affinity of unmodified anti-EGFR antibodies and MS2-anti-EGFR conjugates. By fitting the median fluorescence intensity measurement from each point to

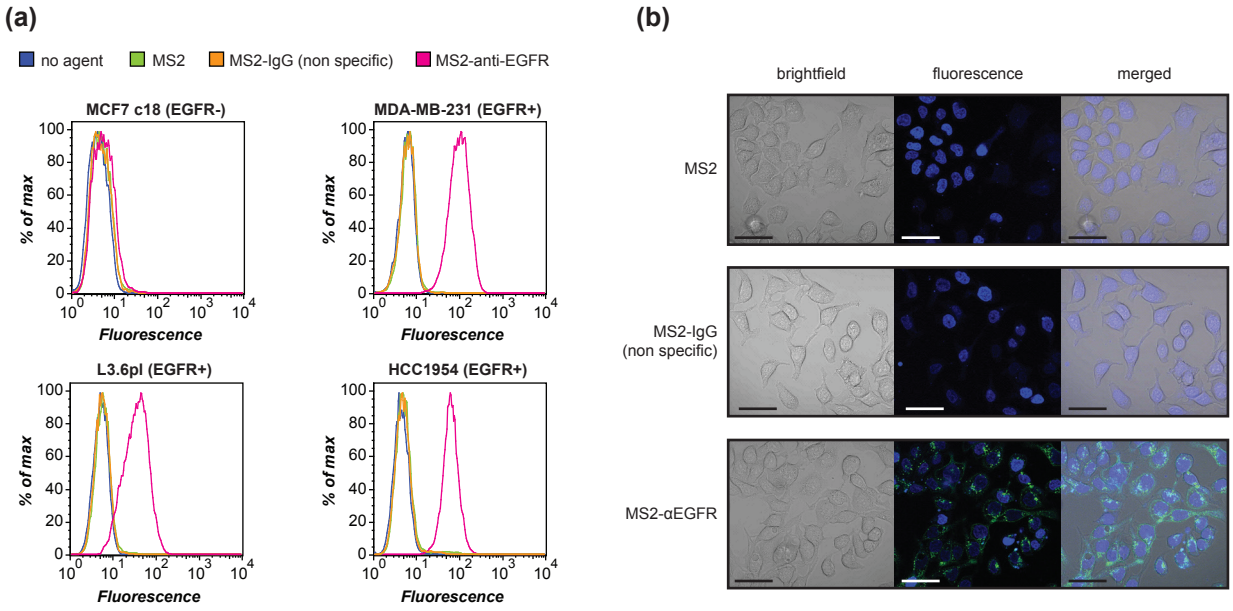

Figure 4.6. Binding studies of MS2-anti-EGFR antibody conjugates. (a) Flow cytometry analysis of the binding of MS2-anti-EGFR Ab conjugates to EGFR negative (MCF7 clone 18) and EGFR positive (MDA-MB-231, L3.6pl, and HCC1954) cell lines. The Oregon Green 488 (OG)-containing MS2-anti-EGFR Ab construct was incubated with these cell lines in DPBS containing 1% FBS binding buffer on ice for 45 min at ~5.5 nM of capsid concentration, which correspond to 1 μM MS2 monomer concentration. The results from flow cytometry showed specific binding of MS2-anti-EGFR conjugates to only the EGFR positive cell lines, while remaining unbound to the EGFR negative cells. MS2-OG and MS2-OG conjugated to non-specific human IgG1 were used as negative control agents and were incubated with cells similarly to the anti-EGFR-MS2 conjugates. None of them were found to bind to any cell lines non-specifically, confirming that the binding of MS2-anti-EGFR conjugates was specifically due to the EGFR/anti-EGFR Ab interaction. (b) Confocal microscopy studies of MS2-Ab binding to live cells. Images were taken after 1 h incubation at 37 ºC of OG-containing MS2, MS2-IgG (non-specific), and MS2-anti-EGFR antibodies construct to live HCC1954 cells, which are EGFR-positive, in DPBS containing 1% FBS binding buffer. Only the MS2-anti-EGFR conjugates were found to bind to the cells, which appeared in the fluorescence channel. Green fluorescent vesicles inside the cells were also noticed, suggesting that the MS2-anti-EGFR conjugates might be internalized into cells. DAPI was used to stain the cell nucleus. The scale bars represent 50 μm.

(a)

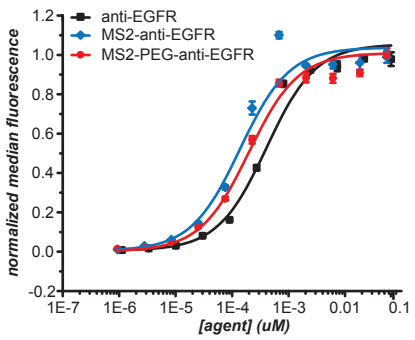

(b)

agents	K_d (nM)	adjusted R-square
anti-EGFR	0.410 ± 0.067	0.982
MS2-anti-EGFR	0.138 ± 0.030	0.985
MS2-PEG-anti-EGFR	0.199 ± 0.033	0.982

Figure 4.7. (a) Comparison of binding affinity of unmodified anti-EGFR antibody, MS2-anti-EGFR, and MS2-PEG-anti-EGFR conjugates. Flow cytometry was used to measure the median fluorescence of MDA-MB-231 cell population after incubation with the samples according to the binding conditions in Figure 4.6. The data were fitted to the Hill equation with fixed Hill coefficient (n) of 1. The K_d values and adjusted R-square values of each fit are listed in table (b). The binding affinity of the Ab in MS2-anti-EGFR with and without the PEG spacer did not seem to be altered as compared to the unmodified Ab.

the Hill equation varying K_d, we obtained the K_d of unmodified anti-EGFR and MS2-anti-EGFR conjugates to be equal to 0.41 ± 0.07 nM and 0.14 ± 0.03 nM, respectively (Figure 4.7). The K_d of anti-EGFR Ab was in excellent agreement to another published study of ^{125}I cetuximab binding to EGFR on MDA-MB-231, which reported a K_d of 0.38 nM [39]. Therefore, the conjugation to MS2 did not worsen the binding affinity, and in fact, the affinity seemed to be slightly better for the MS2-Ab conjugates.

In addition, we generated MS2-Ab conjugates with 5 kDa polyethyleneglycol (PEG) spacer to investigate whether we can futher improve the binding of the MS2-Ab conjugates. If the tangential attachment of the antibodies to the MS2 does lead to a loss in binding, then we hypothesized that the PEG spacer would allow the antibody to orient more favorably in the binding events. First, nitrophenol-containing 5k-PEG was conjugated to antibodies via lysine modification (Figure 4.8). The nitrophenol groups were reduced to aminophenols (AP), and the AP-PEG-Ab conjugates were attached to *p*AF MS2 using the O.C. The binding affinity of MS2-PEG-Ab conjugates was assessed by flow cytometry. Using the Hill equation, the K_d was calculated to be 0.20 ± 0.03 nM, suggesting that PEG spacer did not improve the binding affinity of MS2-Ab constructs.

4.4 Conclusions and Future Prospects

Following the success of targeted MS2-based platforms, here, we developed a new construct with higher complexity using full-sized antibodies as targeting moieties. Given the vast, diverse targets of antibodies, attachment of these biomolecules expands the access of the MS2 vehicles to many more new targets. MS2 can be loaded with up to 180 copies of metal chelators, while the attachment of the antibodies can direct the constructs to specific targets. The combined advantages of signal enhancement of MS2 and the high binding specificity and affinity of antibodies will be useful in many applications. The technique established in this chapter is versatile

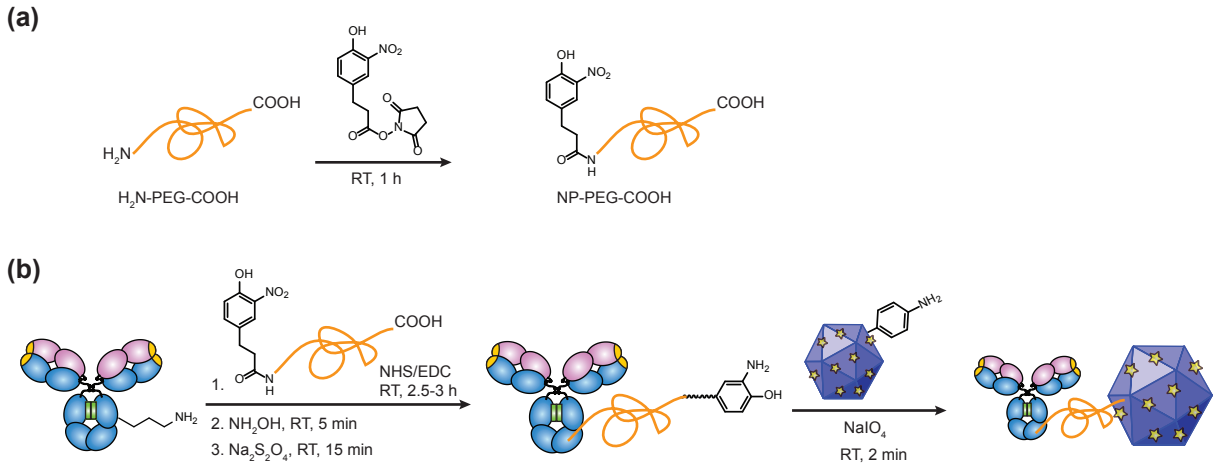

Figure 4.8. Synthetic scheme of MS2-PEG-Ab conjugate formation. (a) Synthesis of nitrophenol-5 kDa polyethylene glycol (PEG)-COOH (NP-PEG-COOH). The amine group on H_2N-PEG-COOH was functionalized with nitrophenol-NHS (NP-NHS) to yield NP-PEG-COOH. (b) Synthesis of 5 k PEG-antibodies and conjugation to *p*AF MS2. First, NP-PEG-COOH was conjugated to antibodies via lysine modification using *N*-hydroxysuccinimide/1-ethyl-3-(3-dimethylaminopropyl)carbodiimide (NHS/EDC) coupling. The reaction was quenched by adding hydroxylamine to hydrolyze any transiently stable species. The nitrophenol groups were then reduced to yield aminophenol-PEG-Ab (AP-PEG-Ab) by addition of $Na_2S_2O_4$. The resulting AP-PEG-Ab was coupled to *p*AF MS2 via oxidative coupling using $NaIO_4$ as an oxidant.

for both mouse and human IgG and is very likely to be applicable to antibodies with other isotypes or antibodies from other species as well. As any molecules smaller than the pore size of MS2 can be attached to the interior surface of MS2, this method to be applied to the generation of targeted imaging or drug delivery agents. Preliminary effort has gone into attaching chelators such as 1,4,7,10-tetraazacyclododecane-1,4,7,10-tetraacetic acid (DOTA) and 1,4,7-triazacyclononane-1,4,7-triacetic acid (NOTA). These chelators can chelate various lanthanide metal ions for MRI contrast enhancement, as well as ^{64}Cu, for mass cytometry and *in vivo* positron emission tomography (PET) imaging applications. The use of this platform for magnetic resonance imaging (MRI) and drug delivery will also be explored.

4.5 Materials and Methods

4.5.1 General experimental procedures and materials

Unless otherwise noted, all chemicals and solvents were of analytical grade and used as received from commercial sources. Water (ddH_2O) used in biological procedures or as the reaction solvent was deionized using a NANOpure purification system (Barnstead, USA). Wild-type anti-HER2 and anti-EGFR human IgG1 monoclonal antibodies were obtained from Eureka Therapeutics, Inc. (Emeryville, CA). Mouse anti-human CD3 and anti-human CD20 antibodies were obtained from Biolegend (San Diego, CA). Goat anti-human IgG (Fcγ specific) PerCP-conjugated $F(ab')_2$ fragments were purchased from Jackson ImmunoResearch Laboratories, Inc. (West Grove, PA). Anti-human IgG1 (Fc specific) FITC-conjugated purified mourse IgG clone 8c/6-39 and non-specific IgG1κ isolated from human myeloma were purchased from Sigma (St. Louis, MO). Anti-mouse IgG AlexaFluor 488-conjugated antibodies were purchased from Life Technologies (Grand Island, NY). All oligonucleotides were obtained from Integrated DNA Technologies (Coralville, IA). All cell culture reagents were obtained from Gibco/Invitrogen Corp. (Carlsbad, CA) unless otherwise noted. Cell culture was conducted using standard techniques. Jurkat, Ramos, and HCC1954 cells were grown in culture-treated flasks (Corning) in RPMI Medium 1640 supplemented with 10% (v/v) fetal bovine serum (FBS, Omega Scientific) and 1% penicillin/streptomycin (P/S, Sigma). MCF7 clone 18, L3.6pl, and MDA-MB-231 cells were grown in culture-treated flasks (Corning) in Dulbecco's Modified Eagle Medium (DMEM) supplemented with 10% (v/v) FBS and 1% P/S. MDA-MB-468 cells were grown in culture-treated flasks (Corning) in L-15 media supplemented with 10% (v/v) FBS and 1% P/S. All cell lines were grown in 5% CO_2 atmosphere, except for MDA-MB-468, which was cultured in 100% air.

4.5.2 Synthesis of nitrophenol-NHS ester

The synthesis of the nitrophenol-NHS ester was performed according to published procedure [33].

4.5.3 Synthesis of nitrophenol-PEG-COOH

10.2 mg of amine-5k-PEG-pentanoic acid (NH_2-PEG-COOH) (0.00204 mmol, 1.0 equiv.) was dissolved in 0.5 mL of DCM in a 1 dram screwcap vial containing a magnetic stirrer. Nitrophenol NHS ester (400 mM in DMSO, 25 μL, 0.0102 mmol, 5.0 equiv.) and triethylamine (2 mg, 2.8 μL, 0.0204 mmol, 10 equiv.) were added sequentially. The reaction turned yellow/orange upon

addition of triethylamine. The reaction mixture was capped and stirred at RT overnight. Solvent was removed under a gentle stream of nitrogen, and the reaction mixture was placed on a high vacuum for ~ 4 h to remove the residual small quantities of DMSO. Excess NP-NHS was precipitated by the addition of 500 μL of water. The insoluble materials were removed by filtration through a 0.45 uM spin filter and washing once with an additional 500 μL of water. The filtrate was spin concentrated with water in 3 kDa MWCO spin concentrators to remove other soluble small molecules. The material was then purified by RP-HPLC, and the obtained material was negative in the ninhydrin test. The combined fractions were extracted with DCM twice, and the solvent was removed under nitrogen stream. The nitrophenol-PEG-COOH product was dissolved in water to give an approximately 5 mM stock solution for use in all subsequent experiments.

4.5.4 Synthesis of anti-EGFR-AlexaFluor 488 conjugates

Antibody solution in 25 mM phosphate buffer pH 8 was prepared by addition of 100 mM pH 8 phosphate buffer to the antibodies supplied in PBS. To this solution is added NHS-AlexaFluor 488 (Life Technologies, Grand Island, NY) from 20 mM DMSO stock (20 equiv.). The mixture was briefly vortexed, and the reaction was allowed to proceed at RT for 1.5 h. The excess dye molecules were removed by using NAP-5 Sephadex size exclusion columns (GE Healthcare, USA) equilibrated with 10 mM pH 7.0 phosphate buffer, followed by spin concentration with a MWCO of 30 kDa (Millipore, Billerica, MA) in 10 mM pH 7.0 phosphate buffer. The resulting anti-EGFR-AlexaFluor 488 conjugates contained ~4.7 dyes per protein molecule, as quantified by absorbance.

4.5.5 Procedure for expression and purification of T19*p*AF N87C MS2 viral capsid

Bacteriophage MS2 T19*p*AF plasmid production and growth has been previously reported [15,32]. The Peter Schultz lab (Scripps Research Institute, La Jolla, CA) provided the tRNA and tRNA synthetase-encoding plasmids necessary for *p*-aminophenylalanine (*p*AF) incorporation [40]. The plasmid containing the amber stop codon mutation in the MS2 coat protein was co-tranformed into DH10B cells with the pDULE plasmid containing the *p*AF aminoacyl tRNA synthetase and tRNA [33]. Position 87 was mutated into a cysteine via Quikchange mutagenesis strategy using the following forward and reverse primers, as previously reported [15].

Forward: 5'–AGCCGCATGGCGTTCGTACTTATGTATGGAACTAACCATTC–3'
Reverse: 5'–GAATGGTTAGTTCCATACATAAGTACGAACGCCATGCGGCT–3'

The T19*p*AF N87C MS2 expression was carried out in minimal media, following the published protocol [15,32,40]. The pellets were thawed and resuspended in 20 ml of 20 mM taurine buffer (pH 9) containing 6.5 mM DTT, 6 mM $MgCl_2$, and 10 μg/ml of DNase and RNase. Following sonication for 10 min, the cells were spun down for 45 min at 11,000 rpm. Next, the supernatant was applied to a DEAE-Sephadex column (GE Healthcare). In 20 mM taurine buffer, pH 9, MS2 eluted first from the DEAE column, and was collected and precipitated using 50 % aqueous ammonium sulfate. The protein pellets were resuspended in 10 mM K_2HPO_4, pH 7.2, and applied to a Sephacryl S1000 column (GE Healthcare, USA). The fractions containing MS2 were then collected and concentrated using Amicon Ultra 100 kD MWCO centrifugal concentrators (Millipore). A yield of ~10 mg/L culture was obtained for T19*p*AF N87C MS2 following two purification rounds.

4.5.6 General procedure for attachment of Oregon Green 488 to interior of T19*p*AF N87C MS2

The cysteine residues on the interior of T19*p*AF N87C MS2 were alkylated with an Oregon Green 488-maleimide (Life Technologies) following published procedures [15]. In brief, to a solution of T19*p*AF N87C MS2 (final monomer concentration of 100 μM) in 10 mM phosphate buffer pH 7.2, OG-maleimide was added from a stock solution of 100 mM in DMF (10 equivalents). The reaction mixture was incubated at room temperature for 4 h. Upon completion, the excess dye was removed using NAP-10 Sephadex size exclusion columns (GE Healthcare, USA) equilibrated with 10 mM pH 7.2 phosphate buffer and subsequent concentration with 100 kDa MWCO spin concentrators (Millipore, Billerica, MA).

4.5.7 General procedure for generating aminophenol-antibody conjugates

First, the antibody solution in 25 mM phosphate buffer pH 8 was prepared by either buffer exchange using spin concentrators or addition of 100 mM pH 8 phosphate buffer to the antibodies supplied in PBS. To this solution is added 5 equivalents of NHS-nitrophenol from either a 5 mM or 10 mM DMSO stock, depending on the reaction scale. The mixture was briefly vortexed and incubated at RT for 1-1.25 h without further agitation. The nitrophenol groups were reduced to aminophenol by addition of a stock solution of 100 mM sodium dithionite ($Na_2S_2O_4$) in 100 mM pH 6.5 phosphate buffer to reach a final concentration of 10 mM. The reduction was carried out at RT for 10-20 min, followed by removal of excess small molecules using 0.5 mL spin concentrators with a MWCO of 30 kDa (Millipore, Billerica, MA) with 10 mM pH 7.0 phosphate buffer. The concentration of the final product can be measured by UV absorbance at 280 nm using A280 of 1.4 yielding 1 mg/mL (~6 μM) as a conversion factor.

4.5.8 General procedure for generating aminophenol-PEG-antibody conjugates

Nitrophenol-PEG-NHS ester was pre-formed by mixing *N*-hydroxysuccinimide (NHS), 1-ethyl-3-(3-dimethylaminopropyl)carbodiimide (EDC), and nitrophenol-PEG-COOH in water. Briefly, NHS (1.2 μL, 100 mM in water) and EDC (1.2 μL, 100 mM in water) were added sequentially to 24 μL of a 5 mM solution of nitrophenol-PEG-COOH in water, and the mixture was incubated at RT for 30 min. To the pre-formed nitrophenol-PEG-NHS ester solution was added 90 μL of antibody (~6.6 μM in PBS). The reaction was allowed to proceed at RT for 2.5-3 h, followed by the addition of 1.2 μL of a 1 M solution of hydroxylamine hydrochloride and incubation for 5 min at RT in order to hydrolyze any unreacted or transiently stable species. Nitrophenol groups on the resulting NP-PEG-Ab conjugates were reduced to aminophenol (AP) to yield AP-PEG-Ab conjugates by adding 20 μL of 100 mM sodium dithionite ($Na_2S_2O_4$) in 100 mM pH 6.5 phosphate buffer, followed by 15 min incubation at RT. All the excess small molecules in the reaction mixture were removed by using 0.5 mL spin concentrators with a MWCO of 30 kDa (Millipore, Billerica, MA) with 10 mM pH 7.0 phosphate buffer.

4.5.9 General procedure for generation MS2-antibody conjugates

A solution of MS2 was added to the above solution of AP-Ab conjugates at a specified ratio of antibody to capsid. In general, the final concentration of the capsid was ~200-300 nM (corresponding to ~ 50 μM MS2 monomer), and the concentration of Ab was ranged from 0.6-6 μM, depending on the ratio of Ab to MS2 capsids. To initiate the oxidative coupling, $NaIO_4$ was added to a final concentration of 500 μM, and the reaction was performed at RT for 5-8 min.

Excess $NaIO_4$ was removed by using NAP-5 Sephadex size exclusion columns (GE Healthcare, USA) equilibrated with 10 mM pH 7.0 phosphate buffer. The resulting product can be further purified by sequential spin concentration using a MWCO of 100 kDa or by FPLC.

4.5.10 General procedure for antibody disulfide reduction and cysteine capping for mass spectrometry analysis

To prepare the antibody conjugates for mass spectrometry analysis, first the oligosaccharides were removed via treatment with Peptide-N-Glycosidase F (PNGase F) following the protocol from the manufacturer (New England Biolabs, Ipswich, MA). Briefly, a buffer exchange into PBS was performed on the antibody samples. In a 1.7 mL Eppendorf tube, 35 µL of protein (~1 mg/mL) was mixed with 5 µL of G7 reaction buffer, 2 µL of PNGase F, and additional PBS to a total volume of 50 µL. The mixture was then incubated at 37 ºC overnight. Immediately following treatment with PNGase F, buffer exchange was performed into 100 mM Tris buffer, pH 8. Dithiothrietol (DTT) and ethylenediaminetetraacetic acid (EDTA) were then added to a final concentration of 10 mM each, and the reaction was incubated at room temperature for 20 min. After the reduction, iodoacetamide was added to a final concentration of 50 mM and the mixture was incubated at 37 ºC for 30 min. The samples were then subjected to buffer exchange into 10 mM Tris buffer pH 8 for mass spectrometry analysis.

4.5.11 Flow cytometry analysis of MS2-Ab conjugates

For the binding experiment, adherent cell lines (HCC1954, MCF7 clone 18, L3.6pl, MDA-MB-231, and MDA-MB-468 cells) were first trypsinized at 37 °C for 5 min, followed by the addition of complete media (L-15 + 10% FBS in the case of MDA-MB-468, RPMI + 10% FBS in the case of HCC1954, or DMEM + 10% FBS for all the other cell lines) to stop trypsinization. For suspension cell lines (Jurkat and Ramos cells), the overnight culture were used without further treatment. Cells were then pelleted and resuspended in binding buffer (Dulbecco's phosphate buffered saline (DPBS) containing 1% FBS or PBS containing 1% BSA) to the density of 2-3 $x10^6$ cells/mL. Aliquots of 100 µL containing 2-3 $x10^6$ cells/mL of cells were incubated with MS2-Ab conjugates containing Oregon Green 488 (OG) or unmodified on the interior at specified final concentrations for 45-60 min on ice. For the OG-containing samples, the cells were washed twice with 150 µL (or once with 500 µL), resuspended in 200 µL of binding buffer, and analyzed by flow cytometry. For the other samples, the cells were washed twice with 150 µL (or once with 500 µL) and resuspended in 100 µL of binding buffer containing 1:1000 dilution of anti-human IgG (Fcγ specific) PerCP-conjugated goat $F(ab')_2$ fragments or anti-mouse IgG AlexaFluor 488-conjugated antibodies (Life Technologies). Another secondary Ab used was anti-human IgG1 (Fc specific) FITC-conjugated purified mouse IgG clone 8c/6-39 (Sigma) at 0.15 µM final concentration. The cells were incubated for 30 min on ice in the dark, then washed twice with 150 µL (or once with 500 µL) and resuspended in 200 µL of binding buffer. The cells were analyzed by flow cytometry to determine the amount of FITC or PerCP fluorescence. For each sample, 10,000 cells were counted. A FACSCalibur flow cytometer (BD Biosciences, USA) equipped with 488 and 633 nm lasers were used for all flow cytometry measurements, usage courtesy of Prof. Carolyn Bertozzi (UC Berkeley). Data was analyzed using FlowJo 8.0 (TreeStar, Ashland, OR).

In the binding affinity studies, the OG-containing MS2-Ab samples were compared with antibodies conjugating to AlexaFluor 488. The Hill equation fitting was calculated using Origin 8.0 software (OriginLab Corporation, Northampton, MA). The obtained Hill plots displayed different

amplitudes for the binding curves, which were taken to arise from three reasons: (1) the use of different dyes, AlexaFluor 488 in antibodies samples and Oregon Green 488 in MS2-Ab samples; (2) the different conjugation efficiency of Ab-PEG-AP and Ab-AP to MS2; and (3) accessibility of MS2-PEG-Ab and MS2-Ab to cell surface. Two hypotheses can be made to account for the difference between MS2-PEG-Ab and MS2-Ab. First, the AP-PEG-Ab may have lower coupling efficiency to MS2 capsid than AP-Ab, resulting in fewer antibodies attached per capsid. Second, due to the PEG spacer, more MS2-PEG-Ab can be packed on cell surface than MS2-Ab without spacer. According to these two hypotheses, more MS2-PEG-Ab can bind to each cell, leading to higher maximum fluorescence as compared to MS2-Ab samples. The plots were therefore normalized based on the maximum median fluorescence of each fit.

4.5.12 Confocal microscopy of MS2-Ab conjugates

Cells were washed with PBS, trypsinized, and trypsin was quenched with complete growth media, as described above. Cells were then resuspended in the growth media at a concentration of 25,000 cells/mL, and 2 mL was added to each 35 mm glass bottom dish (MatTek Corp., Ashland, MA). Cells were allowed to grow at 37 °C with 5% CO_2 for 48-72 h. For incubation with MS2 samples, first, all media was removed from the dishes, and cells were washed once with 1 mL PBS. The MS2 sample was added to each well of the plate at a final concentration of 1 μM (by monomer or ~ 5 nM by capsid concentration) in 150 μL of binding buffer (DPBS containing 1% FBS), and the dishes were incubated at 37 °C with 5% CO_2. After 1 h, the cells were washed three times with PBS (for each wash, 1 mL of PBS was added to wash the cells gently, and was then removed), and 1 mL of phenol red-free media with 10% FBS was added to the cells. 4',6-diamidino-2-phenylindole (DAPI) was added to 1 μM prior to acquisition of the final images. Images were acquired on a Zeiss 510 NLO Axiovert 200M Tsunami microscope equipped with 488 and 633 nm lasers, usage courtesy of Prof. Christopher Chang (UC Berkeley).

4.5.13 Instrumentation and sample analysis

4.5.13.1 Liquid chromatography mass spectrometry (LCMS) analysis of reduced antibody bioconjugates

Acetonitrile (Fisher Optima grade, 99.9%), formic acid (Pierce, 1 mL ampules, 99+%), and water purified to a resistivity of 18.2 MΩ·cm (at 25 °C) using a Milli-Q Gradient ultrapure water purification system (Millipore, Billerica, MA) were used to prepare mobile phase solvents for LCMS. Electrospray ionization mass spectrometry (ESI-MS) of proteins was performed using an Agilent 1260 series liquid chromatograph outfitted with an Agilent 6224 Time-of-Flight (TOF) LCMS system (Santa Clara, CA). The LC was equipped with a Poroshell 300SB-C18 (5 μm particles, 1.0 mm × 75 mm, Agilent, Santa Clara, CA) analytical column. Solvent A was 99.9% water/0.1% formic acid and solvent B was 99.9% acetonitrile/0.1% formic acid (v/v). For each sample, approximately 15 to 30 picomoles of analyte were injected onto the column. Following sample injection, a 20-100% B elution gradient was run at a flow rate of 0.55 mL/min for 7 min. Data was collected and analyzed using Agilent MassHunter Qualitative Analysis B.05.00.

4.5.13.2 High performance liquid chromatography (HPLC)

HPLC was performed on an Agilent 1100 Series HPLC System (Agilent Technologies, USA). Sample analysis for all HPLC experiments was achieved with an inline diode array detector

(DAD). SEC HPLC of MS2-Ab conjugates was accomplished using BioSep GFC s-4000 (Phenomenex, Torrance, CA). The samples were eluted in isocratic flow of 100 mM phosphate buffer pH 6.8 containing 0.02% NaN_3 at 1 mL/min.

4.5.13.3 Gel Analyses

For protein analysis, sodium dodecyl sulfate-polyacrylamide gel electrophoresis (SDS-PAGE) was carried out on a Mini-Protean apparatus from Bio-Rad (Hercules, CA), following the protocol of Laemmli [41]. The protein electrophoresis samples were heated for 10 min at 95 °C in the presence of β-mercaptoethanol to ensure reduction of any disulfide bonds. Gels were run for 60 min at 150 V to allow good separation of the bands. Commercially available markers (Bio-Rad) were applied to at least one lane of each gel for assignment of apparent molecular masses. Visualization of protein bands was accomplished by staining with Coomassie Brilliant Blue R-250 (Bio-Rad).

4.5.13.4 Dynamic Light Scattering (DLS)

DLS measurements were obtained using a Malvern Instruments Zetasizer Nano ZS (Malvern Instruments Ltd., Worcestershire, UK). MS2 samples were prepared at 10 μM (concentration by MS2 monomer) in 10 mM phosphate buffer pH 7.0 and filtered through a 0.22 μm centrifugal filter unit (Millipore Corporation, Billerica, MA) prior to data collection. Data plots are shown as size distribution by number, which weighs large and small particles equally. Diameters were calculated from an average of three measurements.

4.5.13.5 Transmission Electron Microscopy (TEM)

TEM images were taken at the UC Berkeley Electron Microscope Laboratory (UCB EML) using a FEI Tecnai 12 transmission electron microscope (TEM) with 120 kV accelerating voltage. Samples were prepared by pipetting 5 μL onto Formvar-coated copper mesh grids (400 mesh, Ted Pella, Redding, CA) for 5 min, followed by rinsing with 8 μL of dd-H_2O. The grids were then exposed to 8 μL of a solution of uranyl acetate (15 mg/mL in dd-H_2O) for 2 min as a negative stain. Excess stain was then removed and the grids were allowed to dry in air for 10 min.

4.6 Supplementary Information

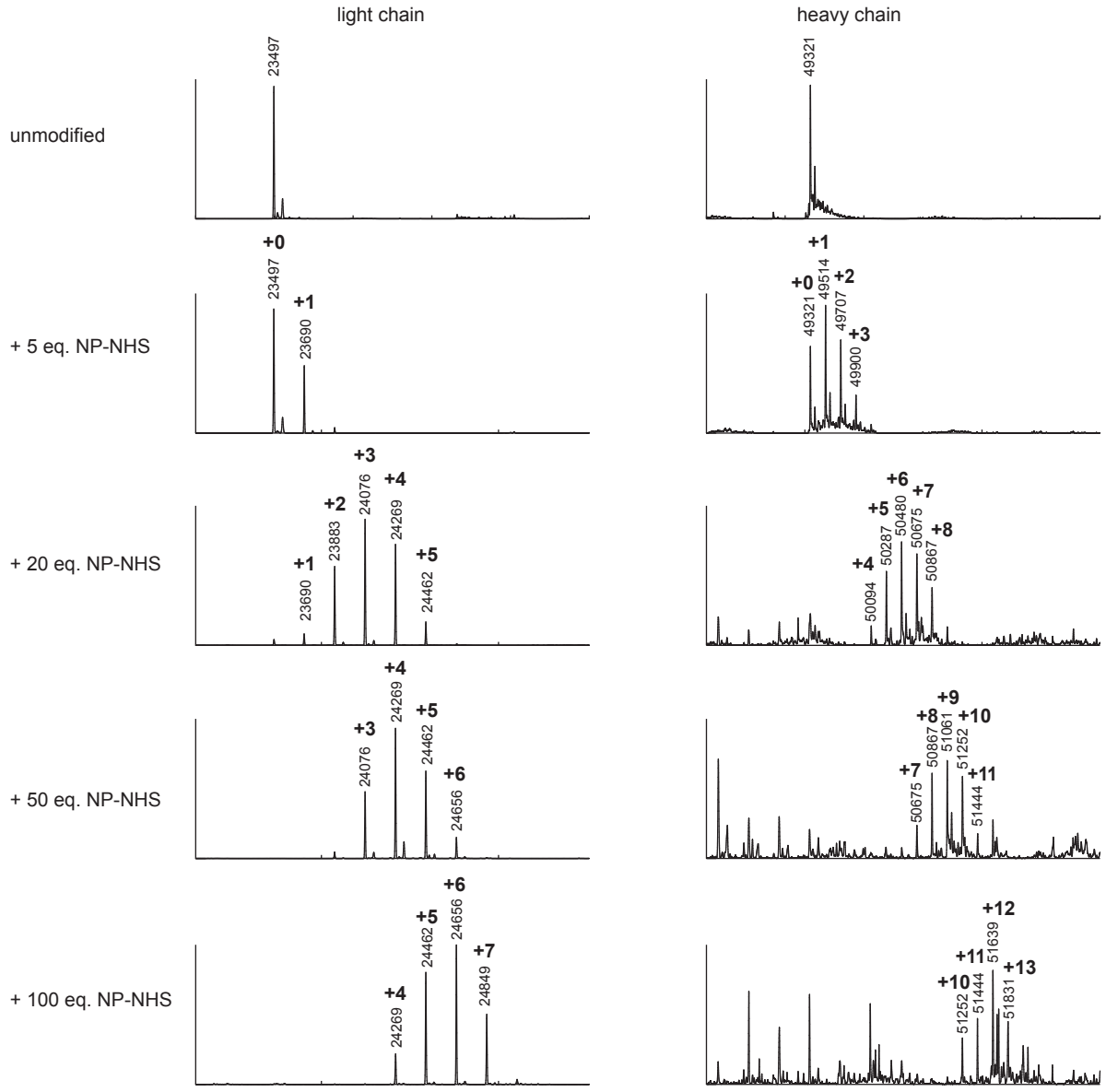

Figure S4.1. Deconvoluted LCMS spectra of the heavy and light chain anti-human IgG1 mouse antibodies after reaction with different numbers of equivalients of NP-NHS. The full-sized antibodies were deglycosylated using PNGase F and reduced with DTT. The reduced cysteines were capped with iodoacetamide before LCMS analysis.

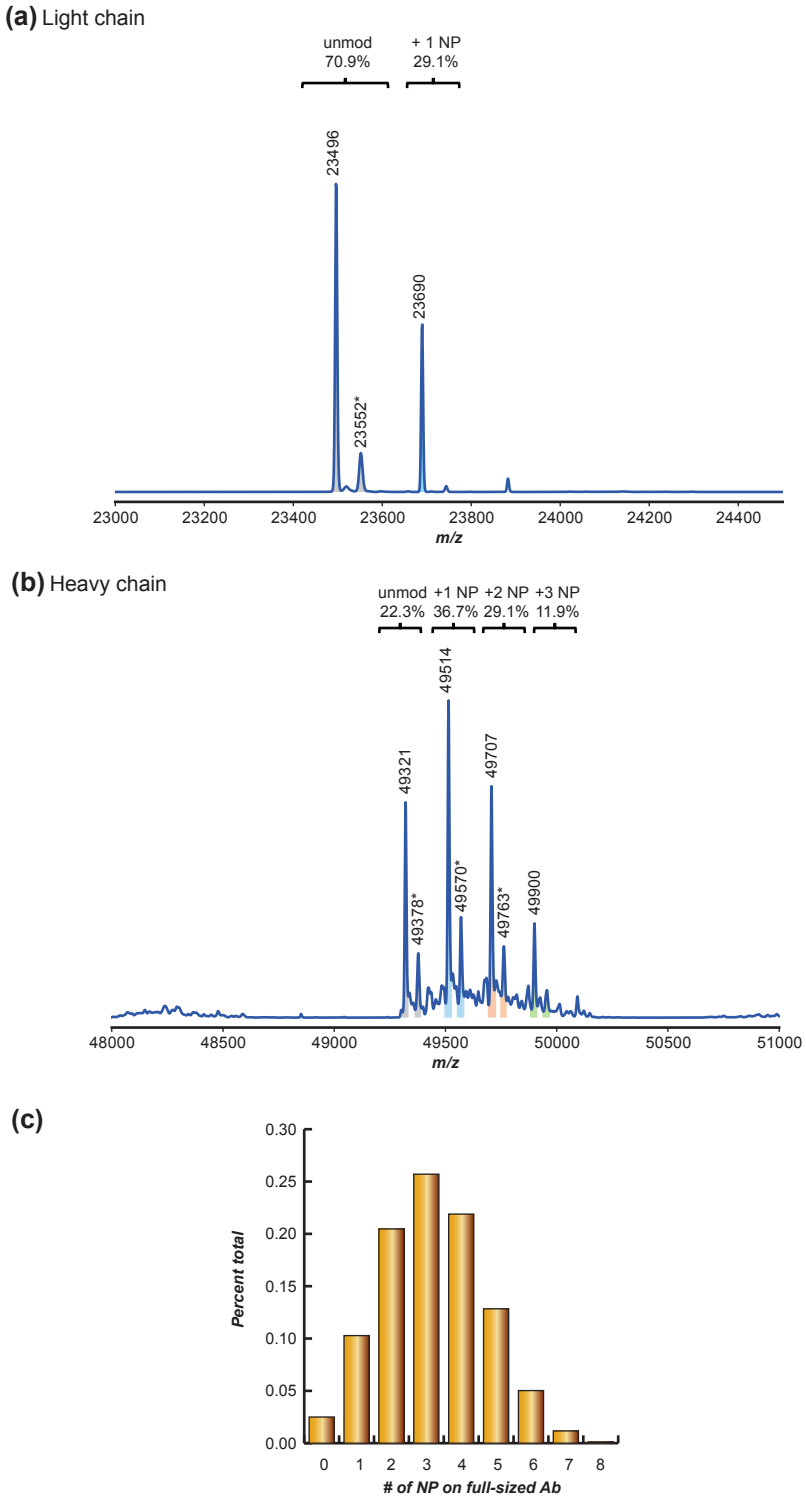

Figure S4.2. Percent modification of each antibody chain after incubation with 5 equivalents of NP-NHS. (a) Deconvoluted LCMS spectrum of the light chain. (b) Deconvoluted spectrum of the heavy chain. The full-sized antibodies were deglycosylated using PNGase F and reduced with DTT. The reduced cysteines were capped with iodoacetamide before LCMS analysis. The asterisk denotes peaks with an additional iodoacetamide attached to the proteins. (c) Product distribution of nitrophenol-modified full-sized antibodies calculated from percent modification of light and heavy chain in (a) and (b).

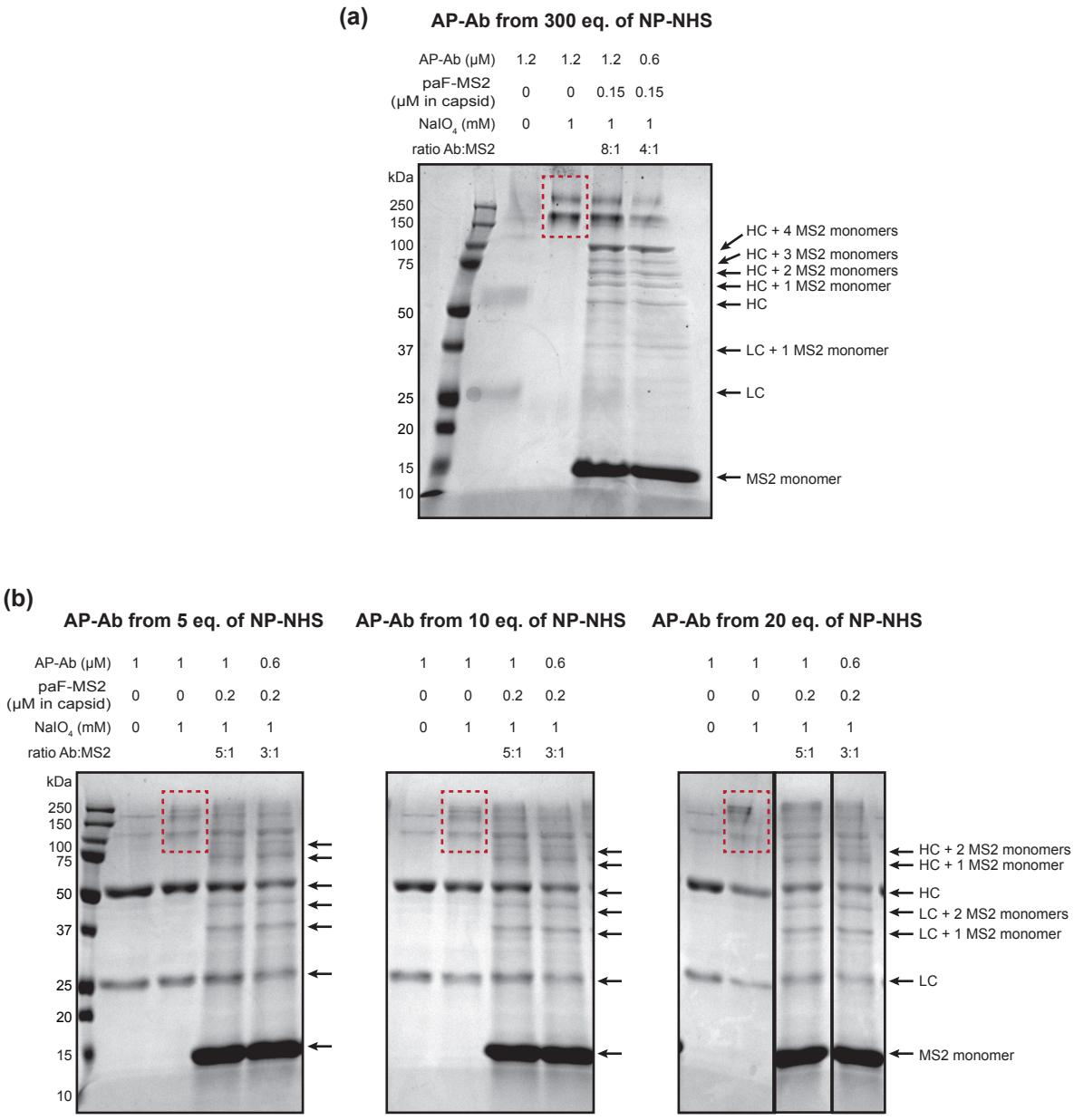

Figure S4.3. SDS-PAGE analysis of reactions between AP-Ab (with different numbers of aminophenol groups appended on Ab) and *p*AF MS2. (a) Ab was first reacted with 300 equiv. of NP-NHS, followed by reaction with pAF MS2 in the presence of $NaIO_4$ in diffrent ratio of Ab:MS2 (lane 3-4). Lane 1 and 2 was AP-Ab by itself in the absence and presence of $NaIO_4$, respectively. (b) AP-Ab made by lower numbers of equivalents of NP-NHS (5, 10, and 20 equiv.). SDS-PAGE analysis was performed under the reducing conditions in both (a) and (b).

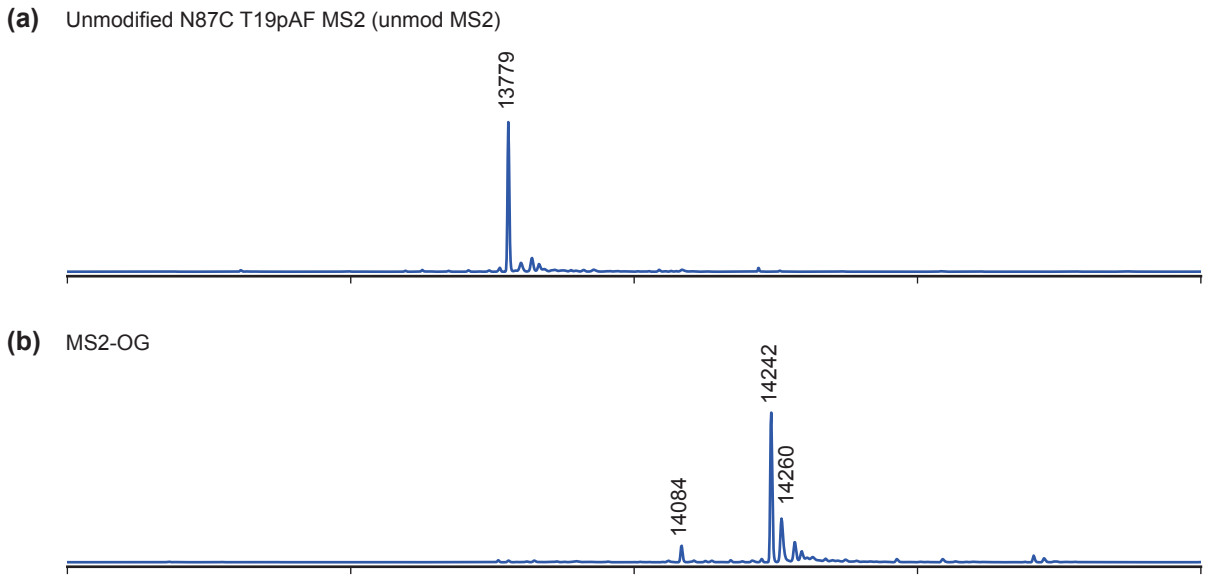

Figure S4.4. LCMS analysis of MS2 conjugating to small molecules at the cysteine residue on the interior. (a) unmodified N87C T19*p*AF MS2 (unmod MS2;expected mass = 13779 Da). (b) N87C T19*p*AF MS2 conjugating to Oregon Green 488 (MS2-OG; expected mass = 14242 Da). The peak at 14260 Da corresponds to the product of the succinimide hydrolysis.

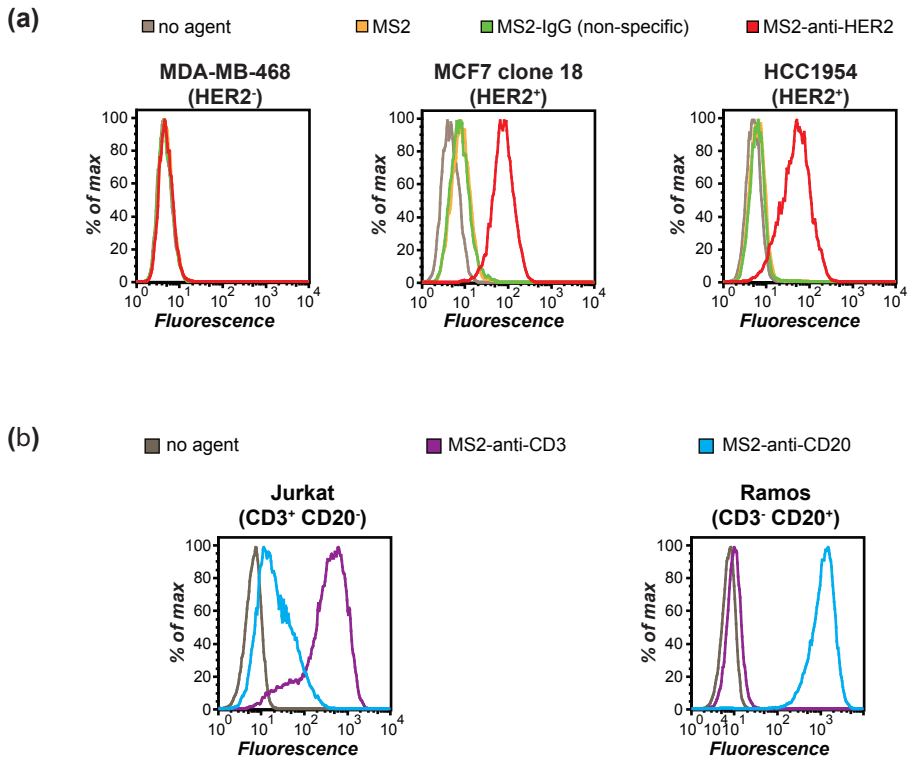

Figure S4.5. Fluorescence flow cytometry analysis of MS2-antibody conjugates. (a) Binding of MS2-anti-HER2 Ab conjugates to HER2 negative, MDA-MB-468, and HER2 positive, MCF7 clone 18 and HCC1954, cell lines. The Oregon Green 488 (OG)-containing MS2-anti-HER2 Ab construct was incubated with these cell lines in PBS containing 1% BSA binding buffer on ice for 45 min at ~5.5 nM of capsid concentration, which corresponds to 1 μM MS2 monomer concentration. The results from flow cytometry showed specific binding of MS2-anti-HER2 conjugates to only the HER2 positive cell lines, while remaining unbound to the HER2 negative cells. MS2-OG and MS2-OG conjugated to non-specific human IgG1 were used as negative control agents and were incubated with cells similarly to the MS2-anti-HER2 conjugates. None of them were found to bind to any cell lines non-specifically, confirming that the binding of MS2-anti-HER2 conjugates were specifically due to HER2/anti-HER2 Ab interaction. (b) Binding of MS2-anti-CD3 and MS2-anti-CD20 Ab conjugates to Jurkat ($CD3^+$ $CD20^-$) and Ramos ($CD3^-$ $CD20^+$) cell lines. The MS2-anti-CD3 and MS2-anti-CD20 constructs were incubated with Jurkat and Ramos cells in DPBS containing 1% FBS binding buffer on ice for 45 min at ~5.5 nM of capsid concentration, followed by washing step and incubation with AlexaFluor 488-conjugated anti-mouse IgG secondary antibody. The MS2-anti-CD3 bound specifically to Jurkat cells, and the MS2-anti-CD20 bound to Ramos cells although it has slight non-specific binding to Jurkat cells.

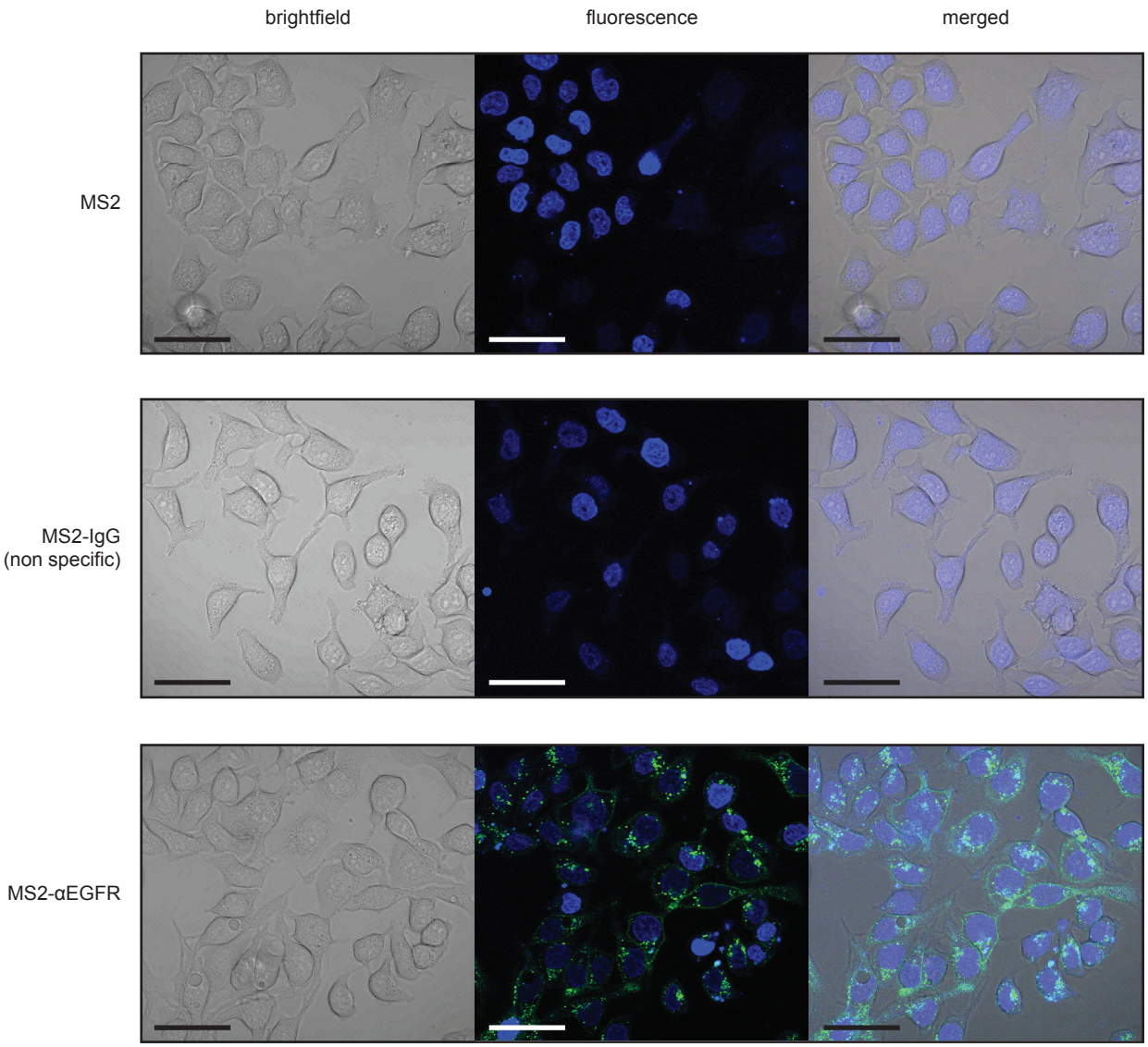

Figure S4.6. Images from the confocal microscopy studies of MS2-Ab binding to live cells, as shown in Figure 4.6b. Several green fluorescent vesicles were found inside the cells after 1 h incubation with the MS2-anti-EGFR conjugates, suggesting that the MS2-anti-EGFR conjugates might be internalized

4.7 References

1. Liu, S.; Maheshwari, R.; Kiick, K. L. *Macromolecules* **2009**, *42*, 3–13.
2. Srivastava, A.; O'Connor, I. B.; Pandit, A.; Gerard Wall, J. *Prog. Polym. Sci.* **2014**, *39*, 308–329.
3. Svenson, S.; Tomalia, D. A. *Adv. Drug Deliv. Rev.* **2005**, *57*, 2106–2129.
4. Lee, C. C.; MacKay, J. A.; Fréchet, J. M. J.; Szoka, F. C. *Nat. Biotechnol.* **2005**, *23*, 1517–1526.
5. Gao, X.; Cui, Y.; Levenson, R. M.; Chung, L. W. K.; Nie, S. *Nat. Biotechnol.* **2004**, *22*, 969–976.
6. Liong, M.; Lu, J.; Kovochich, M.; Xia, T.; Ruehm, S. G.; Nel, A. E.; Tamanoi, F.; Zink, J. I. *ACS Nano* **2008**, *2*, 889–896.
7. Torchilin, V. P. *Nat. Rev. Drug Discov.* **2005**, *4*, 145–160.
8. Tiwari, G.; Tiwari, R.; Sriwastawa, B.; Bhati, L.; Pandey, S.; Pandey, P.; Bannerjee, S. K. *Int. J. Pharm. Investig.* **2012**, *2*, 2–11.
9. Flenniken, M. L.; Liepold, L. O.; Crowley, B. E.; Willits, D. A.; Young, M. J.; Douglas, T. *Chem. Commun. (Camb).* **2005**, 447–449.
10. Flenniken, M. L.; Willits, D. A.; Harmsen, A. L.; Liepold, L. O.; Harmsen, A. G.; Young, M. J.; Douglas, T. *Chem. Biol.* **2006**, *13*, 161–170.
11. Suci, P.; Kang, S.; Gmür, R.; Douglas, T.; Young, M. *Antimicrob. Agents Chemother.* **2010**, *54*, 2489–2496.
12. Wang, Q.; Kaltgrad, E.; Lin, T.; Johnson, J. E.; Finn, M. G. *Chem. Biol.* **2002**, *9*, 805–811.
13. Douglas, T.; Young, M. *Science* **2006**, *312*, 873–875.
14. Kovacs, E. W.; Hooker, J. M.; Romanini, D. W.; Holder, P. G.; Berry, K. E.; Francis, M. B. *Bioconjug. Chem.* **2007**, *18*, 1140–1147.
15. Tong, G. J.; Hsiao, S. C.; Carrico, Z. M.; Francis, M. B. *J. Am. Chem. Soc.* **2009**, *131*, 11174–11178.
16. Wu, W.; Hsiao, S. C.; Carrico, Z. M.; Francis, M. B. *Angew. Chem. Int. Ed. Engl.* **2009**, *48*, 9493–9497.
17. Garimella, P. D.; Datta, A.; Romanini, D. W.; Raymond, K. N.; Francis, M. B. *J. Am. Chem. Soc.* **2011**, *133*, 14704–14709.
18. Destito, G.; Yeh, R.; Rae, C. S.; Finn, M. G.; Manchester, M. *Chem. Biol.* **2007**, *14*, 1152–1162.
19. Ren, Y.; Wong, S. M.; Lim, L.-Y. *Bioconjug. Chem.* **2007**, *18*, 836–843.
20. Behrens, C. R.; Hooker, J. M.; Obermeyer, A. C.; Romanini, D. W.; Katz, E. M.; Francis, M. B. *J. Am. Chem. Soc.* **2011**, *133*, 16398–16401.
21. Hovlid, M. L.; Steinmetz, N. F.; Laufer, B.; Lau, J. L.; Kuzelka, J.; Wang, Q.; Hyypiä, T.; Nemerow, G. R.; Kessler, H.; Manchester, M.; Finn, M. G. *Nanoscale* **2012**, *4*, 3698–3705.

22. Rhee, J.-K.; Baksh, M.; Nycholat, C.; Paulson, J. C.; Kitagishi, H.; Finn, M. G. *Biomacromolecules* **2012**, *13*, 2333–2338.

23. Brown, W. L.; Mastico, R. a.; Wu, M.; Heal, K. G.; Adams, C. J.; Murray, J. B.; Simpson, J. C.; Lord, J. M.; Taylor-Robinson, A. W.; Stockley, P. G. *Intervirology* **2002**, *45*, 371–380.

24. Stephanopoulos, N.; Tong, G. J.; Hsiao, S. C.; Francis, M. B. *ACS Nano* **2010**, *4*, 6014–6020.

25. Farkas, M. E.; Aanei, I. L.; Behrens, C. R.; Tong, G. J.; Murphy, S. T.; O'Neil, J. P.; Francis, M. B. *Mol. Pharm.* **2013**, *10*, 69–76.

26. Hooker, J. M.; Esser-Kahn, A. P.; Francis, M. B. *J. Am. Chem. Soc.* **2006**, *128*, 15558–15559.

27. Capehart, S. L.; Coyle, M. P.; Glasgow, J. E.; Francis, M. B. *J. Am. Chem. Soc.* **2013**, *135*, 3011–3016.

28. Weiner, L. M.; Surana, R.; Wang, S. *Nat. Rev. Immunol.* **2010**, *10*, 317–327.

29. Jiang, X.-R.; Song, A.; Bergelson, S.; Arroll, T.; Parekh, B.; May, K.; Chung, S.; Strouse, R.; Mire-Sluis, A.; Schenerman, M. *Nat. Rev. Drug Discov.* **2011**, *10*, 101–111.

30. Trail, P. *Antibodies* **2013**, *2*, 113–129.

31. Netirojjanakul, C.; Witus, L. S.; Behrens, C. R.; Weng, C.-H.; Iavarone, A. T.; Francis, M. B. *Chem. Sci.* **2013**, *4*, 266–272.

32. Carrico, Z. M.; Romanini, D. W.; Mehl, R. A.; Francis, M. B. *Chem. Commun. (Camb)*. **2008**, 1205–1207.

33. Obermeyer, A. C.; Jarman, J. B.; Netirojjanakul, C.; El Muslemany, K.; Francis, M. B. *Angew. Chem. Int. Ed. Engl*. **2014**, *53*, 1057–1061.

34. Sunada, H.; Magun, B. E.; Mendelsohn, J.; MacLeod, C. L. *Proc. Natl. Acad. Sci.* **1986**, *83*, 3825–3829.

35. Fan, Z.; Lu, Y.; Wu, X.; Mendelsohn, J. *J. Biol. Chem.* **1994**, *269*, 27595–27602.

36. Harding, J.; Burtness, B. *Drugs Today (Barc)*. **2005**, *41*, 107–127.

37. Perez-Torres, M.; Guix, M.; Gonzalez, A.; Arteaga, C. L. *J. Biol. Chem.* **2006**, *281*, 40183–40192.

38. Perera, R. M.; Zoncu, R.; Johns, T. G.; Pypaert, M.; Lee, F.-T.; Mellman, I.; Old, L. J.; Toomre, D. K.; Scott, A. M. *Neoplasia* **2007**, *9*, 1099–1110.

39. Patel, D.; Lahiji, A.; Patel, S.; Franklin, M.; Jimenez, X.; Hicklin, D. J.; Kang, X. *Anticancer Res.* **2007**, *27*, 3355–3366.

40. Mehl, R. A.; Anderson, J. C.; Santoro, S. W.; Wang, L.; Martin, A. B.; King, D. S.; Horn, D. M.; Schultz, P. G. *J. Am. Chem. Soc.* **2003**, *125*, 935–939.

41. Laemmli, U. K. *Nature*. **1970**, *227*, 680–685.